THE UNIVERSITY
of EDINBURGH

Building hepatocytes a home:

New frontiers in bioactive scaffolding techniques for liver tissue engineering

Rhiannon Grant

A thesis submitted for the degree of Doctor of Philosophy

The University of Edinburgh

2018

Declaration

I declare that this thesis has been composed by myself and that this work has not be submitted for any other degree or professional qualification.

Parts of this work have been published as

Grant, R., Hay, D. C., & Callanan, A. (2017). A Drug-Induced Hybrid Electrospun Poly-Capro-Lactone: Cell-Derived Extracellular Matrix Scaffold for Liver Tissue Engineering. Tissue Engineering Part A, 23(13–14), 650–662.

Grant, R., Hay, D. C., & Callanan, A. (2018). From scaffold to structure: the synthetic production of cell derived extracellular matrix for liver tissue engineering. Biomedical Physics & Engineering Express. In Press.

Signed

15th August 2018

Acknowledgements

This work would not have been possible without the help and support of many people.

My research was funded by an Engineering and Physical Sciences Research Council doctoral training partnership, as well as Medical Research Council UK Regenerative Medicine Platform II grant MR/L022974/1 and Medical Research Council Chemistry and Computational Biology of the Niche grant MR/L012766/1. I was generously supported by the Royal Society of Edinburgh, who awarded me a £3797 John Moyes Lessells travel scholarship to work at Lehigh University under Dr Lesley Chow on a project regarding peptide:polymer scaffolds for liver tissue engineering. I was also supported by the Tissue Engineering and Regenerative Medicine Society, the Institute of Physics and Engineering in Medicine and the Tissues, Cells and Engineering Society to attend conferences throughout my PhD.

Some of this work, particularly Chapters 4 and 6 was only possible because of the sacrifice of organ donors and their loved ones, who allowed their organs to be used for this research. Organ donation is an utterly selfless act, enabled by families and loved ones at some of the darkest moments of their lives. That those who are enveloped by such grief can still think of the needs of others speaks to their generosity and altruism, and no words of thanks can ever convey the gratitude that I and my fellow research scientists feel for their sacrifice. I'd also like to thank the NHS and SNBTS staff at the Royal Infirmary of Edinburgh who assist in the organ retrievals; particularly Mr John Hallett and Professor Stuart Forbes for their support and collaboration.

For his tireless support and guidance, I would like to thank my supervisor Dr Anthony Callanan. Uncountable late meetings and cups of tea have been devoted to my research by him, and without his help this thesis would not have been written. His door is never closed; no matter how busy he is or how small or large the question. He is, without a doubt, the best PhD supervisor I could have asked for and his students are lucky to have him. Although he'd never allow me to say it to his face; I believe my scientific career will be founded on the successes he enabled and the lessons he taught me. No words of thanks will ever be enough. I hope he knows that he is a rare credit to the academic community and that I will always be a grateful colleague, and a friend. Thank you Anthony.

I would also like to thank Professor Dave Hay for his supervision and guidance. He helped give me the opportunity, coaching and financial support to pursue this PhD research right through to its successful completion and was always available for help and advice. Thank you Dave.

Steve Mitchell, Dr Vlastimil Srnsen, Dr Alison MacDonald and Katalin Kis provided technical support, advice and assistance during my project without which it could not have been successfully completed, thank you all.

Dr Lesley Chow welcomed me into her group at Lehigh University, generously giving me the opportunity to work with her for four months to learn all things peptide. Peter Schwarzenberg, Paula Camacho and Dami Busari; thank you for welcoming me, being excellent hosts and helping me feel at home. I hope we see each other again soon!

The Callanan Lab and the Institute for Bioengineering was truly a joy to work in. I'd particularly like to thank Todd Burton and Alex Warne for being my first new friends, constant sources of general hilarity, cups of tea (made properly) and a good 'critique' of work when needed. Nimrah Munir, for desserts as needed! Jamie Reid, Tom Bate, Siobhan Dunphy, Maaria Ginai and Billy Shanahan for tolerating my mad science when I needed help, and for litres of tea/wine as and when required.

My beautiful friends. Susan Stewart, Cathy McLaughlin, Hilary Thompson, Sarah Lempriere, Jessica Duncombe; all of you at some point have said something that kept me going when I wanted to sack it all in and go live on a beach in poverty. Thank you for encouraging me, and for doing all the fun, non-work things with me. Here's to many years of friendship to come.

My mum, and my (not so) little brother. Thank you for your unquestioning support and faith in my abilities, I'm not sure where I'd be without you both. Thank you for all the dog sitting, lifts and dinners especially! We're nothing without family.

Tesla. For absolute loyalty and love, for getting me up when I couldn't do it myself and for never allowing me to feel alone.

It truly takes a village for any achievement, and in no way is this achievement mine alone. It belongs to everyone in these acknowledgements, and to everyone in my life. For every hand-hold, step-up, piece of advice and word of encouragement I will pass another on to those behind me, and be their village in turn. Thank you.

Contents

Appendix 3; From scaffold to structure: the synthetic production of cell derived extracellular matrix for liver tissue engineering

List of Figures

List of Tables

List of Abbreviations

2D	2 dimensional
3D	3 dimensional
ADME	Absorption, distribution, metabolism, and excretion
ALB	Albumin
ALD	Acute liver disease
AMC-BAL	Amsterdam medical centre bioartificial liver
BAL	Bioartificial liver
BLSS	Bioartificial liver support system
CARS	Coherent anti-Stokes raman spectroscopy
CD133	Stem cell marker 133/prominin-1
CLD	Chronic liver disease
c-MET /HGFR	Hepatocyte growth factor receptor
COL1A1	Collagen I
COL4A1	Collagen IV
CRISPR	Clustered regularly interspaced short palindromic repeats/Cas9 system
CS	Chondroitin sulfate
CYP	Cytochrome
CYP-450	Cytochrome p-450 reductase
DILI	Drug induced liver injury
DMSO	Dimethyl sulphoxide
DNA	Deoxyribonucleic acid
DPP4	Dipeptidyl peptidase-4
DS	Dermatan sulfate
ECM	Extracellular matrix
EGF	Epidermal growth factor
ELAD	Extracorporeal liver assist device
ELISA	Enzyme-linked immunosorbent assay
ES	Embryonic stem
ESC	Embryonic stem cells
ET-1	Endothelin-1
FGF	Fibroblast growth factor
FN	Fibronectin
GAG	Glycosaminoglycan
GATA1	GATA-binding factor 1/erythroid transcription factor
gDNA	Genomic DNA
hBTC1	Bornstein and Traub Type I collagen (Sigma Type VIII), powder from human placenta-containing scaffold
HE	Hematoxylin and eosin
HFIP	Hexafluoroisopropanol
hFN	Human plasma fibronectin-containing scaffold
HGF	Hepatocyte growth factor
HIV	Human immunodeficiency virus

hLECM	Human liver extracellular matrix-containing scaffold
HPC	Hepatic progenitor cell
hRL521	Human recombinant laminin 521-containing scaffold
HS	Heparan sulfate/heparin
HSC	Hepatic stellate cell
hTERT	Human telomerase reverse transcriptase
ICC	Inverted colloidal crystal
IHC	Immunohistochemisty
iPSC	Induced pluripotent stem cell
KS	Keratan sulfate
Lam-521	Laminin-521
LPS	Lipopolysaccharide
MAPK	Mitogen-activating protein kinases
MDMA	3, 4-methylenedioxy-N-methylamphetamine/ecstasy
MELS	Modular extracorporeal liver assist device
miRNA	Micro RNA
MMP	Matrix metalloproteinase
mRNA	Messenger RNA
MRP2	Multi-drug resistance protein 2
MSC	Adult/Mesenchymal stem cell
NAFLD	Non-alcoholic fatty liver disease
NASH	Non-alcoholic steatohepatitis
N-ECM	No drug treatment (normal) extracellular matrix
NPC	Non-parenchymal cell
PBC	Primary biliary cholangitis
PCL	Polycaprolactone
PCR	Polymerase chain reaction
PDGF	Platelet derived growth factor
PEG	Polyethylene glycol
PLA	Poly-lactic acid
PO	Polymer only scaffold
qRT-PCR/RTQ-PCR	Quantitative reverse transcriptase PCR
RGD	Arginine-Glycine-Aspartic acid (cell binding motif)
RNA	Ribonucleic acid
ROS	Reactive oxygen species
SB-ECM	Sodium butyrate derived extracellular matrix
SD-ECM	Synthetically derived extracellular matrix
SDS	Sodium dodecyl sulphate
SEC	Sinusoidal epithelial cell
SO	Scaffold only
SV40	Simian virus 40
TCP	Tissue culture plastic
TGF-β	Transforming growth factor-beta
TNF-α	Tumour necrosis factor-alpha
TPEF	Two-photon-excited fluorescence
u-PA	Urokinase-type plasminogen activator

V-ECM	Valproic acid derived extracellular matrix
VEGF	Vascular endothelial growth factor
WHO	World health organisation
ZO-1	Zonula occludens-1/Tight junction protein-1

Abstract

Liver disease is one of the top five leading causes of premature death in the UK, with incidence rising sharply by 20% over the last decade, and mortality increasing over 400% since 1970. Liver disease incidence and mortality is rising in stark contrast to trends in the other top healthcare burdens, with stroke, cancer, heart disease and lung disease incidence and mortality rates plummeting and continuing to fall.

Liver disease's hallmark pathology of late diagnosis and rapid acute disease progression leads to an urgent need for donor organs; the only curative treatment for end stage liver disease. However, a chronic and ongoing shortage of suitable organs for transplant means many die before a donor liver can be found, and countless others live with severe, debilitating symptoms at a high cost to both the patient and the healthcare system.

As part of the push for a solution to this problem, tissue engineers are focussing on creating niche microenvironments for hepatocytes which support their survival and function in as close to an in vivo like state as possible; addressing the need for an ideal in vitro model of the human liver and for lab created 'organoids' which could be used to treat patients. Such an environment would allow for the study of new pharmaceuticals, disease biology and hepatocyte behaviour in the laboratory and lead to more effective treatments for patients. While research to date is making inroads into this dilemma, we are yet to see a lab created environment which accurately recapitulates the complex, finely tuned and responsive extracellular matrix (ECM) of the liver. In an effort to address this, researchers have been incorporating bioactivity into scaffold environments for hepatocytes.

This thesis presents three methods of incorporating bioactivity into scaffolds for liver tissue engineering; drug induced ECM biodecoration, synthetically derived ECM biodecoration and decellularized human liver ECM incorporation. Scaffolds were seeded with hepatocyte cells and their response to their microenvironment analysed. Mechanical characterisation and

immunohistochemical analyses demonstrated the differences between the scaffold and the ECM biodecoration, as well as retention of ECM proteins through the manufacturing process. Each method altered the protein production and gene expression of hepatocytes, indicating that these methods provide a viable, translatable platform for creating a niche microenvironment for hepatocytes, supporting and manipulating phenotype and function. These scaffolds offer great potential for tissue engineering and regenerative medicine strategies for liver and a translatable method for other whole organ tissue engineering

Lay Summary

Liver disease is the only increasing cause of death in the UK, last year alone 2 people a week died waiting for a liver transplant. By creating a liver 'on the bench' we could test new drug treatments and study disease causes and progression and reduce this disease burden.

Bioengineering aims to create solutions to the problems of a shortage of donor organs for transplant and a lack of appropriate models in which we can study human biology and diseases. Bioengineers use a combination of materials science; researching new substrates, molecular biology; manipulating cells and proteins to create new environments and fluid dynamics; to create dynamic 'blood-flow' devices in which we can grow and manipulate cells to behave optimally. Eventually we hope to provide artificial organs which we can use to test new drugs, transplant into patients and replace animal models in research.

A particular challenge in liver tissue engineering is creating a replacement for the extracellular matrix (ECM). The ECM is a scaffold for cells to grow on which is a complex combination of organ specific proteins, growth factors and cell signalling molecules. It supports cell growth and modifies/responds to cell behaviour. This project focusses on creating new scaffolds for liver tissue engineering, as a replacement for the native liver ECM.

Research for liver tissue engineering scaffolds has focussed on two avenues; polymeric scaffolds and decellularized tissue. Polymer scaffolds; such as hydrogels, phase separated and electrospun scaffolds provide a reproducible, mechanically stable and consistent environment for liver cells. Decellularized organs, organs which have had all the cells stripped out of them with detergents, theoretically provide all of the biological cues and vascular network that the liver cells need to survive and function well. However, neither of these methods has yet proved sufficient. This project combines the two methods to provide novel environments which can influence liver cells; using engineering to affect a cellular response. Three methods were used to biodecorate electrospun polymer scaffolds. Firstly; an initial

sacrificial cell layer was grown on electrospun scaffolds and treated with protein production altering drugs. This cell layer was decellularized to leave behind a hybrid protein:polymer scaffold to grow liver cells on. The second method was similar; but the sacrificial cell layer was treated with a protein producing vector which increased fibronectin production, an important protein in the liver. Finally, decellularized human liver was incorporated directly into an electrospun scaffold and compared with scaffolds created with single ECM proteins.

Each of the scaffolds altered the behaviour of liver cells; changing gene expression, protein production and cell survival. Bioengineering of scaffolds can be used to alter liver cell behaviour and, in the future, optimise function. Creating novel environments such as these is one step closer to a more realistic platform for cell culture, a replacement for current drug testing models and an alternative to donor derived transplant organs

Justification for thesis research

According to the NHS, liver disease is one of the top five causes of premature death in the UK, with incidence rising sharply by 20% over the last decade[1]. While liver disease incidence is rising, other top healthcare burdens, such as stroke, cancer, heart disease and lung disease mortality rates continue to fall [2,3]. In the UK, 5 people a month die whilst waiting for a donor liver[4].

Liver disease's hallmark pathology of late diagnosis and rapid acute disease progression leads to an urgent need for donor organs; the only curative treatment for end stage liver disease[5]. However, a chronic and ongoing shortage of suitable organs for transplant means many die before a donor liver can be found, and countless others live with severe, debilitating symptoms at a high cost to both the patient and the healthcare system[2].

One of the major obstacles within the liver tissue engineering field is recapitulating the ECM. The ECM is a dynamic, organ specific collection of proteins, cytokines and other small molecules which provides physical support, mediation of cell:cell communication and modulation of cell behaviour[6–8]. Various studies have demonstrated the influence of altered ECM on the behaviour of hepatocytes in culture; including that of diseased ECM[9,10], of synthetically derived ECM[8,11] and of individual ECM components[12,13] on the behaviour of hepatocytes. .

As part of the solution to this problem, tissue engineers are focussing on creating niche microenvironments for main cell type of the liver, the hepatocyte, which support cell survival and function and could be used to treat patients in the future[11,14–16]. Such an environment would also allow for the study of new pharmaceuticals to treat human disease more effectively [17]. While research to date is making inroads into this dilemma, there is yet to be a lab created environment which accurately recapitulates the complex, finely tuned and responsive extracellular matrix (ECM) of the liver[12,18].

Tissue engineers are attempting to solve this problem by engineering liver 'organoids'; laboratory created organs which can function as a liver in vivo[19–22]. The 3D environment exerts extensive influence

on the behaviour and function of hepatocytes[11,21]. With this in mind, tissue engineers employ scaffold manufacturing technologies to create structures which encompass key characteristics of the native 3D ECM[23–28]. Several different methods of creating a scaffold are in use, and they can be made from a myriad of substances; both natural and synthetic[29], and enhanced with bio-decoration methods[11].

There has been particular focus on organ decellularization, which provides an ECM bioscaffold with the 3D site-specific vasculature and highly conserved sinusoidal gradient required for hepatocyte function upon their repopulation of the organ[30]. Decellularized organs have been repopulated with hepatocytes and endothelial cells which subsequently survive and exhibit some level of function, clearly demonstrating the importance of the ECM in supporting hepatocyte survival and phenotype[31–35]. However, decellularization requires a human or animal source of whole, undamaged organs and while research is showing great promise, the field is fragmented and to date no scaffold has been created which allows hepatocytes to function as well as in vivo[36,37].

Detergents such as sodium dodecyl sulphate (SDS), Triton-X100 and sodium deoxycholate (SDOC) are employed to strip the ECM of cells. These detergents disrupt native tissue ultrastructure, decrease glycosaminoglycan (GAG) content and reduce collagen integrity[38,39] as well as disrupt lipid-lipid, lipid-protein and protein-protein interactions[40].

Scaffold manufacture has been employed; using engineering technologies to create a synthetically derived structure which mimics the characteristics of the native ECM. There are several different methods of creating a scaffold, and they can be made from a myriad of substances; both natural and synthetic[29]. Hydrogels have been of particular interest to liver tissue engineers, gels biofunctionalized with collagen I enhance P450 (Cyp450) activity, cell adhesion markers and innate hepatocyte fibronectin production[41]. Gels biofunctionalized with galactose increase albumin production and promoted the proliferation of hepatocytes[42]. Viability and hepatic functions of primary hepatocytes are improved by culturing them in hydrogels made with liver extracellular matrix[43], and when encapsulated in collagen-alginate composite hydrogels[44]. PEG hydrogels have been shown to augment

cell-cell interactions of bipotential mouse embryonic liver (BMEL) cells, subsequently improving their survival and function[45], however incorporating ECM components into scaffolds at the manufacturing stage has proved challenging, with the harsh solvents require to solubilize major components of ECM alter their microstructure and functionality[46,47]. Ongoing research is showing great promise, however to date no scaffold has been created which allows hepatocytes to function as well as in vivo[36,37].

Both ECM components and scaffolds have shown great promise in tissue engineering [12,26,48], and each provides benefits to the cells seeded upon them. With these considerations in mind, this thesis focusses on ECM components obtained from decellularization and protein production/incorporation and scaffold engineering were combined to create novel environments which influence hepatocytes. By manipulating ECM production using pharmaceuticals, producing hepatic ECM components using synthetic biology and combining decellularized proteins and exploiting polymer characteristics novel hybrid polymer-ECM platforms for liver tissue engineering were produced. To validate the platforms produced, cells representative of the liver; HepG2s, THLE3s and primary human hepatocytes, were used.

Hypothesis and Aims

The hypothesis of this project is that hepatocytes can be influenced by novel hybrid scaffold platforms.

The aims are as follows;

1. The manufacture of electrospun polymer scaffolds capable of maintaining hepatocyte survival

2. Combine polymer scaffolds with cutting edge protein production techniques to manufacture practical, reproducible and translatable hybrid polymer:protein scaffolds for liver tissue engineering

3. Assess the impact of polymer only and hybrid scaffolds on hepatocyte survival and behaviour.

Chapter 1

Introduction

1.1 Liver Anatomy

The human liver is the largest solid organ and the largest gland in the human body. In females, the liver weighs 1.2 - 1.4 kg and in males 1.5-1.7 kg, accounting for approximately 2.8% of the total body weight. The liver is located on the upper right side of the body, protected from impact by the lower rib cage. A healthy, perfused liver is reddish brown in colour and is soft, highly malleable and easily lacerated; in addition to being highly vascularised[49]. The liver performs central metabolic, detoxification, synthetic, digestive, endocrine, immunoregulatory, and exocrine functions and is estimated to be vital for over 500 live sustaining processes in the human body[17].

The superior surface of the liver is attached to the diaphragm and anterior abdominal wall by a triangular fold of peritoneum; the falciform ligament. The line of attachment of the falciform ligament divides the liver into right and left lobes. Additionally, the transverse fissure divides the liver additionally into two further lobes; the quadrate and caudate lobes. The gallbladder is attached to the quadrate lobe at the rear of the liver by the cystic duct[49].

The liver is the most richly perfused organ in the human body, containing 13% of the total blood volume at any one time. There are two distinct sources of blood to the liver, the hepatic artery, which provides oxygenated blood to the organ and the portal vein, which provides nutrient dense blood derived from the intestinal tract, spleen, pancreas and gallbladder and provides 80% of the blood flow to the liver, highlighting the liver's pivotal metabolic role. The hepatic vein drains deoxygenated blood from the liver into the inferior vena cava. Bile is drained from the liver via the right and left hepatic ducts, which join the cystic duct to form the common bile duct, draining from the liver to the intestine. The hepatic portal vein, proper hepatic artery and common bile duct are collectively known as the porta hepatis[50].

Figure 1.1; Human liver anatomy

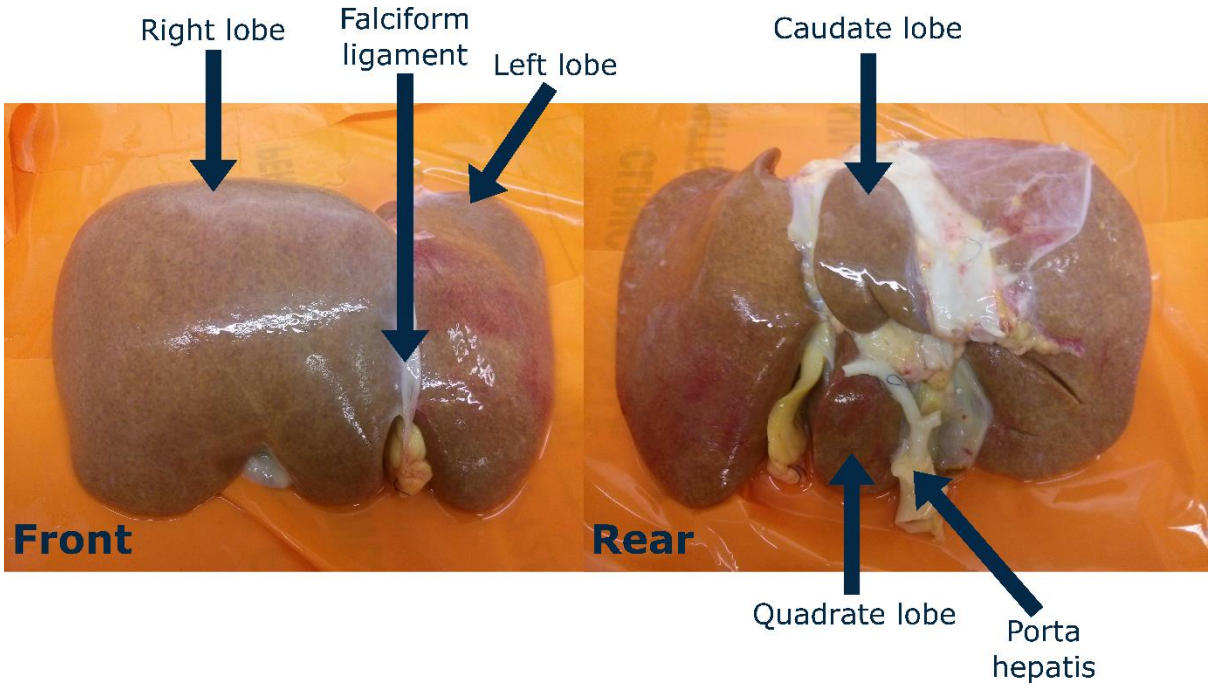

Figure 1.1; Labelled anatomy of the human liver. Donor liver received January 2017.

Each of these arteries, veins and ducts subdivides to feed the smallest histological compartment of the liver; the lobule. Liver lobules are hexagonal honeycomb-like arrangements of cells, approximately 1mm in diameter, fed by the smallest subdivision of the capillary system in the liver; the sinusoids[51,52]. Sinusoids are highly specialised capillaries which are lined by a specialized, discontinuous fenestrated endothelium as opposed to the traditional basement membrane. These sinusoids are in immediate proximity to the Space of Dissé, which borders the liver cells, and allow for unfettered diffusion of metabolites and metabolic products to and from cells[53,54].

Each lobule consists of three zones based on their proximity to the portal triad; the collection of hepatic artery, portal vein and bile ducts. Zone I is closest to the portal triad, and receives the highest level of oxygenation, making the cells within zone I least susceptible to ischemic injury. Conversely, zone II lies adjacent to the central vein of the lobule and receives the lowest level of oxygenation, making the cells within most susceptible to ischemic injury. Additionally, cellular function is related to lobule zonation, with major metabolic processes such as albumin production, ammonia detoxification, urea synthesis, glutamine synthesis, cytochrome p450 drug metabolism, gluconeogenesis, glycolysis,

oxidative phosphorylation, lipogenesis and the TCA cycle all displaying zone based functionality[22,50,55,56].

Figure 1.2; Lobule zonation

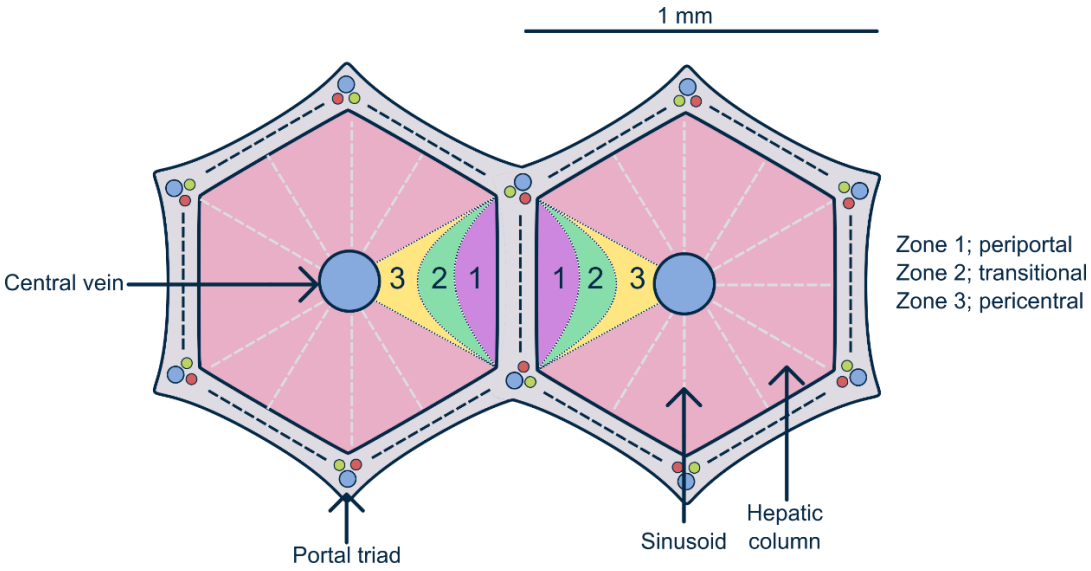

Figure 1.2; Diagram representing the size and zonation of liver lobules, with periportal, transitional and pericentral regions labelled.

1.2 Resident Cells of the Liver

The myriad of functions of the liver are enables by the complex assembly of its highly specialized cell types. Non-parenchymal cells (NPCs) comprise 30-40% of the liver's cellular mass; and includes Kupffer cells (liver macrophages), sinusoidal endothelial cells, stellate cells, biliary epithelial cells and roving immune cells such as leukocytes and lymphocytes[57]. Parenchymal cells, the hepatocytes, make up the majority (60-70%) of the cell mass. The hepatocytes carry out the bulk of the metabolic activity of the liver; producing circulating proteins such as albumin, protease inhibitors and coagulation factors, regulating pH and performing ammonia detoxification[58]. Hepatocytes control the homeostasis of glucose/glycogen, cholesterol, bile and vitamins A and D, as well as metabolize amino acids, heme and bilirubin. The NPCs of the liver exist in functional and structural organisation alongside the hepatocytes, mediating hepatocyte survival and function[59].

Sinusoidal endothelial cells (SECs) line the sinusoids of the liver lobules and lack a consistent basal lamina; resulting in no continuous barrier between the blood and the hepatocytes. SECs possess large pores (0.1-0.3µm) which allow free flow of molecules to and from hepatocytes. However, the SECs also possess lymphatic function, undertaking scavenger receptor mediated clearance of various molecules, including endotoxins and bacteria, recruiting leukocytes and regulating inflammatory cascades. They also possess the ability to behave as antigen presenting cells to circulating T-cells. SECs contribute to the extracellular matrix (ECM) by producing fibronectin and collagen IV. Additionally, they activate transforming growth factor beta (TGF-β) to the active form. SECs also produce autocrine vasoactive compounds, such as endothelin-1 (ET-1), to affect blood flow and uptake from the sinusoidal lumen[60,61].

Hepatic stellate cells (HSCs) reside in the Space of Dissé, between the hepatocytes and the SECs. These cells are considered to be 'stem-like', displaying neuronal and neuroendocrine markers such as *nestin* and CD133 as well as haemopoietic markers such as GATA1. Under normal physiological conditions, stellate cells store vitamin A, but during phases of inflammation they are the source of liver myofibroblasts; playing a pivotal role in hepatic fibrosis progression and regression and maintenance of the extracellular matrix by producing matrix metalloproteinases, hepatocyte-influencing growth factors, and ECM molecules[62–64].

Kupffer cells, or liver macrophages, reside in the microvessels of the sinusoids, ideally situated to screening for pathogens entering the liver and underscoring the role of the liver in acute immune responses; in fact 80% of the body's macrophages are Kupffer cells located in the liver. As macrophages, they play the classical role of clearing cellular debris and exogenous particles and of mediating inflammatory responses by releasing cytokines, chemokines, eicosanoids, proteolytic enzymes, reactive oxygen species (ROS) and nitric oxide[65,66].

Biliary epithelial cells, or cholangiocytes, line the biliary tract and interact directly with their neighbouring hepatocytes to secrete and modify bile; a vital acid for digestion. They maintain

osmolality of the bile secretions and absorb hormones, amino acids, neurotransmitters, and other molecules to mediate homeostasis within the liver lobule[67–70].

Table 1.1; Resident cells of the liver

Cell Type	Location	% of liver cell population	Activity/Function
Hepatocyte	Parenchyma	70%	Protein secretion Bile secretion Cholesterol metabolism Detoxification Urea metabolism Glucose/glycogen metabolism Blood clotting
Biliary epithelial cell (Cholangiocyte)	Bile duct lining	3%	Form bile ducts to transport bile Control rate of bile flow Secrete water and bicarbonate Control pH of bile
Sinusoidal endothelial cell	Sinusoidal lining	19%	Form sinusoidal plexus to facilitate blood circulation Highly specialized to allow transfer of molecules and proteins between serum and hepatocytes Scavenger of macromolecular waste Cytokine secretion Antigen presentation Blood clotting
Kupffer cell	Sinusoid microvessels	2%	Scavengers of foreign material Cytokine secretion Protease secretion Immunomodulation
Hepatic stellate cell	Space of Dissé	2%	Maintenance and modulation of extracellular matrix Vitamin A and retinoid storage Source of myofibroblast cells Cytokine secretion

1.3 Hepatic extracellular matrix

The extracellular matrix (ECM) is a non-cellular component of all tissues, which provides essential support for the cells of the tissue. The ECM, formed by the complex network of water, proteins and polysaccharides surrounding cells in all solid tissues, is among the most important regulators of cellular and tissue functions in the body. As well as being a physical scaffold and structural support for cells,

crucial biochemical and biomechanical signals are initiated by the ECM, necessary for tissue homeostasis, differentiation, and morphogenesis, and considered essential for normal physiology [71,72]. The ECM regulates essential cellular functions, such as adhesion, migration, proliferation, and survival. Cellular response and function is dependent upon the niche microenvironment provided by an organ's ECM, and dysregulation of ECM production and proteolysis is often associated with the development of pathologies. Each tissue has its own specific ECM 'recipe'; driven by a dialogue between various cellular components and the microenvironment within the tissue. Of these, collagen I, collagen II, elastin, fibronectin and laminin are often considered the main structural components, present almost ubiquitously throughout the mammalian body, providing strength, structure, and flexibility. Moreover, the ECM is a highly plastic structure, subject to constant modification and can vary dramatically between tissues [73].

Liver extracellular matrix is a highly specialised cellular microenvironment predicated by the Space of Dissé [74]. Where other organs of the human body possess two basement membranes and a collagen-based ECM between endothelial and epithelial cells, liver lobules have a discontinuous low density basement membrane and an attenuated ECM. This specialised ECM, together with the abundant and large pores of the sinusoidal endothelial cells, ideally facilitates the rapid bidirectional exchange of macromolecules between the blood and hepatocytes and sustains the differentiated stage of the surrounding cells[53,54,75,76].

In a normal liver, ECM represents less than 3% of the relative area on a tissue section, and approximately 0.5% of the wet weight. The hepatic ECM is composed mainly of collagen, fibronectin, laminin and proteoglycans. Liver ECM proteins are mostly detected in the Glisson's capsule, portal tracks, central veins, and in the space of Dissé. Collagen types I, III, IV, and V are the predominant collagens detected in the liver; collagen types I, III, and V are mostly interstitial ECM proteins in the portal and central regions, whereas collagen IV is highly detected in basement membranes[31,77,78]. Fibronectin is abundantly expressed in the hepatic ECM; it is detected in the subcapsular connective

tissue, in septa, and portal areas, and it is the main ECM component in the space of Dissé in normal livers[79,80]. Laminin similarly to collagen IV is a main component of the hepatic basement membranes[12,81–83].

1.3.1 Fibrillar collagens

Fibrillar collagens are ECM proteins which form striated fibrils, providing mechanical structure to the ECM. Collagen I is the most abundant ECM component of the adult liver. Together with the other fibrillary collagens; III and V they comprise the largest proportion of ECM proteins in the liver. Fibrillar collagens are named as such because they possess rigid triple helix amino acid structures and form heterogeneous fibre bundles which infer structural strength to the liver. Collagen I is found in the highest concentrations in the periportal and pericentral regions of the liver lobule, adjacent to the portal triad and the central vein. It contains several binding sites per peptide that attach α1β1 and α1β2 integrins, and interacts with other ECM proteins including other collagens, fibronectin, and proteoglycans[84,85].

Collagen III possesses a similar structure to collagen I, but is most prevalent in the periportal region. It associates strongly with collagen I bundles, providing mechanical integrity to the portal triad region[84,86,87]. Collagen V links multiple collagen types to each other, regulating the formation of collagen fibrils[78].

1.3.2 Non-fibrillar collagens

Non-fibrillar collagens possess fragmented triple-helical structures, and are traditionally classed as a category of basement membrane molecules. They create networks linking other ECM components. Collagen IV is the main non-fibrillar collagen of the liver ECM. It secures non-collagenous components like laminin to the ECM and is mainly concentrated in the discontinuous ECM of the sinusoidal epithelial cells[88].

Collagen VI is present in small amounts in the human liver. They form networks with other collagen molecules, particularly collagen I and III to stabilise collagenous fibre bundles. Collagen VI also interacts with collagen IV to anchor larger structures such as blood vessels and with soluble molecules such as mitogen-activating protein kinases (MAPKs) to function in tissue repair[62,88,89].

1.3.3 Non-collagenous glycoproteins

The most common non-collagenous glycoproteins in the human liver are fibronectin and laminin. Fibronectin is a particularly high molecular weight protein dimer (440KDa) which can be found in two forms; the insoluble cellular and soluble plasma fibronectin. Plasma fibronectin is primarily synthesised by hepatocytes and is the most abundant glycoprotein in the liver. Plasma fibronectin is an essential protein in the clotting process. In healthy liver, cellular fibronectin exists in low levels and is particularly concentrated in the pericentral region, produced primarily by the stellate cells. Cellular fibronectin binds collagen I, perlecan and fibrin and attaches to hepatocytes in the Space of Dissé.

Fibronectin contains a particular cell binding motif, Arginine-Glycine-Aspartic acid (RGD). It's increased presence in the regenerating liver functions as a chemoattractant, cell adhesion molecule and growth factor for migrating cells. During tissue repair, plasma fibronectin at the site of the injury is degraded and remodelled by Kupffer and stellate cells. The hepatocytes then replace this plasma fibronectin with the insoluble cellular fibronectin which is incorporated into the ECM.

Laminins, another RGD-containing ECM molecule, is also produced by hepatic stellate cells and is concentrated around the portal triad and sinusoidal walls. During development, laminins migrate throughout the perisinusoidal region, and have a particularly important role in the maintenance and differentiation of hepatocyte phenotypes, as well as being vital to vascular structural integrity.

1.3.4 Proteoglycans

Proteoglycans are a remarkably variable component of the ECM, macromolecules with a protein core and one or more glycosaminoglycans (GAGs) bound covalently. GAGs are long unbranched

polysaccharides consisting of a repeating disaccharide unit. There are six total GAG types that are classified into four structurally distinct families; heparan sulfate (HS)/heparin, chondroitin (CS)/dermatan sulfate (DS), keratan sulfate (KS), and hyaluronan. Proteoglycans are encoded for by 43 distinct genes, and an exponential number of variants exist due to alternative splicing [90]. Due to the polar nature and specific structural confirmation of GAGs they can bind to a variety of proteins, rendering them negatively charged. Importantly, they can then attract water molecules, keeping the ECM hydrated [91].

Traditionally, proteoglycans are categorised according to their relative size (large or small) and the nature of their protein cores. However this has recently been replaced with a more complex taxonomy, classifying the proteoglycans according to their location, homology and protein core [90]. They are found throughout the cell, cell surface and ECM, and vary greatly according to their function.

Dermatan sulfate, chondroitin sulfate and hyaluronan possess viscoelastic properties which allow them to retain water and influence osmotic pressure [92,93]. Heparan sulfate binds a variety of ligands including FGF (fibroblast growth factor), VEGF (vascular endothelial growth factor) and PDGF (platelet derived growth factor) and is responsible for regulating a wide range of biological processes including coagulation, angiogenesis and developmental processes [94]. Keratan sulfates have a particularly important role in the formation of scar tissue [92,95,96].

All GAGs increase the half-life of soluble growth factors by binding them covalently and protecting them from proteolytic degradation. This process also enhances and controls the presentation of growth factors to cells by clustering them in close proximity to the receptors of cells anchored to the ECM, and concentrating them in specific tissues and regions[97,98].

1.4 Growth factors and the liver

Growth factors are soluble signalling molecules which control cellular responses through specific binding of transmembrane receptors on target cells. They have a wide range of roles, in cell growth

and proliferation as well as differentiation and phenotypic maintenance. Of the 100s of growth factors present in the liver, three have the most significant impact on hepatic function; hepatocyte growth factor (HGF), epidermal growth factor (EGF) and fibroblast growth factor (FGF)[99–102].

HGF is secreted by the HSCs and SECs in the liver, and functions as a very powerful mitogen; stimulating both hepatic progenitor cells and differentiated hepatocytes via the c-MET/HGF receptor and subsequent tyrosine kinase pathways of both epithelial and endothelial cells. HGF has been implicated in liver regeneration and recovery from liver disease, and in the development of particular types of cancer. By binding to the ECM via GAGs, heparin, hyaluronan and collagen; HGFs half-life increases from as low as 4 minutes to several hours, allowing for long term exposure to cells[103,104].

EGF s produced out with the liver, in the Brunner's gland of the duodenum, and is transported into the liver via the portal vein; where is activates cell division and is vital for normal liver regeneration. Exposure to EGF is dependent upon lobule zonation; with hepatocytes in zone 1 (closest to the portal triad) receiving exposure to EGF more rapidly and in higher concentrations than those in zone 3[105,106]. FGF is secreted by HSCs in the perisinusoidal region and influences wound healing, regeneration and angiogenesis in the liver; interacting with the liver ECM in a similar manner to HGF[101,107].

1.5 Liver regeneration

The liver is the only visceral organ capable of regeneration, and can return to 100% of its weight/mass even following a loss of up to 60% of its own bulk[80,108]. The adjustment of liver weight to the needs of the body suggests a complicated set of control points, a 'hepatostat'. Liver regeneration and this mechanism of hepatostat control is a heavily researched process which provides insights into the development of other organs and disease processes. The interaction of all the discussed components; cells, growth factors and ECM molecules in the liver are not only vital for normal function but also for hepatic development and healing/regeneration. A complex and highly conserved cascade of signalling molecules coordinates all liver components to expand and organise new tissue, however the precise mechanisms and methods of controlling hepatic regeneration remain unclear[109].

Loss of or injury to normal liver tissue; either by physical or chemical means initiates the liver regenerative process. Two models of liver regeneration are proposed. One is that the Kupffer cells activate to clear cellular debris, which in turn activates the HSCs and hepatocytes to proliferate within the parenchyma, returning the liver/bodyweight ratio to 100. A second method is proposed where the regenerative capacity of hepatocytes is compromised, e.g. in chronic inflammatory conditions. In this situation, biliary compartment can function as a niche of facultative stem cells that can transdifferentiate into hepatocytes[101,110]. Conversely, in situations when there is a need to repair the damaged biliary epithelium but the proliferative capacity of biliary cells is compromised, the immediate periportal hepatocytes can function as a niche source of facultative stem cells and transdifferentiate into biliary cells[69,101].

Growth factors are vital to the process of liver regeneration. Urokinase-type plasminogen activator (u-PA) is released as quickly as 1 minute following liver injury, and correlates with an increase in its receptor; u-PAR. In addition to releasing plasminogen, u-PA frees matrix-associated HGF; immediately stimulating the surrounding hepatocytes to proliferate[100]. Approximately 1 hour post liver injury, HGF release peaks. During this hour, HSCs, Kupffer cells, and SECs release HGF and EGF to promote further hepatocyte proliferation. Peaks in growth factor production occur at 24 hours and 48 hours post-injury[111].

An important factor in liver regeneration is ECM remodelling. Matrix metalloproteinases (MMPs) are responsible for the degradation of most extracellular matrix proteins during organogenesis, growth and normal tissue turnover[112–114]. Degradation and remodelling of the liver ECM is vital in the regenerative process because it allows the unrestricted proliferation of hepatocytes and other liver cells. In healthy, non-inflamed liver ECM maintenance depends upon the simultaneous action of MMPs and HSCs to remodel and repair the hepatic microenvironment. Healthy adult livers have a moderate amount of ECM turnover, correlating with the small amounts of MMPs constitutively detected in those livers. However in liver injury, various MMPs are upregulated; aiding in the

degradation and replacement of damaged or missing tissue and regulating immune responses via their interactions with other growth factors and cytokines such as transforming growth factor-beta (TGF-β) and tumour necrosis factor-alpha, (TNF-α)[115,116].

1.6 Diseases of the Liver

Liver disease is the only major cause of death still increasing year-on-year, and twice as many people now die from liver disease as did in 1991. Liver disease was described in 2014 as the one 'glaring exception' to the advances made in medicine for the treatment of chronic disorders; with mortality increasing by 400% and incidence in the under-65s rising by 500% since 1970. [3]. There are over 100 types of liver disease, and at least 2 million people in the UK are living with liver disease[3,5].

Figure 1.3; Liver mortality

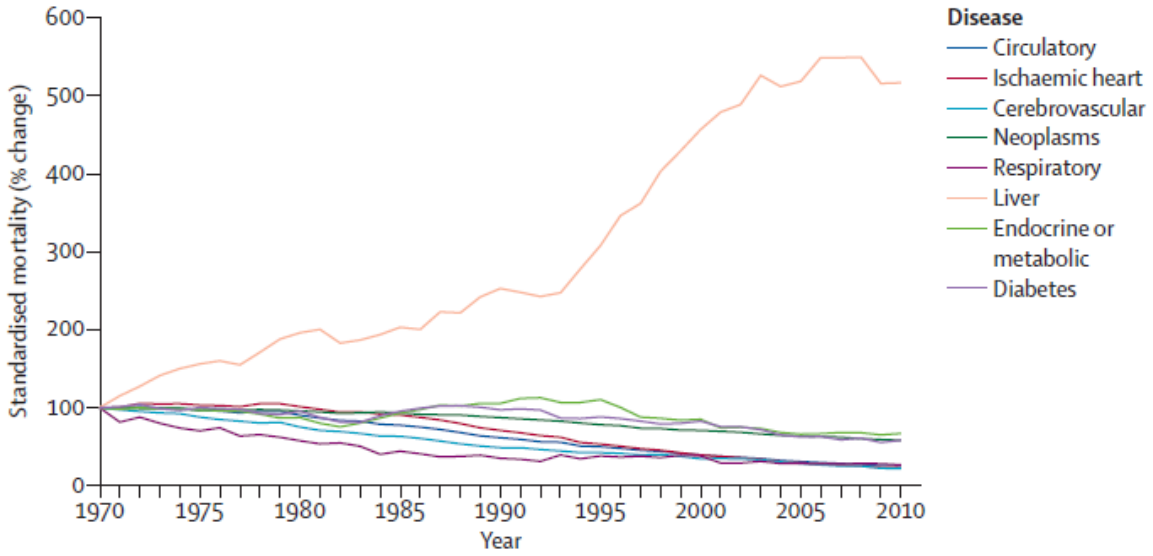

Figure 1.3; Mortality by cause of death year on year. Williams *et al* 2014, The Lancet.

Generally, over 75% of liver tissue needs to be affected before a decrease in hepatic function occurs, leading to late diagnosis of advanced liver conditions. As a result, liver transplant is often the only treatment option available to end-stage disease patients [117]. Due to increasing donor age, a higher incidence of obese donors and a change in the demographics of donor death away from sudden trauma to other causes there is a chronic shortage of donor organs, and many die whilst on the waiting

list. On March 31st 2018 there were 333 people left waiting for donor livers and 56 people died between April 1st 2017 and March 31st 2018 whilst waiting for a donor liver[4].

1.6.1 Acute liver disease

Acute liver disease (ALD) is a rapid loss of liver function and usually occurs in a person who has no pre-existing liver conditions. Loss of function occurs rapidly, as quickly as a matter of days, and indicates that severe hepatic damage has occurred even prior to clinical presentation. With an incidence of fewer than 10 cases per million persons per year in the developed world, acute liver failure is seen most commonly in previously healthy adults in their 30s, and is much rarer than chronic liver disease (CLD). Clinically, patients present with abnormal liver biochemical values and coagulation pathology; without dramatic clinical interventions encephalopathy follows < 8 weeks after onset and 50% of ALD cases are lethal[118].

ALD remains less common in the developed world, where improved public sanitation and vaccination public health measures have reduced the incidence of viral infections which are often responsible for ALD. The most common cause of ALD in the United States and Western Europe is drug induced liver injury (DILI)[17].

1.6.2 Viruses

The hepatitis family of viruses are responsible for the majority of cases of acute liver failure. Hepatitis A and E are implicated heavily; with rates of death of more than 50% reported from the developing world. Hepatitis B can also lead to ALD, with incidence more common in Mediterranean and Asian countries. Patients with reactivation of previously stable subclinical infection with the hepatitis B virus have a particularly high mortality rate. This scenario is most common in patients with treatment-induced immunosuppression during or after therapy for cancer. The identification of at-risk patients and the use of antiviral prophylaxis before the initiation of chemotherapy, immunotherapy, or

glucocorticoid therapy are effective in prevention[119,120]. Other rare viral causes of acute liver failure include herpes simplex virus, cytomegalovirus, Epstein–Barr virus, and parvoviruses[108,118].

1.6.3 Drug-induced liver injury

DILI is responsible for approximately 50% of cases of ALD in the United States and Western Europe. DILI may be dose-dependent and predictable, as exemplified by acetaminophen-induced hepatotoxicity or can present as idiosyncratic, unpredictable, and independent of dose[17,121].

Although DILI can occur after consumption of a single excessive dose of a pharmaceutical, the risk of death is greatest with substantial drug ingestion staggered over longer periods of time rather than at a single time point. DILI is also a risk for patients on complex and extended drug regimens, particularly those taking acetaminophen for the relief of symptoms from hepatic illness or other causes. Malnourished patients and patients with alcoholism are at increased risk[122].

Idiosyncratic DILI is rare, even among patients who are exposed to potentially hepatotoxic medication; due to awareness and strict clinical monitoring practices. Factors such as an older age, increased elevations in blood aminotransferase and bilirubin levels, and coagulopathy are associated with an increased risk of death[123].

1.6.4 Other causes of acute liver disease

Acute ischemic hepatocellular injury occurs in critically ill patients with primary cardiac, circulatory, or respiratory failure; often caused by severe sepsis[124]. This condition primarily requires supportive cardiorespiratory management rather than specific interventions targeted at the liver. The prognosis depends on both the cause of hepatic hypoxia and the severity of liver injury. A similar liver-injury pattern may also be seen in drug-induced liver injury caused by recreational drugs such as MDMA (3, 4-methylenedioxy-*N*-methylamphetamine/ecstasy) or cocaine[125].

Other causes of ALD are neoplastic infiltration, acute Budd–Chiari syndrome, heatstroke, toxic mushroom ingestion, and metabolic disorders such as Wilson's disease. ALD can occur during pregnancy due to the increased hepatic burden caused by the foetus[126].

1.6.5 Chronic liver disease

Chronic liver disease (CLD) refers to a progressive destruction and regeneration of the hepatic parenchyma which results in fibrosis and cirrhosis, the thickening and scarring of the ECM and loss of functional liver cells. In contrast to ALD, this process takes place over a period of at least six months, and often many years. Clinically, CLD is reversible in some cases but only where diagnosed in the early stages. However, patients are often asymptomatic until the hepatic decompensation indicative of major loss of functioning liver tissue occurs. Approximately 40% of patients with late stage CLD are asymptomatic, and the condition is often discovered during routine laboratory or radiographic studies for other conditions, or at autopsy[127].

Global prevalence of CLD is estimated to be between 4.5% and 9.5% of the general population, and ranks 10th as a leading cause of death in developed countries, 14th globally. According to national morbidity statistics, CLD is the 5th leading cause of death in the UK and is estimated to reach the 3rd leading cause by 2020[120].

1.6.6 Chronic viral hepatitis

Hepatitis B and C are precursors to CLD; similarly to that of ALD. Hepatitis B accounts for 0.34% and hepatitis C for 1.68% of all cases of CLD in the United States between 2005 and 2008 and chronic viral hepatitis is heavily implicated as a leading cause of CLD in developing regions and immigrant populations. Of the 12,656 death certificates that listed viral hepatitis in 2004, 42.6% listed hepatitis C as the underlying cause, and a total of 620,000 deaths were reported from HBV-related causes in 2000 of which (94%) liver related. Similarly to ALD, if patients are not diagnosed with hepatitis B/C at

an early stage, the unmediated clinical progression of the virus leads to irreversible liver damage and is currently one of the main etiologic indications for liver transplantation[128].

1.6.7 Alcoholic liver disease

Alcohol is consumed widely and for the majority of adult life; and has long been known to be a major risk factor for all liver diseases. According to the World Health Organisation (WHO), alcohol consumption accounts for 3.8% of global mortality. In 2010, alcohol-attributable liver cirrhosis was responsible for 493,300 deaths (156,900 female deaths and 336,400 male deaths); representing 0.9% (0.7% for women and 1.2% for men) of all global deaths. Alcohol is the primary etiological cause of liver-related death in Western Europe. France and Spain report approximately 30 deaths per 100,000 per year are cause by alcoholic liver disease. Heavy alcohol consumption induces changes in lipid metabolism and an inflammatory response. This results in accumulation of lipids in hepatocytes called hepatic steatosis. Alcohol consumption and alcoholic liver disease also lead to hepatocellular carcinoma via a similar biological pathway[120,129,130].

1.6.8 Non-alcoholic fatty liver disease

Non-alcoholic fatty liver disease (NAFLD) is a collective term for a group of conditions where there is an accumulation of lipid molecules in the livers of patients who drink moderately or not at all. NAFLD affects 20-30% of the Western population and is largely asymptomatic; however incidence is rising rapidly with the concurrence of obesity in the developed world. NAFLD is predicted to affect 50% of the population by 2020[120].

5-6% of patients with NAFD worsen and develop non-alcoholic steatohepatitis (NASH), fibrosis, or cirrhosis. These individuals are at risk of liver failure in approximately 50% of cases. NAFLD is also a precursor to hepatocellular carcinoma; which the WHO estimates has an annual global incidence of over half a million people and a 5 year survival rate of just 10%[2].

1.6.9 Biliary obstruction

Biliary obstruction can be cause by several factors, including gallstones, tumours, biliary atresia, cystic fibrosis and primary biliary cholangitis (PBC). Gallstones, insoluble collections of cholesterol, and tumours can cause physical obstruction of the bile ducts in the liver. PBC is an autoimmune disorder which results in progressive destruction of the small bile ducts of the liver. Biliary obstruction causes cholestasis; an accumulation of bile and other toxins in the liver and cholangiopathy; where the cholangiocytes of the bile ducts die, leading to inflammation and excess collagen deposition; blocking the bile ducts. Over time, the cholestasis and cholangiopathies lead to the fibrosis and cirrhosis typical of CLD[124,131].

In both Western Europe and the US, the incidence of PBC is estimated as 2-3 (peak incidence of 4-6 in women 40 years of age) and 21-40 (59-65 in adult women) per 100,000 persons per year, respectively, and mortality rate of 0.5 per 100,000 per year. Biliary obstruction was implicated in 16% of liver transplants between 1988 and 2014[2].

1.6.10 Other causes of chronic liver disease

CLD can also be caused by similar liver injury patterns to DILI, caused by long term use of acetaminophen, tramadol, cocodamol and concurrent use of heavy medication regiments such as those required for treatment of human immunodeficiency virus (HIV) and tuberculosis. Other causes include Alpha-1-antitrypsin deficiency, Wilson's disease, Haemochromatosis, Tay-Sachs disease, Gaucher disease and Zellweger syndrome[132].

1.7 Cell based approaches for studying the liver

There are several approaches being used to model the liver, study its biology and disease development and provide an alternative to increasingly rare donor livers for patient treatment. Cell culture studies form a key role in this narrative; informing our approach to liver tissue engineering. Liver cells can be

obtained from various sources and used in cell culture studies, in both 2D and 3D. These sources and their applications are summarized in table 1.2.

Table 1.2; Cells for liver studies

Cell	Source	Application	Advantages	Disadvantages
Primary human hepatocytes	Human cadaveric donor livers	Bioartificial liver Implantable devices Cell transplantations Culture studies	Most similar to *in vivo* hepatocytes Host compatible	Limited availability Donor-donor variability Phenotypic drift Poor survival *in vitro*
Primary animal hepatocytes	Porcine liver/rodent liver	Bioartificial liver Implantable devices Cell transplantations Culture studies	More easily available Some similarity to human hepatocytes	Phenotypic drift Poor survival *in vitro* Differences between animal/human hepatic functions Protein-protein incompatibility/immune response
Tumour derived human hepatocyte cell lines	Hepatic carcinomas	Bioartificial liver Implantable devices Culture studies	Easy storage & maintenance Affordable Unlimited *in vitro* proliferation	Tumorigenic Markedly altered phenotype in comparison to primaries Safety concerns Immune response
Immortalized human hepatocyte cell lines	Human hepatocytes immortalized using gene transfection	Bioartificial liver Implantable devices Culture studies	Reduced tumorigenicity compared to tumour derived lines Easy storage & maintenance Affordable Unlimited *in vitro* proliferation	Markedly altered phenotype in comparison to primaries Safety concerns Immune response

Embryonic stem cells (ESCs)	Pluripotent cell obtained from human embryonic tissue	Bioartificial liver Implantable devices Culture studies	Indefinite proliferation Hepatic differentiation capability	Ethical concerns Limited availability Costly maintenance Teratoma formation
Adult stem cells (MSCs)	Adult bone marrow, peripheral blood and amniotic tissue	Implantable devices Cell transplantations	Unlimited availability Minor safety concerns	Trans-differentiation to myofibroblasts Low differentiation efficiency Phenotypic drift
Induced pluripotent stem cells (iPSCs)	Genetically modified adult human cells	Bioartificial liver Implantable devices Culture studies	Indefinite proliferation Hepatic differentiation capability Less ethically divisive than embryonic cells	Limited availability Costly induction and maintenance Dedifferentiation and aberrant phenotypic behaviour
Hepatoblasts	Early stage human foetal liver	Cell transplants	Extensive proliferation *in vitro*	Ethical concerns Limited availability
Human foetal hepatocytes	Human foetal liver	Bioartificial liver Cell transplants Implantable devices	Some proliferation *in vitro* Simple isolation process	Ethical concerns Limited availability Aberrant phenotypic behaviour Possibly tumorigenic
Hepatocyte-like cells	Genetically modified adult cells	Culture studies	Rapid generation No ethical concerns	Aberrant phenotypic behaviour and drift Safety concerns
Hepatic progenitor cells	Bipotential cells from adult donor liver and foetal liver	Cell transplants	Differentiation ability (hepatocytes and biliary cells) Native liver cells	Challenging cell isolation Limited availability Possibly tumorigenic

1.7.1 Primary hepatocytes

Primary human hepatocytes are considered the gold standard for studying the liver *in vitro*. They theoretically represent the closest researchers can come to the behaviour of a hepatocyte *in vivo*, however their availability is limited and their behaviour in culture critiqued heavily by the field[133]. The majority are harvested from discarded cadaveric donor livers which are considered unsuitable for transplant and cryopreserved until they are needed for an experiment. Donor-donor variability, phenotypic instability over culture time and poor plateability/culture survival all compromise their use in routine testing and research. Using porcine primary hepatocytes overcomes the issues of availability and donor-donor variation; however they are subject to the same issues with phenotypic instability and deterioration over culture time. Rat and mouse primary hepatocytes can also be used, however their hepatic profile is markedly different to that of a human. It is commonly accepted that animal models of liver disease are not sufficient alone for the study of liver biology. Of 930 pharmacological compounds withdrawn from the market due to hepatotoxicity, only 17% demonstrated similar levels of toxicity in rodent and non-rodent studies[134]. Some conditions are impossible to replicate in animals; the human Hepatitis C virus does not infect rodents, only chimpanzees and tree shrew, and their clinical progression does not mimic that of the human disease[135]. Rodents metabolise alcohol much more rapidly than humans and do not develop severe liver fibrosis in response to alcohol toxicity[130]. As a result, while readily available; animal sources of primary hepatocytes do not provide results translatable to humans.

1.7.2 Cell lines

To combat the limitations and drawbacks of primary hepatocytes, researchers utilise cell lines. Cell lines are characterized by their unlimited proliferative abilities and stable phenotypes. They are readily available from manufacturers, are affordable and are easy to maintain in culture.

Several tumour derived hepatocyte cell lines are used by researchers, including HepG2, HepC3A, Huh7, HepaRG, and Hep3B cell lines. Each hepatic cell line has been used in several experiments and

provided valuable data, however cell lines show a lower expression of drug metabolizing enzymes (CYPs) in comparison to primaries in culture and the human liver *in vivo*, thought to be a result of reduced transcription of enzyme genes [136]. Additionally, drastic differences in the expression of key hepatic transcription factors and nuclear receptors observed in hepatoma derived cell lines in comparison to primaries/*in vivo* is thought to be linked to the reduction in CYP expression [137]. HepG2s are derived from a hepatic carcinoma, which exhibit some of the required phenotypic traits of liver cells. However microarray studies have revealed significantly altered expression of over 5000 genes in comparison to primary cells and *in vivo* cells [138,139]. HepC3As are derived from HepG2s but exhibit improved albumin and nitrogen metabolizing abilities [140]. However, their lack of urea enzymes and drug metabolizing functions limits their use [137,141]. The HepaRG cell line exhibits an expression pattern closer to that of primaries and *in vivo* in confluent cultures [142]. Proliferating HepaRGs can be treated with dimethyl sulphoxide (DMSO) to force them towards a more primary/*in vivo* like phenotype and express higher levels of CYP3A4, however their gene expression of CYPs is still generally lower than the primaries. Huh7s can also be cultured for several weeks to produce higher levels of CYP3A4, and unlike HepaRGs this is done without differentiation inducers such as DMSO [143].

Non-tumour derived cell lines can also be used. These cells are generally immortalized via gene transfer of the simian virus 40 (SV40) T antigen [144,145] but immortalizing can also be obtained by co-transfection of albumin-promoter-regulated antisense constructs and transcription factors E2F and D1 cyclin [146]. THLE-3/2 and Fa2N4 cell lines both exhibit induction of the major CYPs, however their enzyme activity is very low and only detectable using very sensitive analytical methods. More advanced genetic engineering methods have produced cell lines with reversible immortalization, using Cre-loxP excised oncogenes and suicide genes. The NKNT-3 hepatocyte line and non-parenchymal lines HNNT-2 (endothelials), TWNT-1 (stellates) and MMNK-1 (cholangiocytes) were all immortalized using these advanced methods and can be utilised for co-culture studies.

1.7.3 Embryonic stem cells and induced pluripotent stem cells

Embryonic stem (ES) cells are so prized by researchers for their pluripotency; their ability to proliferate indefinitely and differentiate fully into any tissue. However, due to obvious ethical issues surrounding the use of human ES cells, researcher most often use mouse ES cells. These cells have been used in BAL devices, and several reports of differentiation protocols for hepatocytes exist [147–150]; however none have been used at the scales required to produce a replicate of a human liver. Equally, the need for the use of Matrigel in such protocols introduces a further limitation to their use; Matrigel the trade name for an ECM product derived from Engelbreth-Holm-Swarm mouse sarcoma cells. Matrigel's manufacturers cannot guarantee batch consistency of the product, and the risk of introducing mouse viruses from the Matrigel is a concern.

Induced pluripotent stem cells (iPSCs) go some way to alleviate the concerns associated with ES cells. By circumventing the ethical concerns regarding cell source and using human cells to avoid the immunological challenges presented by animal sources, iPSCs present a potentially limitless source of stem cell derived hepatocytes[151–155]. However, the hepatocytes performance is not yet at the level of primary or *in vivo* cells, and differentiation protocols remain costly, lengthy and laborious.

1.7.4 Adult stem cells

Adult stem cells have been used in BAL devices and transplantation studies. They rely upon the trans-differentiation of mesenchymal stem cells (MSCs) sourced from various adult, live donor tissues to hepatocyte-like cells. MSCs can be injected into the liver and subsequently transdifferentiate into hepatocyte-like cells in the liver. Use of adult stem cells circumvents ethical and immunological issues posed by other cell types, however inappropriate differentiation info myofibroblasts is observed at the injection sites. There are multiple *in vivo* differentiation protocols available to researchers for MSCs, however, as with iPSCs the protocols are costly, lengthy, laborious and are yet to produce a fully differentiated and stable human hepatocyte, limiting their translatability for clinical use [21,82,156].

1.7.5 Hepatic progenitor cells

Hepatic progenitor cells are quiescent stem cells which reside in the liver at low numbers in a healthy state. Anatomically, these cells reside in the area called canals of Hering, which are terminal branches of biliary trees, and produce a mixture of the molecular markers of adult hepatocytes, cholangiocytes and foetal hepatoblasts. In cases of prolonged injury or inflammation of the liver, hepatic progenitor cells begin proliferating and subsequently differentiating into hepatocytes and cholangiocytes [157]. Hepatic progenitor cells have been used in transplant studies in mice, and results are promising, however marker analysis indicates that the progenitor cell population is not homogenous and cells vary in their differentiation capacity, lineage potential and stage of differentiation. This, and the challenges associated with isolating the small number of progenitor cells in the liver, as well as their potential for producing cancer and their links with hepatocellular carcinoma limits their clinical application[70,158].

1.7.6 Human foetal hepatocytes

Whereas adult hepatocytes are limited in their proliferative abilities, human foetal hepatocytes can divide multiple times *in vitro*, and have been immortalized by SV40 large T antigen and hTERT transfection to ensure researchers have an unlimited supply. These cells have been used in culture and transplantation studies, however the exhibit particularly limited urea production and ammonia clearance when compared with primary and *in vivo* hepatocytes. Additionally, when used in BAL devices, foetal hepatocytes are not functionally mature enough for clinical use. Transplantation studies have had promising early results, however ethical considerations regarding the use of foetal cells also limit their clinical applicability, particularly considering the number of cells requires for transplantation[159–162].

1.7.7 Hepatoblasts

Hepatoblasts are similar to human foetal hepatocytes, however are isolated at an earlier stage of gestation and as such possess extensive proliferative abilities *in vitro*. They, like hepatic progenitor cells, can differentiate into both hepatocytes and cholangiocytes in *in vivo* conditions, and animal studies indicate that the hepatoblasts integrate into injured livers and proliferate to renew the liver mass. However, as with other stem and foetal derived cells, ethical issues and availability, as well as challenging differentiation protocols *in vitro* present researchers with challenges for their clinical translation[45,68].

1.7.8 Hepatocyte-like cells

Advances in genetic modification, and particularly the advent of precise tools such as CRISPR gene editing has allowed researchers to generate adult cells which express hepatocyte transcription factors and functional genes; known as hepatocyte like cells or iHeps. iHeps were able to express hepatic genes and undertake hepatic functions and were able to engraft and reconstitute hepatic tissue in mice. By utilising tools like genetic engineering, researchers bypass the complex and costly differentiation protocols required for stem cells, and potentially create an unlimited and ethically preferable source of hepatocytes[145,150–152]. However, concerns regarding the longevity of their gene expression and their phenotypic drift away from a hepatocyte profile, as well as the recent discovery that tools like CRISPR can cause non-target mutations requires further research[163–165].

1.8 Tissue engineering of the Liver

Traditional cell culture is undertaken in 2D, with cell monolayers grown on flat, polystyrene tissue culture plastic dishes. The knowledge gleaned from these cultures in invaluable and has formed the basis of biological studies since Ross Granville Harrison developed cell culture methods in 1910. However, researchers increasingly recognise the artificial environment which 2D cell culture results in has an immeasurable impact upon cells, skewing results and altering everything from their metabolic

profiles to their protein production. Liver cells are known to respond to their 3D microenvironment, altering their albumin and urea production, ammonia clearance, and CYP expression in response to their culture environment[8,28]. The rapid functional deterioration of primary hepatocytes and hepatocytes derived from other sources is a result of their artificial environment in culture. As a result, bioengineers are focussing on creating new niche microenvironments for optimising and altering hepatocyte behaviour and performance[15,166]. Hepatocyte function is highly plastic and regulated by the surrounding ECM, extracellular signalling molecules, cell-cell interactions and the mechanical influence of their environment; none of which researchers have yet fully elucidated the effects of. As a result, bioengineers are also attempting manipulations which are not explicitly 'biomimetic' or recapitulating physiological conditions but still influence hepatocyte behaviour.

Various methods have been employed to mediate this functional deterioration. Arginine free media[167], culturing with various growth factors and DMSO[145], on collagen membranes[168–170], with Matrigel[75,171,172] and on various ECM materials[18,28,173,174] have all been shown to influence hepatocyte function. Devices mimicking the hepatic shear environment, architecture mimicking that of the hepatic lobules and perisinusoidal space and co-culture of hepatocytes with non-parenchymal cells have also shown promise[52,175–178]. These methods can be broadly summarised as shown in table 1.3.

Table 1.3; Tissue engineering of the liver

Environment	Techniques	Advantages	Disadvantages
Scaffold free 3D culture	Spheroid formation Sandwich culture Co-culture	No polymers/foreign materials required	Hi numbers of cells needed Necrosis risk in spheroid centres Foreign proteins required
Micropatterning & bioprinting	Bioink printing Cell encapsulation	Rapid biopatterning Can recapitulate liver structures	Limited on size for now
Scaffolds	Hydrogels Electrospun polymers ECM scaffolds	Repeatable and structurally stable	Risk of degradation/rejection of foreign materials

			Necrosis in hydrogel centres
Decellularized organs	Whole organ decellularization	Vasculature and ECM 'biorecipe' intact	Whole organs still required Incomplete decellularization Remnant detergents Huge numbers of cells required for recellularization
Perfusion and microfluidic devices	Shear devices and lobule mimicking devices	More realistic 'flow' environment Constant oxygen/nutrient exchange	Complex device manufacture and modelling Size limited for now
Bioartificial livers (BALs)	Extracorporeal bioreactors	Can actively (via cells) or passively (via adsorption/filtration) support liver function	Huge numbers of cells required Current clinical trials unsuccessful in replacing liver function

1.8.1 Scaffold free 3D culture techniques

Thus far, the most common non-scaffold based 3D culture methods have been sandwich culture, co-culture of hepatocytes with non-parenchymal cells and spheroid formation. The complex 3D interaction involving of parenchymal cells, non-parenchymal cells and the ECM is believed to be crucial in regulating and maintaining hepatic function *in vivo*; particularly with regard to influencing hepatocyte polarization. Polarization of hepatocytes induces a distinct pattern if transporter protein expression on each of the cell 'faces' and is lost in many 2D and 3D cultures. Sandwich cultures; where hepatocytes are cultures between two layers of ECM, often collagen I or Matrigel, have been employed to maintain this polarization. In this type of model, cell–matrix adhesion from above and below reduces abnormal cytoskeletal flattening and maintains cell–cell contact between adjacent hepatocytes. By promoting polygonal hepatocyte morphology for extended culture periods and improving functionality sandwich cultures with matrix proteins can lead to prolonged hepatocyte

viability[179,180], extended CYP activity[181,182] and increased cell polarization toward more advanced bile canaliculi networks. Co-culture with non-parenchymal cells of the liver is also key to hepatocyte function. Kupffer cells, hepatic stellate cells and sinusoidal endothelial cells have all been used in culture with hepatocytes and are found to be superior when sourced from hepatic tissue; as opposed to traditional 'feeder layer' style co-culture where co-cells are sourced from other more readily available sources such as epidermal fibroblasts[60,177,183]. Ratios of NPCs to hepatocytes has also been shown to influence hepatocyte function[52]. In general, an improvement in hepatocyte function and maintenance of hepatic phenotype is achieved irrespectively of the type of cell used for co-culture. Culturing hepatocytes in conditions which promote aggregation into 'spheroids' also influences the hepatocytes functionality; with breakthrough research postulating that 3D cytoarchitecture and the increased number of homotypic cell-cell contacts between hepatocytes is key to improving the phenotype and function of cultured hepatocytes [44]. However issues with the scale up of spheroid cultures, as well as longevity of the cells and necrosis due to insufficient oxygen diffusion to the centre of spheroid cultures continue to plague the field. Numerous methods including casting arrays, rotational cultures and encapsulation have been developed for the optimization and scale-up of hepatocyte spheroid culture[153,184,185].

1.8.2 Micropatterning and bioprinting

The recent explosion in 3D printing technologies brought about by the 2014 expiration of key patents has led to a rapid expansion of applications; including bioprinting and micropatterning of smaller tissue features such as hepatic lobules[186]. Current research in tissue engineering focuses on the development of compatible methods (printers) and materials (bioinks) that are capable of producing biomimetic scaffolds, vascular structures and cell encapsulation[187]. Organovo's exVive3D™ Liver is a bioprinted human tissue that has been used to provide toxicity assessments to supplement *in vitro* and preclinical animal testing [17,188]. Several groups have reported their novel liver bioinks improver hepatocyte function. Combinations of gelatin-chitosan, agarose-collagen and agarose-chitosan have

been employed, as well as decellularized liver ECM and collagen I [189,190]. A liver-on-a-chip platform has been developed by with hepatic spheroids fabricated via direct write bioprinting using gelatin methacryloyl in a microfluidic bioreactor device. Micropatterned grids of collagen-chitosan hydrogels containing a hepatic cell line and hepatocyte growth factor (HGF) [191] have been implanted into nude mice, demonstrating the translatability of bioprinted liver tissue however concerns exist regarding the safety of crosslinking methods used to stabilise the bioinks and the longevity of cells encapsulated within due to reduced oxygen diffusion through larger constructs [192].

1.8.3 Scaffolds

The shortcomings of other 3D culture methods for hepatocytes have prompted a push for scaffolds for liver tissue engineering. Such scaffolds would be replicable and provide the 3D structure requires to prompt hepatocytes into the desired phenotypic behaviour, as well as overcome concerns regarding the transplantation of unanchored, 'free' cells into human patients. Researchers have used hydrogels[193,194], ECM proteins[173,195] and polymers[28,196,197] to provide 3D environments for hepatocytes; be they biomimetic or otherwise, as well as to elucidate the effect of architecture upon hepatocyte function in a controlled manner. Researchers have reported altering hepatocyte function and maintaining hepatic differentiation using hydrogels and using electrospun polymers, both with and without ECM proteins. RegeneMed 3-D Liver is a liver tissue co-culture system used for screening hepatic ADME, using culture transwells with a nylon mesh. NPCs are seeded in a nylon screen sandwich mesh insert with hepatocytes to form a 3D liver tissue. Liver-specific functions, including production of albumin, fibrinogen, transferrin and urea, can be maintained up to three months, and the induction of CYP1A1, 2C9, and 3A4 activity for two months[198]. Co-culture with Kupffer cells allows for study of the inflammatory response as the release of pro-inflammatory cytokines can be observed with lipopolysaccharide (LPS) exposure[199]. Encapsulating hepatocyte co-cultures (hepatocytes, HSCs and SECs) in collagen-alginate hydrogels was shown to maintain their spheroidal shape, sinusoid-like structures, high viability and stable liver-specific functions for more than 1 month [44]. Collagen-

functionalized microsphere-template poly(ethylene glycol) (PEG) hydrogel scaffolds were shown to promote 3D hepatic sheet morphology; leading to improved albumin production and CYP450 activity as well as enhanced gene expression of cell-adhesion markers which stimulated innate hepatocyte fibronectin production[200]. Non-woven mesh scaffolds were created via total esterification of hyaluronan with benzyl alcohol (HYAFF-11), and seeded with fibroblasts which were subsequently decellularized to leave behind a hybrid ECM:HYAFF-11 scaffold[201]. Rat hepatocytes demonstrated higher proliferation rates and in vitro cell survival up to 4 weeks after seeding in hybrid scaffolds as opposed to HYAFF-11 alone scaffolds, and those seeded on hybrid scaffolds showed cells with a polyhedral morphology and establishing cell–cell contacts. Inverted colloidal crystal (ICC) microporous scaffolds were functionalized with fibronectin or collagen and shown to promote albumin production and liver-specific gene expression of Huh7.5 cells, compared with bare ICC scaffolds; and displayed differing aggregation patterns on fibronectin vs collagen functionalized ICC; possibly due to the distinct mRNA expression levels of cell adhesion-related genes and their interaction with liver specific genes[197]. Specific polymers also have an influence on hepatocyte function; with screening libraries for novel polymers revealing differing effects on differentiation and phenotypic behaviour of hepatocytes[202,203]. Scaffold stiffness has also been investigated with regard to primary hepatocyte function; those cultured on softer heparin gels with a low modulus of 11kPa demonstrated higher albumin synthesis and E-cadherin expression than those cultured on 26kPa and 116kPa gels, however this paper failed to properly disentangle the influence of heparin concentration on the hepatocytes [204,205]. Scaffold development is a rapidly evolving field, with promising results thus far however more targeted research for the future would add value to the field; elucidating the influence of mechanical changes, ECM proteins and scaffold morphology on hepatocyte function.

1.8.4 Decellularized organs

Decellularization refers to the process of removing cellular material to leave behind the surrounding ECM, and can be used to provide a niche environment for cells to repopulate[206]. In the case of whole

organ decellularization; the vascular network and ECM micro and nanoarchitecture are potentially maintained within the ECM and can provide vital cues to the repopulating cells. Decellularization removes potentially immunogenic components such as intracellular protein and DNA while maintaining the multifaceted ultra- structure and composition or bodies within the ECM, such as the sinusoids[207]. There is also strong evidence that ECM is a complex reservoir for growth factors and cytokines, the selective accumulation and release of which are important for robust cell growth, Recent publications by the Badylak group show evidence for microvesicle reservoirs of such factors being both present in the ECM and being tissue specific[208–210]. The first decellularized liver and its potential for hepatocyte survival was reported in 2004, by Lin *et al*.[211] Since then, a multitude of decellularization methods have been reported; including freeze/thaw cycles, immersion and agitation, and perfusion. Most protocols make use of a combination of detergents such as sodium dodecyl sulphate (SDS) and Triton-X100, pH disrupting agents such as ammonium hydroxide and enzymes including trypsin and pepsin with the various physical methods and aim for a remnant DNA concentration of 50ng/mg, <200bp DNA fragment length and a lack of visible nuclear content when visualised with DAPI (4',6-diamidino-2-phenylindole) or hematoxylin and eosin (HE) staining ; criteria proposed by leading researchers[212] as the acceptable conditions for a decellularized tissue to minimise risk of immune response in recipients.

Various protocols have been proposed for the decellularization and recellularization of liver tissue. However none to date have proven perfect for hepatocytes upon repopulation, and while they provide invaluable data for researchers; they still require a source of rare donor organs or require the use of animal tissue. Equally, a lack of uniformity in experimental parameters and cell type used for repopulation is limiting the field's knowledge. More targeted approaches to the process, and co-operation between both research groups and industry is required before researchers can truly reap the potential benefits of organ decellularization[8,28,30,213].

1.8.5 Perfusion devices and microfluidic devices

Hepatocytes and NPCs are known to be influenced by mechanical influences including shear stress and velocity of media flow. The incorporation of continuous flow into a culture system is known to facilitate more *in vivo*-like active transport of oxygen, nutrients and metabolites, as well as influence hepatocyte specific functions such as albumin production, urea synthesis and CYP drug metabolism activity. As a result; some groups are working on developing benchtop lab scale and microfluidic devices which expose cells to flow of media and nutrients. One of the main issues during the development of these devices is the balance between flow and shear stress applied to hepatocytes. The dynamic environment in the liver is particularly complex, with a dual circulatory system providing oxygen and nutrient flow to the hepatocytes and non-parenchymal cells; the portal vein and hepatic artery. Pressure in the portal vein measures between 4 and 10 mmHg, with a low pO_2 of 30 to 40 mmHg. In contrast, pressure in the hepatic artery hovers around 120 mmHg in a healthy individual, with the pO_2 measuring 90-100 mmHg[63,214]. Hepatocytes are extremely sensitive to oxygen concentrations and have a high metabolic demand which infers that they would respond well to high flow rates, however they are also vulnerable to shear stress exceeding 0.03 Pa[215–217]. Hollow fibre bioreactors are a popular choice for hepatocyte culture; with one group demonstrating that with only 0.5ml of media and 20 x 10^6 cells they can maintain enzymatic activity and gene expression of CYP1A2, CYP3A4/5, CYP2C9, CYP2D6, CYP2B6, transporters, and phase II enzymes for up to 3 weeks[218–220]. Another method of controlling the shear hepatocytes are exposed to is the multichamber modular bioreactor, such as those made by Quasi-Vivo®. Different cell types can be cultured in the chambers and connected to each other. Interaction between the different chambers is reliant upon soluble molecules in the cultivation medium, enabling the imitation of exchange between different tissues – imitating the organs of the human body. In the liver module of the Quasi-Vivo® system CYP1A1, 1A2, 2B6, 2C9, 3A4, UGT, MDR1, and MRP2 reached expression levels close to or above those of freshly isolated hepatocytes after two weeks of culture[221]. However, as in other silicone and PDMS based systems, high substrate adsorption can lead to incorrect data interpretation and subsequent errors in

analysis[222]. Microfluidics also provides an avenue for exposing hepatocytes to the challenging flow and shear environments required to optimize their phenotypic profile. Banaeiyan *et al* demonstrated that HepG2s and iPSC derived hepatocytes stabilized albumin secretion and urea synthesis when cultures under flow in microfluidic devices[22]. The hepatocytes also developed 3D tissue-like structure and immature bile-canaliculi networks in the chips. HepaChip® mimics hepatic sinusoids on a microscope slide; with eight micro-chambers containing three cell assembly ridges with the length and width of a human liver sinusoid, and electrodes to enable accurate cell positioning. In short term experiments (3 hours), hepatocytes exhibited significantly higher activity of both CYP3A4, CYP1A2, and phase II enzymes than hepatocytes co-cultivated in 96-well plates in the presence of endothelial cells[223–225]. Arguable however, 96 well plates are not an appropriate control for the experiment and while low media volumes and low required cell numbers are an advantage, the system is highly complex to operate and as such is yet to be widely used.

1.8.6 Bioartificial liver devices

Bioartificial liver devices such as the Extracorporeal Liver Assist Device (ELAD) and HepatAssist incorporate hepatocytes into a purely mechanical, dialysis-based artificial liver support device. Other systems include the Modular Extracorporeal Liver Support (MELS), the Amsterdam Medical Centre Bioartificial Liver (AMC-BAL), and the Bioartificial Liver Support System (BLSS). With no reliable source of high quality human hepatocytes readily available for these systems, they rely upon a variety of cell sources and techniques to detoxify waste molecules such as ammonia, provide synthetic function of albumin and coagulation factors, decrease inflammation, and promote cell regeneration[108,226,227].

1.9 Summary

To summarise, great progress is being made to establish an unlimited source of human hepatocytes; via iPSC and ESC work results as well as provide more appropriate cell lines for study such as iHeps and HepaRGs. The field now recognises the importance of conducting studies in 3D and limiting judgement of 2D derived results, and steps are being taken to provide 3D shear environments for

hepatic cells to study their interactions and metabolism; particularly spheroids and devices such as Kirkstall's Quasi-Vivo® system and the HepaChip® system. However, the field of liver tissue engineering is heterogeneous and somewhat fragmented in its approach. Issues with historical use of products such as Matrigel® and inappropriate extrapolation of results from tissue culture plastic experiments have led to an unclear picture of the behaviour of hepatocytes in 3D environments and *in vivo*. This project therefore aims to use engineering to influence the behaviour and function of hepatocytes; but makes no assumption about 'improvement' or inappropriate comparison to other studies.

Chapter 2

Methods

2.1 Electrospinning

Electrospinning is a method by which ECM-mimicking fibrous mats can be created by drawing fibres from a polymer solution. A high positive voltage is applied to the polymer solution, and the solution is extruded through a needle. The target surface is grounded or has a negative voltage applied to it, and fibres are drawn from the "Taylor cone", which forms at the tip of the needle due to the electric field, towards the target where they accumulate on the surface. The voltages, flow rates, collection surfaces, humidity/temperature and choice of polymer:solvent and their respective concentrations can all be varied to produce different fibres[11,228].

Figure 2.1; Electrospinning schematic

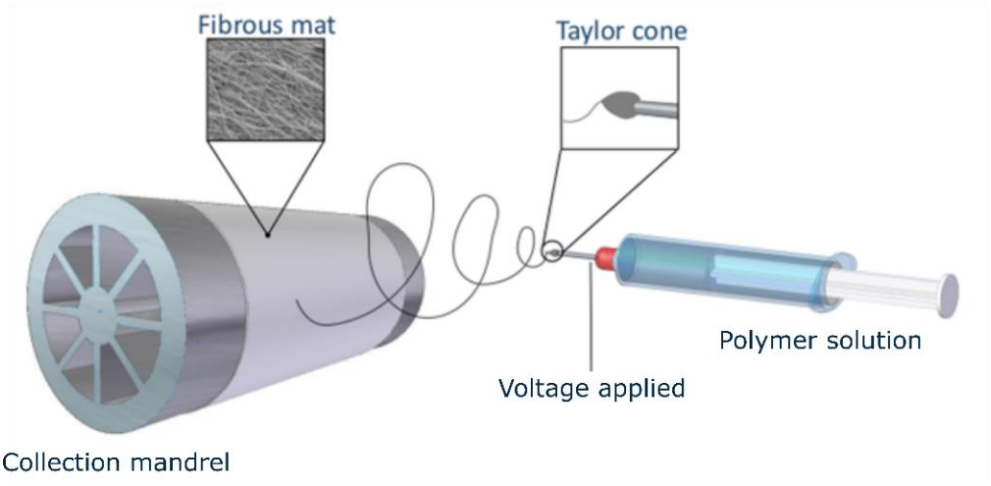

Figure 2.1; Representation of electrospinning method

All fibres were collected on a rotating mandrel covered with aluminium foil at room temperature. Polycaprolactone (PCL) (Mn=80,000 Da) was purchased from Sigma-Aldrich, UK, and polylactic acid (PLA) from Goodfellow, UK. Although no information regarding molecular weight is available PLA, Goodfellow has been used previously and shown to be comparable to the more commonly used Sigma-Aldrich PLA [229]. The solvent 1,1,1,3,3,3-hexafluoro-2-isopropanol (HFIP) was purchased from Manchester Organics, UK. Information regarding purity was requested with each batch to ensure it was comparable to Sigma-Aldrich HFIP, which is commonly used for electrospinning. All

electrospinning solutions were mixed using a roller mixer (SRT9D, Stuart, UK). The mixing speed was kept consistent at 50 RPM, and all mixing was performed at room temperature. Measurements of fibres were undertaken using the ImageJ plugin, DiameterJ [230].

2.2 Scaffold sterilisation

There are several sterilisation techniques available for scaffolds, including the use of 70% ethanol [231]. 70% ethanol has been adopted as the lab standard of sterilisation, as it rapidly kills many different types of bacteria within 10 seconds [232]. Ethanol sterilisation has been shown to be as effective as more complex methods of sterilization. Researchers have demonstrated that plasma treatment alone is an insufficient sterilization method, but that it does enhance the adhesive properties of PCL. By following plasma treatment with ethanol sterilisation, the water contact angle will be reduced due to the reaction of modified PCL groups with ethanol molecules; resulting in lower cell proliferation [233]. Subsequently, ethanol sterilisation was performed prior to plasma treatment on PCL scaffolds.

PLA is not sterilised using ethanol due to its solubility and as such isopropanol was used to sterilise PLA scaffolds. Isopropanol has been shown to be as efficient as ethanol sterilisation within the same time frame [234].

Electrospun scaffolds were cut out using a rubber mallet and a 10mm biopsy punch, placed on a cutting mat. PCL scaffolds were soaked in 70% ethanol for 30 minutes, rinsed three times in phosphate buffered saline for 15 minutes each and allowed to dry completely at room temperature. The scaffords were freeze dried overnight in a FreeZone® 4.5 freeze-drier (Labconco®) before oxygen plasma surface coating (Harrick Plasma) at 10.2W for 30 seconds. Scaffolds were removed from the plasma chamber and placed into an antibiotic/antimycotic treatment solution of Eagles Minimal Essential Media supplemented with 10% foetal bovine serum, 2mM L-glutamine and 100U/ml penicillin, 100µg/ml streptomycin, 0.25µg/ml Fungizone® (amphotericin B) Anti-Anti solution (Gibco) for 1 hour.

PLA scaffolds were soaked in 70% isopropyl alcohol for 10 minutes, rinsed three times in phosphate buffered saline for 15 minutes each and allowed to dry completely at room temperature. Scaffolds were placed into an antibiotic/antimycotic treatment solution of Dulbeccos Minimal Essential Media supplemented with 100U/ml penicillin, 100µg/ml streptomycin, 0.25µg/ml Fungizone® (amphotericin B) Anti-Anti solution (Gibco) for 1 hour.

2.3 Oxygen plasma surface coating

Oxygen plasma surface coating is performed under low pressure oxygen, argon or normal atmospheric composition (air). A high frequency voltage is applied to the coil of a chamber containing this low-pressure gas. This induces the ionization of molecules creating highly reactive free radicals. The presence of oxygen will result in the formation of oxygen containing groups on the surface of the scaffold, rendering the scaffold hydrophilic and sterile for as long as they are stored under sterile liquid conditions[233]. Hydrophobic recovery may take place if stored in air as these groups reorient from the surface into the bulk of the polymer; hence oxygen plasma surface coating was performed immediately before use.

A Harrick Plasma cleaner and PlasmaFlo gas flow mixer (PPC-FMG-2, Harrick Plasma) were used to increase the hydrophilicity of the PCL scaffolds for cell culture. Initial pressure was lowered to 250-400 mTorr before introducing O_2, pressure was stabilised at 500-550 mTorr and medium power (10.2 W) was applied for 30 seconds. Scaffolds were immediately submerged in antibiotic/antimycotic treatment solution of Eagles Minimal Essential Media supplemented with 10% foetal bovine serum, 2mM L-glutamine and 100U/ml penicillin, 100µg/ml streptomycin, 0.25µg/ml Fungizone® (amphotericin B) Anti-Anti solution (Gibco) for 1 hour; preventing hydrophobic recovery.

2.4 Decellularization

The ECM is a known repository of growth factors and bioactive cryptic peptides which possess a diverse range of biological activities such as angiogenesis[235], anti-angiogenesis[236], antimicrobial[237] and

chemotactic[208] effects, as well as the complex macro and micro structure necessary for tissue function[6,53]. Several methods of decellularization have proven successful for liver tissue, including perfusion with detergents, enzymes, freeze thaw cycles and pH extremes[30]. The method chosen for decellularization is important, with the effects of inefficient decellularization and/or the use of overly harsh methods to achieve decellularization adversely affecting the ECM. Remnant cellular components left within the ECM or disruption of the architecture and growth factor content by excessive processing have been shown to promote a proinflammatory process which adversely affects cells downstream. Equally, chemical crosslinking methods used to mask cellular epitopes and/or to increase mechanical properties in many commercially available products significantly disrupts the ligand landscape of the material and prevents the release of cryptic peptides from the matrix material [98,238–240]. Differing decellularization agents have a differing effect on the ECM. The most effective agents for decellularization of each tissue depends on the tissue's cellularity, density, vascularity, lipid content and thickness [241]. Each decellularization method will alter ECM composition and cause some degree of ultrastructure disruption. Minimization of these undesirable effects rather than complete avoidance is the objective of decellularization.

All detergents, whether ionic, non-ionic or zwitterionic solubilize cell membranes and dissociate DNA from proteins, thus removing cellular material from tissue [242]. A blinded comparison of detergents for peripheral nerve decellularization showed better preservation of ultrastructure by non-ionic and zwitterionic detergents but better cell removal by ionic detergents, however a low number of cell bodies in nerves limits the translation of the findings [243]. While Sodium Dodecyl Sulphate (SDS) is effective in removing cell nuclei while preserving tissue mechanics; it has the associated drawback of ultrastructure disruption and growth factor reduction [213,244]. Triton X-100 can effectively remove cell residues from thicker tissues where enzymatic/osmotic methods are insufficient, with the resulting ECM protein loss mediated by decreased adverse immune response *in vivo* [245]. Care should be taken to rinse the tissue clean of residual chemicals following decellularization; particularly in the case of detergents. Cytotoxicity is observed at even low concentrations of residual detergent and will inhibit

recellularization [246]. Ultimately, the decision on which decellularization detergent to use is a balancing act of desirable and undesirable outcomes. Triton X-100 was used to decellularize hybrid ECM:polymer scaffolds due to its effective removal of cell nuclei observed following titration and its recorded ability to reduce adverse immune response *in vivo*. SDS was used to decellularize human liver tissue as it is highly effective at removing all cellular material from organs.

Decellularization is deemed successful where three criteria are met; less than 50ng of remnant DNA per mg of dried tissue, each of those fragments being less than 200bp in size and no visible DAPI staining one the decellularized tissue.

Decellularization of hybrid ECM:Polymer scaffolds was performed using methods adjusted from Lu et al. (2012), under sterile conditions at room temperature (19 - 22°C) and agitation. Scaffolds were washed in phosphate buffered saline (PBS) for 15 minutes and then rinsed in 10mM tris buffered saline (TBS) for 15 minutes.

The scaffolds were submerged in a 0.1% vol/vol Triton X-100 (Sigma-Aldrich) 1.5M potassium chloride (Acros Organics) 50mM TBS for 4 hours. They were rinsed for 15 minutes in 10mM TBS before being submerged in fresh 10mM TBS overnight.

Scaffolds were given a final rinse in 10mM TBS for 15 minutes before being incubated in complete media for 15 minutes and then transferred to new 48 well plates for seeding.

Decellularization of human liver tissue was performed at room temperature (19 – 22°C) in a custom made perfusion decellularization system (Fig 2.2). Tissue was sliced into 3mm thick sections and 35mm diameter punches resected from the sections.

Tissue discs were placed in the decellularization device and secured between discs of 70μm stainless steel filtration mesh. A peristaltic pump (Watson Marlow 302 fixed speed pump) provided a flow rate of 200ml/min. Pressure was adjusted to 24mmHg using plasson pipes.

Tissue was subjected to an initial 4 hours of decellularization using 1L of 0.5% sodium dodecyl sulphate (Sigma) in MilliQ H_2O with 0.1% 100U/ml penicillin, 100µg/ml streptomycin, 0.25µg/ml Fungizone® (amphotericin B) Anti-Anti solution (Gibco). After 4 hours, the decellularization solution was exchanged for fresh solution and the system ran overnight under the same conditions. The tissue was then washed with MilliQ H_2O with 0.1% 100U/ml penicillin, 100µg/ml streptomycin, 0.25µg/ml Fungizone® (amphotericin B) Anti-Anti solution (Gibco) for 4 hours and stored in sterile containers at -20℃ until use.

Figure 2.2; Custom made decellularization device

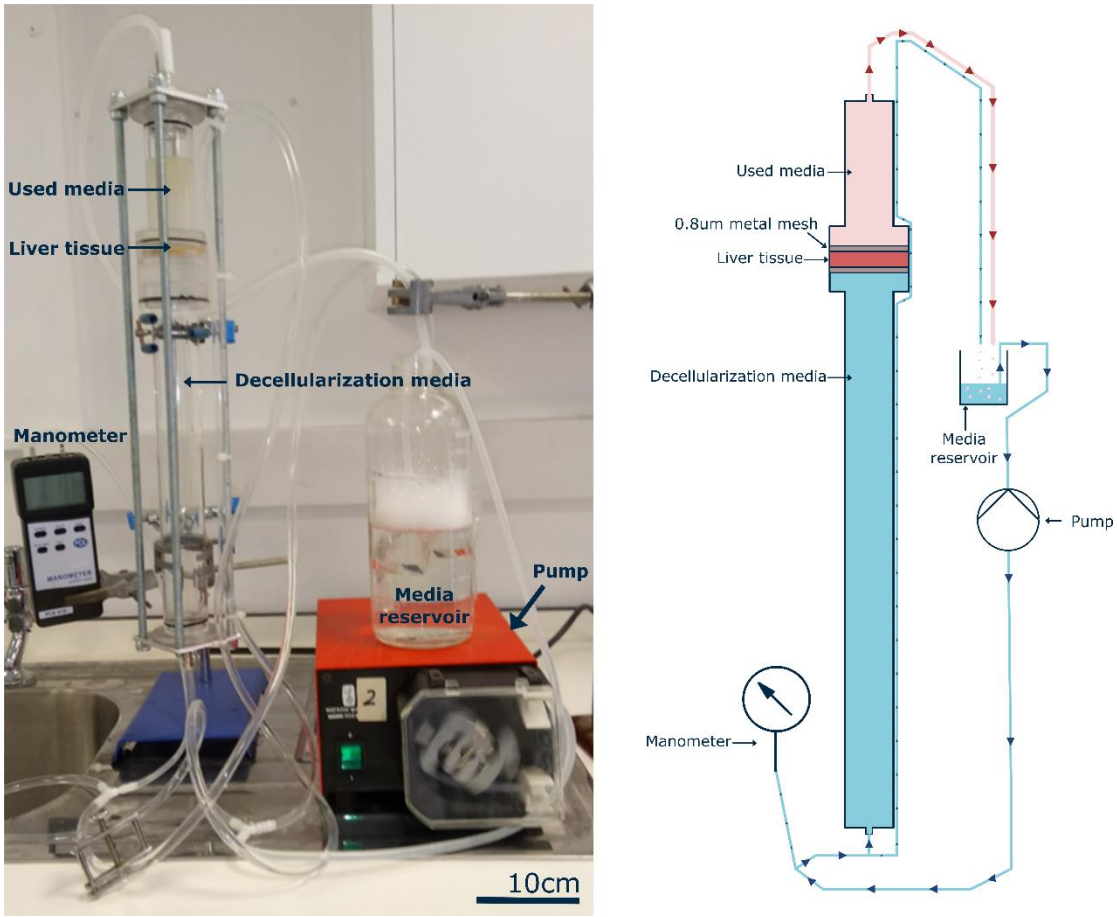

Figure 2.2; Photograph and accompanying schematic of decellularization device which maintains pressurized flow to effectively decellularize tissue biopsies. Scale bar = 10cm.

2.5 Blending proteins for electrospinning

To ensure equal distribution of the ECM proteins throughout the electrospun scaffold, decellularized ECM was suspended in 0.25M acetic acid. Acetic acid damages collagen fibrils to solubilize the ECM, with a corresponding reduction in ECM strength, but it does not affect sulfated glycosaminoglycans (sGAG)[248] and produces cryptic peptides as a by-product of solubilisation; including the Arg-Gly-Asp (RGD) peptide derived primarily from fibronectin, collagen, vitronectin, and osteopontin [241]. The RGD peptide has been used to promote cell adhesion to synthetic substrates [187,249,250].

The decellularized ECM was lyophilized in a FreeZone® 4.5 freeze-drier (Labconco®) before milling in a PM100® planetary ball mill (Retsch®).

The powdered ECM was solubilized in 0.25M acetic acid (Acros Organics) at a concentration of 25µg per ml. Bornstein and Traub Type I collagen (Sigma Type VIII) powder from human placenta, human recombinant laminin 521 (Biolamina), and human plasma fibronectin (Merck) were all solubilized and incorporated into the electrospinning solutions using the same methods. A control scaffold consisting of polymer only in the 9:1 HFIP:0.25M acetic acid was also fabricated.

2.6 Culture of HepG2s

HepG2 cells are a cell line derived from the hepatocellular carcinoma of a 15 year old Caucasian male. According to the supplier (ATCC), HepG2 cells express many of the phenotypic characteristics of hepatocytes, including α-fetoprotein, albumin, α-2 macroglobulin, α-1 antitrypsin, transferrin, α-1 antichymotrypsin, haptoglobin, ceruloplasmin, plasminogen, C4 complement, C3 activator, fibrinogen, α-1 acid glycoprotein, α-2 HS glycoprotein, β-lipoprotein and retinol binding protein. They are nontumorigenic when injected into immunosuppressed mice, however they do produce tumours in semisolid media. They also possess a rearranged chromosome 1[138].

The cells were grown in non-coated culture flasks using Dulbeccos Minimal Essential Media supplemented with 10% foetal bovine serum, 2mM L-glutamine, 100U/ml penicillin and 100µg/ml

streptomycin (all Gibco). They were split when they reached 70% confluence and replated at 1:4 ratios using 0.05% Trypsin-EDTA (Gibco).

2.7 Culture of THLE-3s

THLE-3 cells are a cell line derived from normal primary liver cells derived from the left lobe of a human liver. The cell line was immortalized via infection with SV40 large T antigen; generated by introducing a retroviral vector containing the of BglI-HpaI fragment of SV40 T antigen into the amphotropic packaging cell line PA317. According to the supplier (ATCC), THLE-3 cells express the phenotypic characteristics of normal adult liver epithelial cells. They are nontumorigenic when injected into athymic nude mice, have near-diploid karyotypes, and do not express alpha-fetoprotein. THLE-3 cells metabolize benzo (a) pyrene, N-nitrosodimethylamine, and aflatoxin B1 to their ultimate carcinogenic metabolites that adduct DNA, which indicates that they possess functional cytochrome P450 pathways. Other enzymes involved in metabolism of chemical carcinogens, such as epoxide hydrolase, NADPH cytochrome P450 reductase, superoxide dismutase, catalase, glutathione S-transferases, and glutathione peroxidase are also retained[144,251].

The cells were grown in culture flasks coated with 100µg/cm^2 gelatin (Sigma) using Dulbeccos Minimal Essential Media supplemented with 10% foetal bovine serum, 2mM L-glutamine, 100U/ml penicillin and 100µg/ml streptomycin (all Gibco), 5ng/ml human epithelial growth factor (Corning)., 70ng/ml human insulin (Sigma) 70ng/ml phosphoethanolamine (Sigma) and 70ng/ml hydrocortisone (Sigma). They were split when they reached 70% confluence and replated at 1:3 ratios using 0.05% Trypsin-EDTA (Gibco).

2.8 Culture of 5637 bladder epithelials

The 5637 bladder epithelial cell line is derived from the grade II bladder carcinoma of a 68 year old Caucasian male. The cells are tumourogenic, and produce tumours in nude mice within 21 days of

subcutaneous inoculation with 1 x 10^7 cells in 100% of cases (5/5). One, or occasionally two, Y chromosomes is present in each cell[252].

The cells are grown in non-coated culture flasks using Dulbeccos Minimal Essential Media supplemented with 10% foetal bovine serum, 2mM L-glutamine, 100U/ml penicillin and 100µg/ml streptomycin (all Gibco). They were split when they reached 70% confluence and replated at 1:6 ratios using 0.05% Trypsin-EDTA (Gibco).

2.9 Transfections

Transfection is the process of artificially introducing nucleic acids (either RNA or DNA) into eukaryotic cells, by methods other than viral infection. Transfection is most commonly performed to express a protein of interest in cultured cells (or an animal model) through the use of a plasmid vector or mRNA. Most commonly, researchers use physical methods such as electroporation; using electrical current to compromise the cell membrane and allow nucleic acids to enter the cell or chemical methods like Lipofectamine (Invitrogen). Lipofectamine is a commercially available cationic liposome which provides high transfection efficiency and high levels of transgene expression in a range of mammalian cell types in vitro using a simple protocol[253]. Nucleic acids carry a net negative charge, and for a successful transfection they must cross the similarly negatively charged cell membrane. Lipofectamine's positive charge allows it to complex with the negatively charged nucleic acids which combats the electrostatic repulsion of the cell membrane and allows the complex to be taken up by the cell. Or the cell to express the introduced nucleic acids, the DNA/RNA must reach the nucleus of the cell and become accessible to the transcriptional machinery. In actively dividing cells, transfected nucleic acids are trapped in the nucleus following the reassembly of the nuclear envelope at the end of mitosis. Lipofectamine however, also successfully transfects non-dividing cells such as neurons[254] and primary hepatocytes[253,255] suggesting that the cationic lipofectamine:nucleic acid complex also overcomes the electrostatic repulsion of the intact nuclear envelope.

To perform the transfection, plasmids were purchased from the DNASU Plasmid Repository at Arizona State University. The human fibronectin gene (FN1) was placed into a retroviral expression vector, PJ1520, containing a selective gene for puromycin resistance in mammalian cells. The insert sequence was verified by sequence analysis and restriction enzyme digest by DNASU. The vector was obtained in DH5-alpha T1 phage resistance Escheria coli glycerol stock. The E. coli was cultured under selective conditions; 100µg/ml ampicillin, 34µg/ml chloramphenicol and 7%wt/vol sucrose in LB media. They were purified using the Zyppy™ plasmid miniprep kit (Cambridge Bioscience) following manufacturer's instructions.

Transfections were performed using Invitrogen Lipofectamine 3000®. Following titration experiments, a concentration of 1µg plasmid DNA and 0.75µL lipofectamine reagent per scaffold was chosen. The initial layer of 5637 epithelials was cultured on the scaffolds under standard conditions for 7 days. Transfection was performed on the scaffolds on the 7th day, under serum free conditions. Lipofectamine 3000® was diluted 1:1 with Opti-MEM® reduced serum medium and incubated with the plasmid DNA for 5 minutes at room temperature. The lipofectamine:plasmid complex was then incubated with the scaffold:cell constructs for 30 minutes at 37°C, then an additional 500µL of complete media without antibiotics was added to the constructs and incubated for 2 days.

Scaffold-cell constructs were then placed into selective media containing 150µg/ml puromycin to select for successfully transfected cells.

2.10 Primary cell extraction and culture

Primary human hepatocytes are considered the gold standard cell in hepatology. No other cell accurately recapitulates the phenotypic gene expression and metabolic abilities of primary hepatocytes. Successful and consistent isolation of primary human hepatocytes remains challenging for researchers, however several groups have reported moderate success[133,161,167,256]. Steatotic liver has proven particularly challenging to extract healthy hepatocytes from[59,257]; of particular note with

regards to this work as all livers received were markedly steatotic and from adults weighing up to 160kg.

Percoll® density gradients are used following tissue digestion to remove cell debris, non-parenchymal cells and released proteases from a hepatocyte suspension, and increases the quality and half-life of an isolated hepatocyte suspension[258]. Percoll® is a low-viscosity, non-toxic media composed of colloidal silica coated with polyvinylpyrrolidone (PVP), which gives low osmolality and low viscosity. It is used for the separation of cells, subcellular particles and larger viruses (down to ~ 70S) under gentle conditions which preserve viability and morphological integrity.

Primary human hepatocytes were obtained from tissue donated from organ donors. Tissue was collected as promptly as possible following brain/circulatory death of the donor, however due to obvious logistical reasons collection times and hepatocyte health varied between donors. A total of 6 human livers were collected throughout the course of this body of work; one donor was used for the data presented in Chapter 4, and one donor was used for the data presented in Chapter 6.

Upon receipt of the liver 8-10 small (2cm^2) chunks of liver tissue were incubated in a 10cm^2 petri dish with digest media; Blank DMEM (Gibco), 0.05% Trypsin-EDTA (Gibco), 0.625mg/ml Collagenase I (Sigma) and minced finely with scalpels. The digest was incubated at 37°C for 30 minutes and filtered through a 70µm cell strainer (Corning). The filtrate was centrifuged at 135g for 1 minute at room temperature, then layered onto a gradient of 5ml 1.06g/ml, 5ml 1.08g/ml and 3ml 1.12g/ml Percoll®. The sample was then centrifuged at 750g for 20 minutes at room temperature, and the phase between 1.06g/ml and 1.08g/ml collected. The hepatocytes were cleaned with Williams E media at 135g for 1 minute at room

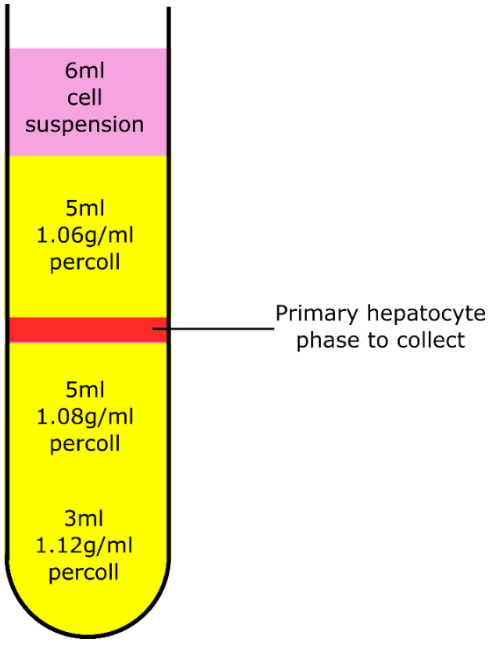

Figure 2.3; Percoll separation of hepatocytes

temperature and plated onto gelatin coated tissue culture plastic (100µg/cm^2 gelatin (Sigma)) or scaffolds as needed. Cell viability was assessed using the Trypan Blue exclusion method[258] prior to plating and was found to be highly variable between donors. The hepatocytes used in chapter 4 exhibited a viability of 72% immediately upon extraction.

The primary hepatocytes were cultured in Williams E media with no phenol red (Gibco) containing 10% Foetal Bovine Serum, 2mM glutamine , 1% Non-essential amino acids , 1% Sodium pyruvate (all Gibco), 2µg/ml Hydrocortisone (Sigma), 0.124 IU/ml Human insulin (Sigma) and 1µg/ml Human epidermal growth factor (Corning). They do not expand or split and were fed according to observations of the culture.

2.11 Live/Dead® Viability/Cytotoxicity assay

To determine cellular viability, cell/scaffold constructs were incubated with 10µm calcein and 2µm ethidium homodimer-1 (Ethd-1) as part of the two colour live/dead assay (Molecular Probes). Calcein is actively converted to calcein-AM in living cells, which then appear green when excited during fluorescence microscopy. Ethd-1 only accumulates in dead cells, which subsequently appear red. The method allows differentiation between dead and viable cells[259].

The scaffolds were rinsed three times in CaCl2/MgCl2 free PBS to remove excess media, and incubated in the two-colour calcein/ethd-1 stain for 30 minutes, then rinsed three times in CaCl2/MgCl2 free PBS and placed onto a standard microscope slide with a 25mm glass coverslip (VWR). All images were captured using a Zeiss Axio Imager fluorescent microscope (COIL, University of Edinburgh) and post processed using ImageJ.

2.12 CellTiter-Blue

CellTiter-Blue® assay is both colorimetric and fluorometric and utilises the dye resazurin to measure metabolic activity. Viable cells reduce resazurin to resorufin; a highly fluorescent molecule. According to the manufacturer (Promega) only viable cells metabolise resazurin, and as such the change in fluorescence is directly proportional to viable cell number[260]. The detection of dye is linear up until

the point of saturation so an estimation of cell number can be made from a tested known number of cells. However, as the result can be saturated and due to known variations in metabolic abilities of hepatocytes[138,159] results were reported throughout as fluorescence, as opposed to cell number.

Cell metabolism was assessed using the CellTiter-Blue® assay according to manufacturer's instructions (Promega, UK). Scaffolds were washed 3 times in PBS and a 1:5 ratio of CellTiter-Blue® assay and appropriate cell culture media was vortexed together. This was added to cell cultures and incubated for 3 hours. On completion 3 x 100 µl of the CellTiter-Blue® solution was added to a black microplate for each sample Importantly, cell/scaffolds constructs were moved into fresh 48 well plates to prevent reading activity from tissue culture plastic bound cells. Measurements were read in a Modulus™ II microplate reader at an excitation wavelength of 525 nm and emission wavelength of 580-640 nm and reported as fluorescence.

2.13 MTT assay

The MTT (3-(4,5-dimethylthiazol-2-yl)-2,5-diphenyltetrazolium bromide) tetrazolium reduction assay (Sigma) is used to indicate cell viability within a culture. MTT is reduced to purple coloured formazan by viable cells with an active metabolism, a product with an absorbance maximum near 570 nm. Dead cells and non-metabolically active cells cannot convert MTT into formazan, thus colour formation serves as a useful and convenient marker of only the viable cells. The exact cellular mechanism of MTT reduction into formazan is not well understood, but likely involves reaction with nicotinamide adenine dinucleotide (NAD) + hydrogen (H) (NADH) or similar reducing molecules that transfer electrons to MTT[261].

Samples were incubated with MTT for 2 hours. Incubation time was limited because of the cytotoxic effect of reagents which utilize NADH from the cell to generate a signal. Formazan accumulates as an insoluble precipitate inside cells as well as being deposited near the cell surface and in the culture medium. Thus, formazan was solubilized prior to recording absorbance readings using acidic

isopropanol (Sigma) and measurements were read in a Modulus™ II microplate reader at a wavelength of 570 nm and reported as absorbance.

2.14 Picogreen DNA quantitation

The Quant-IT™ Picogreen® dsDNA assay utilises a fluorescent probe which binds to DNA, increasing the intensity of fluorescence by over 1000-fold. This fluorescent can then be utilised as a molecule for calculation of the amount of DNA present in a sample, when comparing to a DNA standard of known concentration[262].

Cell seeded scaffolds were digested in a solution of CaCl2 and MgCl2 free PBS (Sigma), containing 2.5 U/ml papain extract (Sigma) 5 mM cysteine-HCl (Sigma) and 5 mM EDTA (Sigma) and incubated overnight at 60°C. Picogreen solution was added to the digests and fluorescent intensity measurements read in a Modulus™ II microplate reader at an excitation wavelength of 480 nm and emission wavelength of 510-570 nm. A standard λ dsDNA curve of graded known concentrations was used to calibrate fluorescence intensity vs dsDNA concentration.

2.15 Albumin assay

Quantitation of albumin levels produced by hepatocyte cultures was undertaken using the commercially available bromocresol green (BCG) albumin quantitation kit (Sigma). The addition of samples containing albumin protein to a solution of BCG in a 0.075 M succinate buffer at a pH of 4.2 produces an increase in absorbance at 628 nm. The absorbance-concentration relationship is linear for samples containing up to 6 g/dL of albumin. Bilirubin, moderate lipemia, and salicylate presence in the samples do not interfere with the analysis. The use of an anionic surfactant (sodium dodecyl sulphate) reduces the absorbance of the blank, prevents turbidity and improves linearity of the absorbance results[263].

For each experiment, albumin production was established 24hr timescales at various time points, and results read at an absorbance of 620 nm in a Modulus™ II microplate reader. Results were quantified by comparison of absorbance with a calibration curve of known albumin concentration.

2.16 Immunohistochemistry and cell imaging

Imaging of cell/scaffold constructs was performed using fluorescently conjugated molecules. Phalloidin is used to image the cytoplasm of cells via its interaction with actin filaments. Phalloidin binds directly to actin subunits but does not bind to monomeric G-actin[264], and was purchased conjugated with alexafluor-514 (Sigma) to allow for visualisation. 4',6-diamidino-2-phenylindole (DAPI) binds to the A-T rich region of DNA increasing the DNA's fluorescence intensity and allowing for visualisation[265]. A fluorescently conjugated E-Cadherin antibody (Abcam) was used to visualise cell membranes. E-Cadherin is a calcium-dependent cell-cell adhesion molecule with pivotal roles in epithelial cell behaviour, tissue formation, and suppression of cancer and is found in the cell membrane of healthy hepatocytes with appropriate phenotypes[266]. Fluorescently conjugated antibodies for Collagen I (Stratech), Laminin (Stratech) and Fibronectin (Sigma) were used to visualise the presence of these proteins in both ECM and in blended scaffolds, due to their significant roles in the human hepatic ECM[53].

Scaffolds seeded with cells, decellularized hybrid scaffolds and blended scaffolds were washed 3 times in TBS/PBS and fixed using 3.7% (v/v) formalin solution in TBS/PBS overnight, then washed again 3 times in TBS/PBS. A 0.2% (v/v) TritonX-100 solution in TBS/PBS was used for permeabilization for 5 minutes before washing 3 times in TBS/PBS.

Cells lines were stained with primary antibodies overnight using 1µl per 1 ml PBS with 0.1 % bovine serum albumin at 4℃ and then washed 3 times in TBS/PBS. Nucleic acids were visualised using a 300 nM DAPI solution in PBS for 20 minutes, then washed 3 times in TBS/PBS. Scaffolds were affixed to glass microscope slides (VWR) with mowiol mounting medium (Sigma) for imaging performed using a

Zeiss Axio Imager fluorescent microscope (COIL, University of Edinburgh) and post processed using ImageJ.

The images in Chapter 4 were obtained using a custom multi-photon microscope. This system consists of a mode-locked ND:YVO4 laser source (PicoTrain, Spectra Physics) to generate both a Stokes pulse (6 ps, 1064 nm) and drive an optical parametric oscillator (OPO) (Levante Emerald, APE). The OPO provides a tuneable excitation pulse across 700-1000 nm allowing coherent anti- Stokes Raman scattering (CARS), second harmonic generation (SHG) and two-photon excitation fluorescence (TPEF) microscopy. The two pulse trains are coupled into an inverted microscope (Nikon BV 'C1', Amsterdam, Netherlands) and focused onto the sample with a 25 times water-immersion objective lens with a numerical aperture of 1.05 (XLPlan N, Olympus). Images from the CARS and TPEF signals were recorded on two photomultiplier tubes (R3896, Hamamatsu). The lateral and depth resolution of this objective was measured to be 0.25 and 1.1 µm, , respectively. The CARS signal was generated from the asymmetrical CH2 stretch of the scaffold at 812.5 nm (2911 cm-1 wavenumbers). The same OPO beam was used to excite the broad two-photon spectrum in the Phalloidin and DAPI. The signals were separated with two dichroic filter cubes at 649 nm, 570 nm, along with band pass filters with transmission peaks at 660 nm, 585 nm, 545 nm for the CARS, Phalloidin-iFluor™ and DAPI, respectively.

All images are representative of scaffold conditions.

2.17 Scanning electron microscopy

Scanning electron microscopy (SEM) utilises a focused electron beam to scan the surface of microscopy samples. The signals generated reveal information regarding the topography of the material and generate an image for subsequent analysis.

Glutaraldehyde is used as a fixative for SEM because it causes the rapid penetration of small HCHO molecules, which initiate the structural stabilization and thorough crosslinking of the tissue;

maintaining the ultrastructure of biological samples for SEM[267]. A secondary fixation with osmium tetroxide is undertaken to reduce charging of samples during imaging [268]. Biological samples were fixed in 2.5% v/v glutaraldehyde (Fisher Scientific) in 0.1M phosphate buffer (PB) (pH 7.4) at 4℃ overnight. They were then rinsed three times in 0.1M PB before being post-fixed in 1% v/v osmium tetroxide (Electron Microscopy Supplies) buffered with 0.1M PB. Samples were again rinsed three times in 0.1M PB and dehydrated through an ethanol gradient (30-100%) and were dried by placing them in hexamethyldisilazane (HMDS, Sigma) which was allowed to evaporate off at room temperature overnight. Samples were mounted the samples onto SEM chucks using double sided carbon tape.

A Hitachi S4700 fuelled emission scanning electron microscope (SEM) (Hitachi) with a 5kV accelerating voltage and a working distance of 12 mm was used to image scaffolds. Samples were coated using a Polaron splutter coater using gold-palladium (60:40).

2.18 Mechanical testing

Mechanical testing is used in this study to characterise polymer and protein:polymer scaffolds and elucidate any mechanical influences cells may be exposed to.

Young's modulus is a ratio of the force applied to a material against the change in its length. It is derived from the stress (σ) and strain (ε) measurements taken during the mechanical testing. Stress is defined as force (F) per unit area (A): $\sigma = \frac{F}{A}$ and strain is the change in length (ΔL) divided by the original sample length (L): $\varepsilon = \frac{\Delta L}{L}$. Thus, Young's modulus (E) is defined as $E = \frac{\sigma}{\varepsilon}$. Young's modulus is calculated before the elastic limit after which plastic deformation takes place; in a linear material Hooke's law applies assuming a linear and elastic response.

Non-linear materials have more complex properties and can be analysed using the tangential modulus at different values of strain. Dynamic (complex) modulus (E*) is used to calculate the properties of non-linear or viscoelastic materials and requires dynamic mechanical testing with an oscillatory force.

This is represented by a storage (E') and loss (E'') modulus where stress and strain possess a phase difference and as such the stress strain graph is non-linear $E^* = E' + iE''$.

Ultimate tensile strength is the maximum stress that can be applied to a material before failure, although for polymers this is typically long after the elastic limit.

Tension testing characterizes Young's modulus and reveal elasticity of constructs. A uniaxial tensile load is applied to a specimen with known, uniform geometry, and the extension of the gage is recorded as a function of the applied load. Given the dimensions of the specimen, it is straightforward to obtain a stress-strain graph, and to extract *E*, σγ and σf[269]. The most common error in tensile testing is introduced when handling and mounting the samples. This is combatted my taking multiple measurements from multiple samples to reduce sample error, and by using a c-shaped mount to stabilise samples with a uniform support structure. Tensile testing was undertaken using Instron 3367 dual column universal testing system with Bluehill 3 software. The system was fitted with Instron biopulse submersible pneumatic side action grips and a 50N load cell. A gauge length of 20mm and an extension rate of 20mm/min were used for all tensile tests. Analyses was conducted using the incremental modulus method as previously described [24,26]. Samples were fixed to 'C' shaped card templates to allow consistent set up during tensile testing, and sizes were measured using digital callipers for accuracy. Samples were tested until failure.

Nanoindentation was also used to characterise hybrid scaffolds. This is a powerful tool for testing small samples such as these scaffolds. A 100µm diameter flat diamond tip is projected into the sample, and the depth of penetration (δ) is measured as a function of the applied load (P)[270]. By estimating the area of contact under the indenter from the depth of indentation, Young's modulus is calculated[271,272]. Nanoindentation is limited by several factors including accidental indentation of 'support' structures, particularly when testing small, thin, non-homogenous samples. This is combatted again by testing multiple samples and by testing in a 12 x 12 array of nano-indentation points to represent the non-homogenous samples more accurately.

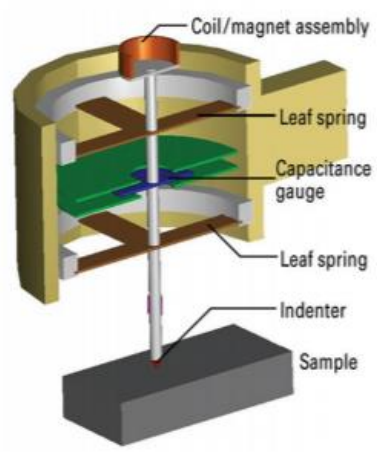

Figure 2.4; Schematic diagram of the actuating and sensing mechanisms of the Nano Indenter G200.

Nanoindentation experiments were undertaken to establish the dynamic properties of scaffolds and decellularized ECM/scaffold constructs using the Keysight/Agilent G200 nano indenter testing system. During the nanoindentation test, indentation load and displacement curves are recorded as the indenter tip is pressed into the test material's surface with a prescribed loading and unloading profile, allowing the determination of local mechanical properties. The displacement resolution of the DCM II is 0.2 picometer and produces noise levels < 1 angstrom, and as such is considered sensitive enough to measure changes in biological sample's mechanical profiles. Scaffolds and constructs were subject to indentation by a DCM II actuator flat-ended cylindrical punch (D = 100µm) using a max load of 1g-f. All nanoindentation experiments were carried out on fresh, hydrated, unfixed samples which were adhered to the chuck using double sided tape. A total of 36 indentations were carried out on each sample, 50nm apart. Indent sites were selected using the high precision X-Y stage within the testing system (Agilent). Poisson's ratio for biological materials and cells is assumed to be 0.5, as proteins of the ECM such as fibronectin and collagen act as ideal elastomers and thus a Poisson's ratio of 0.5 was used [273–275]. Allowable drift rate was 0.1nm/s. A NanoSuite (Keysight Technologies) test method "G-Series DCM CSM Flat Punch Complex Modulus" was used for all testing [271,272].

Compression testing was undertaken to establish the dynamic properties of the hybrid polymer:ECM scaffolds using the Instron 3367 dual column universal testing system with Bluehill 3 software. Each sample was compressed to 10% strain at a crosshead speed of 0.5% strain min−1. Incremental compressive moduli were calculated from 0%–2.5%, 2.5%–5%, 5%–7.5% and 7.5%–10%, adapted from previous methodology[24,26].

2.19 rtQ-PCR

The reverse transcription real-time polymerase chain reaction (RT-qPCR) is used to quantify the levels of RNA expressed by a cell culture. The RNA is transcribed into complementary DNA (cDNA) using the reverse transcriptase reaction. This cDNA is then used as a template for real-time PCR (qPCR), producing DNA.

qPCR requires 3 steps: denaturation, annealing, and elongation. These steps occur repeatedly in cycles; doubling the amount of DNA after each cycle. As each cycle takes place a fluorescent dye, SybrGreen, binds to newly formed DNA. The cycle in which fluorescence is first detected is designated the threshold cycle (Ct), and is used to quantify the amount of RNA present in the original sample.

Quantification was performed using the $2^{-\Delta\Delta Ct}$ method [276]. The $2^{-\Delta\Delta Ct}$ method compares the Ct values of a gene of interest in both a reference sample (TG_R) and a subject sample (TG_S), with a housekeeping reference gene used as a normaliser (HK_R, HK_S). Equations used are as follows;

Difference in Ct value between the target gene and the housekeeping gene.

$$\Delta Ct = TG - HK$$

Difference between ΔCt of the subject sample and ΔCt of the reference sample.

$$\Delta\Delta Ct = \Delta Ct_S - \Delta Ct_R$$

Relative expression of the gene of interest compared to a reference sample. The reference sample is taken to be 1.

$$Relative\ expression = 2^{-\Delta\Delta Ct}$$

Standard deviation of samples in RT-qPCR, accounting for error in reference control.

$$SD = \sqrt{HK\frac{R}{2} + TG\frac{R}{2} + HK\frac{S}{2} + TG\frac{S}{2}}$$

To further clarify, in the $2^{-\Delta\Delta Ct}$ method identical expression would be 1, any number between 0 - 1 represents a decrease in expression and any number larger than 1 represents an increase in expression. By representing results graphically on log axis equal representation is given to both up and down regulation of genes. Errors in data can arise from TG_R, TG_s, HK_R and HK_S, thus it is therefore important to calculate the standard deviation of each of these means and propagate errors correctly. If standard deviation (SD) is calculated following data manipulation, then the propagation of errors throughout the manipulation is not accounted for. SD therefore must be propagated using the $2^{-\Delta\Delta Ct}$ equation to represent graphically, as either standard error (SE) or confidence interval (CI). This method ensures error in each measured data set is properly accounted for and represented accurately [276].

Standard error of the $2^{-\Delta\Delta Ct}$ method

$$Upper = 2^{-(\Delta\Delta Ct - CI)}$$

$$Lower = 2^{-(\Delta\Delta Ct + CI)}$$

RT-qPCR was performed in a two-step process. Cells and scaffolds were homogenised using Trizol® (Life Technologies) and subjected to phase separation [277] using chloroform (Sigma Aldrich). RNA was isolated by harvesting the clear supernatant and purified using the commercially available silica membrane/chaotropic agent based [278] RNeasy kit (Qiagen) as per the manufacturer's instructions. The cDNA was synthesised from a reverse transcription reaction using an ImProm-II kit (Promega), according to the manufacturer's instructions, and a PCR machine (Applied Biosystems Proflex PCR system) using Cycle 1.

<u>Cycle 1</u>

Anneal – 5 minutes @ 25°C

Extend – 60 minutes @ 42°C

Inactivation – 15 minutes @ 70°C

cDNA was used in a qPCR reaction with the SensiFAST™ SYBR®Hi-ROX kit (Bioline) according to the manufacturer's protocol using Cycle 2.

Cycle 2

Initial denaturation – 2 minutes @ 95°C

40 cycles of;

Denaturation – 15 seconds @ 95°C

Annealing/Extension – 1 minute @ 60°C (or 5°C below lowest primer T_M)

Gene expression levels were normalised using expression of the housekeeping gene Glyceraldehyde 3-phosphate dehydrogenase (GAPDH) and presented as a relative expression. The $2^{-\Delta\Delta Ct}$ method was used to calculate relative RNA levels of Albumin (Alb), Cytochrome P450 Family 1 Subfamily A Polypeptide 1 (Cyp1A1), Cytochrome P450 Family 1 Subfamily A Polypeptide 2 (Cyp1A2), Cytochrome P450 Family 2 Subfamily B Polypeptide 6 (Cyp2B6), Cytochrome P450 Family 3 Subfamily A Polypeptide 4 (Cyp3A4), Collagen Type I alpha 1 (Col1A1), Collagen Type 4 alpha 1 (Col4A1) and Fibronectin Type 1 (FN1) were investigated. Forward and reverse primers (Sigma) were designed using the free to access NCBI PrimerBLAST [279] and are detailed in Table 7. Errors in graphs were calculated from a magnitude of the standard deviations of both the housekeeping gene and the target gene of both the sample and the control to ensure errors were carried forward. Data was presented on a logarithmic scale to give equal relevance in terms of graphical representation to both increases and decreases in expression. As ΔΔCt was manipulated by a log factor, the values represented by the error bar represented also underwent the same manipulation, thus maintaining their relevance to the manipulated dataset.

Table 2.1; Primer Sequences

Albumin (Alb)	For - CCTGTTGCCAAAGCTCGATG Rev - GAAATCTCTGGCTCAGGCGA
Cytochrome P450 Family 1 Subfamily A Polypeptide 1 (Cyp1A1)	For - AATTTCGGGGAGGTGGTTGG Rev - GATGTGGCCCTTCTCAAAGGT

Cytochrome P450 Family 1 Subfamily A Polypeptide 2 (Cyp1A2)	For - CTTCGCTACCTGCCTAACCC Rev - GTCCCGGACACTGTTCTTGT
Cytochrome P450 Family 2 Subfamily B Polypeptide 6 (Cyp2B6)	For - TGCCCCTTTTGGGAAACCTT Rev - ATGAGGGCCCCCTTGGATTT
Cytochrome P450 Family 3 Subfamily A Polypeptide 4 (Cyp3A4)	For- TTTTTGGATCCATTCTTTCTCTCAA Rev- TCCACTCGGTGCTTTTGTGT
Collagen Type I alpha 1 (Col1A1)	For - GGACACAGAGGTTTCAGTGGT Rev - GCACCATCATTTCCACGAGC
Collagen Type 4 alpha 1 (Col4A1)	For - GACCCCCGGGAGAAATAGGT Rev - TTTGAAAAAGCAATGGCACTCC
Fibronectin Type 1 (FN1)	For - GAACAAACACTAATGTTAATTGCCC Rev - TCTTGGCAGAGAGACATGCTT
Glyceraldehyde-3-Phosphate Dehydrogenase (GAPDH)	For – GTCTCCTCTGACTTCAACAG Rev - GTTGTCATACCAGGAAATGAG

2.20 Statistical analysis

All statistical analyses were performed in Origin and Minitab software. Where n is used n = number of biological replicates. All experiments were performed with a minimum of 3 biological replicates to allow for statistical analysis. Multiple comparisons tests have been used following the Ryan Joiner test for normality and Bartlett's test for the homogeneity of variances; a test which tells us if populations have similar variances. ANOVA and some Design of Experiments (DOE) tests rely upon underlying data possessing similar variance. Selecting the correct multiple comparison/post hoc test avoids errors caused by α inflation induced by performing multiple t-tests upon groups with unequal variance.

The Tukey post hoc test tests each experimental group against each control group while maintaining the experiment wise error rate (α_E) at the pre-established α level. The Tukey test relies upon equal population variance, and so is used where Bartlett's test result is not significantly different i.e. the null hypothesis of population variances being equal is not rejected.

The Games-Howell test does not assume equal variances and sample sizes. The test was designed based on Welch's degrees of freedom correction and uses Tukey's studentised range distribution. The Games-Howell test is performed on the ranked variables similar to other nonparametric tests, and is used where Bartlett's test result is significantly different i.e. the null hypothesis of population variances being equal is rejected.

Fisher's LSD test is the least robust of the post hoc tests, and performs pairwise comparisons between <3 groups, as unlike Tukey and Games Howell, the Fisher's LSD test does not while maintaining the experiment wise error rate (α_E) at the pre-established α level for over 3 groups of comparisons[280–282].

2.21 Ethical approval for donor human liver work

All human tissue used in this study was provided by NHS Organ Donation and Transplant and NHS Blood and Transplant. No organs/tissues were procured from prisoners. Ethical approval was granted for the project from the North of Scotland Research Ethics Committee, ref 16/NS/0083. Informed consent for organ donation for research purposes was obtained in accordance with the Helsinki Declaration. A total of 6 donor livers were obtained over the duration of this project and tissue from one donor was used for the study detailed in Chapter 4, and tissue from one donor was used for the study detailed in Chapter 6.

Chapter 3

Drug induced hybrid protein:polycaprolactone scaffolds for liver tissue engineering

3.1 Introduction

The extracellular matrix (ECM) is a non-cellular component of all tissues which provides essential support for the cells of the tissue or organ. Each tissue type has its own specific ECM 'recipe', composed of water, proteins and polysaccharides, driven by a dialogue between various cellular components and the microenvironment within the tissue[283,284]. Additionally, the ECM is a dynamic structure, subject to constant modification in response to environmental influences such as 3D cell culture[73] and which varies massively between tissues[285]. ³⁰

Multiple methods have been employed in an attempt to provide hepatocytes with an optimal environment; in particular decellularization of whole livers and novel 3D tissue engineered scaffolds. Decellularization provides a whole organ ECM based bioscaffold with the potential to maintain the 3D site-specific architecture and highly conserved sinusoidal ECM gradient required for hepatocyte function upon their repopulation of the organ[30]. Several studies have repopulated decellularized organs with hepatocytes and endothelial cells which subsequently survive and exhibit some level of function[31–35,286]. However, this approach still requires precious donor organs, whether human or animal and with all of their immunogenic potential and methods used are not without their drawbacks[287,288]. Detergents such as sodium dodecyl sulphate (SDS), Triton-X100 and sodium deoxycholate (SDOC) are employed to strip the ECM of cells. These detergents disrupt native tissue ultrastructure, decrease glycosaminoglycan (GAG) content and reduce collagen integrity[38,39] as well as disrupt lipid-lipid, lipid-protein and protein-protein interactions[40]. Scaffold manufacture employs engineering technologies to create a synthetically derived structure which mimics the characteristics of the native ECM. There are several different methods of creating a scaffold, and they can be made from a myriad of substances; both natural and synthetic[29]. Hydrogels have been of particular interest to liver tissue engineers, gels biofunctionalized with collagen I enhance P450 (Cyp450) activity, cell adhesion markers and innate hepatocyte fibronectin production[41]. Gels biofunctionalized with galactose increase albumin production and promoted the proliferation of hepatocytes[42]. Viability and

hepatic functions of primary hepatocytes are improved by culturing them in hydrogels made with liver extracellular matrix[43], and when encapsulated in collagen-alginate composite hydrogels[44]. PEG hydrogels have been shown to augment cell-cell interactions of bipotential mouse embryonic liver (BMEL) cells, subsequently improving their survival and function[45], however incorporating ECM components into scaffolds at the manufacturing stage has proved challenging, with the harsh solvents require to solubilize major components of ECM alter their microstructure and functionality[46,47]. Ongoing research is showing great promise, however to date no scaffold has been created which allows hepatocytes to function as well as in vivo[36,37].

Both ECM components and scaffolds have shown great promise in tissue engineering [12,26,48]. With these considerations in mind, decellularization and scaffold engineering were combined to create a novel environment in which hepatocytes thrive (Fig 3.1). Two different histone deacetylase inhibitors (iHDACs) were used to manipulate the cellular environment and alter the ECM production; sodium butyrate (NaBut) is widely used in industry to increase yield recombinant protein yields in mammalian cells. Valproic acid (ValA) is an FDA approved anti-convulsant which also functions as an iHDAC to increase recombinant protein yields [289]. Histone deacetylase inhibitors (iHDACs) can influence gene expression via their role in deacetylation; the process by which DNA renders itself less transcriptionally active. Inhibiting this process in cells results in hyperacetylation of histones and subsequently and increase in transcriptional activity [290]. By manipulating ECM production using pharmaceuticals and exploiting polymer characteristics a novel hybrid polymer-ECM platform for liver tissue engineering was produced. To validate the platform cells representative of the liver (HepG2s) were used.

Figure 3.1 Method schematic

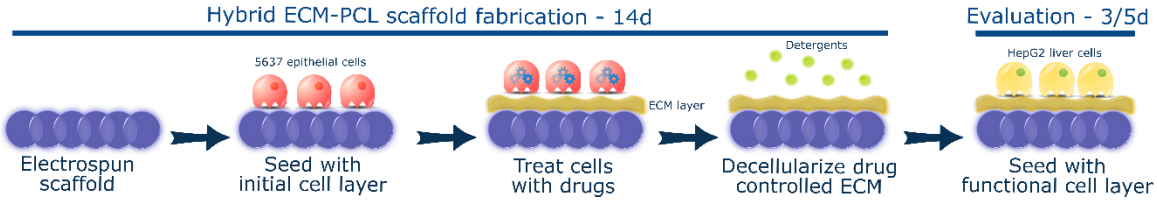

3.2 Methods

All methods were performed according to protocols laid out in Chapter 2. Specific details are described forthwith.

3.2.1 Electrospinning

A 12% wt/vol solution of poly-capro-lactone (Sigma-Aldrich) and hexafluoroisopropanol (Manchester Organics) was used to electrospin scaffolds according to the following parameters;

Table 3.1; Electrospinning parameters

Volume per hour	Total volume	Mandrel:needle distance	Positive charge	Negative charge	Mandrel rotation	Needle movement
1.8ml	8ml	21 cm	12kV	-2kV	250rpm	100mm/s

3.2.2 Oxygen plasma surface treatment

10mm discs of scaffold were subjected to oxygen plasma surface treatment (Harrick Plasma) at 10.2W for 30 seconds. Scaffolds were removed from the plasma chamber and placed into antibiotic/antimycotic treatment solution for 1 hour prior to initial seeding.

3.2.3 Initial Layer Cell Seeding and Culture

Scaffolds were removed from the antibiotic/antimycotic treatment solution and rinsed three times for 15 minutes each in complete media; Eagles Minimal Essential Media supplemented with 10% foetal bovine serum, 2mM L-glutamine, 100U/ml penicillin and 100µg/ml streptomycin (Gibco). They were then placed into a fresh 48 well tissue culture plate.

5637 human urinary bladder epithelials (ATCC) were trypsinized using standard methods from tissue culture flasks and counted using the trypan blue exclusion method. 1 x 10^4 cells at passage 23 were suspended in 100µl of complete media and seeded directly on to the scaffolds. The cells were allowed

to incubate in this small volume on the scaffolds for 2 hours, before an additional 400µl of complete media was added.

Media was changed after 24 hours to either 750µM Valproic Acid (VA) or 750µM Sodium Butyrate (NaB) (Sigma-Aldrich) in complete media and subsequently changed every 48 hours. Controls were scaffold only, i.e. not seeded with an initial cell layer and no drug treatment i.e. the initial layer cultured in drug free complete media only. Drug concentrations and initial layer cells were chosen following results of a drug response curve for each iHDAC (data not shown). Valproic acid and sodium butyrate are used as epigenetic control mechanisms of gene transcription. They function by inhibiting histone deacetylases (as iHDACs) to modulate chromatin structure, creating an open, transcriptionally active euchromatin configuration at gene coding and regulatory regions of the chromosome. This renders the chromatin accessible to transcription factors, and facilitates gene transcription [290]. Valproic acid and sodium butyrate are both commonly used in industry, particularly antibody production due to their ability to upregulate protein production in such a manner [289,291]. This initial layer of cells was cultured for 7 days at 37ºC and 5% CO_2 in a humidified incubator.

3.2.4 Decellularization

Decellularization was performed using methods adjusted from Lu et al. (2012), under sterile conditions at room temperature (19 - 22ºC) and agitation. Scaffolds were washed in phosphate buffered saline (PBS) for 15 minutes and then rinsed in 10mM tris buffered saline (TBS) for 15 minutes.

The scaffolds were submerged in a 0.1% vol/vol Triton X-100 (Sigma-Aldrich) 1.5M potassium chloride (Acros Organics) 50mM TBS for 4 hours. They were rinsed for 15 minutes in 10mM TBS before being submerged in fresh 10mM TBS overnight.

Scaffolds were given a final rinse in 10mM TBS for 15 minutes before being incubated in complete media for 15 minutes and then transferred to new 48 well plates for seeding.

3.2.5 Functional layer Cell Seeding and Culture

HepG2 cells were trypsinized using standard methods from tissue culture flasks and counted using the trypan blue exclusion method. 3 x 10^5 cells at passage 17 were suspended in 100µl of complete media and seeded directly on to the scaffolds. The cells were allowed to incubate in this small volume on the scaffolds for 2 hours, before an additional 400µl of complete media was added.

Media was changed after 24 hours and changed every 48 hours after the initial 24 hour adherence and recovery period. This functional layer (FL) of cells was cultured using standard methods for either 3 or 5 days at 37ºC and 5% CO_2 in a humidified incubator.

3.2.6 Live/Dead® Viability/Cytotoxicity assay

To determine cellular viability, cell/scaffold constructs were incubated with 10µm calcein and 2µm ethidium ho-modimer-1 (Ethd-1) for 30 minutes as part of the two colour live/dead assay (Molecular Probes). Calcein is actively converted to calcein-AM in living cells, which then appear green when excited during fluorescence microscopy. Ethd-1 only accumulates in dead cells, which subsequently appear red. The method allows differentiation between dead and viable cells. The scaffolds were rinsed three times in $CaCl_2$/$MgCl_2$ free PBS to remove excess dye and placed onto a standard microscope slide with a 25mm glass coverslip (VWR). All images were captured using a Zeiss Axio Imager fluorescent microscope (COIL, University of Edinburgh) at 40x magnification and post processed using ImageJ.

3.2.7 CellTiter-Blue® Cell viability assay

The assay was performed according to manufacturer's instruction (Promega). For each condition group, n = 3. Importantly, cell/scaffolds constructs were moved into fresh 48 well plates to prevent reading activity from tissue culture plastic bound cells. Measurements were read in a Modulus™ II microplate reader at an excitation wavelength of 525 nm and emission wavelength of 580-640 nm and reported as fluorescence.

3.2.8 Picogreen DNA quantification

The Quant-IT™ Picogreen® dsDNA assay kit (Life Technologies™) was employed to establish the efficiency of the decellularization method in removing cellular material and to estimate cell number on the cell/scaffold constructs. The assay was performed according to manufacturer instructions. In brief, constructs (n = 6) were digested in a solution of $CaCl_2$ and $MgCl_2$ free PBS (Sigma), containing 2.5 U/ml papain extract (Sigma) 5 mM cysteine-HCl (Sigma) and 5 mM EDTA (Sigma) and incubated overnight at 60°C. Picogreen solution was added to the digests and fluorescent intensity measurements read in a Modulus™ II microplate reader at an excitation wavelength of 480 nm and emission wavelength of 510-570 nm. A standard λ dsDNA curve of graded known concentrations was used to calibrate fluorescence intensity vs dsDNA concentration.

3.2.9 Sectioning and staining

The samples were rinsed three times in PBS (Gibco) for 15 minutes each, then fixed in 4% v/v formalin buffered in saline for 15 minutes at room temperature. After rinsing with fresh PBS, constructs were embedded in low melting temperature polyester wax (Electron Microscopy Supplies) using methods adapted from Steele et al. (2014). In brief, samples are dehydrated through 70-100% ethanol, then incubated in 50:50 ethanol:wax overnight at 45ºC overnight with agitation. The samples were moved into 100% wax for 3 hours at 45ºC and then fresh 100% wax for 1 hour at 45ºC. Samples were embedded and allowed 72 hours to fully cure before sectioning. Immunohistochemical staining was undertaken using antibodies for Collagen I (Stratech), Laminin (Stratech) and Fibronectin (Sigma). All images were captured using a Coherent Anti-Stokes Raman Scattering (CARS) system (Bioimaging Facility, University of Edinburgh) at 10x and 100x magnification and post processed using ImageJ.

3.2.10 Scanning Electron Microscopy

SEM was used to characterise the scaffold architecture. Samples were rinsed three times in PBS for 15 minutes each, then fixed in 2.5% v/v glutaraldehyde (Fisher Scientific) in 0.1M phosphate buffer (PB) (pH 7.4) at 4ºC overnight. They were then rinsed three times in 0.1M PB before being post-fixed in 1% v/v osmium tetroxide (Electron Microscopy Supplies) buffered with 0.1M PB. Samples were again rinsed three times in 0.1M PB and dehydrated through an ethanol gradient (30-100%). They were dried by placing them in hexamethyldisilazane (HMDS, Sigma) which was allowed to evaporate off at room temperature overnight. The samples were mounted onto SEM chucks using double sided carbon tape and coated them with a thin layer of gold and palladium alloy (Polaron Sputtercoater).

All images were captured at 5 kV using a Hitachi S-4700 SEM (BioSEM, University of Edinburgh).

3.2.11 Mechanical Testing

Nanoindentation experiments were undertaken to establish the dynamic properties of scaffolds and decellularized ECM/scaffold constructs using the Keysight/Agilent 5200 nano indenter testing system.

Scaffolds and constructs were subject to indentation by a DCM II actuator flat-ended cylindrical punch (D = 100µm) using a max load of 1g-f. All nanoindentation experiments were carried out on fresh, hydrated, unfixed samples which were adhered to the chuck using double sided tape. A total of 36 indentations were carried out on each sample, 50nm apart. Indent sites were selected using the high precision X-Y stage within the testing system (Agilent). Poissons ratio was assumed to be 0.5 for each sample [273,274]. Allowable drift rate was 0.1nm/s. A NanoSuite (Keysight Technologies) test method "G-Series DCM CSM Flat Punch Complex Modulus" was used for all testing [271,272].

3.2.12 Gene Expression analysis

RNA was extracted from constructs using standard Trizol (Fisher Scientific) methods and purified using Qiagen's RNeasy spin column system. cDNA was synthesised using the Promega's ImProm-II™ Reverse Transcription System.

Quantitative real-time polymerase chain reaction (qRT-PCR) was performed using the LightCycler® 480 Instrument II (Roche Life Science) and Sensifast™ SYBR® High-ROX (Bioline) system. Results were normalized to HepG2s of the same passage number grown on tissue culture plastic and compared to the housekeeping gene Glyceraldehyde-3-Phosphate Dehydrogenase (GAPDH). Analysis was performed using the 2–[delta][delta] Ct method [276], n = 4. Albumin (Alb), Cytochrome P450 Family 1 Subfamily A Polypeptide 1 (Cyp1A1), Cytochrome P450 Family 1 Subfamily A Polypeptide 2 (Cyp1A2), Cytochrome P450 Family 3 Subfamily A Polypeptide 4 (Cyp3A4), Collagen Type I alpha 1 (Col1A1), Collagen Type 4 alpha 1 (Col4A1) and Fibronectin Type 1 (FN1) were investigated, forward and reverse primers (Sigma) are detailed in Table 3.2.

Table 3.2; QRT-PCR Primers

Albumin (Alb)	For - CCTGTTGCCAAAGCTCGATG Rev - GAAATCTCTGGCTCAGGCGA
Cytochrome P450 Family 1 Subfamily A Polypeptide 1 (Cyp1A1)	For - AATTTCGGGGAGGTGGTTGG Rev - GATGTGGCCCTTCTCAAAGGT
Cytochrome P450 Family 1 Subfamily A Polypeptide 2 (Cyp1A2)	For - CTTCGCTACCTGCCTAACCC Rev - GTCCCGGACACTGTTCTTGT
Cytochrome P450 Family 3 Subfamily A Polypeptide 4 (Cyp3A4)	For- TTTTTGGATCCATTCTTTCTCTCAA Rev- TCCACTCGGTGCTTTTGTGT
Collagen Type I alpha 1 (Col1A1)	For - GGACACAGAGGTTTCAGTGGT Rev - GCACCATCATTTCCACGAGC
Collagen Type 4 alpha 1 (Col4A1)	For - GACCCCCGGGAGAAATAGGT Rev - TTTGAAAAAGCAATGGCACTCC
Fibronectin Type 1 (FN1)	For - GAACAAACACTAATGTTAATTGCCC Rev - TCTTGGCAGAGAGACATGCTT
Glyceraldehyde-3-Phosphate Dehydrogenase (GAPDH)	For – GTCTCCTCTGACTTCAACAG Rev - GTTGTCATACCAGGAAATGAG

3.2.13 Statistical Analysis

One-way ANOVAs and Tukey post-hoc testing were performed and graphs generated using Origin software (OriginLab, Northampton, MA). A minimum of n = 3 and max of n = 6 was used for all analysis. Study groups were as follows; Scaffold only, No drug treatment, treatment with Valproic acid and treatment with Sodium butyrate. HepG2 cells were grown on each scaffold for 3 and 5 day time points.

3.3 Results

3.3.1 Scaffold production

Scaffold imaging was performed using scanning electron microscopy and fibres assessed for average diameter using DiameterJ[230]. The average fibre size was 1.14µm. Analyses was also performed post oxygen plasma surface treatment. The average fibre size following oxygen plasma surface treatment was found to be 1.25µm.

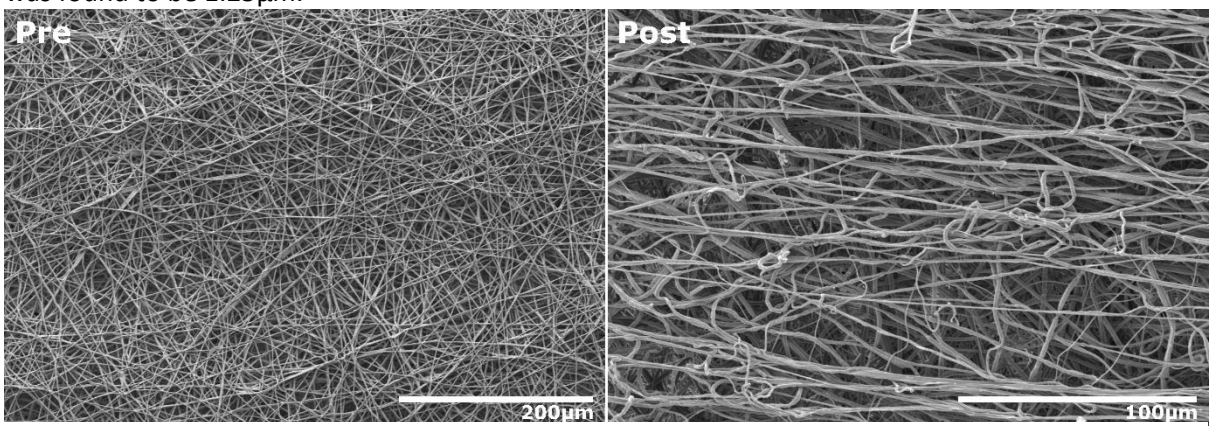

Figure 3.2; Electrospun fibres pre and post oxygen plasma surface treatment

The scaffolds were assessed for consistency and fibre size via scanning electron microscopy and subsequent image analysis. n = 4. 200x (Pre) and 400x (Post) magnification.

3.3.2 Decellularization

Decellularization was confirmed using Picogreen DNA quantitation. Remnant DNA falls well below the threshold remnant DNA concentration of 50ng/mg[212], thus scaffolds are considered successfully decellularized.

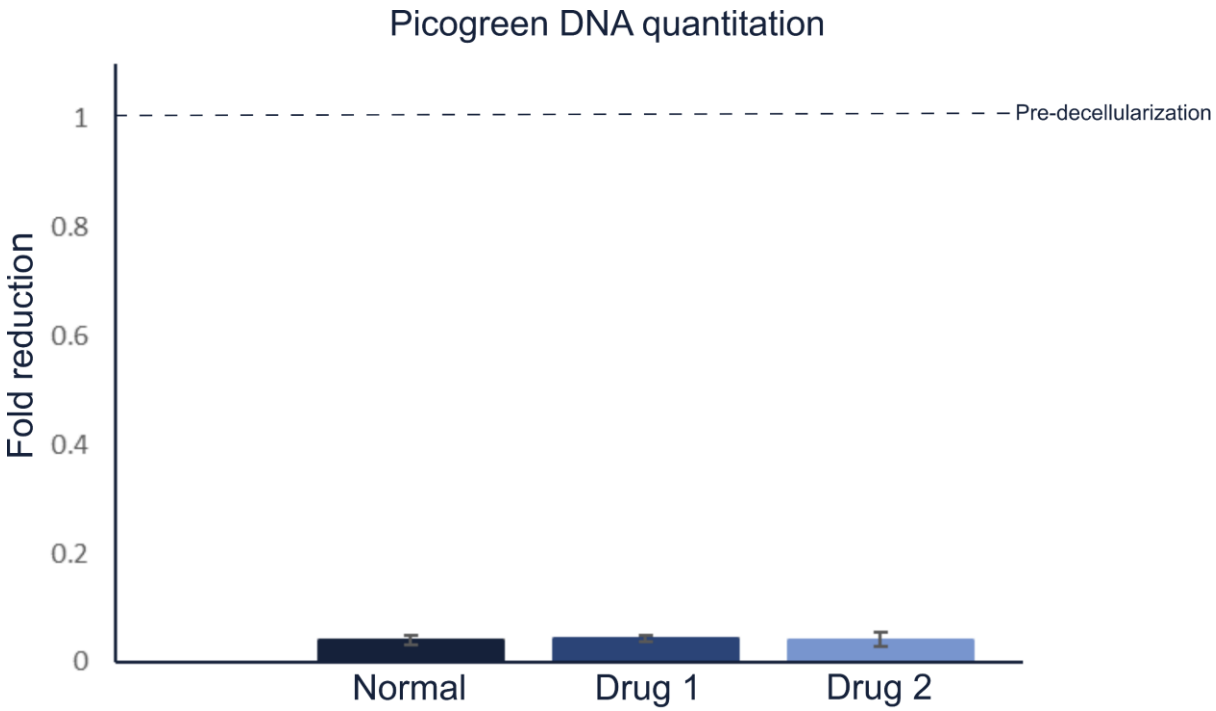

Figure 3.3; Decellularization of initial layer

Decellularization was confirmed using the Quant-IT™ Picogreen® dsDNA assay and scanning electron microscopy (not shown). Additionally, CellTiter-Blue® Cell viability assay was performed on the decellularized scaffolds and showed no activity, and staining with DAPI (4',6-diamidino-2-phenylindole) demonstrated a lack of visible nuclear content (data not shown).

3.3.3 Cell attachment and survival on scaffolds

When compared to N-ECM, a lower number of HepG2s adhered to each of the drug induced scaffold-ECM constructs, and to the scaffold alone (Fig. 3.4); demonstrating that 'normal' ECM is efficient for cell seeding purposes. SO, VA-ECM and NaB-ECM conditions demonstrate longer term maintenance or the HepG2s however (Fig. 3.4) and results are confirmed by both CellTiter-Blue® viability (Fig. 3.4B) and Picogreen® DNA quantitation (Fig. 3.4A). Live/Dead® Viability/Cytotoxicity images (Fig. 3.5) further demonstrates the metabolic viability of the functional HepG2 cell layer (FL), although it should be noted that imaging reveals the FL was not yet confluent at 5 days culture, as further confirmed by SEM images (Fig. 3.6).

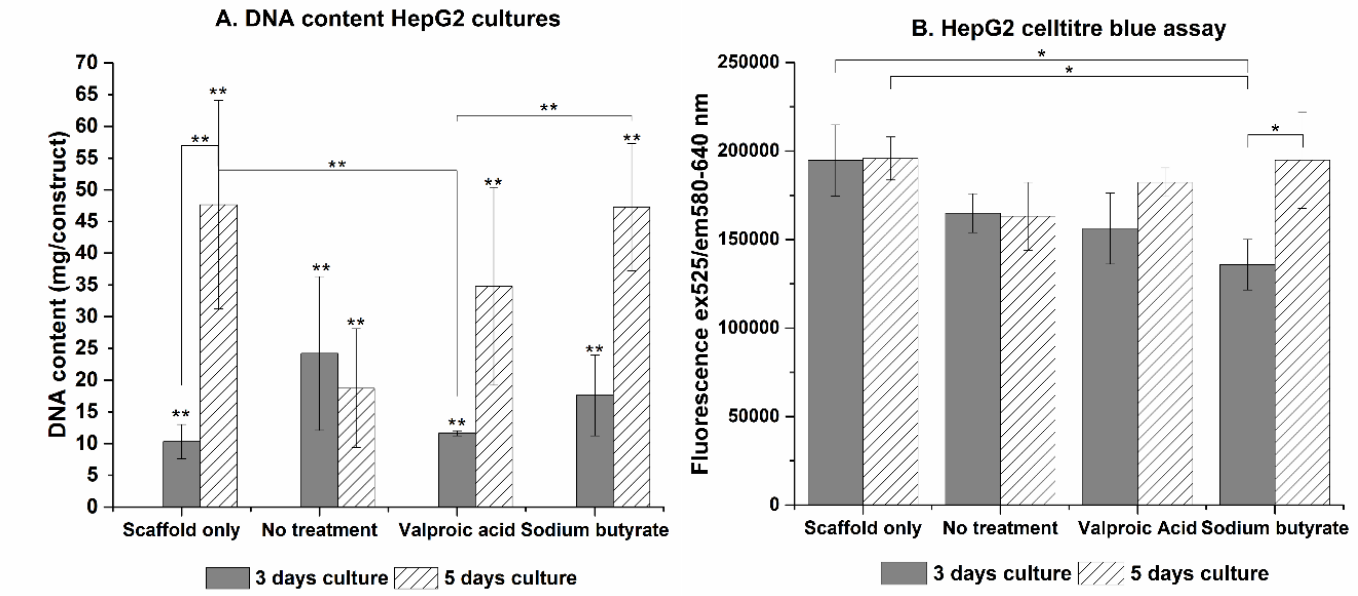

Figure 3.4; Seeding efficiency/viability on scaffolds

Cell adherence was assessed by Quant-IT™ Picogreen® dsDNA assay (A) and further confirmed by CellTiter-Blue® Cell viability assay (B). One-way ANOVA with Tukey post hoc testing. * = $p < 0.05$ ** = $p < 0.01$. Error bars represent SD.

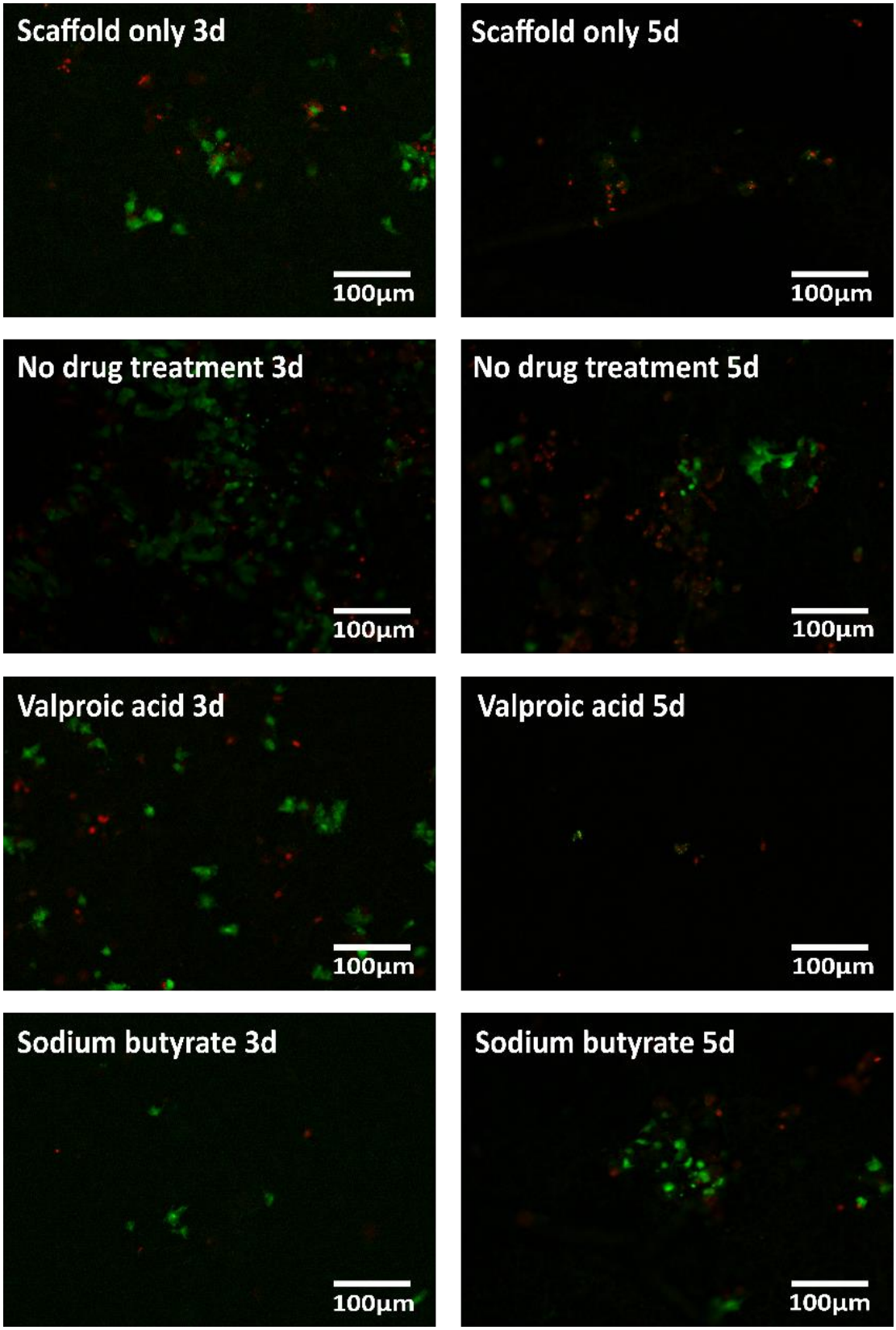

Figure 3.5; Live/Dead® Viability/Cytotoxicity assay

Viability of the FL was assessed by Live/Dead® Viability/Cytotoxicity staining assay. Results demonstrate the FL is metabolically viable at all assessed time points. 40x magnification.

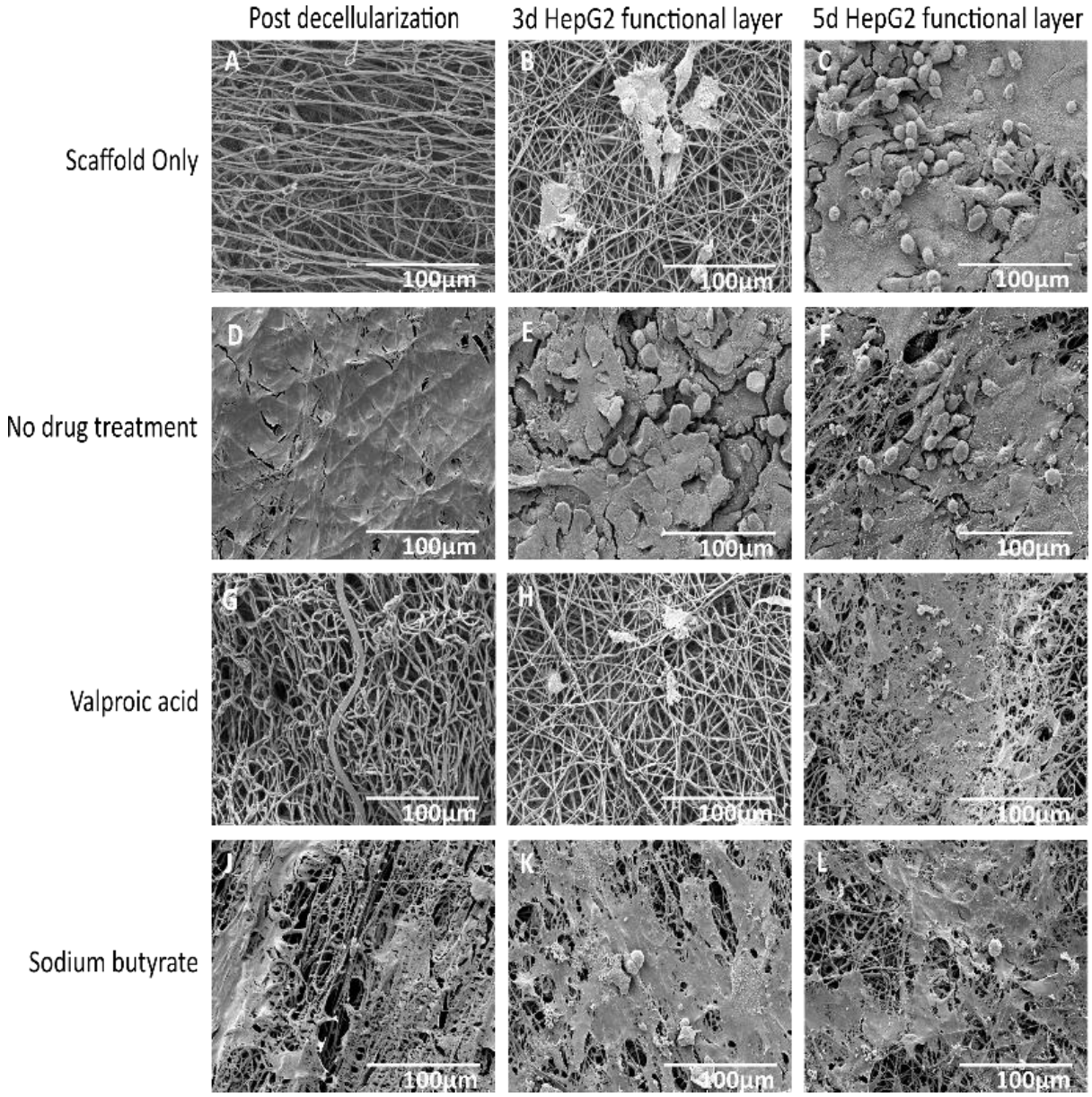

Figure 3.6; SEM of Scaffold-ECM constructs and functional cell layers

Scanning electron microscopy images of the decellularized scaffold-ECM constructs and functional cell layers at three and five days culture. Topographical differences are clearly evident on decellularized constructs. 500x magnification.

3.3.4 Mechanical characterisation of scaffolds

Interestingly, mechanical differences between the scaffold construct were negligible (Fig. 3.7). No significant differences in storage (Fig. 3.7A) or loss (Fig. 3.7B) modulus between the four conditions (Tables 3.3 and 3.4).

Testing was performed at frequencies experienced by the human liver in vivo[292]. Storage modulus (G') ranged from 3.58±0.12 to 4.64±0.43 MPa and loss modulus (G'') from 0.55±0.03 to 1.17±0.07 at the frequencies detailed in tables 3.3 and 3.4. This reassures us that differences in cell attachment, viability and function are due to differences in the biochemical and topographical profile of the hybrid scaffolds, as opposed to potential dynamic differences to which cells are known to be so sensitive[293–296].

Table 3.3; Storage modulus G' at mechanical excitation frequencies

Frequency (Hz)	**Storage modulus, G' (MPa)**								
	1	1.75	3.05	5.31	9.27	16.18	28.23	49.26	85.96
Scaffold only	3.77±0.21	3.73±0.20	3.73±0.20	3.76±0.21	3.79±0.21	3.83±0.21	3.87±0.22	3.89±0.22	3.85±0.22
No drug treatment	3.63±0.12	3.58±0.12	3.58±0.12	3.59±0.12	3.62±0.12	3.65±0.12	3.68±0.13	3.69±0.13	3.66±0.13
Valproic acid	4.43±0.36	4.39±0.36	4.40±0.36	4.44±0.37	4.49±0.38	4.55±0.39	4.60±0.40	4.65±0.41	4.64±0.43
Sodium butyrate	4.33±0.28	4.27±0.28	4.26±0.27	4.29±0.28	4.32±0.28	4.36±0.28	4.40±0.29	4.42±0.29	4.39±0.30

Table 3.4; Loss modulus G'' at mechanical excitation frequencies

Frequency (Hz)	**Loss modulus, G'' (MPa)**								
	1	1.75	3.05	5.31	9.27	16.18	28.23	49.26	85.96
Scaffold only	0.61±0.04	0.62±0.04	0.61±0.04	0.62±0.04	0.65±0.04	0.7±0.04	0.77±0.04	0.88±0.05	1.05±0.06
No drug treatment	0.55±0.03	0.56±0.03	0.55±0.03	0.57±0.03	0.59±0.03	0.64±0.03	0.71±0.03	0.82±0.04	0.98±0.04
Valproic acid	0.65±0.04	0.66±0.04	0.65±0.04	0.67±0.04	0.70±0.04	0.75±0.05	0.84±0.05	0.97±0.05	1.17±0.07
Sodium butyrate	0.58±0.03	0.59±0.03	0.58±0.03	0.60±0.03	0.63±0.03	0.68±0.03	0.76±0.03	0.88±0.04	1.07±0.05

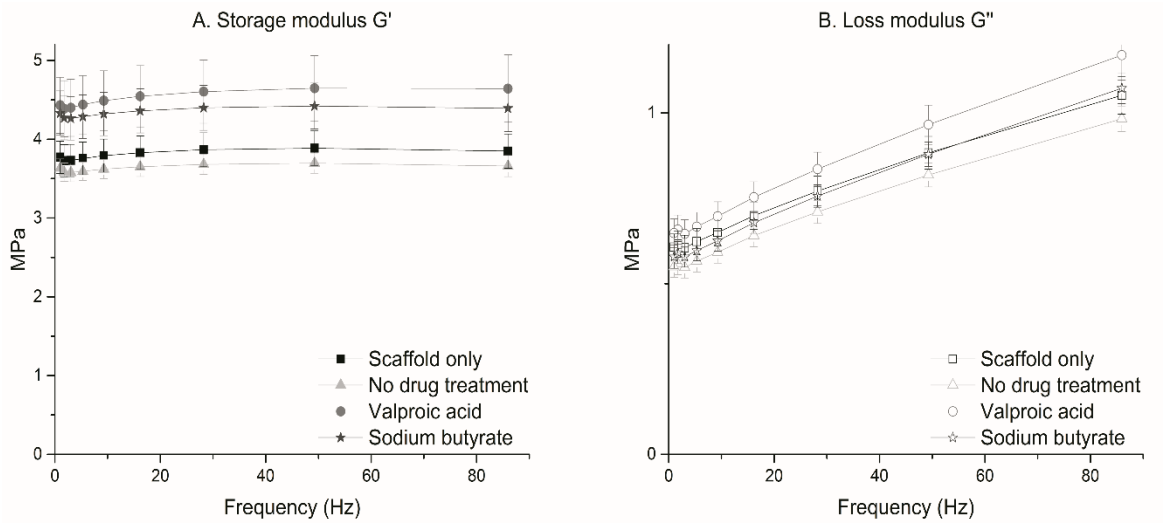

Figure 3.7; Mechanical characterization of decellularized scaffolds

Decellularized ECM/scaffold constructs were subject to nanoindentation experiments to assess their dynamic properties. Results demonstrate no significant differences in storage (A) or loss (B) modulus between the four conditions (Tables 3.3 and 3.4).

3.3.5 Biochemical characterisation of the hybrid polymer-ECM scaffolds

Differences in the biochemical profile of the different ECMs were demonstrated by immunohistochemistry performed on the hybrid scaffold sections (Fig. 3.8). Hepatic phenotype has long been known to be influenced by ECM proteins; particularly Collagen I, Laminin and Fibronectin[12,53,179], all of which are present on the scaffolds to varying degrees. Laminin is of particular importance in the regenerating liver and for cell adhesion, and is increased in injured or developing states[6,297]. Laminin is present in each construct, but appear to be most prevalent in NaB-ECM scaffolds (Fig. 3.8J). These constructs demonstrate higher 'maintenance' of the HepG2s; that is cell number and viability increases between 3 days and 5 days (Fig. 3.3). Collagen I is one of the major components of normal liver ECM[53,179]. Collagen I is most prevalent on NaB-ECM scaffold constructs (Fig. 3.8I), followed by VA-ECM (Fig. 3.8E) and N-ECM (Fig. 3.8A) scaffold constructs. When compared to the N-ECM scaffold constructs, these demonstrate improved maintenance of the HepG2 cell layer (Fig. 3.3), although not in comparison to the SO conditions. Fibronectin is also ubiquitous in healthy liver ECM[53,298] and is present under each of the conditions, but is most prevalent on NaB-ECM scaffolds

(Fig. 3.8K). Scanning electron microscopy of the hybrid scaffolds appears to confirm the fibrillary nature of the Collagen I enriched NaB (Fig. 3.6J) and VA-ECMs (Fig. 3.6G) and the smoother morphology of the Laminin enriched N-ECM (Fig. 3.6D). The ECMs present have penetrated the scaffold in each case, and each protein is present on each scaffold, indicating the robustness and reproducibility of the method (Supplementary Fig. 1 n = 3).

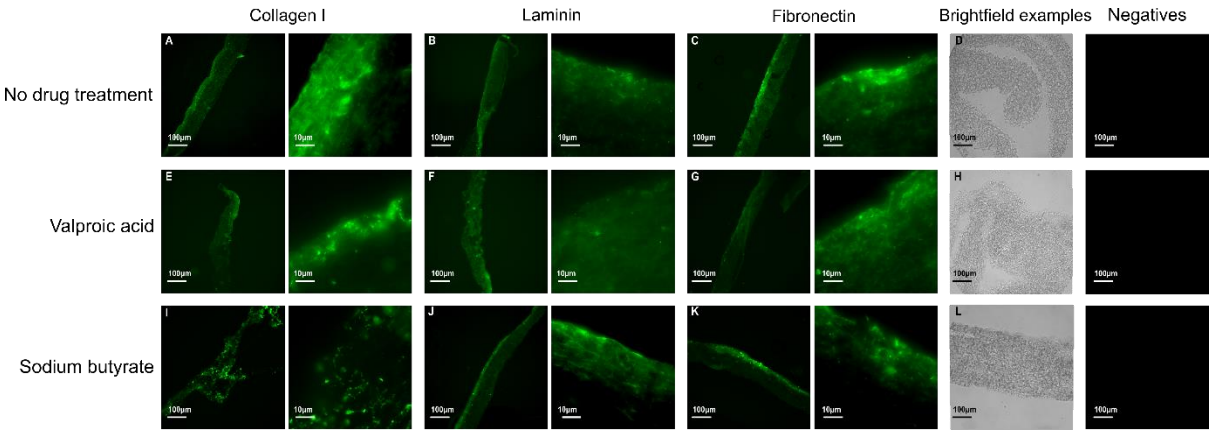

Figure 3.8; Immunohistochemical investigation

Immunohistochemistry staining of the decellularized ECM/scaffold constructs revealed significant differences in ECM components. Stains were performed for Collagen I, Laminin and Fibronectin, post processed using ImageJ . 10x and 100x magnification.

3.3.6 Gene expression of HepG2s in response to hybrid polymer-ECM scaffolds

Multiple genes associated with liver function were assayed for gene expression (Fig. 3.9). Albumin expression is a marker of liver cell differentiation and function and Cytochrome P450 (CYP) are involved in metabolism of toxic compounds and products of endogenous metabolism such as bilirubin in the liver [150,155]. Albumin mRNA expression increases between day 3 and day 5 as expected, but at day 5 is upregulated in comparison to HepG2s grown on tissue culture plastic in all conditions; with the highest levels observed in SO and N-ECM conditions. Additionally, albumin mRNA expression is downregulated at day 3 in SO and NaB-ECM conditions (Fig. 3.9A). Cyp1A1 mRNA expression is consistently upregulated in comparison to tissue culture plastic (Fig. 3.9B). Cyp1A2 mRNA expression is hugely upregulated in comparison to tissue culture plastic (~1000 – 38,000-fold), with the highest levels observed at 3 days on VA-ECM scaffold constructs, and levels at day 5 consistently lower than

those at day 3 (Fig. 3.9C). Cyp3A4 mRNA expression follows a similar pattern, barring the NaB-ECM scaffolds; where expression levels at day 5 are higher than those of day 3. Additionally, the highest levels of expression are observed on SO at day 3 of culture (Fig. 9D). Additionally, three ECM genes were analysed, as key components of the liver microenvironment; Fibronectin (Fig. 3.9E), Collagen I (Fig. 3.9F) and Collagen IV (Fig. 3.9G). While hepatocytes are not the major producers of ECM proteins in the liver[53], the expression of such genes are of interest with regards to the cells further modulation of its environment considering the plastic nature of the ECM[283].

Fibronectin mRNA levels are higher in each condition than in that of HepG2s grown on tissue culture plastic, and highest levels are observed at day 3 on VA-ECM scaffold constructs, subsequently dropping to less than a third of day 3 levels by day 5. This may be in response to fibronectin levels observed in Figure 3.6, where the highest fibronectin levels observed (Fig. 3.6K) correspond with the lowest mRNA expression in the HepG2s. Collagen I mRNA expression is upregulated in every condition. Levels increase at day 5 in SO and NaB-ECM conditions; N-ECM and VA-ECM conditions follow the opposite trend with lowest levels observed in NaB-ECM conditions at day 3. The highest level of gene expression is observed on the scaffold with correspondingly increased Collagen I levels; NaB-ECM (Fig. 3.7I). Collagen IV mRNA levels are decreased in comparison to tissue culture plastic. While the authors refrain from speculation without further analysis, the alterations in mRNA levels indicate that the drug induced ECMs have a profound effect on liver cellular behaviour.

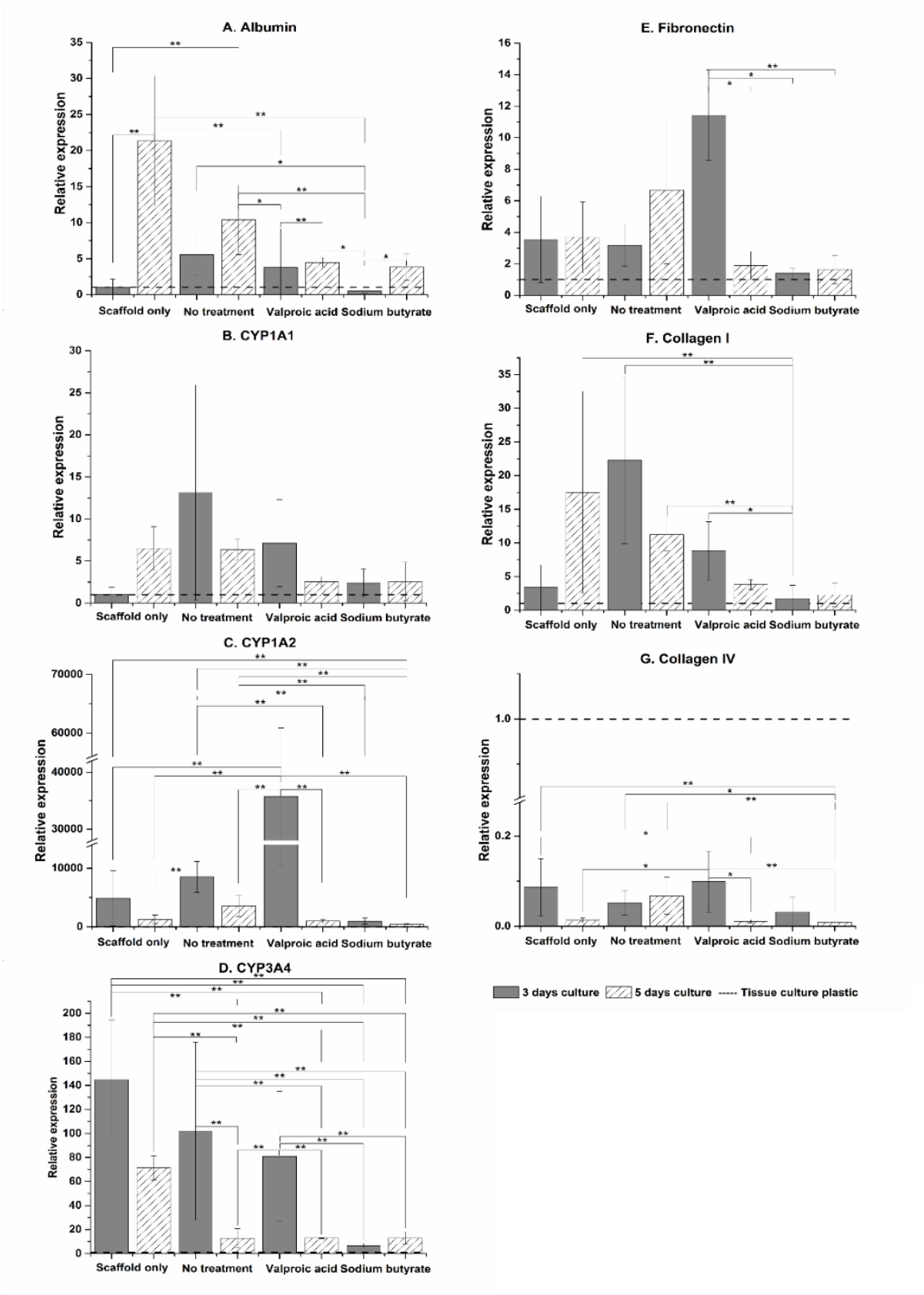

Figure 3.9; Q-PCR analysis of functional cell layer

Quantitative analysis of gene expression was undertaken on the functional cell layer at three and five days culture, compared to that of HepG2s of the same passage and culture periods grown on tissue culture plastic. mRNA levels of Albumin (A), Cyp1A1 (B), Cyp1A2 (C), CYP3A4 (D), Fibronectin (E) Collagen I (F), and Collagen IV (G) are represented as fold difference relative to tissue culture plastic controls and relative to the housekeeping gene GAPDH. One-way ANOVA with Tukey-post hoc testing and n = 4. * = $p < 0.05$ ** = $p<0.01$. Error bars represent SD.

3.4 Discussion

Fabrication of a hybrid polymer-ECM scaffold is an important avenue for liver tissue engineering, addressing the need for donor organs and combatting issues regarding animal-sourced biomaterials and creating a platform which can produce consistent, bioactive scaffolds for liver cell survival and function.

In this chapter, an electrospun fibre approach was taken in the study to mimic the morphology of healthy fibrillary collagen [24,299], which may explain cells favouring environments observed to contain more Collagen I. PCL was used for the fabrication of electrospun scaffolds as it possesses FDA approval for use in medical devices due to its biodegradable nature and elasticity [26]. Oxygen plasma surface treatment altered the hydrophilicity of the PCL to allow cell adhesion.

These results indicate not only that the iHDACs used significantly alter the production and consistency of the ECM, but that this technique is robust and reproducible and the ECM it produces, when harnessed in combination with 3D scaffolding technologies, creates a biofuctionalized scaffold which significantly alters the behaviour of liver cells. These results address the aims of this thesis to assess the response of hepatocytes to novel liver tissue engineering scaffolds.

While the ECM produced by a bladder epithelial may be different to that of a liver cell; several decellularized ECM products on the market are in clinical use to regenerate tissues from which they are not derived, including ALLOPATCH HD™, MatriStem® and Tutoplast® Pericardium[300]. Hepatocytes are regularly cultured on 'ECM' surfaces which are not derived from liver, commonly using Matrigel®, a product derived from murine sarcoma which is as yet undefined and experiences batch to batch variability[12,154,301–303]. Ass discussed in the justification for this research, the promising field of whole organ decellularization is hampered by the availability of human livers, and researchers are subsequently investigating alternative organ and cells sources, such as spleen, bone marrow mesenchymal stem cells[174,304 174]and various animal sources of livers[36]. One of the main advantages of using decellularized native liver ECM is conservation of the highly conserved sinusoidal ECM gradient

required to allow hepatocytes to repopulate in their specific niches. The complex extracellular matrix of the liver remains a topic of investigation in each of its states; diseased, regenerating and healthy[6,53,54,124].

To assess the performance of the hybrid scaffolds, the attachment and function of a commonly used liver cell line, HepG2s, at 3 and 5 day time points when cultured in vitro on the hybrid scaffolds versus scaffold alone was assessed. HepG2s were derived from the hepatocarcinoma of a 15 year old Caucasian male. They are often used because they are virus free, possess liver specific functions such as ammonia metabolism and albumin synthesis and secrete some growth factors such as insulin and insulin-like growth factor II[138]. Cell attachment and viability was analysed, and gene expression of both liver function genes and ECM genes at both 3 and 5 day time points. Additionally, decellularization of the ECM producing cell layer was validated and immunohistochemical analyses of the hybrid scaffold-ECM constructs upon which the HepG2s were seeded was performed.

While this work is a robust proof of principle regarding manipulation of ECM production, and has produced a novel hybrid polymer-ECM scaffold with great potential for liver tissue engineering, further work is required to analyse results and increase translatability. Although HepG2s are a highly valuable research resource, they are derived from a carcinoma and as such criticism of their in vitro relevance abounds within the scientific community. It is important to undertake future work using primary or stem cell derived hepatocytes to combat such criticism. Furthermore, while hepatocytes are the major parenchymal cell of the liver (making up more than 70% of the cellular mass), they do not exist in isolation and the non-parenchymal cells play an essential role in the in vivo liver[124,305]; future studies should look to include these cells. In addition, recognising the value of proteomic and functional assays (such as ELISAs) in analysing the function of the primary/stem cell derived hepatocytes will be important for future validation of the scaffolds, however at this time these were deemed unnecessary considering the critique of the HepG2 cell line. Additionally, care should be taken to ensure decellularization agents are completely removed from the scaffolds, due to their deleterious

effect on both cells and ECM [287]. While such considerations are of importance, this study clearly demonstrates the potential of these hybrid polymer-ECM scaffolds for tissue engineering and provides a robust initial platform for further research.

3.5 Conclusion

This chapter developed a new method of creating hybrid polymer-ECM scaffolds by manipulating cells using electrospun scaffold technologies, clinically relevant iHDACs and methods easily modified to other organs in the human body. To do so, a sacrificial, ECM-producing cell layer was seeded onto a novel electrospun scaffold and then treated with valproic acid or sodium butyrate in order to biofuctionalize the scaffold with cell-derived ECM components. Scaffolds with untreated cells and no initial cell layer at all were used as controls. The initial cell layer was removed with a detergent based decellularization method, and the resulting hybrid polymer-ECM scaffolds seeded with a liver cell line for validation. The work was validated using robust methods such as Q-PCR, mechanical quantification and scanning electron microscopy. Drug induced hybrid polymer-ECM scaffolds had a significant positive influence on the gene expression profile, attachment and survival of liver cells. This data demonstrates promise as a unique method of inducing and altering the production of ECM and that the hybrid scaffolds exert influence upon cells in vitro, as well as future potential as an implantable treatment platform for liver disease patients.

These scaffolds are a useful tool for the development of 3D liver cell platforms which can be used for in vivo cell analysis and novel pharmaceutical research.

Chapter 4

Drug induced hybrid protein:poly-L-lactic acid scaffolds and primary human hepatocytes

4.1 Introduction

Strategies to mimic the *in vivo* ECM include decellularization of organs, use of recombinant and purified proteins and synthetic scaffolds such as hydrogels and electrospun polymers[26,48,203,306]. However, the use of these alone have proved insufficient for longer term maintenance, survival and optimisation of hepatocyte behaviour. Using such techniques has been beneficial to the field; scientists can maintain liver organoids; lab grown collections of hepatocytes and occasionally non-parenchymal cells in the lab for a considerable amount of time and these organoids and spheroids maintain some semblance of hepatic function[108]. Unfortunately, to date no environment has been manufactured which allows hepatocytes to function as they do *in vivo* or provides a viable, clinically translatable alternative to whole organ transplant[73]. Equally, primary human hepatocytes are generally considered the gold standard for studying hepatocyte biology, however, they are a rare resource and as such are under-represented in the liver tissue engineering research field[307]. Yet, a minimum number of studies have been able to transition their promising early stage research into the next stage by undertaking further, translational studies using primary human hepatocytes.

Drug-induced hybrid electrospun poly-capro-lactone:cell-derived ECM scaffolds for liver tissue engineering have been used previously[11]. These scaffolds were manufactured using a sacrificial, ECM-producing cell layer which was seeded onto a novel electrospun scaffold and then treated with histone deacetylase inhibitors (iHDACs)[290,291,308,309] to biofuctionalize the scaffold with ECM components. The initial cell layer was removed with a detergent-based decellularization method, and the resulting hybrid polymer-ECM scaffolds seeded with HepG2s for validation. Drug-induced hybrid polymer-ECM scaffolds had a significant positive influence on the gene expression profile, attachment, and survival of liver cells. These scaffolds represent a unique method of inducing and altering the production of ECM and of exerting an influence on phenotypic behaviour of cells, as well as future potential as an implantable treatment platform for liver disease patients. However, these scaffolds ECM layer was produced by a bladder epithelial cell line. An obvious improvement is to use a more hepatic relevant

cell line to biodecorate the scaffolds. Equally, use of a more clinically relevant cell; such as a primary or IPSC hepatocyte to validate the scaffolds adds to the robustness of the work and further highlights the translatability of the drug induced hybrid scaffold methods.

With this background in mind the next generation of drug-induced hybrid electrospun scaffolds were manufactures; using poly-lactic-acid as a biocompatible and biodegradable polymer for the scaffolds and using sodium butyrate and valproic acid as previously described to alter the ECM biodecoration by a sacrificial liver cell line; THLE-3s. These scaffolds were decellularized and frozen until primary human liver cells, obtained from a donated cadaveric human liver were available. The scaffolds were defrosted and seeded with primary hepatocytes to validate the scaffolds. Results demonstrate that the ECM on the scaffolds is drastically altered by the drug treatment; displaying different mechanical and biochemical properties. Albumin production, cell survival and gene expression of the primary hepatocytes were all altered in response to the hybrid drug induced ECM:PLA scaffolds.

This work further demonstrates the translatability of the hybrid protein:polymer scaffolds and further elucidates the impact of differing ECM profiles on the behaviour of primary human hepatocytes.

Figure 4.1; Method schematic

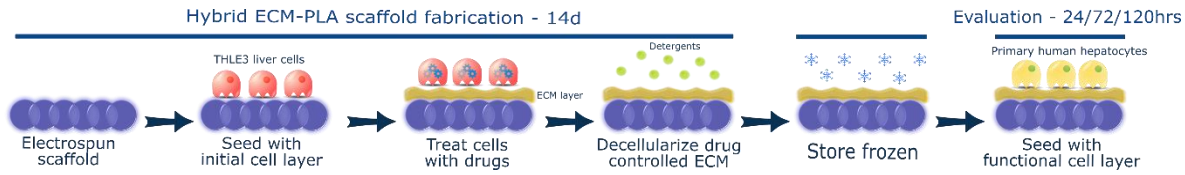

4.2 Materials and Methods

All methods were performed according to protocols laid out in Chapter 2. Specific details are described forthwith.

4.2.1 Ethics and Governance

All human tissue used in this chapter was provided by NHS Organ Donation and Transplant and NHS Blood and Transplant. No organs/tissues were procured from prisoners. Ethical approval was granted for the project from the North of Scotland Research Ethics Committee, ref 16/NS/0083. Informed consent for organ donation for research purposes was obtained in accordance with the Helsinki Declaration. Tissue from one donor liver was used for this chapter.

4.2.2 Electrospinning

A 22% wt/vol solution of poly-L-lactic acid (Goodman) and 10ml hexafluoroisopropanol (Manchester Organics) was used to electrospin scaffolds under the following parameters;

Table 4.1; Electrospinning parameters

Volume per hour	Total volume	Mandrel:needle distance	Positive charge	Negative charge	Mandrel rotation	Needle movement
2.5ml	7.5ml	23 cm	16kV	-3kV	300rpm	100mm/s

4.2.3 Scaffold Preparation

10mm discs of scaffold were cut from the dry fibre sheet and sterilised using isopropyl alcohol for 10 minutes, rinsed three times in phosphate buffered saline for 15 minutes each and were placed into antibiotic/antimycotic treatment for 1 hour.

4.2.4 Initial Layer Cell Seeding and Culture

Scaffolds were removed from the antibiotic/antimycotic treatment solution and rinsed three times for 15 minutes each in complete media; Eagles Minimal Essential Media supplemented with 10% foetal

bovine serum, 2mM L-glutamine, 100U/ml penicillin and 100µg/ml streptomycin (Gibco). They were then placed into a fresh 48 well tissue culture plate.

THLE-3 immortalized normal human liver epithelials (ATCC) were trypsinized using standard methods from tissue culture flasks and counted using the trypan blue exclusion method. 3.5 x 10^4 cells at passage 4 were suspended in 100µl of complete media and seeded directly on to the scaffolds. The cells were allowed to incubate in this small volume on the scaffolds for 3 hours to allow attachment, before an additional 400µl of complete media was added.

Media was changed after 24 hours to either 750µM Valproic Acid (VA-ECM) or 750µM Sodium Butyrate (NaB-ECM) (Sigma-Aldrich) in complete media and changed every 48 hours. Controls were polymer only (PO), i.e. not seeded with an initial cell layer at all and no drug treatment (N-ECM) i.e. the initial layer was cultured in drug free complete media only and never exposed to either iHDAC. Drug concentrations and initial layer cells were chosen following results of a drug response curve for each iHDAC (data not shown). Valproic acid and sodium butyrate are used as epigenetic control mechanisms of gene transcription. They function by inhibiting histone deacetylases (as iHDACs) to modulate chromatin structure, creating an open, transcriptionally active euchromatin configuration at gene coding and regulatory regions of the chromosome. This renders the chromatin accessible to transcription factors, and facilitates gene transcription [290]. Valproic acid and sodium butyrate are both commonly used in industry, particularly antibody production due to their ability to upregulate protein production in such a manner [289,291]. This initial layer of cells was cultured for 7 days at 37ºC and 5% CO_2 in a humidified incubator. A control set of scaffolds was processed with the complete media, but with no initial layer cells and is referred to as the polymer only (PO) condition throughout.

4.2.5 Decellularization

Decellularization was performed using methods adjusted from Lu et al. (2012), under sterile conditions at room temperature (19 - 22ºC) and with agitation.

Scaffolds were given a final rinse in 10mM TBS for 15 minutes before being transferred to 500µl fresh, cell-culture grade PBS in new 48 well culture plates. Plates were sealed with parafilm and flash-frozen in a dry ice:ethanol bath. Samples were stored at -80ºC until use.

4.2.6 Primary hepatocyte extraction

The donor liver had been subject to ex situ normothermic perfusion as part of another groups ongoing research[310] prior to collection. Upon receipt of the donated liver 8-10 small ($2cm^2$) chunks of liver tissue were subjected to digestion and Percoll density centrifugation to obtain primary human hepatocytes.

The hepatocytes plated onto tissue culture plastic or scaffolds as needed.

4.2.7 Functional layer Cell Seeding and Culture

The primary hepatocytes were seeded at 3×10^5 cells, suspended in 100µl of complete media and placed directly on to the scaffolds. The cells were allowed to incubate in this small volume on the scaffolds for 2 hours, before an additional 400µl of complete media was added.

The primary hepatocytes were cultured in Williams E media with no phenol red (Gibco) containing 10% Foetal Bovine Serum, 2mM glutamine, 1% Non-essential amino acids , 1% Sodium pyruvate (all Gibco), 2µg/ml Hydrocortisone (Sigma), 0.124 IU/ml Human insulin (Sigma) and 1µg/ml Human epidermal growth factor (Corning). They do not expand or split, and media was changed every 24 hours. This functional layer (FL) of cells was cultured using standard methods for either 24, 72 or 120 hours at 37ºC and 5% CO_2 in a humidified incubator.

4.2.8 Live/Dead® Viability/Cytotoxicity assay

To determine cellular viability, cell/scaffold constructs were incubated with 10µm calcein and 2µm ethidium homodimer-1 (Ethd-1) for 30 minutes as part of the two colour live/dead assay (Molecular Probes). All images were captured using a Zeiss Axio Imager fluorescent microscope (COIL, University of Edinburgh) at 40x magnification and post processed using ImageJ.

4.2.9 MTT® Cell viability assay

The MTT (3-(4,5-dimethylthiazol-2-yl)-2,5-diphenyltetrazolium bromide) tetrazolium reduction assay (Sigma) was used to indicate cell viability.

The primary hepatocyte functional cell layer was incubated with MTT for 2 hours at the 24, 72 and 120-hour time points. Incubation time was limited because of the cytotoxic effect of reagents which utilize NADH from the cell to generate a signal. Thus, the formazan produced was solubilized prior to recording absorbance readings using acidic isopropanol (Sigma) and measurements were read in a Modulus™ II microplate reader at a wavelength of 570 nm and reported as absorbance. For each condition group, minimum n = 4.

4.2.10 Albumin quantification

A bromocresol green (BCG) albumin assay (Sigma) was used to quantify serum albumin produced by the primary hepatocyte functional cell layer over 24 hours at 24, 72 and 120 hours. The assay was performed according to manufacturer's instructions and results read at an absorbance of 620 nm in a Modulus™ II microplate reader. For each condition group, minimum n = 5.

4.2.11 Picogreen® DNA quantification

The Quant-IT™ Picogreen® dsDNA assay kit (Life Technologies™) was employed to establish the efficiency of the decellularization method in removing cellular material and to estimate cell number on the cell/scaffold constructs. The assay was performed according to manufacturer instructions. For each condition group, minimum n = 5.

4.2.12 Immunohistochemistry

Constructs were stained using antibodies for Collagen I (Stratech), Laminin (Stratech) and Fibronectin (Sigma). Top down images of cells on the scaffolds were obtained by staining with DAPI (Sigma) and Phalloidin (Sigma). All images were captured using a custom multi-photon microscope at the Institute for Bioengineering Bioimaging Facility, University of Edinburgh. A mode-locked ND:YVO4 laser source

(PicoTrain, Spectra Physics) was used to generate both a Stokes pulse (6 ps, 1064 nm) and drive an optical parametric oscillator (OPO) (Levante Emerald, APE). The OPO provides a tuneable excitation pulse across 700-1000 nm allowing coherent anti- Stokes Raman scattering (CARS), second harmonic generation (SHG) and two-photon excitation fluorescence (TPEF) microscopy.

4.2.13 Scanning Electron Microscopy

SEM was used to characterise the scaffold architecture. The samples were mounted onto SEM chucks using double sided carbon tape and coated them with a thin layer of gold and palladium alloy (Polaron Sputter coater).

All images were captured at 5 kV using a Hitachi S-4700 SEM (BioSEM, University of Edinburgh).

4.2.14 Mechanical Testing

Compression testing was undertaken to establish the dynamic properties of the hybrid polymer:ECM scaffolds using the Instron 3367 dual column universal testing system with Bluehill 3 software. Each sample was compressed to 10% strain at a crosshead speed of 0.5% strain min−1. Incremental compressive moduli were calculated from 0%–2.5%, 2.5%–5%, 5%–7.5% and 7.5%–10%, adapted from previous methodology [24,26].

4.2.15 Gene Expression analysis

RNA was extracted from constructs using standard Trizol (Fisher Scientific) methods and purified using Qiagen's RNeasy spin column system. cDNA was synthesised using the Promega's ImProm-II™ Reverse Transcription System.

Quantitative real-time polymerase chain reaction (qRT-PCR) was performed using the LightCycler® 480 Instrument II (Roche Life Science) and Sensifast™ SYBR® High-ROX (Bioline) system. Results were normalized to primary hepatocytes of the same extraction grown on polymer only scaffolds and compared to the housekeeping gene Glyceraldehyde-3-Phosphate Dehydrogenase (GAPDH). Analysis was performed using the 2–[delta][delta] Ct method [276,311], n = 5. Albumin (Alb), Cytochrome P450

Family 1 Subfamily A Polypeptide 2 (Cyp1A2), Cytochrome P450 Family 2 Subfamily B Polypeptide 6 (Cyp2B6), Cytochrome P450 Family 3 Subfamily A Polypeptide 4 (Cyp3A4), Collagen Type I alpha 1 (Col1A1), Collagen Type 4 alpha 1 (Col4A1) and Fibronectin Type 1 (FN1) were investigated, forward and reverse primers (Sigma) are detailed in Table 4.2.

Table 4.2; qRT-PCR primers used

Albumin (Alb)	For - CCTGTTGCCAAAGCTCGATG Rev - GAAATCTCTGGCTCAGGCGA
Cytochrome P450 Family 1 Subfamily A Polypeptide 2 (Cyp1A2)	For - CTTCGCTACCTGCCTAACCC Rev - GTCCCGGACACTGTTCTTGT
Cytochrome P450 Family 2 Subfamily B Polypeptide 6 (Cyp2B6)	For - TGCCCCTTTTGGGAAACCTT Rev - ATGAGGGCCCCCTTGGATTT
Cytochrome P450 Family 3 Subfamily A Polypeptide 4 (Cyp3A4)	For- TTTTTGGATCCATTCTTTCTCTCAA Rev- TCCACTCGGTGCTTTTGTGT
Collagen Type I alpha 1 (Col1A1)	For - GGACACAGAGGTTTCAGTGGT Rev - GCACCATCATTTCCACGAGC
Collagen Type 4 alpha 1 (Col4A1)	For - GACCCCCGGGAGAAATAGGT Rev - TTTGAAAAAGCAATGGCACTCC
Fibronectin Type 1 (FN1)	For - GAACAAACACTAATGTTAATTGCCC Rev - TCTTGGCAGAGAGACATGCTT
Glyceraldehyde-3-Phosphate Dehydrogenase (GAPDH)	For – GTCTCCTCTGACTTCAACAG Rev - GTTGTCATACCAGGAAATGAG

4.2.16 Statistical Analysis

One-way ANOVAs with Games-Howell and Tukey post-hoc testing was performed using Minitab 18 Statistical Software. Multiple comparisons tests were used following the Ryan Joiner test for normality and Bartlett's test for the homogeneity of variances. The Tukey post hoc test was used where Bartlett's test result is not significantly different i.e. the null hypothesis of population variances being equal is not rejected. The Games-Howell test does not assume equal variances and sample sizes and was performed on the ranked variables similar to other nonparametric tests. The Games-Howell post hoc test is used where Bartlett's test result is significantly different i.e. the null hypothesis of population variances being equal is rejected. Error bars indicate standard deviation. A minimum of n = 3 and max of n = 6 was used for all analysis. * = p value <0.05, ** = p value <0.01, *** = p value <0.001.

Methods are as previously described in published papers[128,129].

4.3 Results

4.3.1 Mechanical profiling of scaffolds

The Young's modulus at 0-40% strain analysis by one-way ANOVA and Games-Howell post hoc analysis (n=3, p = <0.05) showed a significant difference between V-ECM scaffolds and all other conditions; indicating that the use of valproic acid to alter ECM production has significantly altered the mechanical qualities and structure of the ECM and resulting in a stiffer environment for scaffolds. ND-ECM and NaB-ECM both exhibit lower Young's modulus than both PO and V-ECM scaffolds, indicating that a 'normal' , non-drug derived ECM and a NaB derived ECM are less stiff than a scaffold with no ECM 'PO', as would be expected from a hydrated, protein-based ECM in comparison to an electrospun polymer mat.

Table 4.3; Young's modulus (MPa) of each scaffold.

Strain	Polymer only	No drug treatment	Valproic acid	Sodium butyrate
0-10%	0.00021 ± 0.00009	0.00011 ± 0.00007	0.00042 ± 0.00049	0.00017 ± 0.00005
10-20%	0.00020 ± 0.00009	0.00021 ± 0.00009	0.01543 ± 0.01639	0.00016 ± 0.00006
20-30%	0.00050 ± 0.00049	0.00024 ± 0.00015	0.07181 ± 0.06190	0.00023 ± 0.00011
30-40%	0.00724 ± 0.00994	0.00177 ± 0.00160	0.46913 ± 0.43570	0.00028 ± 0.00016

4.3.2 Scanning electron microscopy

Scanning electron microscopy reveals visibly altered ECM in each condition (Fig 4.2).

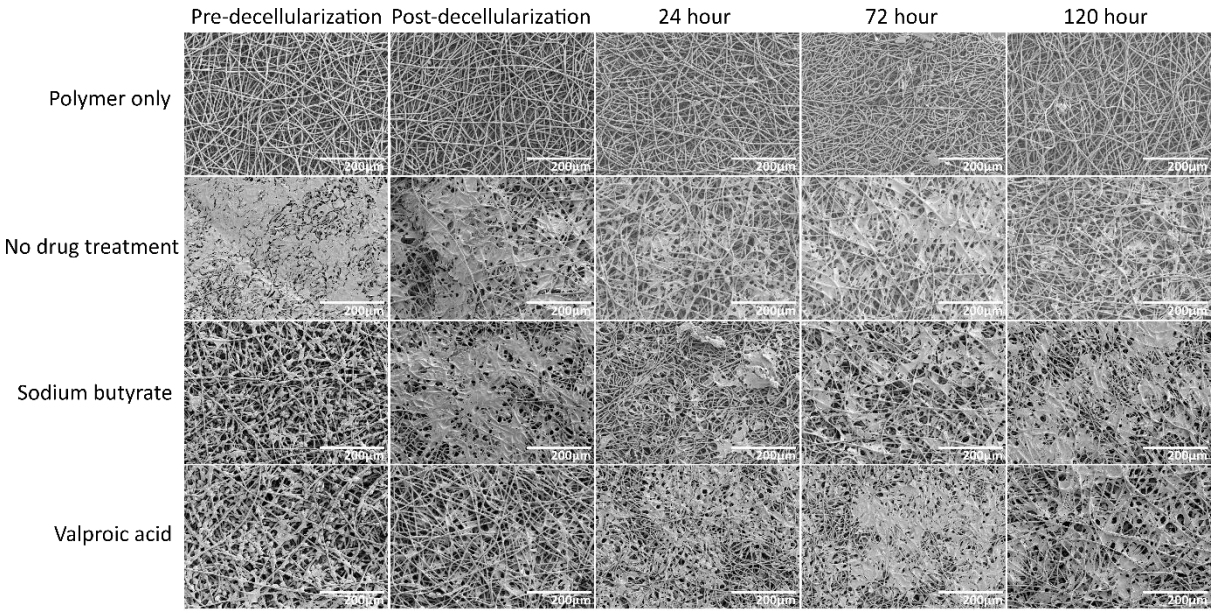

Figure 4.2; SEM of Scaffold-ECM constructs and functional cell layers

Scanning electron microscopy images of the decellularized scaffold-ECM constructs and functional cell layers at 24, 72 and 120 hours culture. Topographical differences are clearly evident on decellularized constructs. 500x magnification.

This phenomenon was also observed in previous studies; with each drug exerting a different effect on the visual appearance of the ECM. Equally, SEM imaging demonstrates a confluent initial cell layer and complete decellularization of the initial cell layer of THLE-3s. Decellularization was confirmed by use of Picogreen DNA analysis (Fig 4.3). Primary human hepatocytes are evident on the scaffolds at 24, 72 and 120 hours on each scaffold.

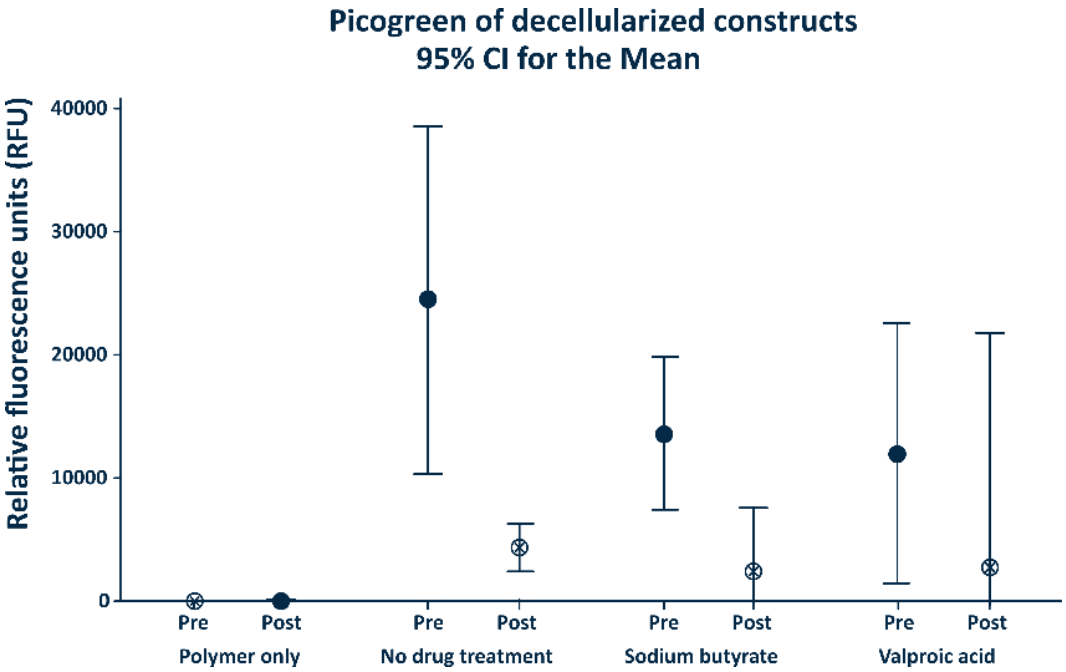

Figure 4.3; Decellularization of initial layer

Decellularization was confirmed using the Quant-IT™ Picogreen® dsDNA assay and scanning electron microscopy (Fig 4.2).

4.3.3 Cell survival and metabolism

As demonstrated in the SEM imaging (Fig 4.2) primary human hepatocytes have adhered to the scaffold successfully. This is confirmed by Picogreen DNA analysis of the scaffolds (Fig 4.4). As expected, due to early cell death DNA levels drop off after 24 hours. They recover slightly, although not significantly, at 120 hours. MTT absorbance results (Fig 4.5) demonstrate that cells are metabolically active at each time point, and that this metabolic activity increases over time.

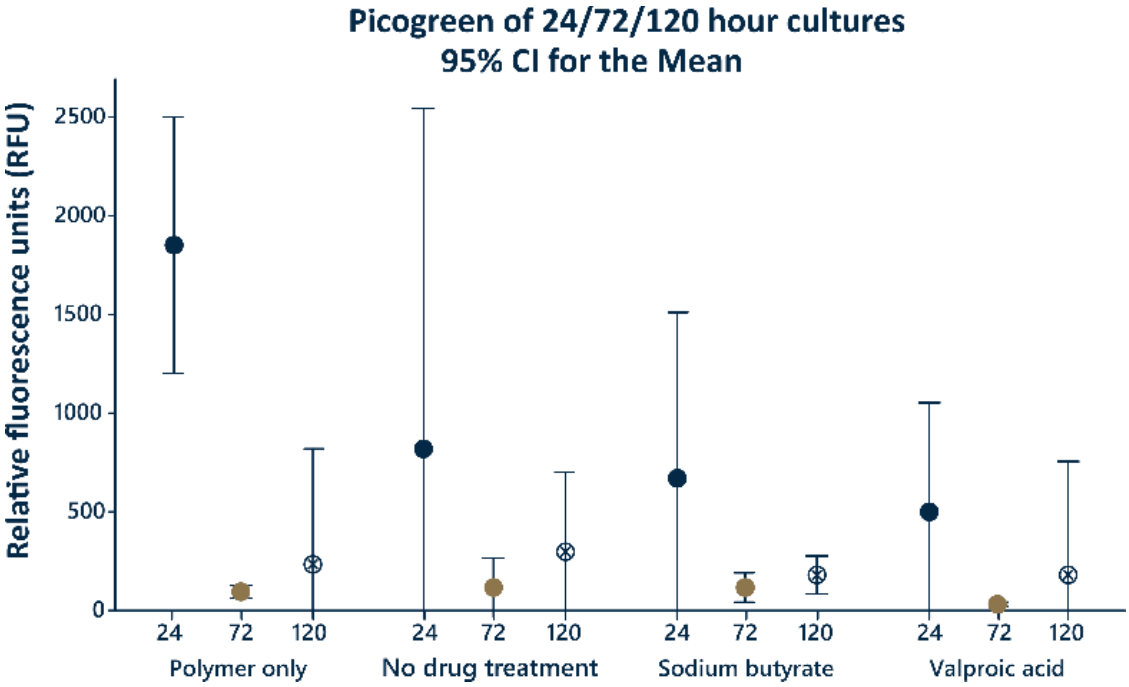

Figure 4.4; Seeding efficiency/viability on scaffolds

Cell adherence was assessed by Quant-IT™ Picogreen® dsDNA assay and further confirmed by MTT absorbance assay (Fig 4.5). One-way ANOVA with Tukey post hoc testing. * = $p < 0.05$ ** = $p < 0.01$. Error bars represent SD.

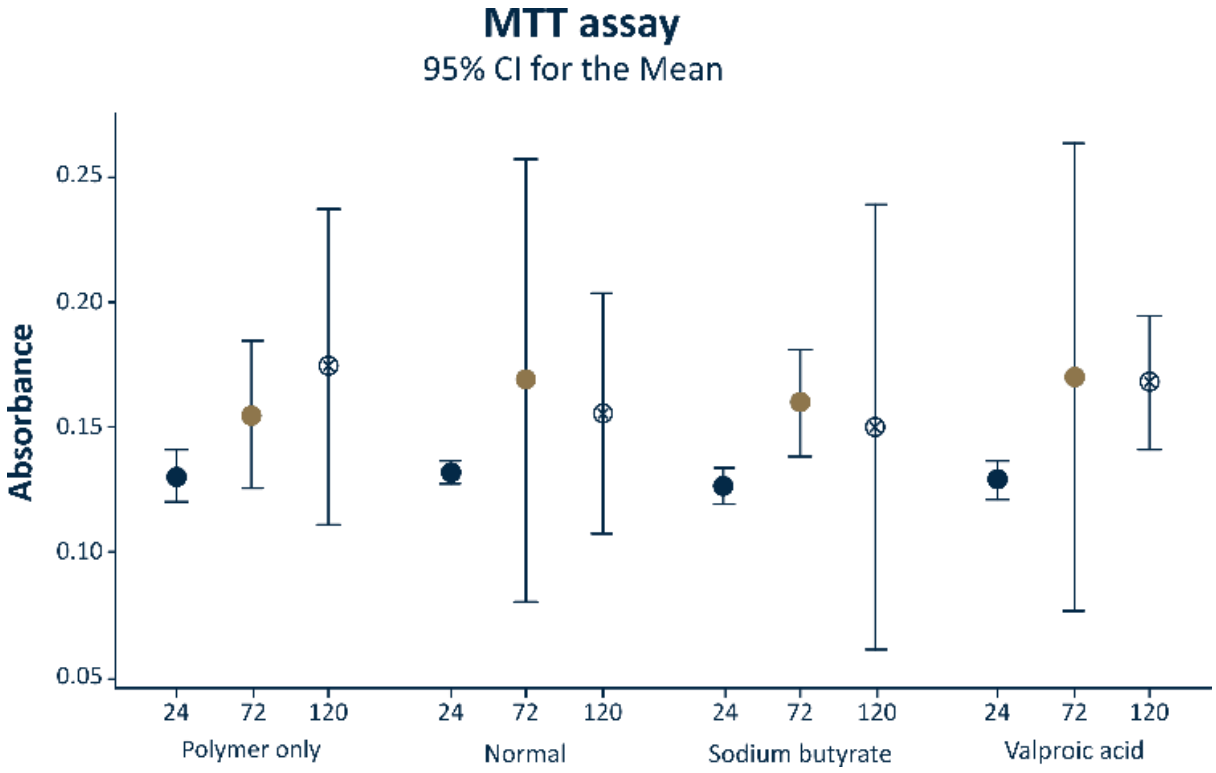

Figure 4.5; Seeding efficiency/viability on scaffolds

Cell metabolism was confirmed by MTT absorbance assay. One-way ANOVA with Tukey post hoc testing. * = p <0.05 ** = p<0.01. Error bars represent SD.

4.3.4 Immunohistochemistry

Differences in the biochemical profile of the different ECMs were demonstrated by immunohistochemistry performed on the hybrid scaffold sections (Fig 4.6). As discussed previously, hepatic phenotype and behaviour has long been known to be influenced by ECM composition; particularly Collagen I, Laminin and Fibronectin[12,53,179], all of which are present on the scaffolds to varying degrees (stained in red). The PLA fibres are clearly visible in each. Laminin is of particular importance in the regenerating liver and for cell adhesion, and is increased in injured or developing states[6,297]. Laminin seem most prevalent on VA-ECM scaffold constructs (Fig 4.6H), followed by NaB-ECM (Fig 4.6G) and N-ECM (Fig 4.6F) scaffold constructs. Collagen I is one of the major components of normal liver ECM[53,179]. Collagen I appears most prevalent on NaB-ECM scaffold constructs (Fig 4.6C), followed by VA-ECM (Fig 4.6D) and N-ECM (Fig 4.6B) scaffold constructs. These results were also seen in a previous iteration of this work[11]. When compared to the N-ECM scaffold constructs, these

demonstrate improved albumin production (Fig 4.6). Fibronectin is also ubiquitous in healthy liver ECM[53,298]. Fibronectin staining is present in each construct (Fig 4.6J, 4.6K & 4.6L).

Figure 4.6; Immunohistochemical investigation

Immunohistochemistry staining of the decellularized ECM/scaffold constructs revealed differences in ECM components. Stains were performed for Collagen I, Laminin and Fibronectin,post processed using ImageJ.

Staining was also undertaken to visualise the hepatocytes adhered to the scaffolds (Fig 4.7). Cells are visible in each condition and at each time point, although spread far apart. This reflects the relatively low seeding density of the hepatocytes.

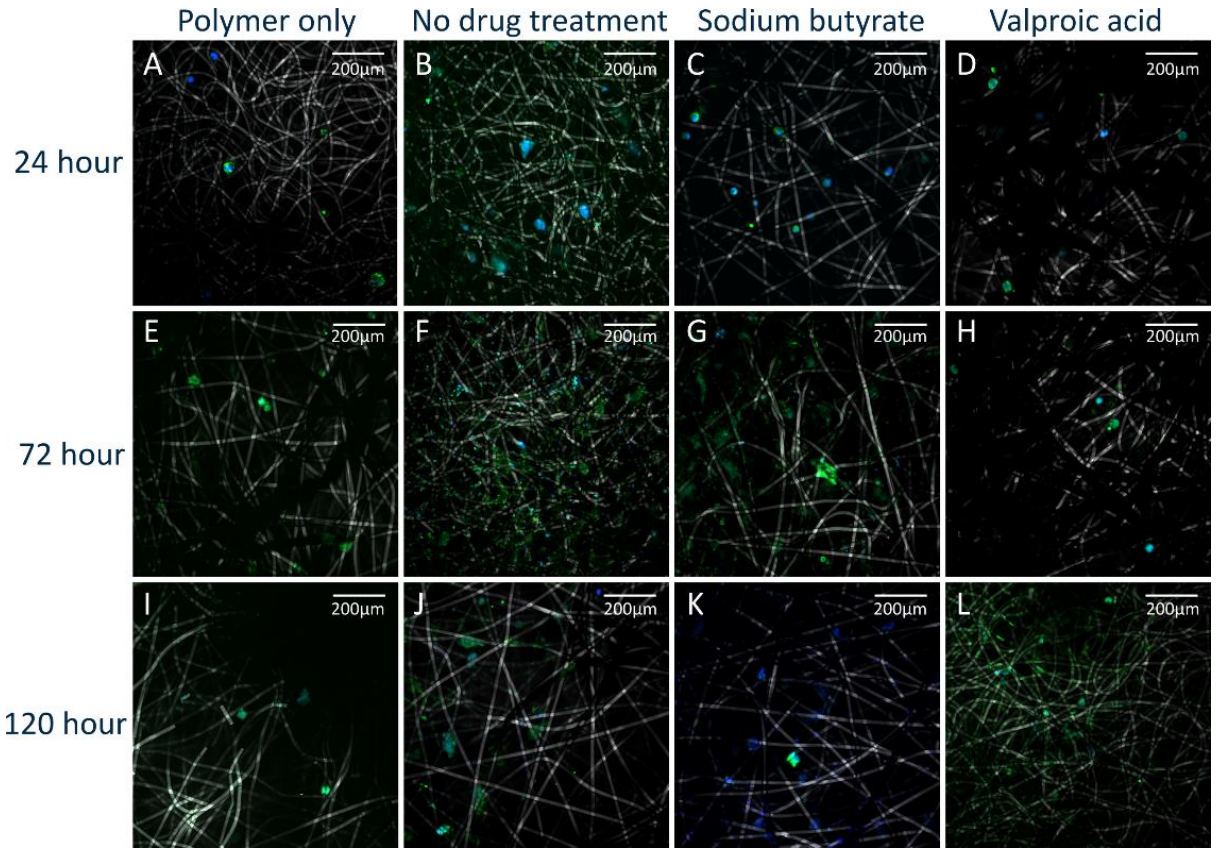

Figure 4.7; Cell imaging

Dapi and phalloidin staining of cell/scaffold constructs revealed cells present at each timepoint, post processed using ImageJ.

4.3.5 Albumin production

Figure 4.8 reveals that albumin is being produced by the primary human hepatocytes in each condition and at each time point. Importantly, albumin levels are significantly higher than those produced on tissue culture plastic at 24 hours on every scaffold. On PO scaffolds, albumin production increases significantly between 72 and 120 hours. Importantly, the pattern of albumin production reassuringly tallies that of the MTT metabolic analyses (Fig 4.5), indicating an initial metabolic drop off and then recovery over the 120-hour culture period.

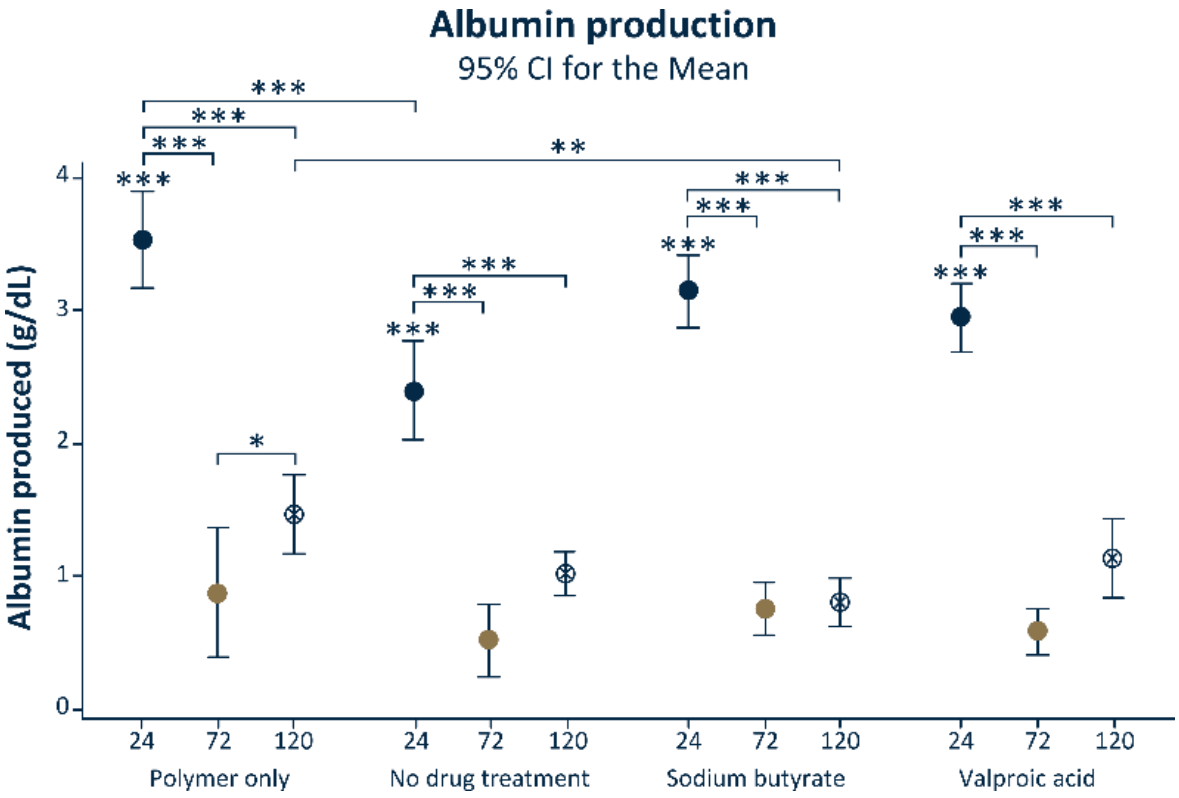

Figure 4.8; Albumin production on scaffolds

Cell function was assayed by checking for albumin protein production. One-way ANOVA with Tukey post hoc testing. * = p <0.05 ** = p<0.01. Error bars represent SD.

4.3.6 Gene expression

Gene expression analysis demonstrates significant differences between conditions and time points (Fig 4.9). Albumin gene expression (Fig 4.9A) is altered between PO at 24 hours on ND-ECM and 72 hours on V-ECM. Differences are also seen at 72 hours between ND-ECM, V-ECM and NaB-ECM as well as between each time point on N-ECM. Of not is that the gene expression follows a similar pattern to that of the albumin production; high at 24 hours then dropping off at 72 hours before recovering at 120 hours in each condition. CYP1A2 expression (Fig 4.9B) is altered at 24 hours between PO-ECM, N-ECM, V-ECM and NaB-ECM with changes also seen between time points on N-ECM. Col4A1 expression (Fig 4.9F) demonstrated changes between time points in the N-ECM condition, and FN1 (Fig 4.9G) expression is significantly altered at 24 hours between all conditions, similarly to that of CYP1A2 expression.

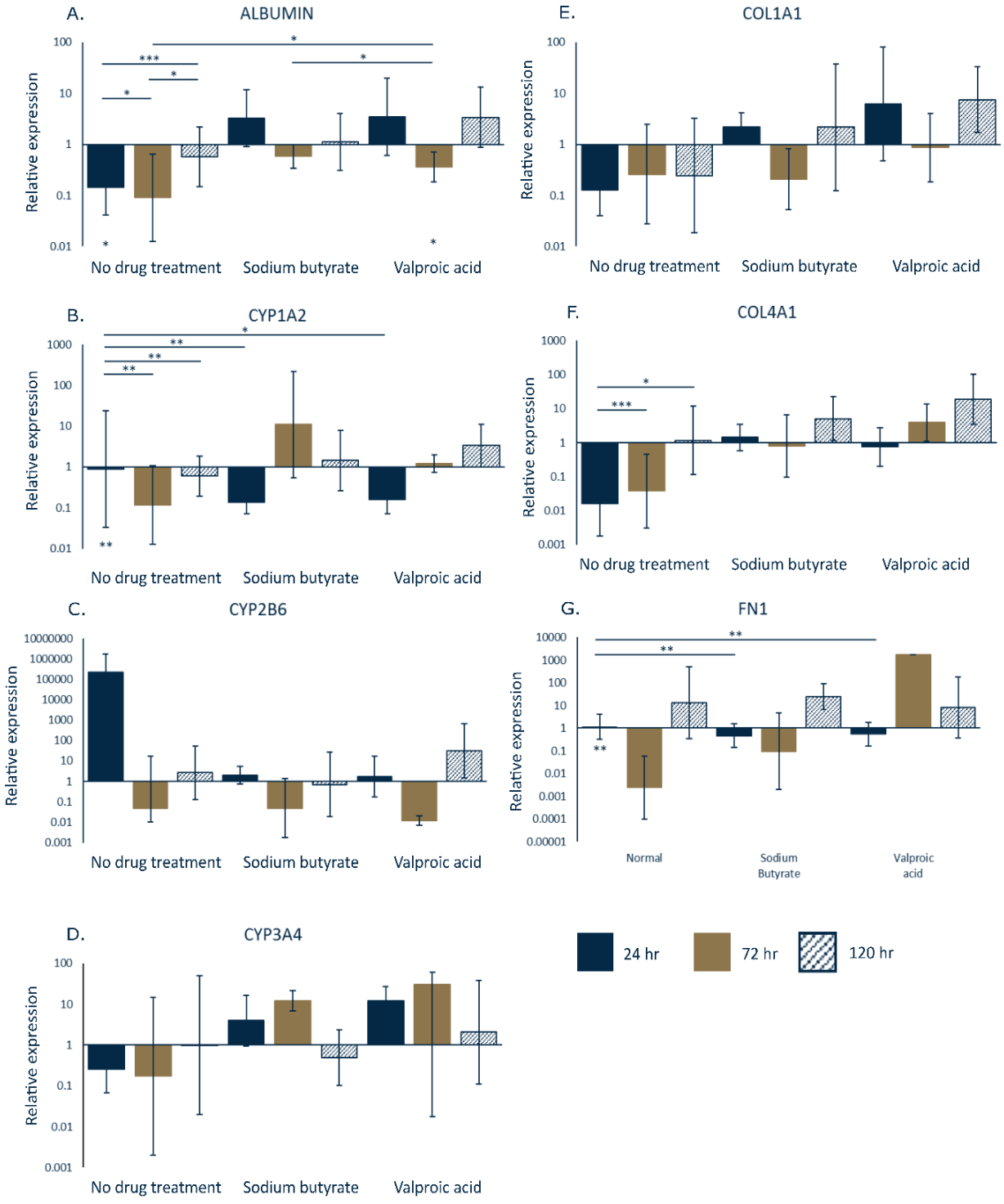

Figure 4.9; Q-PCR analysis of functional cell layer

Quantitative analysis of gene expression was undertaken on the functional cell layer 24, 72 and 120 hours culture, compared to that of the polymer only condition at each time point. mRNA levels of Albumin (A), CYP1A2 (B), CYP2B6 (C), CYP3A4 (D), Collagen I (E) Collagen IV (F), and Fibronectin (G) are represented as fold difference relative to tissue culture plastic controls and relative to the housekeeping gene GAPDH. One-way ANOVA with Games-Howell post hoc testing and minimum n = 4. * = $p < 0.05$ ** = $p < 0.01$. Error bars represent SD.

4.4 Discussion

The production of an alternative to whole organ transplant for treatment of liver disease patients is a vital avenue for research in the face of increasing donor shortages, treatment costs and disease burden on national healthcare systems. Equally, the analysis of primary hepatocyte behaviour on manufactured culture environments is vital to the field of liver biology. A platform which can produce consistent, high quality scaffolds for liver cell survival and function would go some way to furthering knowledge of hepatocyte biology, liver disease and provide a potential treatment and drug testing bed without involving the use of animals and animal tissues.

An electrospun fibre approach was taken in the study to mimic the morphology of healthy fibrillary collagen [24,299], a major constituent of the human liver extracellular matrix *in* vivo. PLA was used for the fabrication of electrospun scaffolds due to its biodegradable nature and elasticity [26], and it's previous use in liver scaffolding studies [228,312], and favourable cell adhesion in initial tests.

The hepatic ECM is a highly plastic biomaterial, subject to constant modification and varies massively between tissues [285], and between healthy and diseased livers [283,284]. As the ECM is such a dynamic structure, it stands to reason that its production and maintenance will be influenced by its surrounding environment in 3D culture [73]. Following on from the work presented in Chapter 3, which revealed that histone deacetylase inhibitors (iHDACs) do indeed alter ECM production in culture, iHDACs were used again to manipulate the cellular environment and alter the ECM production. Sodium butyrate (NaBut) is widely used in industry to increase yield recombinant protein yields in mammalian cells. Valproic acid (ValA) is an FDA approved anti-convulsant which also functions as an iHDAC to increase recombinant protein yields [289]. Histone deacetylase inhibitors influence gene expression via their role in deacetylation; the process by which DNA renders itself less transcriptionally active. Inhibiting this process in cells results in hyperacetylation of histones and subsequently increases transcriptional activity [290]. Once again, results indicate not only that the iHDACs significantly alter the production and consistency of the ECM, but that this technique is robust and reproducible and the ECM it produces,

when harnessed in combination with 3D scaffolding technologies, creates a biofuctionalized scaffold which significantly alters the behaviour of liver cells. Equally, these scaffolds can be simply stored by freezing and remain biologically active for subsequent seeding of primary human hepatocytes.

Previous work took advantage of a bladder epithelial cell line for the initial ECM producing cell layer, however in this instance THLE-3 liver cells were used; a cell line derived from normal primary liver cells derived from the left lobe of a human liver. The cell line was immortalized via infection with SV40 large T antigen and expresses the phenotypic characteristics of normal adult liver epithelial cells. They are nontumorigenic when injected into athymic nude mice, have near-diploid karyotypes, and do not express alpha-fetoprotein. THLE-3 cells metabolize benzo(a)pyrene, N-nitrosodimethylamine, and aflatoxin B1 to their ultimate carcinogenic metabolites that adduct DNA, which indicates that they possess functional cytochrome P450 pathways [144,251]. THLE-3s were used to address minor concerns that the ECM produced by the initial cell layer is not a 'liver ECM' and that this may have an influence on the functional cell layer. However, multiple studies and product continue to use inter-organ and even multi-animal sources of ECM. Several decellularized ECM products on the market are in clinical use to regenerate tissues from which they are not derived, including ALLOPATCH HD™, MatriStem® and Tutoplast® Pericardium[300]. Indeed, hepatocytes are often cultured on 'ECM' surfaces which are not derived from liver, commonly using Matrigel®, a product derived from murine sarcoma which is as yet undefined and experiences batch to batch variability [12,154,301–303]. The promising field of whole organ decellularization is hampered by the availability of human livers, and researchers are subsequently investigating alternative organ and cells sources, such as spleen, bone marrow mesenchymal stem cells [174,304] [174]and various animal sources of livers [36]. With this body of knowledge in mind, the hypothesis that hepatocytes may respond equally favourably to non-liver ECM and remain open to other sources of ECM for hybrid scaffold manufacture is not unwarranted.

The use of primary human hepatocytes was undertaken to address concerns regarding the more commonly used cell lines. Previous work to assess the performance of the hybrid scaffolds, was

undertaken using HepG2s; derived from the hepatocarcinoma of a 15-year-old Caucasian male. They are often used because they are virus free, possess liver specific functions such as ammonia metabolism and albumin synthesis and secrete some growth factors such as insulin and insulin-like growth factor II [138], however they are limited in their translatability because they are derived from a carcinoma and are tumourigenic. By taking advantage of the rare resource provided by donor human livers, the clinical translatability of the hybrid scaffold platform is increased and further knowledge of the behaviour of primary human hepatocytes in engineered culture environment is elucidated. Cell attachment and metabolic viability, and gene expression of both liver function genes and ECM genes at both 24, 72 and 120-hour time points. Additionally, the decellularization of the ECM producing cell layer was validated and immunohistochemical analyses of the hybrid scaffold-ECM constructs upon which the HepG2s were seeded performed.

This work is a robust body of 'next stage' research regarding manipulation of ECM production, and has produced a repeatable method of hybrid polymer-ECM scaffolds with great potential for liver tissue engineering and shown that these scaffolds can be stored frozen for future use and maintain bioactivity and sterility. Further work is required to analyse results and increase translatability. Primary human hepatocytes are a highly valuable research resource; however, the donors are derived from a pool of individuals whose organs are rejected for whole organ transplant into living recipients. This indicates that their livers, and therefore their hepatocytes are not in the utmost of health. Further work should ideally be undertaken using healthy human donor hepatocytes. Furthermore, while hepatocytes are the major parenchymal cell of the liver (making up more than 70% of the cellular mass), they do not exist in isolation and the non-parenchymal cells play an essential role in the in vivo liver [124,305]; future studies should look to include a co-culture element. In addition, recognising the value of proteomic and functional assays (such as ELISAs) in analysing the function of the primary/stem cell derived hepatocytes will be important for future validation of the scaffolds, however at this time these were deemed unnecessary considering the health of the donor hepatocytes Additionally, care should be taken to ensure decellularization agents are completely removed from the scaffolds, due to

their deleterious effect on both cells and ECM [287]. While such considerations are of importance, this chapter clearly demonstrates the potential of these hybrid polymer-ECM scaffolds for tissue engineering, provides a robust initial platform for further research and addresses the hypothesis and aims of this thesis to produce novel hybrid scaffolds which influence liver cell behaviour.

4.5 Conclusion

This chapter developed a new method of creating hybrid polymer-ECM scaffolds by manipulating cells using electrospun scaffold technologies, clinically relevant iHDACs and methods easily modified to fulfil good manufacturing practice (GMP) regulation. To do so, a sacrificial, ECM-producing cell layer was seeded onto a novel electrospun scaffold and then treated with valproic acid or sodium butyrate to biofuctionalize the scaffold with ECM components. Scaffolds with untreated cells and no initial cell layer at all were used as controls. The initial cell layer was removed with a detergent based decellularization method, and the resulting hybrid polymer-ECM scaffolds were stored at -80°C until a source of donor primary human hepatocytes was available for use as a functional cell layer. The work was validated using robust methods such as Q-PCR, mechanical quantification and scanning electron microscopy. Drug induced hybrid polymer-ECM scaffolds had a significant positive influence on the gene expression profile and albumin production of primary human hepatocytes. This data demonstrates promise as a unique method of inducing and altering the production of ECM and that the hybrid scaffolds exert influence upon cells in vitro, as well as future potential as an implantable treatment platform for liver disease patients and testing bed for development of novel pharmaceuticals and treatments for liver disease, as well as the study of primary hepatocyte biology and behaviour.

Chapter 5

The production of synthetically derived fibronectin scaffolds for liver tissue engineering

5.1 Introduction

Synthetic biology and genetic engineering are vital tools for tissue engineers and have been used to alter gene expression, enhance intracellular imaging and study fundamental processes in hepatocytes[313–315]. Recently, synthetic biology tools have been successfully employed to direct both stem cell lineage and fate in 3D constructs[316,317], in the manipulation of biofilms for cell culture[318] and in the production of therapeutic proteins in *in vivo* systems[319,320] demonstrating the ability of synthetic biology techniques to manipulate 3D environments and thus their potential benefit to the field of tissue engineering. Ground-breaking CRISPR[321–323] and minicircle vector[324–326] technologies have made the idea of therapeutic gene editing in humans a viable reality. However concerns exist regarding the safety and subsequently, the translatability of such tools with regards to patient treatment; particularly with the recent revelation that the much lauded CRISPR technology causes mass deletions and mutations *in vivo*[165,327]. Heavily publicised and tragic events such as the 1999 death of 18 year old Jesse Gelsinger[328] and the 2002 clinical trial in which four children developed leukaemia following gene therapy for their Severe Combined Immune Deficiency disease[329] have led to obvious worries regarding the safety of gene therapies.

The inflammatory and immune modulating effects of damage-associated molecular patterns (DAMPs) such as foreign DNA fragments[330] are well documented, however clinical use of decellularized ECM in exogenic and allogenic form has demonstrated great promise, giving no immune response and showing regenerative potential, despite emerging evidence of remnant nucleic acid reservoirs and their influence on cells[331]. This paves the way for using synthetic biology to tissue engineer the ideal ECM environment.

Table 5.1; the advantages of a combinatorial approach to tissue engineering of liver environments.

Polymer scaffolds		**Decellularized tissues**		**Vector technology**		**Combinatorial approach**
✓	Reproducible	✓	Provides biochemical cues of ECM	✓	Customizable protein profile	✓	Mechanically & proteomically customizable
✓	Mechanically customizable	✓	Vasculature exists within tissue	✓	Rapid production of desired proteins	✓	Cell lines used - donors avoided
×	Does not provide complex biochemical cues of ECM	×	Limited donors & donor safety	×	Vector safety concerns	✓	Vectors removed - safety concerns abated

With the potential of synthetic biology for manipulation of protein production in mind, this chapter developed a novel bio-active hybrid scaffold which possesses the potential for customization of the ECM microenvironment. To date, this is the only work where synthetic biology and electrospinning have been combined. The scaffolds were successfully decellularized, and validated the platform using cells representative of the liver, HepG2s.

Figure 5.1; Method schematic

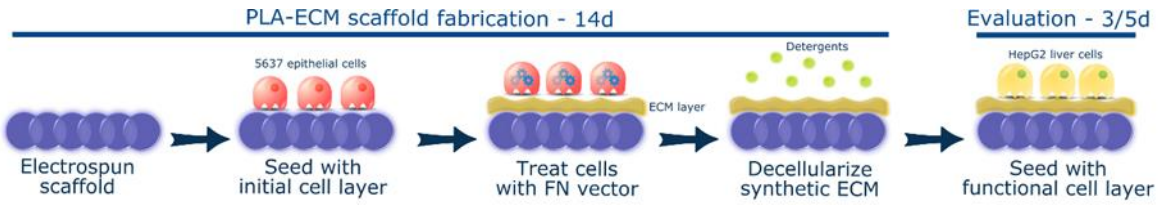

5.2 Materials and Methods

All methods were performed according to protocols laid out in Chapter 2. Specific details are described forthwith.

5.2.1 Electrospinning

A 10% wt/vol solution of poly-L-lactic acid (Goodman) and hexafluoroisopropanol (Manchester Organics) was used to electrospin the scaffolds under the following parameters;

Table 5.2; Electrospinning parameters

Volume per hour	Total volume	Mandrel:needle distance	Positive charge	Negative charge	Mandrel rotation	Needle movement
0.5ml	10ml	14 cm	16kV	-3kV	250rpm	100mm/s

The mandrel was coated in non-stick aluminium foil for collecting the electrospun fibres. The sheets of electrospun fibres were allowed to dry overnight in a fume hood when the electrospinning session was completed. The average fibre size was 1.48µm as calculated by ImageJ plugin 'DiameterJ' [230].

5.2.2 Scaffold Preparation

10mm discs of scaffold were cut from the dry fibre sheet and sterilised with isopropyl alcohol. Scaffolds were placed into an antibiotic/antimycotic treatment for 1 hour.

5.2.3 Initial Layer Cell Seeding and Culture

Scaffolds were removed from the antibiotic/antimycotic treatment solution and rinsed three times for 15 minutes each in complete media; Dulbeccos Minimal Essential Media supplemented with 10% foetal bovine serum, 2mM L-glutamine, 100U/ml penicillin and 100µg/ml streptomycin (Gibco). They were then placed into a fresh 48 well tissue culture plate.

5637 human urinary bladder epithelials (ATCC) were cultured and expanded as per supplier recommendations, using the media described above. Cells for scaffold seeding were trypsinized using

0.25% Trypsin-EDTA (Gibco) from tissue culture flasks and counted using the trypan blue exclusion method. 1 x 10^5 cells at passage 23 were suspended in 100µl of complete media and seeded directly on to the scaffolds. The cells were allowed to incubate in this small volume on the scaffolds for 2 hours, before an additional 400µl of complete media was added.

Media was changed after 24 hours using standard methods and subsequently changed every 48 hours. Controls were scaffold only, i.e. not seeded with an initial cell layer and a 'normal' initial layer i.e. untransfected cells. Initial layers of cells were cultured for 7 days at 37ºC and 5% CO_2 in a humidified incubator.

5.2.4 Fibronectin Vector

Vectors were obtained from the DNASU plasmid repository. In brief, the human fibronectin gene (FN1) was placed into a retroviral expression vector, PJ1520. The insert sequence was verified by sequence analysis and restriction enzyme digest by DNASU. The vector was obtained in DH5-alpha T1 phage resistance *Escheria coli* glycerol stock. The E. coli were cultured under selective conditions; 100µg/ml ampicillin, 34µg/ml chloramphenicol and 7%wt/vol sucrose in LB media. Plasmid extractions were performed using Cambridge Bioscience's Zyppy™ plasmid extraction kit following manufacturer's methods.

5.2.5 Transfections

Transfections were performed using Invitrogen Lipofectamine 3000®. Following titration experiments, a concentration of 1µg plasmid DNA and 0.75µL lipofectamine reagent per scaffold was chosen. The initial layer of 5637 epithelials was cultured on the scaffolds under standard conditions for 7 days. Transfection was performed on the 7th day. Scaffold-cell constructs were then placed into selective media containing 150µg/ml puromycin. The cell-scaffold constructs were cultured under selection for a further 7 days to allow production of the vector derived fibronectin before being decellularized.

5.2.6 Decellularization

Decellularization was performed under sterile conditions at room temperature (19 - 22ºC) and with agitation and then transferred to new 48 well plates for seeding.

5.2.7 Functional layer Cell Seeding and Culture

HepG2 cells were trypsinized using standard methods from tissue culture flasks and counted using the trypan blue exclusion method. 1 x 10^5 cells at passage 17 were suspended in 100µl of complete media and seeded directly on to the scaffolds. The cells were allowed to incubate in this small volume on the scaffolds for 2 hours, before an additional 400µl of complete media was added.

Media was changed after 24 hours and changed every 48 hours after the initial 24 hour adherence and recovery period. This functional layer (FL) of cells was cultured using standard methods for either 3 or 5 days at 37ºC and 5% CO_2 in a humidified incubator.

5.2.8 Live/Dead® Viability/Cytotoxicity assay

To determine cellular viability, cell/scaffold constructs were incubated with 10µm calcein and 2µm ethidium ho-modimer-1 (Ethd-1) for 30 minutes as part of the two colour live/dead assay (Molecular Probes). All images were captured using a Zeiss Axio Imager fluorescent microscope (COIL, University of Edinburgh) at 40x magnification and post processed using ImageJ.

5.2.9 CellTiter-Blue® Cell viability assay

The assay was performed according to manufacturer's instruction (Promega). For each condition group, n = 5. Importantly, cell/scaffolds constructs were moved into fresh 48 well plates to prevent reading activity from tissue culture plastic bound cells. Measurements were read in a Modulus™ II microplate reader at an excitation wavelength of 525 nm and emission wavelength of 580-640 nm and reported as fluorescence. For all groups, minimum n = 5.

5.2.10 Albumin quantification

A bromocresol green (BCG) albumin assay (Sigma) was used to quantify serum albumin produced by the HepG2 functional cell layer over 24 hours at 3 and 5 day time points. The assay was performed according to manufacturer's instructions and results read at an absorbance of 620 nm in a Modulus™ II microplate reader. For all groups, minimum n = 5.

5.2.11 Picogreen® DNA quantification

The Quant-IT™ Picogreen® dsDNA assay kit (Life Technologies™) was employed to establish the efficiency of the decellularization method in removing cellular material and to estimate cell number on the cell/scaffold constructs. Fluorescent intensity measurements were read in a Modulus™ II microplate reader at an excitation wavelength of 480 nm and emission wavelength of 510-570 nm. For all groups, minimum n = 5.

5.2.12 Sectioning and staining

The samples were rinsed three times in PBS (Gibco) for 15 minutes each, then fixed in 4% v/v formalin buffered in saline for 15 minutes at room temperature. After rinsing with fresh PBS, constructs were embedded in low melting temperature polyester wax (Electron Microscopy Supplies) using methods adapted from Steele et al. (2014). In brief, samples are dehydrated through 70-100% ethanol, then incubated in 50:50 ethanol:wax overnight at 45ºC overnight with agitation. The samples were moved into 100% wax for 3 hours at 45ºC and then fresh 100% wax for 1 hour at 45ºC. Samples were embedded and allowed 72 hours to fully cure before sectioning. Immunohistochemical staining was undertaken using antibodies for Collagen I (Stratech), Laminin (Stratech) and Fibronectin (Sigma). All images were captured using a Zeiss Axio Imager system (Centre Optical Instrumentation Laboratory, University of Edinburgh) at 40x magnification and post processed using ImageJ.

5.2.13 Scanning Electron Microscopy

SEM was used to characterise the scaffold architecture. Samples were mounted onto SEM chucks using double sided carbon tape and coated with a thin layer of gold and palladium alloy (Polaron Sputtercoater). All images were captured at 5 kV using a Hitachi S-4700 SEM (BioSEM, University of Edinburgh).

5.2.14 Mechanical Testing

Nanoindentation experiments were undertaken to establish the dynamic properties of scaffolds and decellularized ECM/scaffold constructs using the Keysight/Agilent 5200 nano indenter testing system.

Scaffolds and constructs were subject to indentation by a DCM II actuator flat-ended cylindrical punch (D = 100µm) using a max load of 1g-f. All nanoindentation experiments were carried out on fresh, hydrated (suspended in PBS), unfixed samples in a stainless steel well chuck. A total of 36 indentations were carried out on each sample, 50nm apart. Indent sites were selected using the high precision X-Y stage within the testing system (Agilent). Poissons ratio was assumed to be 0.5 for each sample [273,274]. Allowable drift rate was 0.1nm/s. A NanoSuite (Keysight Technologies) test method "G-Series DCM CSM Flat Punch Complex Modulus" was used for all testing [271,272].

5.2.15 Gene Expression analysis

RNA was extracted from constructs using standard Trizol (Fisher Scientific) methods and purified using Qiagen's RNeasy spin column system. cDNA was synthesised using the Promega's ImProm-II™ Reverse Transcription System.

Quantitative real-time polymerase chain reaction (qRT-PCR) was performed using the LightCycler® 480 Instrument II (Roche Life Science) and Sensifast™ SYBR® High-ROX (Bioline) system. Results were normalized to HepG2s of the same passage number grown on tissue culture plastic and compared to the housekeeping gene Glyceraldehyde-3-Phosphate Dehydrogenase (GAPDH). Analysis was performed using the 2–[delta][delta] Ct method [276,311], n = 5. Albumin (Alb), Cytochrome P450 Family

1 Subfamily A Polypeptide 1 (Cyp1A1), Cytochrome P450 Family 1 Subfamily A Polypeptide 2 (Cyp1A2), Cytochrome P450 Family 3 Subfamily A Polypeptide 4 (Cyp3A4), Collagen Type I alpha 1 (Col1A1), Collagen Type 4 alpha 1 (Col4A1) and Fibronectin Type 1 (FN1) were investigated, forward and reverse primers (Sigma) are detailed in Supplementary Table 1.

5.2.16 Statistical Analysis

One-way ANOVAs with Fishers, Games-Howell and Tukey[280–282] post-hoc testing were performed using Minitab 17 Statistical Software and graphs generated using Origin software (OriginLab, Northampton, MA). Error bars indicate standard deviation. A minimum of n = 3 and max of n = 6 was used for all analysis.

5.3 Results

5.3.1 Cell attachment and survival on scaffolds

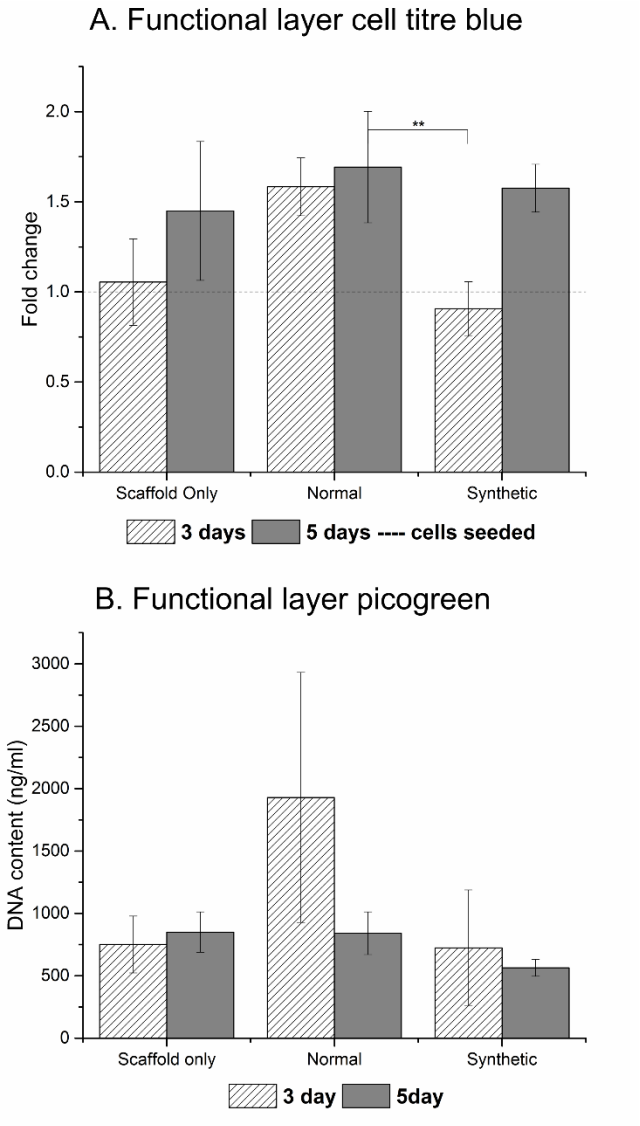

Figure 5.2; Cell titre blue and Picogreen results

Cell titre blue assay indicating metabolic activity (A) and DNA quantitation of the functional layer (B). One way ANOVA with Games Howell post hoc testing, ** = p value <0.01.

When compared to normal ECM derived from untransfected cells (N-ECM) and the scaffold alone (SO), a lower number of HepG2s adhered to the synthetically derived vector driven (SD-ECM) scaffold-ECM constructs (Fig. 5.2). According to the CellTiter-Blue® results (Fig. 5.2A), the SD ECM layer maintained the growth of the HepG2s between days 3 and 5. However, this result is not concurrent with the Picogreen® DNA quantitation (Fig. 5.2B). This is most likely due to different data extraction methods and validation methods in the Picogreen and CellTiter-Blue assays. Both assays possess depth dependencies with regards to their efficiency and effectiveness in extracting data from fibrous scaffold constructs. Additionally, the assays were validated using 2D monolayer cell cultures. This would explain high standard deviations in the Picogreen® DNA quantitation dataset and slight different trends observed between the assays. These finding are corroborated by my recent published work of cells on electrospun scaffolds [28]. Live/Dead® Viability/Cytotoxicity images (Fig. 5.3)

demonstrate the metabolic viability of the functional HepG2 cell layer (FL), and that at day 5 the cells appear to be confluent and living, with low levels of cell death in each condition.

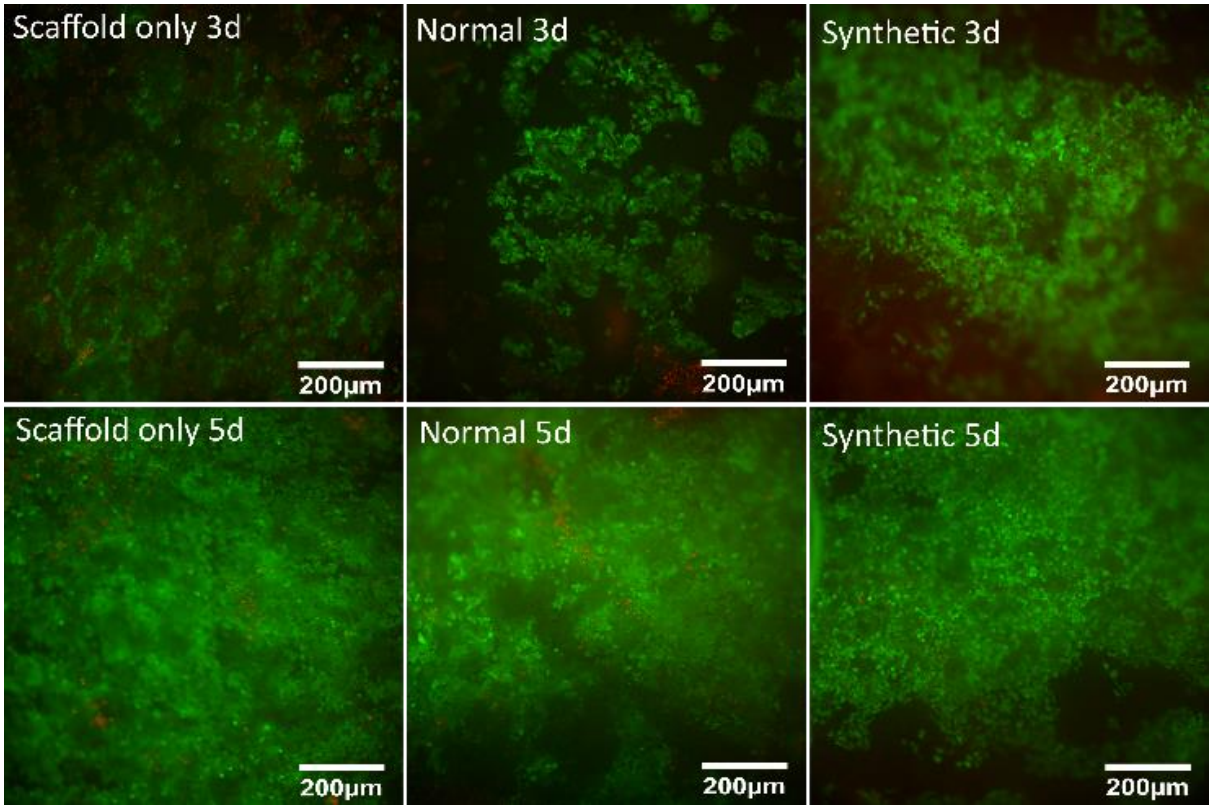

Figure 5.3; Live/Dead® Viability/Cytotoxicity assay

Viability of the FL was assessed by Live/Dead® Viability/Cytotoxicity staining assay. Results demonstrate the FL is metabolically viable at all assessed time points. 40x magnification.

5.3.2 Mechanical characterisation of scaffolds

Reassuringly, both storage (G') and loss (G") modulus demonstrate significant differences between the three conditions (Fig. 5.4). Fibronectin is known to influence both the mechanical profile of the ECM[85,332] and influence the maintenance and structure of other vital ECM proteins, such as collagen[333]. Equally, cells are known to respond to the mechanical and topographical influence a scaffold exerts[296]. Testing was performed at frequencies experienced by the human liver in vivo [292]. Storage modulus (G')

ranged from 22.92±9.14 to 12.29±0.14 MPa and loss modulus (G'') from 2.45±0.93 to 0.15±0.02 MPa at the frequencies detailed in tables 5.3 and 5.4.

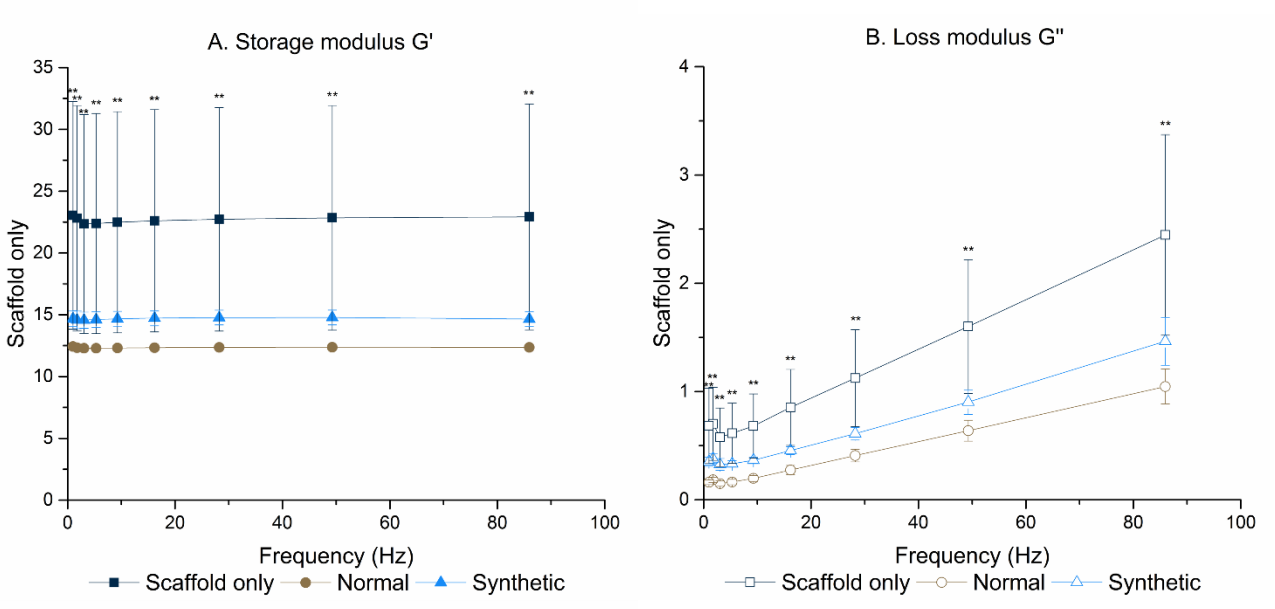

Figure 5.4; Mechanical characterization of decellularized scaffolds

Decellularized ECM/scaffold constructs were subject to nanoindentation experiments to assess their dynamic properties. Results demonstrate significant differences in storage (A) or loss (B) modulus between the three conditions (Tables 3.3 and 3.4). One way ANOVA with Games Howell post hoc testing, ** = p value <0.01.

Table 5.3; Storage modulus G' at mechanical excitation frequencies

Frequency (Hz)	**Storage modulus, G' (MPa)**								
	85.961	49.262	28.231	16.179	9.272	5.313	3.045	1.745	1
Scaffold only	22.92 ±9.14	22.84 ±9.10	22.72 ±9.05	22.60 ±9.00	22.48 ±8.95	22.38 ±8.91	22.34 ±8.86	22.82 ±9.11	23.04 ±9.20
Normal	12.36 ±0.14	12.37 ±0.14	12.36 ±0.14	12.33 ±0.14	12.31 ±0.14	12.29 ±0.14	12.29 ±0.14	12.33 ±0.14	12.43 ±0.14
Synthetic	14.64 ±0.61	14.78 ±0.59	14.77 ±0.59	14.73 ±0.59	14.67 ±0.61	14.61 ±0.62	14.56 ±0.65	14.58 ±0.71	14.68 ±0.65

Table 5.4; Loss modulus G'' at mechanical excitation frequencies

Frequency (Hz)	**Loss modulus, G'' (MPa)**								
	85.961	49.262	28.231	16.179	9.272	5.313	3.045	1.745	1
Scaffold only	2.45 ±0.93	1.60 ±0.62	1.12 ±0.45	0.85 ±0.35	0.68 ±0.30	0.61 ±0.28	0.58 ±0.27	0.70 ±0.34	0.69 ±0.35
Normal	1.05 ±0.16	0.64 ±0.10	0.41 ±0.06	0.28 ±0.04	0.20 ±0.03	0.16 ±0.02	0.15 ±0.02	0.18 ±0.02	0.16 ±0.02
Synthetic	1.46 ±0.22	0.90 ±0.11	0.61 ±0.06	0.45 ±0.04	0.37 ±0.03	0.33 ±0.03	0.33 ±0.05	0.38 ±0.04	0.35 ±0.04

5.3.3 Biochemical characterisation of the hybrid polymer-ECM scaffolds

Differences in the biochemical profile of the different ECMs were demonstrated by immunohistochemistry performed on decellularized hybrid scaffold sections (Fig. 5.5). Hepatic cells are very responsive to extracellular matrix proteins; particularly Collagen I, Laminin and Fibronectin

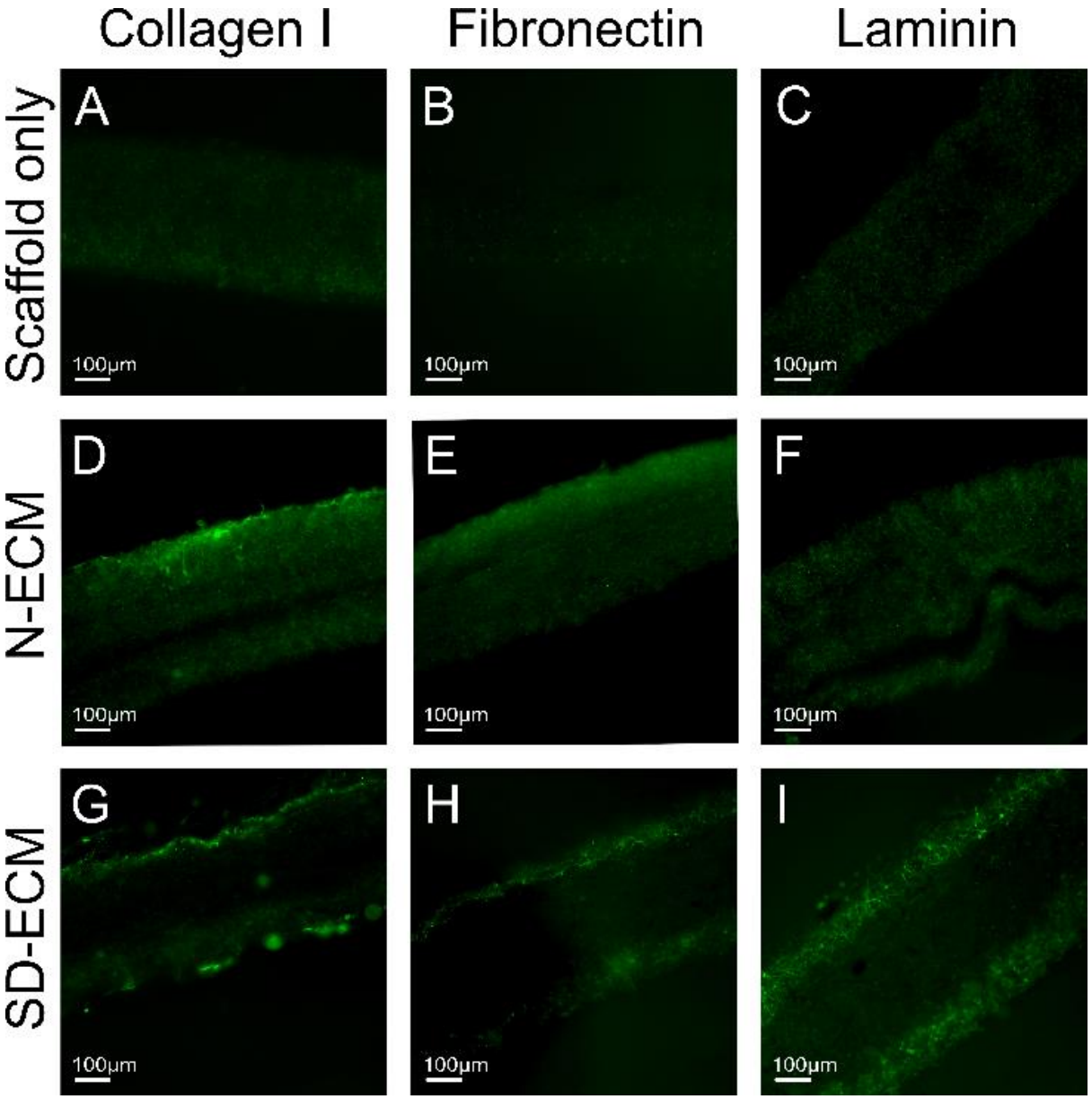

Figure 5.5; Immunohistochemical investigation

Immunohistochemistry staining of the decellularized ECM/scaffold constructs revealed significant differences in ECM components. Stains were performed for Collagen I, Laminin and Fibronectin, post processed using ImageJ . Staining demonstrates retention of major liver ECM proteins Collagen I (D, G), Fibronectin (E, H) and Laminin (F, I) following decellularization. Additionally, SO condition shows no positive staining as expected (A, B, C).

[78,166,174]. Fibronectin is ubiquitous in healthy liver [12,53], and antibody staining reveals altered levels of fibronectin in the synthetically derived ECM, as expected due to the introduction of the fibronectin vector (Fig. 5.5H). ECM proteins do not exist in isolation, and fibronectin is known to influence the generation and laydown of other ECM proteins including collagen I and laminin [333,334], as evidenced in Fig. 5.5G and 5.5I when compared to N-ECM. The N-ECM is collagen I rich (Fig. 5.5D) with some fibronectin and laminin also present (Fig. 5.5E & 5.5F). Of note is that the SD-ECM appears to be concentrated on the outer layers of the electrospun scaffold. This could be due to the transfected cells being in fewer number than those which were not transfected (N-ECM), so they did not penetrate the scaffold to the same extent.

5.3.4 Gene expression of HepG2s in response to hybrid polymer-ECM scaffolds

Genes associated with both liver function and ECM production were assayed for gene expression (Fig. 5.6). Albumin expression, a marker of appropriate liver cell differentiation and function, appears upregulated between day 3 and day 5 in each condition, confirming appropriate development of the cells. At day 5, expression is significantly upregulated in comparison to HepG2s grown on tissue culture plastic (TCP) on the SD-ECM constructs; with the highest levels of expression observed in SO and SD-ECM conditions. Additionally, albumin mRNA expression is downregulated in comparison to TCP at day 3 in all conditions (Fig. 5.6A). Cytochrome P450s (CYP) are a family of enzymes involved in metabolism of xenobiotics and toxic compounds in the liver[160,335,336]. Cyp1A1 mRNA expression is significantly altered in comparison to TCP (Fig. 5.6B); upregulated at day 3 and downregulated at day 5. Cyp1A2 mRNA expression is consistently significantly downregulated in all but one condition; day 3 N-ECM (Fig. 5.6C). Cyp3A4 mRNA expression is upregulated in every condition, with a significant upregulation observed in response to SD-ECM (Fig. 5.6D). In addition, three ECM genes important for normal liver composition were assayed [53,77]; Fibronectin (Fig. 5.6E), Collagen I (Fig. 5.6F) and Collagen IV (Fig. 5.6G). Considering the plastic nature of ECM, these genes are of interest with regards to

ongoing modification of the tissue microenvironment despite hepatocytes not being the main producers of ECM proteins in the liver [53,283].

Collagen I is consistently upregulated, with significant upregulation observed at day 5 on SD-ECM. Equally, Fibronectin mRNA expression is significantly upregulated on day 5 SD-ECM constructs, though downregulated at day 3 on SO and N-ECM constructs. Collagen IV mRNA expression is consistently upregulated in each condition, with significant changes observed in all but day 3 N-ECM and SD-ECM. While such alterations in gene expression are promising, this chapter refrains from further assumption regarding cell response without further proteomic and functional analyses.

Table 5.5; RT-PCR primers

Albumin (Alb)	For - CCTGTTGCCAAAGCTCGATG Rev - GAAATCTCTGGCTCAGGCGA
Cytochrome P450 Family 1 Subfamily A Polypeptide 1 (Cyp1A1)	For - AATTTCGGGGAGGTGGTTGG Rev - GATGTGGCCCTTCTCAAAGGT
Cytochrome P450 Family 1 Subfamily A Polypeptide 2 (Cyp1A2)	For - CTTCGCTACCTGCCTAACCC Rev - GTCCCGGACACTGTTCTTGT
Cytochrome P450 Family 3 Subfamily A Polypeptide 4 (Cyp3A4)	For- TTTTTGGATCCATTCTTTCTCTCAA Rev- TCCACTCGGTGCTTTTGTGT
Collagen Type I alpha 1 (Col1A1)	For - GGACACAGAGGTTTCAGTGGT Rev - GCACCATCATTTCCACGAGC
Collagen Type 4 alpha 1 (Col4A1)	For - GACCCCCGGGAGAAATAGGT Rev - TTTGAAAAAGCAATGGCACTCC
Fibronectin Type 1 (FN1)	For - GAACAAACACTAATGTTAATTGCCC Rev - TCTTGGCAGAGAGACATGCTT
Glyceraldehyde-3-Phosphate Dehydrogenase (GAPDH)	For – GTCTCCTCTGACTTCAACAG Rev - GTTGTCATACCAGGAAATGAG

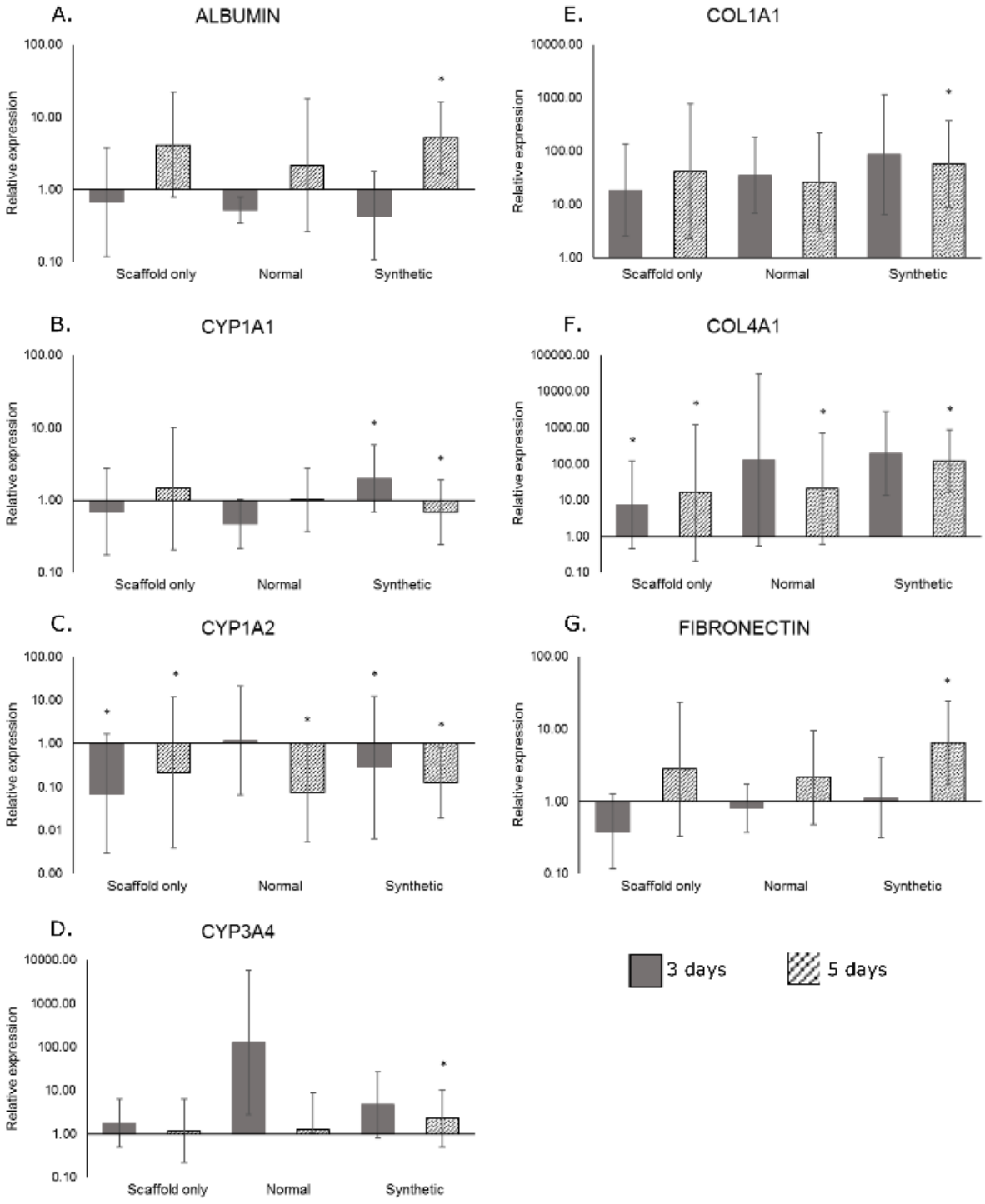

Figure 5.6; Q-PCR analysis of functional cell layer

Quantitative analysis of gene expression was undertaken on the functional cell layer at three- and five-days culture, compared to that of HepG2s of the same passage and culture periods grown on tissue culture plastic. mRNA levels of Albumin (A), CYP1A1 (B), CYP1A2 (C), CYP3A4 (D), Collagen I (E) Collagen IV (F), and Fibronectin (G) are represented as fold difference relative to tissue culture plastic controls and relative to the housekeeping gene GAPDH. One-way ANOVA with post hoc testing and n = 4. * = $p < 0.05$ ** = $p<0.01$. Error bars represent SD.

5.3.5 Albumin production

Albumin levels are indicative of hepatocyte health and response to the microenvironment [78]. Each condition results in differing levels of albumin production, with significant differences in protein levels observed between SO and SD-ECM at both 3 days and 5 days (Fig. 6), indicating that the N-ECM encouraged albumin production more than SD-ECM

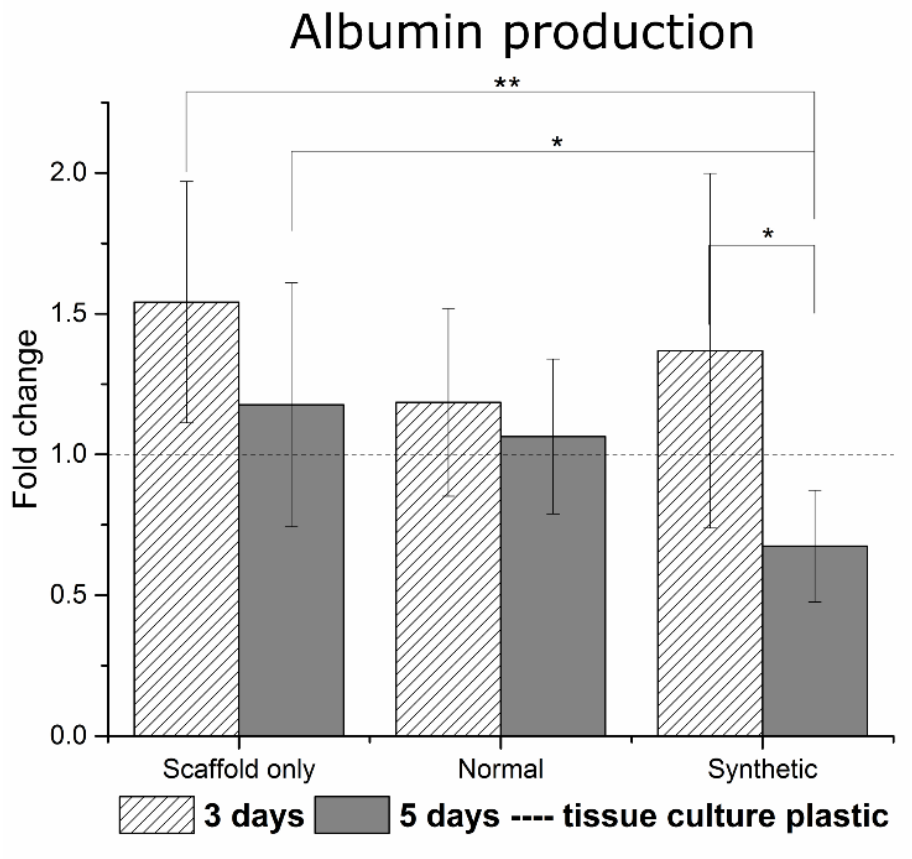

.

Figure 5.7; BCG albumin assay

Albumin production between conditions, showing significant changes between SO and SD-ECM conditions at both time points. One way ANOVA with Games Howell post hoc testing, * = p value <0.05. ** = p value <0.01.

5.3.6 Confirmation of decellularization

Decellularization was confirmed using Picogreen® DNA quantitation (Fig. 5.8G) and histological staining (Fig. 5.8A-F). A tenfold reduction in DNA combined with visual confirmation of an absence of

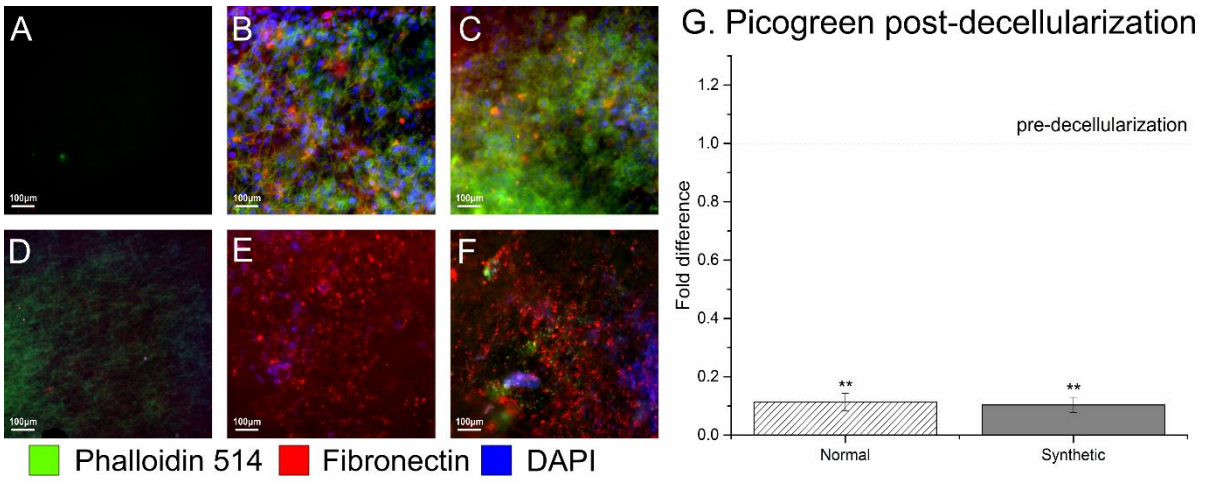

Figure 5.8; Confirmation of decellularization

Effectively decellularized constructs, with minimum remnant DNA detected by IHC (E,F) or picogreen (G). Scaffolds pre-decellularization shown in (A), (B) and (C). One way ANOVA with Games Howell post hoc testing, ** = p value <0.05. Scaffold only (A, D), N-ECM (B,E) and SD-ECM (C, F).

DAPI nuclear staining and Phalloidin-514 actin staining on decellularized constructs, plus the presence of fibronectin antibody staining on both the N-ECM and SD-ECM decellularized constructs (Fig. 5.8E&F) provides evidence of efficient decellularization methods, and that synthetically derived fibronectin is present on the hybrid scaffolds.

5.4 Discussion

The extracellular matrix provides a microenvironment for cells which is not yet fully understood, nor replicable by existing manufacturing methods[30,337–339]. By manipulating human cells to produce a customizable blend of ECM components, and combining this with replicable electrospun scaffolds and decellularization methods the shortage of donor derived ECM bioscaffolds and the issues regarding animal-sourced biomaterials are negated[30,287]. Additionally, this platform has the potential to be used to model not only 'healthy' ECM microenvironments, but also those of disease and developing states.

Fibrous electrospun scaffolds mimic the morphology of healthy fibrillary collagen[24,25,340,341]. PLA was used to fabricate the scaffolds, chosen for its compatibility with hepatocytes[166] and its use in multiple types of medical device due to its predictable biodegradation rate and mechanical properties[342,343].

Fibronectin was chosen as the protein to synthetically overexpress due to its vital role in the liver[85,344] and its interaction with other ECM components such as collagen and laminin[332,333]. Fibronectin is a large dimeric adhesive glycoprotein which exists in both cellular and plasma forms, with roles in regenerating tissues, embryonic development and regulation of cell behaviours such as adhesion and migration[345]. The role of fibronectin in the liver is still unclear, with inhibition of fibronectin production or deposition improving fibrosis outcomes[10,65]. However, its vital role in the hepatic ECM is demonstrated by mutant mice who were specifically null in only the liver for both plasma and cellular fibronectin. The fibronectin-null livers not only develop highly disorganized/diffuse collagenous ECM networks, but when fibrogenesis was induced the null livers experienced more extensive fibrosis; thought to be due to fibronectins role in regulating TGF-β1 bioavailability[344]. Additionally, homozygous fibronectin null mutants display early embryonic lethality, while heterozygotes (with 50% of the normal plasma fibronectin levels) appear normal; suggesting a dose dependent role for fibronectin in development[346].

As an initial assessment of these novel hybrid scaffolds the attachment and function of a commonly used liver cell line, HepG2s was investigated, when cultured on the synthetically derived hybrid

scaffolds versus a wild type 'normal' hybrid scaffold and the scaffold alone. The HepG2 cell line was derived from the hepatocarcinoma of a 15 year old Caucasian male. They are often used because they are virus free, possess liver specific functions such as ammonia metabolism and albumin synthesis and secrete some growth factors[138]. Cell attachment and viability, albumin production and gene expression of both liver function genes and ECM genes at 3 and 5 day time points were assayed. Additionally, the decellularization method was validated and both immunohistochemical and Raman spectrum analyses (data not shown) were undertaken of the hybrid scaffold-ECM constructs upon which the HepG2s were seeded.

These results indicate not only that synthetically derived ECMs provide a viable method of biofunctionalising electrospun polymer scaffolds, but that the composition of the synthetically derived ECM-polymer hybrid scaffolds influences liver cells. That albumin production is significantly altered between SO and SD-ECM conditions, but not N-ECM conditions supports this assertion. Gene expression of key hepatic genes was altered on day 5 of SD-ECM conditions in every gene tested, whereas SO and N-ECM conditions only influence CYP1A2 and COL4A1 expression; demonstrating that the composition of the ECM is highly influential in tissue engineering. This in turn leads to questions regarding donor-donor variability of current decellularization work and its influence upon hepatic behaviour and a need for more reproducible hepatic microenvironments that this platform provides.

While this study forms a robust initial proof of principle regarding the exploitation of synthetic biology for scaffold manufacture, and has produced a novel hybrid synthetically derived ECM- polymer scaffold with great potential for liver tissue engineering, further work is required to analyse results and increase translatability. Vector technologies and synthetic biology present obvious concerns with regards to patient safety[319,347], and care should be taken to ensure all bacterial/ viral constructs are removed from the ECM layer. Detergent based methods used to strip the ECM of cells can be detrimental to the bioscaffold[287,288], disrupting native tissue ultrastructure, decreasing glycosaminoglycan (GAG) content and reducing collagen integrity[38,39] as well as disrupting lipid-lipid,

lipid-protein and protein-protein interactions[40]. Care should be taken to optimise this procedure in the future. HepG2s provide a convenient method of initial viability testing of the scaffolds, but they are derived from a carcinoma and as such criticism of their clinical relevance is well placed. Further studies will utilise primary or stem cell derived hepatocytes to combat such criticism. Additionally, recognition of the value of further proteomic and functional assays (such as ELISAs and Alkaline Phosphatase quantitation) in analysing the function of hepatocytes. Further, the importance of ensuring decellularization agents are removed from the constructs should not be underestimated, due to their influence upon cells and ECM[35,287]. While such criticisms are important to consider, this work clearly demonstrates the potential of synthetic biology for the design of bespoke ECMs and provides a robust initial platform upon which further, improved studies can be built.

5.5 Conclusion

This study demonstrates a novel method of creating a biologically bespoke hybrid ECM-polymer scaffold for liver tissue engineering, addressing the aims and hypothesis of this thesis. In order to achieve this, a sacrificial ECM-producing cell layer was transfected using a protein producing fibronectin vector on an electrospun scaffold, biofunctionalising the scaffold with a biologically bespoke ECM. Scaffolds with wild type untransfected cells and no initial cell layer at all were used as controls. The sacrificial cell layer was successfully removed with a detergent based method and the hybrid synthetically derived ECM-polymer scaffolds seeded with HepG2 liver cells for validation. Results were validated using multiple well characterized methods, including mechanical quantitation, Q-PCR and immunohistochemistry. The synthetically derived PLA-ECM scaffolds exert biological influence upon liver cells, manipulating their microenvironment and resulting in alterations in gene expression profile, protein synthesis and cell attachment and survival. These differences are not recapitulated in the polymer only scaffolds, indicating the ECM component of the hybrid scaffolds exerts a separate influence to the polymer alone. Such data demonstrates promise as a unique

method of creating biologically bespoke ECMs and exerting influence upon cell populations both *in vivo* and *in vitro*.

These novel scaffolds exhibit great promise both as an implantable patient treatment for liver tissue engineering, for adaptation to other tissues and as a useful tool for development of 3D liver cell culture platforms with potential for both *in vivo* cell analysis and novel pharmaceutical research.

Chapter 6

Blended protein and decellularized human liver:poly-L-lactic acid scaffolds for liver tissue engineering

6.1 Introduction

In an effort to address the shortage of ECM like environments for hepatocytes, researchers have been incorporating bioactivity into scaffold environments for hepatocytes[11,12,15]. Decellularized extracellular matrix is the obvious avenue for such research[30,348], and while results are promising a decellularized liver still requires a donor liver and recellularization. Obstacles such as necrosis, immune reaction and residual decellularization agents are all yet to be fully addressed for decellularized whole organs to be a truly viable option[36,213,348,349]. Individual ECM components in the form of gelatin[298,350], collagen[43,44,351], laminin[77,83,297] and fibronectin[65,80,352] have all been employed; each influencing the hepatocytes survival and function and providing insight into the complex cell-matrix interactions present in the hepatic microenvironment. However each protein individually represents a small fraction of the bioactive molecules present in the ECM and when used in isolation cannot recapitulate the healthy hepatic matrix[77,78,353].

With this work in mind this chapter develops a new scaffold for liver tissue engineering; for the first time incorporating human liver ECM (hLECM) directly into the fibres of electrospun polymer scaffolds. By combining the best of current scaffolding technology; reproducible polymeric scaffolds and efficiently decellularized human donor liver this work produced a niche bioinfluential microenvironment which influences the function of cultured human hepatocytes.

Figure 6.1 Method schematic

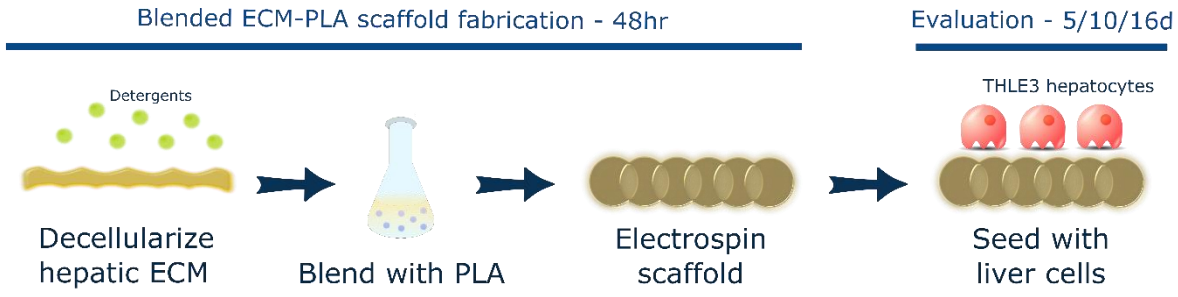

6.2 Methods

All methods were performed according to protocols laid out in Chapter 2. Specific details are described forthwith.

6.2.1 Ethics and Governance

All human tissue used in this study was provided by NHS Organ Donation and Transplant and NHS Blood and Transplant. No organs/tissues were procured from prisoners. Ethical approval was granted for the project from the North of Scotland Research Ethics Committee, ref 16/NS/0083. Informed consent for organ donation for research purposes was obtained in accordance with the Helsinki Declaration. Tissue from one liver was used in this study.

6.2.2 Decellularization

Decellularization of human liver tissue was performed at room temperature (19 - 22ºC) in a custom made perfusion decellularization system (Fig 2.2, Chapter 2 Methods). Decellularized tissue was stored at -20ºC ant defrosted at room temperature prior to use.

6.2.3 Preparation of hLECM

Decellularization was confirmed using the Quant-IT™ Picogreen® dsDNA assay kit (Life Technologies™), performed according to manufacturer's instructions. The ECM was lyophilized in a FreeZone® 4.5 freeze-drier (Labconco®) before milling in a PM100® planetary ball mill (Retsch®).

6.2.4 Preparation of proteins for electrospinning

The powdered hLECM was solubilized in 0.25M acetic acid (Acros Organics) at a concentration of 25µg per ml. Bornstein and Traub Type I collagen (Sigma Type VIII), powder from human placenta (hBTC1), human recombinant laminin 521 (hRL521) (Biolamina), and human plasma fibronectin (hFN) (Merck) were all solubilized similarly and incorporated into the electrospinning solutions using the same

methods. A control scaffold consisting of polymer only in the 9:1 HFIP:0.25M acetic acid was also incorporated into the study.

6.2.5 Preparation of electrospinning solutions

A 22% wt/vol solution of poly-L-lactic acid (Goodman) and 9ml hexafluoroisopropanol (Manchester Organics) was dissolved overnight at room temperature with agitation. 1ml of 0.25M acetic acid (Acros Organics) containing 25µg protein was added to the 22% poly-L-lactic acid:HFIP solution and combined at room temperature under agitation for 1 hour.

6.2.6 Electrospinning

Blended solutions were used to electrospin scaffolds under the following parameters;

Table 6.1; Electrospinning parameters

Volume per hour	Total volume	Mandrel:needle distance	Positive charge	Negative charge	Mandrel rotation	Needle movement
2.5ml	7.5ml	23 cm	16kV	-3kV	300rpm	100mm/s

The average fibre size of each scaffold is reported in Table 6.2;

Table 6.2; Fibre sizes

Scaffold	Polymer only	hBTC1	hFN	hRL521	ECM
Average fibre Size (µm)	1.82	1.60	1.72	1.17	2.01

6.2.7 Scaffold Preparation

10mm discs of scaffold were cut from the dry fibre sheet and sterilized in 30% isopropyl alcohol then placed into an antibiotic/antimycotic treatment.

6.2.8 Cell Seeding and Culture

THLE-3 cells were trypsinized using standard methods from tissue culture flasks and counted using the trypan blue exclusion method. 1 x 10^5 cells at passage 14 were suspended in 100µl of complete media

and seeded directly on to the scaffolds. The cells were allowed to incubate in this small volume on the scaffolds for 2 hours, before an additional 400µl of complete media was added.

Media was changed after 24 hours and changed every 48 hours after the initial 24 hour adherence and recovery period. This functional layer (FL) of cells was cultured using standard methods for either 5, 10 or 16 days at 37ºC and 5% CO_2 in a humidified incubator.

6.2.9 Live/Dead® Viability/Cytotoxicity assay

To determine cellular viability, cell/scaffold constructs were incubated with 10µm calcein and 2µm ethidium homodimer-1 (Ethd-1) for 30 minutes as part of the two colour live/dead assay (Molecular Probes). Calcein is actively converted to calcein-AM in living cells, which then appear green when excited during fluorescence microscopy. Ethd-1 only accumulates in dead cells, which subsequently appear red. The method allows differentiation between dead and viable cells. The scaffolds were rinsed three times in $CaCl_2$/$MgCl_2$ free PBS to remove excess dye and placed onto a standard microscope slide with a 25mm glass coverslip (VWR). All images were captured using a Zeiss Axio Imager fluorescent microscope (COIL, University of Edinburgh) at 40x magnification and post processed using ImageJ.

6.2.10 CellTiter-Blue® Cell viability assay

The assay was performed according to manufacturer's instruction (Promega). For each condition group, minimum n = 5. Importantly, cell/scaffolds constructs were moved into fresh 48 well plates to prevent reading activity from tissue culture plastic bound cells. Measurements were read in a Modulus™ II microplate reader at an excitation wavelength of 525 nm and emission wavelength of 580-640 nm and reported as fluorescence.

6.2.11 Albumin quantification

A bromocresol green (BCG) albumin assay (Sigma) was used to quantify serum albumin produced by the THLE-3 functional cell layer over 24 hours at 5, 10 and 16 day time points. The assay was performed

according to manufacturer's instructions and results read at an absorbance of 620 nm in a Modulus™ II microplate reader. For each condition group, minimum n = 5.

6.2.12 Picogreen® DNA quantification

The Quant-IT™ Picogreen® dsDNA assay kit (Life Technologies™) was employed to establish the efficiency of the decellularization method in removing cellular material and to estimate cell number on the cell/scaffold constructs. The assay was performed according to manufacturer instructions. Fluorescent intensity measurements were read in a Modulus™ II microplate reader at an excitation wavelength of 480 nm and emission wavelength of 510-570 nm. Minimum n= 5 for each group.

6.2.13 Sectioning and staining

The samples were rinsed three times in PBS (Gibco) for 15 minutes each, then fixed in 4% v/v formalin buffered in saline for 1 hour at room temperature. After rinsing with fresh PBS, constructs were stained using antibodies for Collagen I (Stratech), Laminin (Stratech) and Fibronectin (Sigma). Additionally, top down images of cells on the scaffolds were obtained by staining with DAPI (Sigma), Phalloidin (Sigma) and E-Cadherin (Abcam). All images were captured using a Zeiss Axio Imager system (Centre Optical Instrumentation Laboratory, University of Edinburgh) at 40x magnification and post processed using ImageJ.

6.2.14 Scanning Electron Microscopy

SEM was used to characterise the scaffold architecture. Samples were mounted the samples onto SEM chucks using double sided carbon tape and coated them with a thin layer of gold and palladium alloy (Polaron Sputtercoater). All images were captured at 5 kV using a Hitachi S-4700 SEM (BioSEM, University of Edinburgh).

6.2.15 Mechanical Testing

Tensile testing was undertaken to establish the dynamic properties of scaffolds and hLECM using the Instron 3367 dual column universal testing system with Bluehill 3 software. The system was fitted

with Instron biopulse submersible pneumatic side action grips and a 50N load cell. A gauge length of 20mm and an extension rate of 20mm/min were used for all tensile tests. Analyses was conducted using the incremental modulus method as previously described[24,26].

Six samples of each scaffold with a width of 10mm and a gauge length of 80mm were obtained from each sheet. Samples were fixed to 'C' shaped card templates to allow consistent set up during tensile testing. Samples were tested until failure. N=6.

6.2.16 Gene Expression analysis

RNA was extracted from constructs using standard Trizol (Fisher Scientific) methods and purified using Qiagen's RNeasy spin column system. cDNA was synthesised using the Promega's ImProm-II™ Reverse Transcription System.

Quantitative real-time polymerase chain reaction (qRT-PCR) was performed using the LightCycler® 480 Instrument II (Roche Life Science) and Sensifast™ SYBR® High-ROX (Bioline) system. Results were normalized to THLE-3s of the same passage number grown on tissue culture plastic and compared to the housekeeping gene Glyceraldehyde-3-Phosphate Dehydrogenase (GAPDH). Analysis was performed using the 2–[delta][delta] Ct method [276,311], n = 5. Albumin (Alb), Cytochrome P450 Family 1 Subfamily A Polypeptide 1 (Cyp1A1), Cytochrome P450 Family 1 Subfamily A Polypeptide 2 (Cyp1A2), Cytochrome P450 Family 3 Subfamily A Polypeptide 4 (Cyp3A4), Collagen Type I alpha 1 (Col1A1), Collagen Type 4 alpha 1 (Col4A1) and Fibronectin Type 1 (FN1) were investigated, forward and reverse primers (Sigma) are detailed in Supplementary Table 1.

6.2.17 Statistical Analysis

One-way ANOVAs with Games-Howell and Tukey post-hoc testing was performed using Minitab 18 Statistical Software. Multiple comparisons tests were used following the Ryan Joiner test for normality and Bartlett's test for the homogeneity of variances. The Tukey post hoc test was used where Bartlett's test result is not significantly different i.e. the null hypothesis of population variances being equal is

not rejected. The Games-Howell test does not assume equal variances and sample sizes and was performed on the ranked variables similar to other nonparametric tests. The Games-Howell post hoc test is used where Bartlett's test result is significantly different i.e. the null hypothesis of population variances being equal is rejected. Error bars indicate standard deviation. A minimum of n = 3 and max of n = 6 was used for all analysis. * = p value <0.05, ** = p value <0.01, *** = p value <0.001.

Methods are as previously described in published papers[128,129].

6.3 Results

This chapter's results demonstrate a method of incorporating proteins directly into a scaffold environment and of making impactful use of a valuable tissue resource which would otherwise be wasted. Protein:polymer scaffolds containing human liver ECM exert a significant positive influence on the gene expression profile, albumin production, attachment, and survival of liver cells which cannot be recapitulated by individual ECM components. These scaffolds show great potential not only for the future of liver tissue engineering and patient treatment and are easily adaptable for other organs and tissues.

6.3.1 Mechanical characterization of scaffolds

Tensile testing revealed significant increases in the Young's Modulus between the ECM scaffold and every other scaffold (Fig 6.2), indicating that incorporating human liver ECM into the scaffold results in a significantly stiffer environment for hepatocytes. Interestingly, hRL521 scaffolds were significantly more elastic than both hBTC1 and hFN scaffolds (Table 3). Such results demonstrate that the mechanical influence of varying ECM compositions influence on cell behaviour and function cannot be discounted in studies and must be considered when analysing biological results.

Table 6.3; Elasticity (0-10% strain)

Scaffold	Polymer only	hBTC1	hFN	hRL521	ECM
Average Young's Modulus (MPa)	11.11 ±1.88	12.53 ±1.96	13.2 ±1.40	8.15 ±1.35	18.49 ±1.40

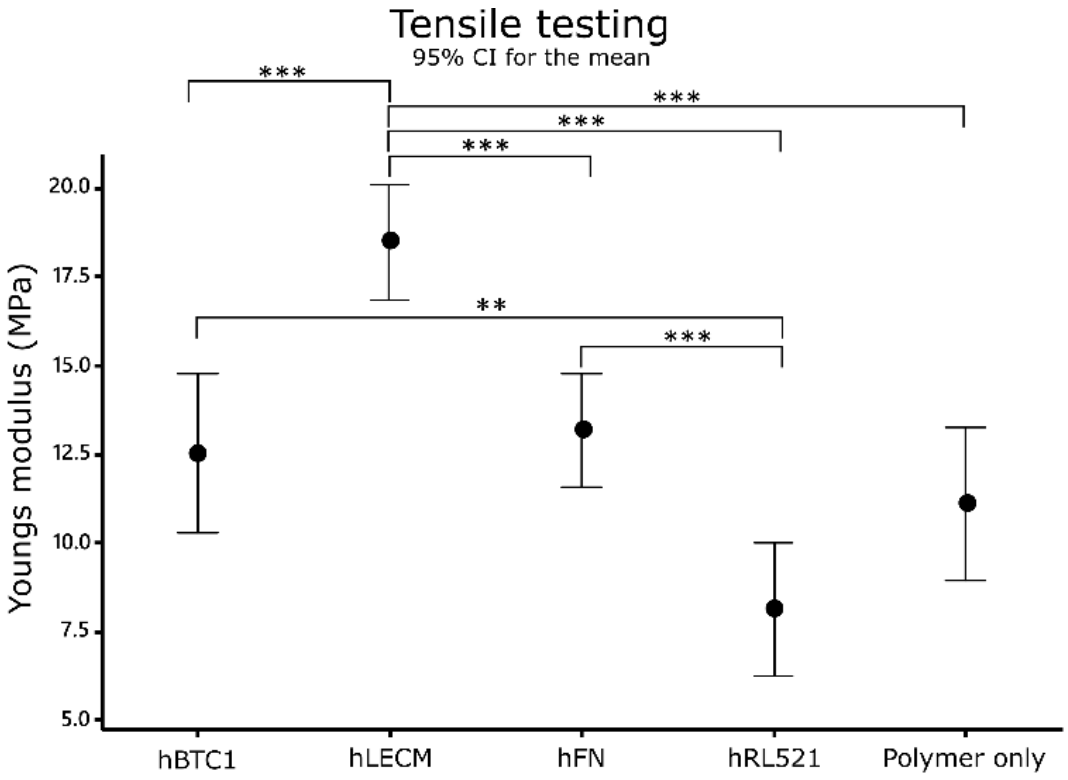

Figure 6.2; Mechanical testing

Incorporating human liver ECM into the scaffold produces a significantly stiffer environment for hepatocytes. hRL521 scaffolds are significantly more elastic than both hBTC1 and hFN scaffolds. N= 6, Data shown as mean ± 95% confidence interval with statistics performed using One way ANOVA with Games Howell post hoc analyses

6.3.2 Histological characterisation of the scaffolds

The presence of the various proteins was demonstrated by immunohistochemistry performed on the scaffolds (Fig 6.3). Collagen I, Laminin and Fibronectin were chosen because of their long established influence on hepatic cells [78,149,166]. Fibronectin is ubiquitous in healthy liver, collagen I is the largest component of the healthy liver extracellular matrix and laminin is of particular importance in the differentiation of liver cells as well as for cell adhesion and liver regeneration [12,53]. Each is clearly present in their respective single protein scaffolds, as well as in varying degrees in the ECM scaffold, with no false positive staining observed in the control polymer only condition. Reassuringly, this indicates that the antigens to which the primary antibodies bind were not affected by the

solubilisation or electrospinning process, and therefore that some bioactivity is maintained throughout the scaffold fabrication process.

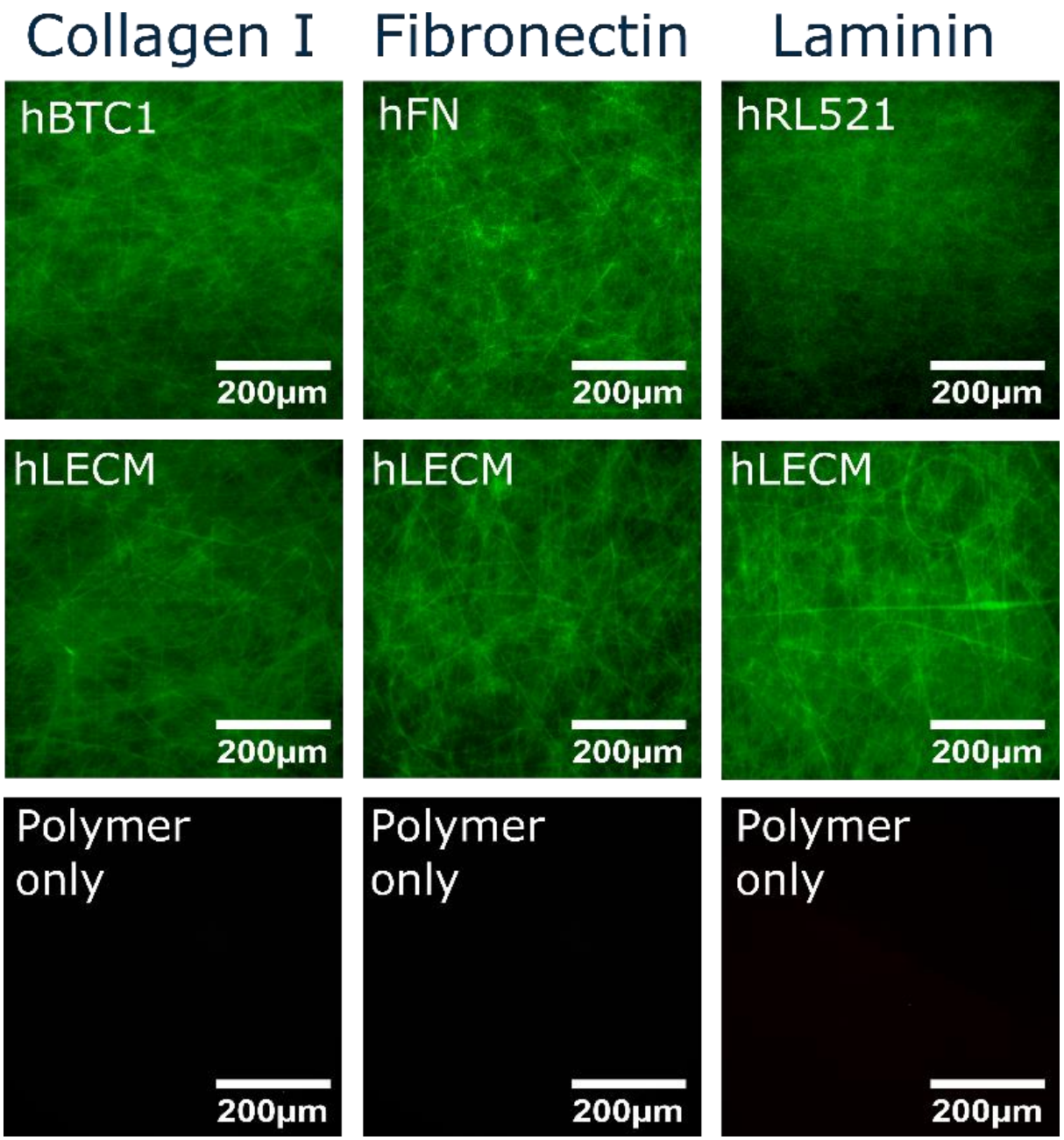

Figure 6.3; Immunohistochemistry

Collagen I, Fibronectin and Laminin are all present in their respective single protein scaffolds, as well as in varying degrees in the ECM scaffold, with no false positive staining observed in the control polymer only condition. Stains were performed for Collagen I, Laminin and Fibronectin, post processed using ImageJ. 10x magnification.

6.3.3 Cell attachment and survival on scaffolds

Every scaffold maintains the survival of the THLE-3 liver cells and the number of cells increases significantly between each time point (Fig 6.4A). Interestingly, between conditions the only significant difference observed is between the polymer only and hLECM scaffolds at day 5, with higher

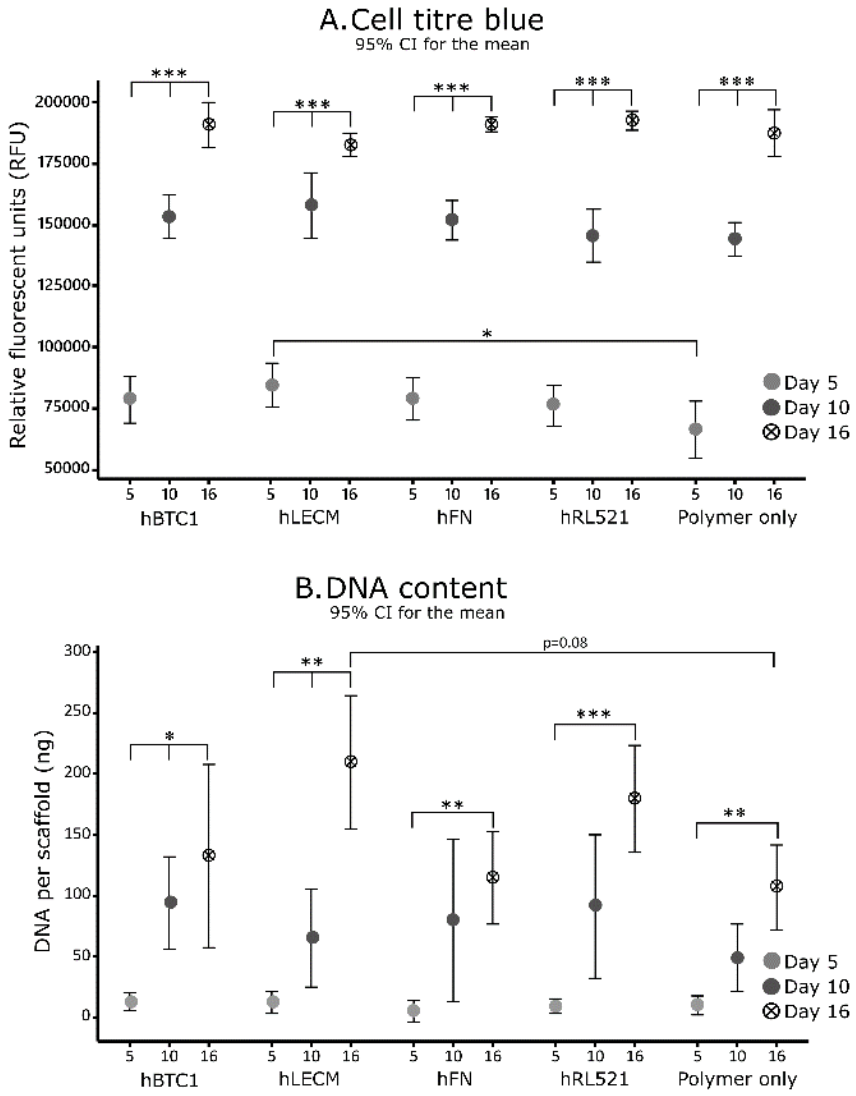

Figure 6.4; Cell viability – Cell titre blue and picogreen DNA quantitation

Cell adherence was assessed by CellTiter-Blue® Cell viability assay (A) and further confirmed by Quant-IT™ Picogreen® dsDNA assay (B). Minimum n = 5. Data shown as mean ± 95% confidence interval with statistics performed using One-way ANOVA with Tukey post hoc testing. * = $p < 0.05$ ** = $p < 0.01$, *** = $p < 0.001$. Each condition maintains cell survival and the number of cells increases significantly between each time point (Fig 4A). A significant increase in fluorescence is observed between the polymer only and hLECM scaffolds at day 5 indicating that the presence of human liver ECM has a positive influence on the early expansion and/or metabolic activity of hepatocytes. A consistent pattern is observed in the DNA concentration (Fig 4B) on the scaffolds.

fluorescence observed on the hLECM scaffolds indicating that the presence of human liver ECM in the scaffold has a positive influence on the early expansion and/or metabolic activity of hepatocytes.

Reassuringly, a similar pattern is observed in the DNA concentration (Fig 6.4B) on the scaffolds, with a difference observed between polymer only and hLECM conditions once again; more DNA is present on the hLECM scaffolds indicating the presence of more cells. Live/dead viability/cytotoxicity images (Fig 6.5) further demonstrate the continuing metabolic viability of the hepatocytes at the latest time point (16d), with a confluent population of viable cells present on the scaffold and a low level of cell death on each scaffold. Presence of a dense cell layer is further confirmed by SEM imaging (Fig 6.6), with a carpet of cells visible in each condition at 16d.

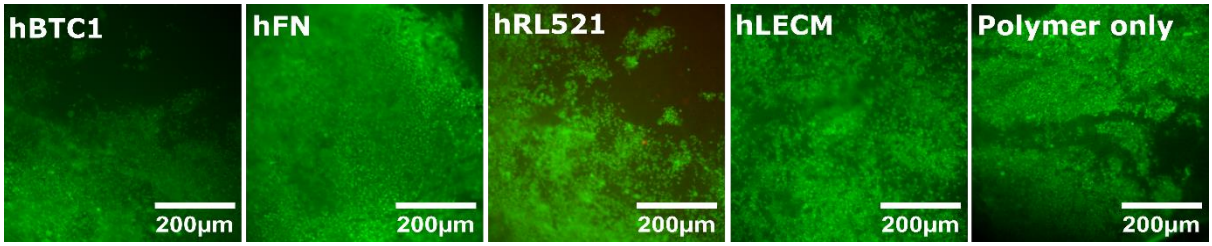

Figure 6.5; Cell viability – Live Dead

Live/Dead® Viability/Cytotoxicity staining analyses demonstrates continuing metabolic viability of the hepatocytes at the latest timepoint (16d), with a confluent population of viable cells and a low level of cell death on each scaffold. Viability of the FL was assessed by. Results demonstrate the FL is metabolically viable at all assessed time points. 10x magnification.

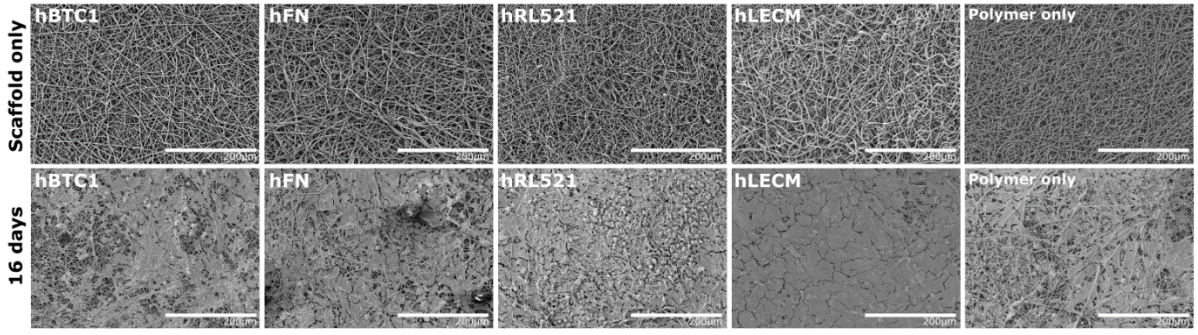

Figure 6.6; SEM analysis

The scaffolds were assessed for consistency and fibre size via scanning electron microscopy and subsequent image analysis. Fibres diameter was determined by DiameterJ 34, n = 4. 250x magnification. Presence of a dense cell layer is further confirmed by SEM imaging with a carpet of cells visible in each condition at 16d.

6.3.4 Gene expression of THLE-3s in response to hybrid polymer-ECM scaffolds

Genes associated with both liver function and ECM production were assayed for gene expression (Fig 6.7). Albumin (Fig 6.7A), a marker of appropriate liver cell differentiation and function, and Cytochrome P450s (CYP1A1 Fig 6.7B, CYP1A2 Fig 6.7C and CYP3A4 Fig 6.7D), a family of enzymes involved in metabolism of xenobiotics and toxic compounds in the liver [160,335,336] were both studied. In addition, three ECM genes important in normal liver composition were assayed [53,77]; Fibronectin (FN1 Fig 6.7E), Collagen I (COL1A1 Fig 6.7F) and Collagen IV (COL4A1 Fig 6.7G). Considering the constantly altering and responsive nature of ECM, these genes are of interest with regards to ongoing modification of the tissue microenvironment despite hepatocytes not being the sole producers of ECM proteins in the liver [53,283]. Results were normalised to the polymer only condition to assay the influence of the protein component of the scaffolds on gene expression.

Only the human liver ECM scaffold maintains albumin expression in the expected pattern, increasing over time; as seen in primary hepatocytes and other liver cell lines [354]. CYP1A1 is consistently downregulated in comparison to the polymer only scaffolds in every condition over the 16 days. CYP1A2 is down regulated in comparison to polymer only, with significant changes observed on hRL521 and hBTC1 scaffolds at day 16. CYP1A2 is upregulated at day 16 on liver ECM, indicating an improvement in metabolic capability for hepatocytes grown in the hLECM scaffolds. All the single protein environments increase the expression of CYP3A4 in comparison to the polymer only environment. These changes in metabolic genes demonstrate the importance of protein microenvironment for hepatocyte function. hLECM scaffolds caused an increase in COL1A1 expression over the 16 days, with expression 100 times higher at 16 days than on the polymer only environment. Significant changes were observed between days 5 and 10, and 10 and 16 of hFN and hRL521 scaffolds, and between days 5 and 16, and 10 and 16 on hBTC1 scaffolds. COL4A1 was downregulated over time on all the single protein scaffolds, but increases over time on the scaffolds which incorporate hLECM, although is overall reduced in comparison to polymer only. Significant changes were observed

between days 5 and 16 on hBTC1 and days 10 and 16 on hRL521 scaffolds in FN1 expression. Reduction in expression of FN1 was slight in comparison to polymer only scaffolds.

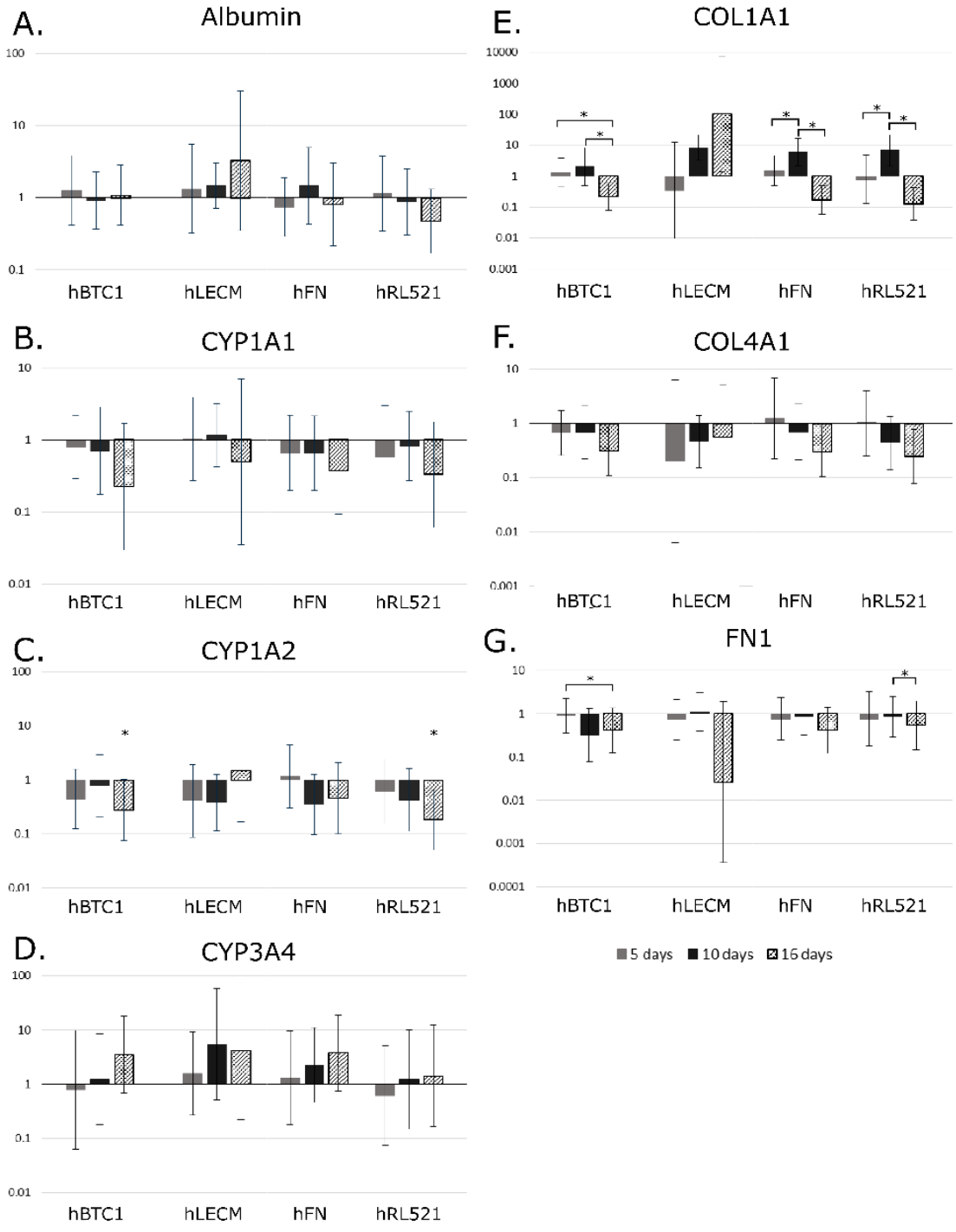

Figure 6.7; Q-PCR of key hepatic genes

Quantitative analysis of gene expression was undertaken on the functional cell layer at five, ten and sixteen days of culture, compared to that of the same culture periods grown on polymer only scaffolds. Results are represented as fold difference relative to tissue culture plastic controls and relative to the housekeeping gene GAPDH. One-way ANOVA with Games Howell and Tukey post hoc testing and minimum n = 5. * = p <0.05 ** = p<0.01, *** = p<0.001. Error bars = SD.

6.3.5 Albumin production

Albumin levels are indicative of hepatocyte health and response to the microenvironment [11,78]. hBTC1, polymer only and liver ECM all exhibit increasing production of albumin over time (Fig 6.8), as expected in a healthy hepatocyte culture and correlating with gene expression patterns observed in Fig 6.7. Interestingly, a significant increase in albumin production is observed on liver ECM scaffolds when compared with hRL521 scaffolds at day 10, and compared to hBTC1 scaffolds at day 5; indicating that hLECM is important for the production of albumin and that individual ECM components are not sufficient to boost the production of albumin.

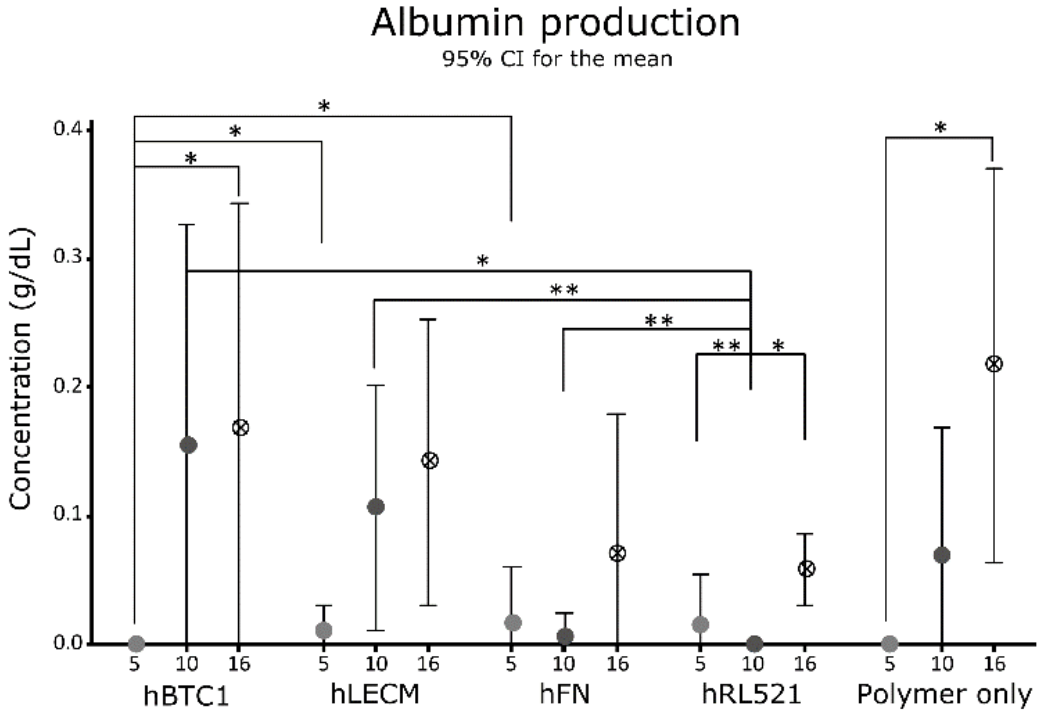

Figure 6.8; Albumin production

Serum albumin produced by the THLE-3 cells over 24 hours at 5, 10 and 16 day timepoints. n = 6. Data shown as mean ± 95% confidence interval with statistics performed using One-way ANOVA with Games Howell and Tukey post hoc testing and minimum n = 5. * = $p < 0.05$ ** = $p<0.01$, *** = $p<0.001$.

6.3.6 Validation of tissue decellularization

Picogreen was employed to validate the decellularization process and ensure minimal DNA was present in the scaffolds. Results reassure us that our decellularization process is effective.

Table 6.4; Remnant DNA in scaffolds

Scaffold	Native liver	Decellularized liver	Polymer only	hBTC1	hFN	hRL521	hLECM
DNA (ng p/mg)	340.57	0	0	0	0	0	0

6.4 Discussion

A bioactive scaffold for hepatocyte culture is an important avenue for tissue engineering, meeting the need for an environment which supports the behaviour and function of hepatocytes in as close to an *in vivo* like state as possible. An optimised environment for hepatocytes can address the need for appropriate *in vitro* models and the shortage of treatment options and donor livers for patients. By combining a valuable and underused resource such as human liver tissue with the reproducibility of polymeric scaffold manufacture a platform that can produce consistent, bioinfluential scaffolds for liver cell survival and function is developed.

An electrospun fibre was chosen as the basis of these scaffolds as their fibrous nature mimics the morphology of native fibrillary collagen I in the liver extracellular matrix. PLA was used for this study because of its history of use in medical devices due to its biodegradation profile and compatibility with cellular environments. It is of note that the fibre diameter of each scaffold varied between proteins despite being electrospun under identical parameters. This method was employed to ensure the proteins were exposed to the same levels of electrical charge, solvent concentration and spinning time. The influence of fibre size when culturing upon electrospun scaffolds is yet to be fully elucidated, with evidence that variations between 0.3-1.3µm do not influence cell behaviour[340,355].

The livers used in this study are an underutilised resource. The donors are approved for transplant, but for varying reasons the liver may not be taken for transplant. In this situation, approved researchers are contacted and offered the tissue. The livers would otherwise be disposed of as clinical waste. This platform provides a method of using these livers to create niche, biologically active microenvironments for hepatocytes without the concerns that come with the more commonly used animal sourced tissue. Equally, the decellularization process developed as part of this work is effective and importantly, does not rely upon an intact vasculature for efficient decellularization unlike other successful work. This means that traumatically injured livers which are beyond surgical repair, those with occluded vasculature or partial lobes of liver. While the field of whole organ decellularization is

a promising avenue for tissue engineers, it remains that the field is hampered by a lack of suitable whole organs. This method circumvents the need for whole organs. The platform vastly enlarges the pool of tissue available for this avenue of research and makes use of a precious resource donated by bereaved families which would otherwise go to waste when unsuitable for transplant.

These results indicate that hLECM has an influence on hepatocytes which cannot be recapitulated by individual ECM components, confirming that there is a complex and not fully understood relationship between cells and the native extracellular matrix. This method is robust, reproducible and by harnessing ECM protein in conjunction with 3D scaffolding technologies a bioactive scaffold which significantly alters the behaviour of liver cells was produced.

ECM products are in clinical use, with products such as SIS, ALLO- PATCH HD®, MatriStem®, and Tutoplast® all being used in regenerative medicine for the benefit of patients. Equally, the decellularization method completely removed the potentially immunogenic DNA from the ECM, allaying translational concerns.

To assess scaffold performance THLE-3 cells were used; a non-tumorigenic line derived from the left lobe of a normal adult human liver[144]. Their adherence, growth and performance was assessed at 5, 10 and 16 days post-replating when cultured *in vitro* on the scaffolds containing hFN, hRL521, hBTC1 and hLECM versus scaffolds containing no protein; polymer only. Cell attachment and viability was assayed, as was gene expression of both liver function genes and ECM genes at both 5, 10 and 16 day time points. Additionally, retention of ECM proteins in the scaffolds through the electrospinning process and the effective decellularization of the human liver ECM were validated.

This work has resulted in a robust platform for the production of blended protein:polymer scaffolds and a reproducible method of liver decellularization which does not rely on obtaining an entire organ. This chapter developed bioactive scaffold for liver tissue engineering which influence the behaviour and function of THLE-3 human hepatocytes. There is vast potential for the application of these scaffolds and methodology in the field of liver tissue engineering and the wider tissue engineering

community however further work is required to analyse the scaffolds influence on the cells and further improve the translatability of this work. While cell lines such as THLE-3s are undisputedly a highly valuable research resource, criticism of cell lines behaviour *in vitro* and the translatability of such results abounds within the scientific community [144,251]. It is important to undertake future work using primary or stem cell-derived hepatocytes[22,155,356–358] and incorporate other important stimuli such as fluid flow to combat such criticism[37,99,175]. Furthermore, while the parenchymal hepatocytes make up more than 70% of the cellular mass, they do not exist in isolation and non-parenchymal and immune cells play an essential role in the in vivo liver; future studies should look to consider co-culture[75,142,153].

The value of proteomic and functional assays (such as enzyme-linked immunosorbent assays) in analysing the function of the hepatocytes will be vital in any future studies. At this juncture these tests were deemed unnecessary considering the critiques of cell lines. Additionally, while every care was taken to ensure the complete removal of decellularization agents in the manufacture of these scaffold, this should be validated to ensure further translatability of this work, considering the deleterious effects of remnant detergent on cells [213,246,287].

While such concerns are valid, this work clearly demonstrates the potential of blended ECM scaffolds for liver tissue engineering, utilising an underused and valuable resource of human liver tissue rejected for transplant and provides an robust initial platform for further research.

6.5 Conclusion

This work established a robust platform for the production of reproducible blended protein:polymer scaffolds for liver tissue engineering by combining human liver ECM with electrospun polymer manufacturing technologies. To do so, this chapter develops a consistent and effective method of decellularizing the tissue using a pressurised flow device. The ECM was successfully solubilized and incorporated directly into the fibres via the electrospinning solution. Additional scaffolds for comparison containing hFN, hBTC1 and hRL521 were manufactured. These were all compared to a scaffold manufactured with no protein. The protein:polymer scaffolds were seeded with a liver cell

line to assess their biological influence. The work was validated using robust methods such as Q-PCR, mechanical quantification, and SEM. Liver ECM containing protein:polymer scaffolds exert a significant positive influence on the gene expression profile, albumin production, attachment, and survival of liver cells.

The results presented here demonstrate great promise as a method of incorporating liver ECM and other proteins directly into a scaffold environment and of making impactful use of a valuable tissue resource which would otherwise be wasted. These scaffolds show great potential not only for the future of liver tissue engineering and patient treatment but are easily adaptable for other organs and tissues. Additionally, they are a useful tool for the development of 3D liver cell platforms, which can be used for in vivo cell analysis and novel pharmaceutical research.

Chapter 7

Discussion and Conclusions

7.1 Discussion

The aim of this PhD project was to investigate the effect of bioengineered scaffolds on the behaviour and function of hepatocytes in culture; within the remit of the liver tissue engineering field. In each chapter I utilised different method of combining ECM components with an electrospun polymer scaffold and investigated the hybrid scaffold's influence on cells representative of the human liver. Specifically, the aims and objectives of this project were as follows;

1. The manufacture of electrospun polymer scaffolds capable of maintaining hepatocyte survival

2. Combine polymer scaffolds with cutting edge protein production techniques to manufacture practical, reproducible and translatable hybrid polymer:protein scaffolds for liver tissue engineering

3. Assess the impact of polymer only and hybrid scaffolds on hepatocyte survival and behaviour.

Each of these aims has been addressed via the development of novel hybrid scaffolds to influence hepatocyte cell behaviour, survival and function.

Electrospun polymer scaffolds biodecorated with drug induced[11] and synthetically derived[228] ECMs influence on both cell lines and primary human hepatocytes have been studied. Blended electrospun scaffolds containing single ECM proteins and decellularized human ECM effect on cell line derived hepatocytes have also been investigated.

Chapter 3 used histone deacetylase inhibitors to alter the ECM produced by a bladder cell epithelial line when cultured on an electrospun PCL scaffold. The constructs were decellularized, and displayed significant changes in their mechanical properties, as well as an altered biochemical profile. A HepG2 cell line was cultured on the decellularized constructs, and displayed markedly altered survival, metabolic activity and gene expression between the conditions. With the critique of this work in mind, namely the use of tumour-derived cell lines, I proceeded to further the translatability of this work in Chapter 4. A non-cancer liver cell line was used to derive the ECM component of the hybrid scaffolds, and PLA was used due to its favourable biodegradable nature and superior cell adhesion properties.

These scaffolds were decellularized and subsequently stored until a source of primary human hepatocytes was available. These scaffolds also demonstrated altered mechanical properties and biochemical profiles. They were seeded with the primary hepatocytes and the differences in ECM proteins and mechanical changes induced a subsequent alteration in the behaviour of the hepatocytes. Albumin production demonstrated changes in each condition, as did gene expression data; with particular note taken of the correlation between albumin gene expression patterns and albumin production.

Chapter 5 took advantage of synthetic biology techniques to introduce a protein producing vector into the ECM producing initial layer of cells. Mechanical changes were reassuringly present, as was a change in the biochemical profile of the ECM when assessed using immunohistochemistry. Hep-G2 cells were subsequently cultured on the decellularized constructs and demonstrated changes in cell survival, gene expression and albumin production.

Chapter 6 made use of decellularized human tissue to create a novel blended scaffold environment for THLE-3 liver cells. Scaffolds containing decellularized human liver, fibronectin, laminin-521 and collagen I were compared to elucidate the influence of single ECM proteins vs whole ECM. Drastic mechanical differences were observed between scaffolds, and immunohistochemistry demonstrated retention of the proteins in the electrospun scaffolds. Interestingly, Only the human liver ECM scaffold maintains albumin expression in the expected pattern, increasing over time; as seen in primary hepatocytes and other liver cell lines [354] with the same pattern observed in albumin production. Initial results indicate that hLECM has an influence on hepatocytes which cannot be recapitulated by individual ECM components, leading us to conclude that there is a complex and not fully understood relationship between cells and the native extracellular matrix.

Electrospinning was chosen as the scaffold fabrication method because of its morphological similarity to collagen fibres[359]. PLA and PCL were used for the electrospinning process due to their biocompatibility[360] and use in existing medical devices[361,362]. PLA in particular was chosen as cells grew

preferentially on PLA fibres in initial tests. However, other scaffold fabrication methods may be appropriate for combination with ECM proteins, including hydrogels[193,194], phase-separated[363] and hollow fibre[364] scaffolds. Novel polymers which influence hepatic behaviour are also, of course, an option and some work is focussing on finding novel substrates for liver tissue engineering[202,306,365,366].

Immortal cell lines were used throughout this work. Critique of the use of cell lines is discussed in depth by multiple publications, however as a 'proof-of-concept' tool, they are invaluable to researchers[111,138,172]. They allow us to assess biocompatibility and differences between experimental conditions without the need for ethical approval for use of animal or human tissue donors or the complexities or economic burden of primary cell extractions and culture. Where cell lines are used, this work is very conservative in its extrapolation to the *in vivo* condition and care is taken to use non-cancer derived cell lines where possible.

Primary human hepatocytes are considered the gold standard human liver cell model[367]; although availability of human liver tissue and difficulties in isolating viable cells limits their widespread use. Many factors influence the successful extraction of hepatocytes (I.e. their viability and yield), including donor age and gender, the presence of steatosis or fibrosis and levels of donor serum enzymes[133,368]. Two-step perfusion methods are said to give the highest yields of hepatocytes, however such methods require intact and unimpeded vasculature; not always a possibility in donated human tissue[369]. As such, a collagenase digestion method was utilised here, and iso-density percoll centrifugation used to separate viable parenchymal cells from cell aggregates, debris, and nonparenchymal cells[258]. By ensuring Ithe hepatocytes are separated from the non-parenchymal cells a homogenous cell population which can be used for qRT-PCR analyses is obtained, as opposed to a co-culture which could not be easily assayed for hepatocyte gene expression. Cell purity could be further analysed using flow cytometry and the expression of CD95 on hepatocytes, however data suggests these methods reliably result in >90% purity[370].

qRT-PCR allows for the quantification of gene expression, however gene expression does not always equate production of proteins due to the complex post-translational mechanisms involved[371,372]. Contamination of RNA samples is also a concern during the process; primers were designed to encompass exon junctions to avoid gDNA amplification (if contamination was present). Following purification, optical density was used to determine the quantity of RNA and presence of contamination from phenol/DNA[373]. Using these methods increases reliability and reassures that RNA expression is truly being assayed, as opposed to DNA content. Further work to assay cell function could confirm gene expression results, a next stage analysis would be an enzyme linked immunoabsorbant assay (ELISA) or mass spectrometry to quantify proteins produced.

Oxidation-reduction (redox) assays like MTT and CellTiter Blue are both stable, homogenous assays commonly used to indicate mitochondrial activity and therefore metabolic viability in cells. One of the disadvantages is optical interference. Additionally some culture additives can give false positive results[374]. However, by combining these assays with other indicators of cell life and metabolic activity such as LiveDead and the BCG Albumin production assay reliability Is increased.

Cell and protein imaging were performed using immunohistochemical (IHC) staining and fluorescent imaging in the majority of cases. In addition to these techniques, in chapter 4, CARS and TPEF imaging were used. IHC staining is a qualitative technique; blocking with buffers such as gelatine or bovine serum albumin must be performed to prevent non-specific binding of proteins. Antigen retrieval may be required to allow antibody binding. Inappropriate fixation can limit the resolution of molecules of interest by masking or damaging antibody binding sites. Samples less than 3um thick may produce very weak staining. However IHC as a technique is commonly used as a qualitative technique and is considered, when used with appropriate negative and positive controls, to be indicative of antigen presence[375]. CARS is an effective technique for imaging and was utilised here to image polymer scaffolds and to assess the presence of ECM proteins and cells. Exploiting this technique in conjunction with TPEF allowed images of a single plane along the Z-axis, producing high quality images. Overall, it

is an effective qualitative method for determining the presence of particular markers and has been used here and previously to confirm the presence of desired cells[376]

Liver tissue engineering is a rapidly evolving field, with multiple internationally renowned scientists focussing on the urgent need for an alternative to whole organ transplant. The need for a reliable cell source is possibly the most heavily researched field, with several groups focussing on the development of hepatocyte-like cells derived from iPSCs and progenitor cells with a view to producing an unlimited supply of functional human hepatocytes with minimal ethical concerns regarding their source. Co-culture of parenchymal and non-parenchymal cells is the focus of several groups, with liver spheroid technology proving promising[153]; hepatocytes can be maintained for 100s of days in such conditions[377], and early stage work is being undertaken using these in animal transplant studies and fluidic devices[378]. Decellularization of whole organs has become a major focus of the liver tissue engineering community, recognising the opportunity to combine expertise in deriving large numbers of hepatocyte-like cells from progenitors and iPSCs with which to recellularize an otherwise useless organ. Some work is being undertaken to elucidate the influence of 3D culture variables, such as shear and oxygen concentration on hepatocytes, with a view to combining this knowledge with scaffolding expertise to produce liver 'devices' which can be used to dialyse toxins from patients' bloodstreams or implant in place of an organ.

The field of hepatocyte biology has given us insight into the behaviour of liver cells in vivo, and of the progress and treatment options for liver disease. However, critics argue the field is heterogeneous and fractured. Historic use of products such as Matrigel and gelatin to grow cells in culture, as well as premature extrapolation of results gained from these cells to in vivo and 3D systems has led to an unclear picture of the true behaviour of primary parenchymal and non-parenchymal cells. Researchers are beginning to pull the field together, with molecular biologists, cell culture experts and bioengineers working together to gain a true picture of the hepatic niche, with projects like HepatoSys, a consortium of German research centres studying the physiology and pathophysiology of the human

liver using systems biology. As a result of this heterogeneous background, this thesis is particularly careful not to make assumptions about expected hepatocyte behaviour and aim to present all data as a valuable contribution to the field of liver tissue engineering with no comment made on 'improving' function or 'preferred' conditions for the hepatocytes used in these studies.

The work demonstrated here combines scaffolding, synthetic biology and decellularization techniques to produce hybrid, bioactive environments for hepatocyte culture. Polymer scaffolds have been previously been utilised in liver tissue engineering studies, primarily via their use in fibre-based bioreactors and hydrogels. To date, research using electrospun polymers for liver tissue engineering has been minimal despite its advantages in manufacture, mechanical properties and collagen-like fibrillar nature. The polymers used in these studies are prevalent in the tissue engineering community due to their biocompatibility, biodegradation profile, mechanical properties, low cost and simplicity of manufacture. While other polymers may be more beneficial to hepatocytes, the lack of robust research into the influence of scaffolding materials and polymers on hepatocyte behaviour this research provides a basis upon which to perform further studies. Screening-methods for novel materials such as those used by the Hay group at University of Edinburgh may prove invaluable in finding an ideal polymer for liver tissue engineering[196,365].

While decellularization of whole organs is proving beneficial and providing a wealth of insight into liver biology and function, it none-the-less requires an ongoing source of whole, undamaged and healthy livers. By combining these techniques with novel ECM generating methods as has been achieved in this project, the need for whole organs is circumvented and provide a bioactive environment with a demonstrative influence on hepatocytes. By taking advantage of methods used by industrial protein production; drugs to alter protein yield/production and synthetic biology to derive extracellular matrix proteins, novel scaffold manufacturing methods and environments for hepatocyte culture were created without the use of rare whole organs. When the opportunity to obtain human liver tissue presented itself, the work within this thesis provided the advantage of knowledge in decellularization

to investigate for the first time the influence of single ECM components in comparison to 'complete' human ECM, providing insight into the interactions of ECM components and hepatocytes.

7.2 Further work

Critique of each study is present within their respective chapters; however, one major criticism is the lack of proteomic analyses of the scaffolds. Mass spectrometry (MS)-based high-throughput proteomics is the core technique for large-scale protein characterization[303,379]. Due to the extreme complexity of proteomes, sophisticated separation techniques and advanced MS instrumentation is required to conduct such studies, and these would most likely be outsourced to specialist centres such as the University of Dundee's FingerPrint proteomics facility. For early-stage research such as this, this was not deemed an effective use of limited resources but remains a clear next step for future work. Equally, use of cell lines has limited the translatability of this research. Cell lines were used due to their ready availability and, particularly in the case of Chapter 5, survival of the transfection process. Wherever possible 'normal' cell lines such as the THLE-3s were used to address critique of cancer derived cell lines. Future work should address this issue with the use of cells such as HepaRGs, iPSCs and primary human hepatocytes.

Co-culture with non-parenchymal cells of the liver and with circulating cells such as red blood cells is also key to understanding and improving hepatocyte function. Kupffer cells, hepatic stellate cells and sinusoidal endothelial cells have all been used in co-culture with hepatocytes and are found to induce improvement in hepatocyte function and maintenance of hepatic phenotype irrespective of the type of cell used for co-culture. Such work is a vital next step for promising liver tissue engineering such as these hybrid scaffolds.

Further methods of analysing the hepatocytes response to the scaffold environments and hepatic characterisation should be included in the next round of experimentation. Analysis of hepatocyte polarization by analysis of the tight junction protein ZO-1[143,380], apical export protein MRP2[19,381] and bile canalicular protein DPP4[160] should be assessed. The functional ability of formed bile canaliculi

should be evaluated by accumulation of fluorescein within the cells[21,160,382]. Mature hepatic protein production in addition to that of albumin should also be assessed, namely prealbumin, α-fetoprotein, fibrinogen, haptoglobulin, α2-macroglobulin and fibronectin[150,160,301]. Heatmap analysis of the metabolic functions of the hepatocytes could prove useful when comparing results to studies from other groups[383].

Functional studies would be invaluable for the ultimate aim of creating an environment which supports hepatic cell survival and function. Acetaminophen toxicity studies[384] and analysis of the CYP450 reductase enzyme production using ELISA or western blotting[44,142,149] would demonstrate the translatability of these platforms. The scaffolds could easily be incorporated into flow devices such as Kirkstall's QuasiVivo[221] or scaled up for larger systems similar to the Extracorporeal Liver Assist Device (ELAD)[227] to assess the cells function and behaviour under flow and shear stress.

Finally, now that these methods have been established within the group, future researchers could work towards a more directed ECM; recapitulating disease environments or specific regions of the liver such as the sinusoid to study the influence of disease ECM or cell location on the hepatocyte and investigate methods of manipulating such behaviour or creating benchtop disease systems.

7.3 Conclusion

The aims for this project were laid out as

1. The manufacture of electrospun polymer scaffolds capable of maintaining hepatocyte survival

2. Combine polymer scaffolds with cutting edge protein production techniques to manufacture practical, reproducible and translatable hybrid polymer:protein scaffolds for liver tissue engineering

3. Assess the impact of polymer only and hybrid scaffolds on hepatocyte survival and behaviour.

Each of these aims has been addressed in this body of work. Novel methods have been employed to deliver scaffolds which can be used to influence the survival and behaviour of hepatocytes. Each study presented in this thesis represents the initial, 'proof-of-concept' stage of a new environment for liver

tissue engineering. Each condition tested exerted a differing influence on the survival, metabolic activity, gene expression and protein production of the hepatocytes cultured upon it.

In Chapter 3 drug-derived ECM:PCL scaffolds displayed significant changes in their mechanical properties, as well as an altered biochemical profile. HepG2s cultures on the constructs displayed markedly altered survival, metabolic activity and gene expression between the conditions. This work represents this first use of pharmaceuticals to manipulate ECM production for liver tissue engineering.

In Chapter 4, the work from chapter 3 was furthered by the use of a liver cell line to derive the ECM component of the hybrid scaffolds, and a switch to PLA for its favourable biodegradable nature and superior cell adhesion properties. The drug derived ECM:PLA scaffolds also demonstrated altered mechanical properties and biochemical profiles. They were seeded with primary human hepatocytes and the differences in ECM proteins and mechanical changes induced a subsequent alteration in albumin production and gene expression.

Chapter 5 produced a synthetically derived fibronectin enriched ECM:PLA scaffold which displayed mechanical and biochemical differences between conditions. Hep-G2 cells were subsequently cultured scaffolds and I observed changes in cell survival, gene expression and albumin production. This chapter represents the first combinatorial approach to synthetic biology and electrospun scaffold production for liver tissue engineering,

Chapter 6 produced a to create a novel blended human ECM:PLA scaffold for THLE-3 liver cells. Scaffolds containing decellularized human liver, fibronectin, laminin-521 and collagen I were compared to elucidate the influence of single ECM proteins vs whole ECM. The drastic mechanical differences and immunohistochemical profiles of the scaffolds induced changes in THLE-3 cell behaviour. Results indicate that hLECM has an influence on hepatocytes which cannot be recapitulated by individual ECM components, raising questions regarding the relationship between cells and the native extracellular matrix. This study is the first time whole human licer ECM has been

combined with electrospinning and compared to its individual recombinant constituents at the same concentrations and with the same scaffold manufacturing method employed.

The hybrid scaffolds developed in this work are a powerful platform for the future manipulation of liver cell behaviour. They provide a non-invasive, animal-free culture environment for hepatocytes which, with development, has the potential to contribute greatly to the fields of drug development, disease biology, personalised medicine and tissue engineering.

References

1. NHS Blood and Transplant. Organ donation and transplantation 2017. *NHS Blood Transpl.* 2017 (2017).
2. Blachier, M., Leleu, H., Peck-Radosavljevic, M., Valla, D.-C. & Roudot-Thoraval, F. The burden of liver disease in Europe: A review of available epidemiological data. *J. Hepatol.* **58,** 593–608 (2013).
3. Williams, R. *et al.* The Lancet Commissions Addressing liver disease in the UK : a blueprint for attaining excellence in health care and reducing premature mortality from lifestyle issues of excess consumption of alcohol , obesity , and viral hepatitis. *Lancet* **384,** 1953–1997 (2014).
4. NHS Blood and Transplant. *Organ Donation and Transplantation activity report*. (2018).
5. Williams, R. *et al.* Implementation of the Lancet Standing Commission on Liver Disease in the UK. *Lancet* **386,** 2098–2111 (2015).
6. Martinez-Hernandez, A. & Amenta, P. S. The extracellular matrix in hepatic regeneration. *Faseb J.* **9,** 1401–1410 (1995).
7. Mazza, G. *et al.* Rapid production of human liver scaffolds for functional tissue engineering by high shear stress oscillation-decellularization. *Sci. Rep.* **7,** (2017).
8. Grant, R., Hay, D. & Callanan, A. From scaffold to structure: the synthetic production of cell derived extracellular matrix for liver tissue engineering. *Biomed. Phys. Eng. Express* (2018).
9. Baiocchini, A. *et al.* Extracellular Matrix Molecular Remodeling in Human Liver Fibrosis Evolution. (2016).
10. Altrock, E. *et al.* Inhibition of fibronectin deposition improves experimental liver fibrosis. *J. Hepatol.* **62,** 625–633 (2015).
11. Grant, R., Hay, D. & Callanan, A. A Drug-Induced Hybrid Electrospun Poly-Capro-Lactone: Cell-Derived Extracellular Matrix Scaffold for Liver Tissue Engineering. *Tissue Eng. Part A* **23,** 650–662 (2017).
12. Cameron, K. *et al.* Recombinant Laminins Drive the Differentiation and Self-Organization of hESC-Derived Hepatocytes. *Stem Cell Reports* **5,** 1–13 (2015).
13. Finoli, A., Schmelzer, E., Over, P., Nettleship, I. & Gerlach, J. C. Open-Porous Hydroxyapatite Scaffolds for Three-Dimensional Culture of Human Adult Liver Cells.
14. Shinozawa, T., Yoshikawa, H. Y. & Takebe, T. Reverse Engineering Liver Buds Through Self-Driven Condensation And Organization Towards Medical Application. *Dev. Biol.* **420,** 1–9 (2016).
15. Lucendo-Villarin, B. *et al.* Stabilizing Hepatocellular Phenotype Using Optimized Synthetic Surfaces. *J. Vis. Exp.* e51723–e51723 (2014).
16. Yanagi, Y. *et al.* In vivo and ex vivo methods of growing a liver bud through tissue connection. *Sci. Rep.* **7,** (2017).
17. Ware, B. R. & Khetani, S. R. Engineered Liver Platforms for Different Phases of Drug Development. *Trends Biotechnol.* **35,** 172–183 (2017).

18. Mazza, G. *et al.* Decellularized human liver as a natural 3D-scaffold for liver bioengineering and transplantation. *Sci. Rep.* **5,** (2015).

19. Huch, M. *et al.* Long-term culture of genome-stable bipotent stem cells from adult human liver. *Cell* **160,** 299–312 (2015).

20. Ye, J., Shirakigawa, N. & Ijima, H. Hybrid organoids consisting of extracellular matrix gel particles and hepatocytes for transplantation. *J. Biosci. Bioeng.* (2015).

21. Takebe, T. *et al.* Vascularized and complex organ buds from diverse tissues via mesenchymal cell-driven condensation. *Cell Stem Cell* **16,** 556–565 (2015).

22. Banaeiyan, A. A. *et al.* Design and fabrication of a scalable liver-lobule-on-a-chip microphysiological platform. *Biofabrication* **9,** (2017).

23. Nichol, J. W. *et al.* Cell-laden microengineered gelatin methacrylate hydrogels. *Biomaterials* **31,** 5536–44 (2010).

24. McCullen, S. D., Autefage, H., Callanan, A., Gentleman, E. & Stevens, M. M. Anisotropic Fibrous Scaffolds for Articular Cartilage Regeneration. *Tissue Eng. Part A* **18,** 2073–2083 (2012).

25. Accardi, M. A. *et al.* Effects of fiber orientation on the frictional properties and damage of regenerative articular cartilage surfaces. *Tissue Eng. Part A* **19,** 2300–10 (2013).

26. Steele, J. A. M. *et al.* Combinatorial scaffold morphologies for zonal articular cartilage engineering. *Acta Biomater.* **10,** 2065–2075 (2014).

27. Noszczyk, B. H. *et al.* Biocompatibility of electrospun human albumin: a pilot study. *Biofabrication* **7,** 015011 (2015).

28. Grant, R., Hay, D. C. & Callanan, A. A Drug-Induced Hybrid Electrospun Poly-Capro-Lactone: Cell-Derived Extracellular Matrix Scaffold for Liver Tissue Engineering. *Tissue Eng. Part A* **23,** 650–662 (2017).

29. Naderi, H., Matin, M. M. & Bahrami, A. R. Review paper: critical issues in tissue engineering: biomaterials, cell sources, angiogenesis, and drug delivery systems. *J. Biomater. Appl.* **26,** 383–417 (2011).

30. He, M. & Callanan, A. Comparison of methods for whole organ decellularisation in tissue engineering of bio-artificial organs. *Tissue Eng. Part B Rev.* **19,** (2012).

31. De Kock, J. *et al.* Simple and quick method for whole-liver decellularization: A novel in vitro three-dimensional bioengineering tool? *Arch. Toxicol.* **85,** 607–612 (2011).

32. Baptista, P. M. *et al.* The use of whole organ decellularization for the generation of a vascularized liver organoid. *Hepatology* **53,** 604–617 (2011).

33. Barakat, O. *et al.* Use of decellularized porcine liver for engineering humanized liver organ. *J. Surg. Res.* **173,** e11–e25 (2012).

34. Wu, Q. *et al.* Optimizing Perfusion-Decellularization Methods of Porcine Livers for Clinical-Scale Whole-Organ Bioengineering. *Biomed Res. Int.* **2015,** 1–9 (2015).

35. Zhou, P. *et al.* Decellularization and Recellularization of Rat Livers With Hepatocytes and Endothelial Progenitor Cells. *Artif. Organs* n/a-n/a (2016).

36. Faulk, D. M., Wildemann, J. D. & Badylak, S. F. Decellularization and Cell Seeding of Whole Liver Biologic Scaffolds Composed of Extracellular Matrix. *J. Clin. Exp. Hepatol.* **5,** 69–80

(2015).

37. Kogel, J. Van Der, Bussink, J., Coxon, A., Polverino, A. & M, P. Fluid flow regulation of revascularization and cellular organizationin a bioengineered liver platform. *Tissue Eng. Part C Methods* 1–22 (2016).

38. Woods, T. & Gratzer, P. F. Effectiveness of three extraction techniques in the development of a decellularized bone-anterior cruciate ligament-bone graft. *Biomaterials* **26,** 7339–7349 (2005).

39. Funamoto, S. *et al.* The use of high-hydrostatic pressure treatment to decellularize blood vessels. *Biomaterials* **31,** 3590–3595 (2010).

40. Cebotari, S. *et al.* Detergent decellularization of heart valves for tissue engineering: Toxicological effects of residual detergents on human endothelial cells. *Artif. Organs* **34,** 206–210 (2010).

41. Kim, M. H. *et al.* Phenotypic regulation of liver cells in a biofunctionalized three-dimensional hydrogel platform. *Integr. Biol.* (2016).

42. Vasanthan, K. S., Sethuraman, S. & Parthasarathy, M. Electrochemical evidence for asialoglycoprotein receptor - mediated hepatocyte adhesion and proliferation in three dimensional tissue engineering scaffolds. *Anal. Chim. Acta* **890,** 83–90 (2015).

43. Lee, J. S. *et al.* Liver extracellular matrix providing dual functions of two-dimensional substrate coating and three-dimensional injectable hydrogel platform for liver tissue engineering. *Biomacromolecules* **15,** 206–18 (2014).

44. No, D. Y., Jeong, G. S. & Lee, S.-H. Immune-protected xenogeneic bioartificial livers with liver-specific microarchitecture and hydrogel-encapsulated cells. *Biomaterials* **35,** 8983–91 (2014).

45. Underhill, G. H., Chen, A. a, Albrecht, D. R. & Bhatia, S. N. Assessment of hepatocellular function within PEG hydrogels. *Biomaterials* **28,** 256–70 (2007).

46. Zeugolis, D. I. *et al.* Electro-spinning of pure collagen nano-fibres - Just an expensive way to make gelatin? *Biomaterials* **29,** 2293–2305 (2008).

47. Dong, B., Arnoult, O., Smith, M. E. & Wnek, G. E. Electrospinning of collagen nanofiber scaffolds from benign solvents. *Macromol. Rapid Commun.* **30,** 539–542 (2009).

48. Chung, S. *et al.* Responsive poly (γ-glutamic acid) fibres for biomedical applications. *J. Mater. Chem. B* **1,** 1397 (2013).

49. Gray, H. & Vandyke Carter, H. *Gray's Anatomy: the Anatomical Basis of Clinical Practice*. (Churchill Livingstone/Elsevier, 1858).

50. Crawford, A. R., Lin, X. Z. & Crawford, J. The normal adult human liver biopsy: a quantitative reference standard. *Hepatology* **28,** 323–331 (1998).

51. Kang, Y. B., Sodunke, T. R., Cirillo, J., Bouchard, M. J. & Noh, H. Liver on a chip: Engineering the liver sinusoid. in *2013 Transducers & Eurosensors XXVII: The 17th International Conference on Solid-State Sensors, Actuators and Microsystems (TRANSDUCERS & EUROSENSORS XXVII)* 301–304 (IEEE, 2013).

52. Du, Y. *et al.* Mimicking liver sinusoidal structures and functions using a 3D-configured microfluidic chip. **17,** 782 (2014).

53. Martinez-Hernandez, A. & Amenta, P. S. The hepatic extracellular matrix I. Components and

distribution in normal liver. *Virchows Arch. A Pathol. Anat. Histopathol.* **423,** 1–11 (1993).

54. Martinez-Hernandez, A. & Amenta, P. S. The hepatic extracellular matrix II. Ontogenesis, regeneration and cirrhosis. *Virchows Arch. A Pathol. Anat. Histopathol.* **423,** 77–84 (1993).

55. Ruprecht, V. *et al.* How cells respond to environmental cues – insights from bio-functionalized substrates. *J. Cell Sci.* jcs.196162 (2016).

56. Liu, Z. *et al.* Three-dimensional hepatic lobule-like tissue constructs using cell-microcapsule technology. *Acta Biomater.* **50,** 178–187 (2017).

57. Damm, G. *et al.* Human parenchymal and non-parenchymal liver cell isolation, culture and characterization. *Hepatol. Int.* **7,** 951–958 (2013).

58. Bachmann, A. *et al.* 3D Cultivation Techniques for Primary Human Hepatocytes. *Microarrays* **4,** 64–83 (2015).

59. Alexandrova, K. *et al.* Large-Scale Isolation of Human Hepatocytes for Therapeutic Application. *Cell Transplant.* **14,** 845–853 (2005).

60. Kang, Y. B., Rawat, S., Cirillo, J., Bouchard, M. & Noh, H. Layered long-term co-culture of hepatocytes and endothelial cells on a transwell membrane: Toward engineering the liver sinusoid. *Biofabrication* **5,** 1–24 (2013).

61. Braet, F. & Wisse, E. Structural and functional aspects of liver sinusoidal endothelial cell fenestrae: a review. *Comp. Hepatol.* **1,** 1 (2002).

62. Fullár, A. *et al.* Response of Hepatic Stellate Cells to TGFB1 Differs from the Response of Myofibroblasts. Decorin Protects against the Action of Growth Factor. *Pathol. Oncol. Res.* **23,** 287–294 (2017).

63. Yi, S.-H., Zhang, Y., Tang, D. & Zhu, L. Mechanical force and tensile strain activated hepatic stellate cells and inhibited retinol metabolism. *Biotechnol. Lett.* (2015).

64. Rashid, S. T. *et al.* Proteomic analysis of extracellular matrix from the hepatic stellate cell line LX-2 identi fi es CYR61 and Wnt-5a as novel constituents of fi brotic liver. *J. Proteome Res.* (2012).

65. Kawelke, N. *et al.* Fibronectin protects from excessive liver fibrosis by modulating the availability of and responsiveness of stellate cells to active TGF-β. *PLoS One* **6,** e28181 (2011).

66. Larkin, A. L., Rodrigues, R. R., Murali, T. M. & Rajagopalan, P. Designing a Multicellular Organotypic 3D Liver Model with a Detachable, Nanoscale Polymeric Space of Disse. *Tissue Eng. Part C Methods* **19,** 875–84 (2013).

67. Tabibian, J. H., Masyuk, A. I., Masyuk, T. V, O'Hara, S. P. & LaRusso, N. F. Physiology of cholangiocytes. *Compr. Physiol.* **3,** 541–565 (2013).

68. Takayama, K. *et al.* Long-term self-renewal of human ES/iPS-derived hepatoblast-like cells on human laminin 111-coated dishes. *Stem cell reports* **1,** 322–35 (2013).

69. Michalopoulos, G. K., Barua, L. & Bowen, W. C. Transdifferentiation of Rat Hepatocytes Into Biliary Cells After Bile Duct Ligation and Toxic Biliary Injury. *Hepatology* **41,** 535–544 (2005).

70. Lu, W.-Y. *et al.* Hepatic progenitor cells of biliary origin with liver repopulation capacity Europe PMC Funders Group. *Nat Cell Biol* **17,** 971–983 (2015).

71. Brown, B. N. & Badylak, S. F. Extracellular matrix as an inductive scaffold for functional tissue reconstruction. *Transl. Res.* **163,** 268–85 (2014).

72. Frantz, C., Stewart, K. M. & Weaver, V. M. The extracellular matrix at a glance. *J. Cell Sci.* **123,** 4195–200 (2010).

73. Faulk, D. M., Johnson, S. A., Zhang, L. & Badylak, S. F. Role of the extracellular matrix in whole organ engineering. *J. Cell. Physiol.* **229,** 984–9 (2014).

74. Laurila, P. & Leivo, I. Basement membrane and interstitial matrix components form separate matrices in heterokaryons of PYS-2 cells and fibroblasts. *J. Cell Sci.* **104 (Pt 1,** 59–68 (1993).

75. Kang, Y. B. (Abraham), Rawat, S., Cirillo, J., Bouchard, M. & Noh, H. (Moses). Layered long-term co-culture of hepatocytes and endothelial cells on a transwell membrane: toward engineering the liver sinusoid. *Biofabrication* **5,** 045008 (2013).

76. Kikkawa, Y., Mochizuki, Y., Miner, J. H. & Mitaka, T. Transient expression of laminin alpha1 chain in regenerating murine liver: restricted localization of laminin chains and nidogen-1. *Exp. Cell Res.* **305,** 99–109 (2005).

77. Saad, B. *et al.* Crude liver membrane fractions and extracellular matrix components as substrata regulate differentially the preservation and inducibility of cytochrome P-450 isoenzymes in cultured rat hepatocytes. *Eur J Biochem* **213,** 805–814 (1993).

78. Loneker, A. E., Faulk, D. M., Hussey, G. S., D'Amore, A. & Badylak, S. F. Solubilized liver extracellular matrix maintains primary rat hepatocyte phenotype in-vitro. *J. Biomed. Mater. Res. A* 1–9 (2015).

79. Pujades, C., Forsberg, E., Enrich, C. & Johansson, S. Changes in cell surface expression of fibronectin and fibronectin receptor during liver regeneration. *J. Cell Sci.* **102 (Pt 4,** 815–820 (1992).

80. Moriya, K., Sakai, K., Yan, M. H. & Sakai, T. Fibronectin is essential for survival but is dispensable for proliferation of hepatocytes in acute liver injury in mice. *Hepatology* **56,** 311–321 (2012).

81. Domogatskaya, A., Rodin, S. & Tryggvason, K. Functional diversity of laminins. *Annu. Rev. Cell Dev. Biol.* **28,** 523–53 (2012).

82. Noro, A. *et al.* Laminin production and basement membrane deposition by mesenchymal stem cells upon adipogenic differentiation. *J. Histochem. Cytochem.* **61,** 719–30 (2013).

83. Lucendo-Villarin, B. *et al.* Maintaining hepatic stem cell gene expression on biological and synthetic substrata. *Biores. Open Access* **1,** 50–3 (2012).

84. Gordon, M. K. & Hahn, R. a. Collagens. *Cell Tissue Res.* **339,** 247–57 (2010).

85. Klaas, M. *et al.* The alterations in the extracellular matrix composition guide the repair of damaged liver tissue. *Sci. Rep.* **6,** 27398 (2016).

86. Rothan, H. a *et al.* Three-dimensional culture environment increases the efficacy of platelet rich plasma releasate in prompting skin fibroblast differentiation and extracellular matrix formation. *Int. J. Med. Sci.* **11,** 1029–38 (2014).

87. Zamir, E. *et al.* Molecular diversity of cell-matrix adhesions. *J. Cell Sci.* **112 (Pt 1,** 1655–1669 (1999).

88. Llacua, A., de Haan, B. J. & de Vos, P. **Laminin and collagen IV inclusion in immunoisolating microcapsules reduces cytokine-mediated cell death in human pancreatic islets**. *J. Tissue Eng. Regen. Med.* (2017).

89. Cescon, M., Gattazzo, F., Chen, P. & Bonaldo, P. Collagen VI at a glance. 1–7 (2015).

90. Iozzo, R. V. & Schaefer, L. Proteoglycan form and function: A comprehensive nomenclature of proteoglycans. *Matrix Biol.* **42,** 11–55 (2015).

91. Mouw, J. K., Ou, G. & Weaver, V. M. Extracellular matrix assembly: a multiscale deconstruction. *Nat. Rev. Mol. Cell Biol.* **15,** 771–785 (2014).

92. Faissner, A. & Reinhard, J. The extracellular matrix compartment of neural stem and glial progenitor cells. *Glia* n/a-n/a (2015).

93. Mizumoto, S., Yamada, S. & Sugahara, K. Molecular interactions between chondroitin–dermatan sulfate and growth factors/receptors/matrix proteins. *Curr. Opin. Struct. Biol.* **34,** 35–42 (2015).

94. Harisi, R. & Jeney, A. Extracellular matrix as target for antitumor therapy. 1387–1398 (2015).

95. Pomin, V. H. Keratan sulfate: An up-to-date review. *Int. J. Biol. Macromol.* **72,** 282–289 (2015).

96. Funderburgh, J. L. Keratan sulphate biosynthesis. **54,** 187–194 (2010).

97. Barallobre-Barreiro, J., Baig, F., Fava, M., Yin, X. & Mayr, M. Glycoproteomics of the Extracellular Matrix: A Method for Intact Glycopeptide Analysis Using Mass Spectrometry. *J. Vis. Exp.* e55674–e55674 (2017).

98. Reing, J. E. *et al.* The effects of processing methods upon mechanical and biologic properties of porcine dermal extracellular matrix scaffolds. *Biomaterials* **31,** 8626–8633 (2010).

99. Bedossa, P. & Paradis, V. Liver extracellular matrix in health and disease. *J. Pathol.* **200,** 504–15 (2003).

100. Taipale, J. & Keski-Oja, J. Growth factors in the extracellular matrix. *FASEB J.* **11,** 51–59 (1997).

101. Limaye, P. B. *et al.* Mechanisms of hepatocyte growth factor-mediated and epidermal growth factor-mediated signaling in transdifferentiation of rat hepatocytes to biliary epithelium. *Hepatology* **47,** 1702–1713 (2008).

102. Brizzi, M. F., Tarone, G. & Defilippi, P. Extracellular matrix, integrins, and growth factors as tailors of the stem cell niche. *Curr. Opin. Cell Biol.* **24,** 645–651 (2012).

103. Nakamura, T. & Mizuno, S. The discovery of hepatocyte growth factor (HGF) and its significance for cell biology, life sciences and clinical medicine. *Proc. Jpn. Acad. Ser. B. Phys. Biol. Sci.* **86,** 588–610 (2010).

104. Yao, L.-B. *et al.* In situ splitting after selective partial portal vein ligation or simultaneous hepatic artery ligation promotes liver regeneration. *Sci. Rep.* **8,** 8699 (2018).

105. Gebhardt, R. & Matz-Soja, M. Liver zonation: Novel aspects of its regulation and its impact on homeostasis. *World J. Gastroenterol.* **20,** 8491–504 (2014).

106. McCarty, W. J., Usta, O. B. & Yarmush, M. L. A Microfabricated Platform for Generating Physiologically-Relevant Hepatocyte Zonation. *Sci. Rep.* **6,** 26868 (2016).

107. Shan, Z. *et al.* Fibroblast growth factors 19 and 21 in acute liver damage. *Ann. Transl. Med.* **6,** 257–257 (2018).

108. Nicolas, C. T. *et al.* Concise Review: Liver Regenerative Medicine: From Hepatocyte

Transplantation to Bioartificial Livers and Bioengineered Grafts. *Stem Cells* 42–50 (2016).

109. Michalopoulos, G. K. Hepatostat: Liver regeneration and normal liver tissue maintenance. *Hepatology* **65,** 1384–1392 (2017).

110. Yanger, K. *et al.* Robust cellular reprogramming occurs spontaneously during liver regeneration. *Genes Dev.* **27,** 719–724 (2013).

111. Alwahsh, S. M., Rashidi, H. & Hay, D. C. Liver cell therapy: is this the end of the beginning? *Cell. Mol. Life Sci.* 1–18 (2017).

112. Bhatia, S. N., Underhill, G. H., Zaret, K. S. & Fox, I. J. Cell and Tissue Engineering for Liver Disease.

113. Duarte, S., Baber, J., Fujii, T. & Coito, A. J. Matrix metalloproteinases in liver injury, repair and fibrosis.

114. Stephan, J.-P. *et al.* Albumin stimulates the accumulation of extracellular matrix in renal tubular epithelial cells. *Am. J. Nephrol.* **24,** 14–9 (2004).

115. Bonnans, C., Chou, J. & Werb, Z. Remodelling the extracellular matrix in development and disease. *Nat. Rev. Mol. Cell Biol.* **15,** 786–801 (2015).

116. Eggink, L. L. & Hoober, J. K. A biologically active peptide mimetic of N-acetylgalactosamine/galactose. *BMC Res. Notes* **2,** 23 (2009).

117. British Association for the Study of the Liver & British Society of Gastroenterology. *A Time to Act: Improving Liver Health and Outcomes in Liver Disease*. *The National Plan for Liver Services UK* (2009).

118. Bélanger, M. & Butterworth, R. F. Acute liver failure: A critical appraisal of available animal models. *Metab. Brain Dis.* **20,** 409–423 (2005).

119. Billerbeck, E. *et al.* Mouse models of acute and chronic hepacivirus infection. *Science (80-.).* **357,** 204–208 (2017).

120. Younossi, Z. M. *et al.* Changes in the Prevalence of the Most Common Causes of Chronic Liver Diseases in the United States From 1988 to 2008. *Clin. Gastroenterol. Hepatol.* **9,** 524–530.e1 (2011).

121. Church, R. J. *et al.* Candidate biomarkers for the diagnosis and prognosis of drug-induced liver injury: An international collaborative effort. *Hepatology* (2018).

122. Starkey Lewis, P. J. *et al.* Circulating microRNAs as potential markers of human drug-induced liver injury. *Hepatology* **54,** 1767–1776 (2011).

123. Vliegenthart, A. D. B., Berends, C., Potter, C. M. J., Kersaudy-Kerhoas, M. & Dear, J. W. MicroRNA-122 can be measured in capillary blood which facilitates point-of-care testing for drug-induced liver injury. *Br. J. Clin. Pharmacol.* **83,** 2027–2033 (2017).

124. Godoy, P. *et al. Recent advances in 2D and 3D in vitro systems using primary hepatocytes, alternative hepatocyte sources and non-parenchymal liver cells and their use in investigating mechanisms of hepatotoxicity, cell signaling and ADME*. *Archives of Toxicology* **87,** (2013).

125. Ellis, A. J., Wendon, J. A., Portmann, B. & Williams, R. Acute liver damage and ecstasy ingestion. *Gut* **38,** 454–458 (1996).

126. Ostapowicz, G. *et al.* Results of a Prospective Study of Acute Liver Failure at 17 Tertiary Care Centers in the United States. 947–955 (2002).

127. Liu, Y. *et al.* Animal models of chronic liver diseases. *AJP Gastrointest. Liver Physiol.* **304,** G449–G468 (2013).

128. Xiao, J. *et al.* Disease Burden from Hepatitis B Virus Infection in Guangdong Province, China. *Int. J. Environ. Res. Public Health* **12,** 14055–67 (2015).

129. Rehm, J., Samokhvalov, A. V. & Shield, K. D. Global burden of alcoholic liver diseases. *J. Hepatol.* **59,** 160–168 (2013).

130. Brandon-Warner, E., Schrum, L. W., Schmidt, C. M. & McKillop, I. H. Rodent Models of Alcoholic Liver Disease: Of Mice and Men. *Alcohol* **46,** 3279–3288 (2012).

131. Ono, Y. *et al.* Regeneration and Cell Recruitment in an Improved Heterotopic Auxiliary Partial Liver Transplantation Model in the Rat. *Transplantation* **101,** 92–100 (2017).

132. Marcdante, K. J. & Nelson, W. E. (Waldo E. *Nelson essentials of pediatrics*. (Saunders/Elsevier, 2011).

133. Green, C. J. *et al.* The isolation of primary hepatocytes from human tissue: optimising the use of small non-encapsulated liver resection surplus. *Cell Tissue Bank.* **18,** 597–604 (2017).

134. Coleman, R. a. Human Tissue in the Evaluation of Safety and Efficacy of New Medicines: A Viable Alternative to Animal Models? *ISRN Pharm.* **2011,** 1–8 (2011).

135. Billerbeck, E. *et al.* Mouse models of acute and chronic hepacivirus infection. *Science (80-.).* **357,** 204–208 (2017).

136. Donato, M. T., Lahoz, A., Castell, J. V & Gómez-Lechón, M. J. Cell lines: a tool for in vitro drug metabolism studies. *Curr Drug Metab.* **9,** 1–11 (2008).

137. Elkayam, T., Amitay-Shaprut, S., Dvir-Ginzberg, M., Harel, T. & Cohen, S. Enhancing the drug metabolism activities of C3A--a human hepatocyte cell line--by tissue engineering within alginate scaffolds. *Tissue Eng.* **12,** 1357–68 (2006).

138. Costantini, S., Di Bernardo, G., Cammarota, M., Castello, G. & Colonna, G. Gene expression signature of human HepG2 cell line. *Gene* **518,** 335–45 (2013).

139. Qiu, G.-H. *et al.* Distinctive pharmacological differences between liver cancer cell lines HepG2 and Hep3B. *Cytotechnology* **67,** 1–12 (2015).

140. el Mouelhi, M., Didolkar, M. S., Elias, E. G., Guengerich, F. P. & Kauffman, F. C. Hepatic drug-metabolizing enzymes in primary and secondary tumors of human liver. *Cancer Res.* **47,** 460–6 (1987).

141. Wang, L. *et al.* Comparison of porcine hepatocytes with human hepatoma (C3A) cells for use in a bioartificial liver support system. *Cell Transplant.* **7,** 459–468 (1998).

142. Nelson, L. J. *et al.* Human Hepatic HepaRG Cells Maintain an Organotypic Phenotype with High Intrinsic CYP450 Activity/Metabolism and Significantly Outperform Standard HepG2/C3A Cells for Pharmaceutical and Therapeutic Applications. *Basic Clin. Pharmacol. Toxicol.* **120,** 30–37 (2017).

143. Sainz, B., TenCate, V. & Uprichard, S. L. Three-dimensional Huh7 cell culture system for the study of Hepatitis C virus infection. *Virol. J.* **6,** 103 (2009).

144. Pfeifer, a M. *et al.* Simian virus 40 large tumor antigen-immortalized normal human liver epithelial cells express hepatocyte characteristics and metabolize chemical carcinogens. *Proc. Natl. Acad. Sci. U. S. A.* **90,** 5123–5127 (1993).

145. Schippers, I. J. *et al.* Immortalized human hepatocytes as a tool for the study of hepatocytic (de-)differentiation. *Cell Biol. Toxicol.* **13,** 375–386 (1997).

146. WERNER, A. *et al.* Cultivation and Characterization of a New Immortalized Human Hepatocyte Cell Line, HepZ, for Use in an Artificial Liver Support System. *Ann. N. Y. Acad. Sci.* **875,** 364–368 (1999).

147. Hay, D. C. Rapid and scalable human stem cell differentiation: now in 3D. *Stem Cells Dev.* **22,** 2691–2 (2013).

148. Hay, D. C. *et al.* Direct Differentiation of Human Embryonic Stem Cells to Hepatocyte-like Cells Exhibiting Functional Activities. *Cloning Stem Cells* **9,** 51–62 (2007).

149. Cameron, K., Lucendo-Villarin, B., Szkolnicka, D. & Hay, D. C. Serum-Free Directed Differentiation of Human Embryonic Stem Cells to Hepatocytes. *Methods Mol. Biol.* **1250,** 105–11 (2015).

150. Hay, D. C. *et al.* Highly efficient differentiation of hESCs to functional hepatic endoderm requires ActivinA and Wnt3a signaling. *Proc. Natl. Acad. Sci. U. S. A.* **105,** (2008).

151. Takebe, T. *et al.* Engineering of human hepatic tissue with functional vascular networks. *Organogenesis* **10,** 260–267 (2014).

152. Koike, H. *et al.* Nutritional modulation of mouse and human liver bud growth through a branched-amino acid metabolism. *Development* (2017).

153. Sekine, K., Takebe, T. & Taniguchi, H. Liver Regeneration Using Cultured Liver Bud. in *Methods in molecular biology (Clifton, N.J.)* **1597,** 207–216 (2017).

154. Takebe, T. *et al.* Generation of a vascularized and functional human liver from an iPSC-derived organ bud transplant. *Nat. Protoc.* **9,** 396–409 (2014).

155. Takebe, T. *et al.* Vascularized and functional human liver from an iPSC-derived organ bud transplant. *Nature* **499,** 481–4 (2013).

156. Bi, H. *et al.* Liver extracellular matrix promotes BM-MSCs hepatic differentiation and reversal of liver fibrosis through activation of integrin pathway. *J. Tissue Eng. Regen. Med.* (2016).

157. Lu, W.-Y. *et al.* Hepatic progenitor cells of biliary origin with liver repopulation capacity. *Nat. Cell Biol.* (2015).

158. Hsieh, W.-C. *et al.* Galectin-3 regulates hepatic progenitor cell expansion during liver injury. *Gut* **64,** 312–21 (2015).

159. Palakkan, A. A., Hay, D. C., Pr, A. K., Tv, K. & Ross, J. A. Liver tissue engineering and cell sources: Issues and challenges. *Liver Int.* **33,** 666–676 (2013).

160. Palakkan, A. A. *et al.* Polarisation and functional characterisation of hepatocytes derived from human embryonic and mesenchymal stem cells. *Biomed. reports* **3,** 626–636 (2015).

161. Hughes, R. D. *et al.* Isolation of hepatocytes from livers from non-heart-beating donors for cell transplantation. *Liver Transplant.* **12,** 713–717 (2006).

162. Ye, J., Shirakigawa, N. & Ijima, H. Fetal liver cell-containing hybrid organoids improve cell viability and albumin production upon transplantation. (2016).

163. Godoy, P. *et al. Gene networks and transcription factor motifs defining the differentiation of stem cells into hepatocyte-like cells*. *Journal of Hepatology* (European Association for the Study of the Liver, 2015).

164. Vunjak-Novakovic, G., Bhatia, S., Chen, C. & Hirschi, K. HeLiVa platform: integrated heart-liver-vascular systems for drug testing in human health and disease. *Stem Cell Res. Ther.* **4 Suppl 1,** S8 (2013).

165. Kosicki, M., Tomberg, K. & Bradley, A. Repair of double-strand breaks induced by CRISPR–Cas9 leads to large deletions and complex rearrangements. *Nat. Biotechnol.* **36,** 765–771 (2018).

166. Torok, E. *et al.* Primary Human Hepatocytes on Biodegradable Poly(l-Lactic acid) Matrices: A Promising Model for Improving Transplantation Efficiency With Tissue Engineering. *Liver Transplant.* **13,** 465–466 (2011).

167. Bhogal, R. H. *et al.* Isolation of primary human hepatocytes from normal and diseased liver tissue: a one hundred liver experience. *PLoS One* **6,** e18222 (2011).

168. Bale, S. S. *et al.* Long-Term Coculture Strategies for Primary Hepatocytes and Liver Sinusoidal Endothelial Cells. *Tissue Eng. Part C Methods* **21,** (2015).

169. Simpson, D. G. *et al.* Electrospun collagen: A tissue engineering scaffold with unique functional properties in a wide variety of applications. *J. Nanomater.* **2011,** (2011).

170. Boess, F. *et al.* Gene expression in two hepatic cell lines, cultured primary hepatocytes, and liver slices compared to the in vivo liver gene expression in rats: Possible implications for toxicogenomics use of in vitro systems. *Toxicol. Sci.* **73,** 386–402 (2003).

171. Hughes, C. S., Postovit, L. M. & Lajoie, G. A. Matrigel: a complex protein mixture required for optimal growth of cell culture. *Proteomics* **10,** 1886–1890 (2010).

172. Luckert, C. *et al.* Comparative analysis of 3D culture methods on human HepG2 cells. *Arch. Toxicol.* **91,** 393–406 (2017).

173. Saldin, L. T., Cramer, M. C., Velankar, S. S., White, L. J. & Badylak, S. F. Extracellular Matrix Hydrogels from Decellularized Tissues: Structure and Function. *Acta Biomater.* (2016).

174. Gao, R. *et al.* Hepatocyte Culture in Autologous Decellularized Spleen Matrix. *Organogenesis* (2015).

175. Khetani, S. & Bhatia, S. Microscale culture of human liver cells for drug development. *Nat. Biotechnol.* **26,** 120–6 (2007).

176. Lee, P. J., Hung, P. J. & Lee, L. P. An artificial liver sinusoid with a microfluidic endothelial-like barrier for primary hepatocyte culture. *Biotechnol. Bioeng.* **97,** 1340–1346 (2007).

177. Ortega-Prieto, A. M. *et al.* 3D microfluidic liver cultures as a physiological preclinical tool for hepatitis B virus infection. *Nat. Commun.* **9,** 682 (2018).

178. Mi, S., Yi, X., Du, Z., Xu, Y. & Sun, W. Construction of a liver sinusoid based on the laminar flow on chip and self-assembly of endothelial cells. *Biofabrication* **10,** 025010 (2018).

179. Dunn, J. C., Yarmush, M. L., Koebe, H. G. & Tompkins, R. G. Hepatocyte function and extracellular matrix geometry: long-term culture in a sandwich configuration. *FASEB J.* **3,** 174–7 (1989).

180. Dunn, J. C. Y., Tompkins, R. G. & Yarmush, M. L. Long-term in vitro function of adult hepatocytes in a collagen sandwich configuration. *Biotechnol. Prog.* **7,** 237–245 (1991).

181. Bell, C. C. *et al.* Characterization of primary human hepatocyte spheroids as a model system for drug-induced liver injury, liver function and disease. *Sci. Rep.* **6,** 25187 (2016).

182. Kern, A., Bader, A., Pichlmayr, R. & Sewing, K.-F. Drug metabolism in hepatocyte sandwich cultures of rats and humans. *Biochem. Pharmacol.* **54,** 761–772 (1997).

183. Liu, Y. *et al.* Micropatterned coculture of hepatocytes on electrospun fibers as a potential in vitro model for predictive drug metabolism. *Mater. Sci. Eng. C* **63,** 475–484 (2016).

184. Kilbride, P. *et al.* Impact of Storage at -80°C on Encapsulated Liver Spheroids After Liquid Nitrogen Storage. *Biores. Open Access* **5,** 146–54 (2016).

185. Bécavin, T. *et al.* Well-organized spheroids as a new platform to examine cell interaction and behaviour during organ development. *Cell Tissue Res.* 1–15 (2016).

186. Murphy, S. V & Atala, A. 3D bioprinting of tissues and organs. *Nat. Biotechnol.* **32,** 773–785 (2014).

187. Chow, L. W. & Fischer, J. F. Creating biomaterials with spatially organized functionality. *Exp. Biol. Med. (Maywood).* **241,** 1025–32 (2016).

188. Lucendo-Villarin, B., Rashidi, H., Cameron, K. & Hay, D. C. Pluripotent stem cell derived hepatocytes: using materials to define cellular differentiation and tissue engineering. *J. Mater. Chem. B* **4,** 3433–3442 (2016).

189. Moglia, R. *et al.* Solvent-free fabrication of polyHIPE microspheres for controlled release of growth factors. *Macromol. Rapid Commun.* **35,** 1301–1305 (2014).

190. Lee, H. *et al.* Development of liver decellularized extracellular matrix bioink for 3D cell printing-based liver tissue engineering. (2017).

191. Knowlton, S. & Tasoglu, S. Spotlight : A Bioprinted Liver-on-a-Chip for Drug Screening Applications. *Trends Biotechnol.* **xx,** 1–2 (2016).

192. Nguyen, D. G. *et al.* Bioprinted 3D Primary Liver Tissues Allow Assessment of Organ-Level Response to Clinical Drug Induced Toxicity In Vitro. *PLoS One* **11,** e0158674 (2016).

193. Zhong, C., Xie, H.-Y., Zhou, L., Xu, X. & Zheng, S.-S. Human hepatocytes loaded in 3D bioprinting generate mini-liver. *Hepatobiliary Pancreat. Dis. Int* **15,** 512–518 (2016).

194. Saheli, M. *et al.* Three-Dimensional Liver-derived Extracellular Matrix Hydrogel Promotes Liver Organoids Function. *J. Cell. Biochem.* (2017).

195. Cho, C. S. *et al.* Galactose-carrying polymers as extracellular matrices for liver tissue engineering. *Biomaterials* **27,** 576–85 (2006).

196. Hay, D. C. *et al.* Unbiased screening of polymer libraries to define novel substrates for functional hepatocytes with inducible drug metabolism. *Stem Cell Res.* **6,** 92–102 (2011).

197. Shirahama, H. *et al.* Fabrication of Inverted Colloidal Crystal Poly(ethylene glycol) Scaffold: A Three-dimensional Cell Culture Platform for Liver Tissue Engineering. *J. Vis. Exp.* (2016).

198. Chang, S.-Y., Weber, E. J., Van Ness, K. P., Eaton, D. L. & Kelly, E. J. Liver and kidney on chips: Microphysiological models to understand transporter function. *Clin. Pharmacol. Ther.* 1–23 (2016).

199. Ogoke, O., Oluwole, J. & Parashurama, N. Bioengineering considerations in liver regenerative medicine. *J. Biol. Eng.* **11,** 46 (2017).

200. Kim, I. G. *et al.* Bioactive cell-derived matrices combined with polymer mesh scaffold for osteogenesis and bone healing. *Biomaterials* **50,** 75–86 (2015).

201. Zavan, B. *et al.* Extracellular matrix-enriched polymeric scaffolds as a substrate for hepatocyte cultures: in vitro and in vivo studies. *Biomaterials* **26,** 7038–45 (2005).

202. Hay, D. C. *et al.* Unbiased screening of polymer libraries to define novel substrates for functional hepatocytes with inducible drug metabolism. *Stem Cell Res.* **6,** 92–102 (2011).

203. Celiz, A. D. *et al.* Discovery of a Novel Polymer for Human Pluripotent Stem Cell Expansion and Multilineage Differentiation. *Adv. Mater.* n/a-n/a (2015).

204. You, J. *et al.* Characterizing the effects of heparin gel stiffness on function of primary hepatocytes. *Tissue Eng Part A* **19,** 2655–2663 (2013).

205. Gheibi, P., Son, K. J., Stybayeva, G. & Revzin, A. Harnessing endogenous signals from hepatocytes using a low volume multi-well plate. *Integr. Biol. (United Kingdom)* **9,** 427–435 (2017).

206. Sabetkish, S. *et al.* Whole-organ tissue engineering: Decellularization and recellularization of three-dimensional matrix liver scaffolds. *J. Biomed. Mater. Res. - Part A* 1498–1508 (2014).

207. Keane, T. J., Swinehart, I. T. & Badylak, S. F. Methods of tissue decellularization used for preparation of biologic scaffolds and in vivo relevance. *Methods* **84,** 25–34 (2015).

208. Haraszti, R. A. *et al.* High-resolution proteomic and lipidomic analysis of exosomes and microvesicles from different cell sources. *J. Extracell. Vesicles* **5,** 1–14 (2016).

209. Huleihel, L. *et al.* Matrix-bound nanovesicles within ECM bioscaffolds. (2016).

210. Huleihel, L., Scarritt, M. E. & Badylak, S. F. The Influence of Extracellular RNA on Cell Behavior in Health, Disease, and Regeneration. *Curr. Pathobiol. Rep.* **5,** 13–22 (2017).

211. Lin, P., Chan, W. C. W., Badylak, S. F. & Bhatia, S. N. Assessing porcine liver-derived biomatrix for hepatic tissue engineering. *Tissue Eng.* **10,** 1046–53 (2004).

212. Gilbert, T. W., Gilbert, S., Madden, M., Reynolds, S. D. & Badylak, S. F. Morphologic assessment of extracellular matrix scaffolds for patch tracheoplasty in a canine model. *Ann. Thorac. Surg.* **86,** 967-74; discussion 967-74 (2008).

213. White, L. J. *et al.* The impact of detergents on the tissue decellularization process: a ToF-SIMS study. *Acta Biomater.* (2016).

214. Vinci, B. *et al.* In vitro liver model using microfabricated scaffolds in a modular bioreactor. *Biotechnol. J.* **5,** 232–241 (2010).

215. Tilles, A. W., Baskaran, H., Roy, P., Yarmush, M. L. & Toner, M. Effects of oxygenation and flow on the viability and function of rat hepatocytes cocultured in a microchannel flat-plate bioreactor. *Biotechnol. Bioeng.* **73,** 379–89 (2001).

216. Powers, M. J. *et al.* A microfabricated array bioreactor for perfused 3D liver culture. *Biotechnol. Bioeng.* **78,** 257–269 (2002).

217. Tanaka, Y., Yamato, M., Okano, T., Kitamori, T. & Sato, K. Evaluation of effects of shear stress on hepatocytes by a microchip-based system. *Meas. Sci. Technol.* **17,** 3167–3170 (2006).

218. Hoffmann, S. A. *et al.* Analysis of drug metabolism activities in a miniaturized liver cell bioreactor for use in pharmacological studies. *Biotechnol. Bioeng.* **109,** 3172–3181 (2012).

219. Nussler, A. K. *et al.* The suitability of hepatocyte culture models to study various aspects of drug metabolism. *ALTEX* **18,** 91–101 (2001).

220. Mueller, D. *et al.* Real-time in situ viability assessment in a 3D bioreactor with liver cells using resazurin assay. *Cytotechnology* **65,** 297–305 (2013).

221. Sbrana, T. & Ahluwalia, A. Engineering Quasi-Vivo in vitro organ models. *Adv. Exp. Med. Biol.* **745,** 138–53 (2012).

222. Unger, J. K., Kuehlein, G., Schroers, A., Gerlach, J. C. & Rossaint, R. Adsorption of xenobiotics to plastic tubing incorporated into dynamic in vitro systems used in pharmacological research--limits and progress. *Biomaterials* **22,** 2031–7 (2001).

223. Schütte, J. *et al.* "Artificial micro organs"—a microfluidic device for dielectrophoretic assembly of liver sinusoids. *Biomed. Microdevices* **13,** 493–501 (2011).

224. Ho, C.-T. *et al.* Liver-cell patterning Lab Chip: mimicking the morphology of liver lobule tissue. *Lab Chip* **13,** 3578 (2013).

225. Ho, C.-T., Lin, R.-Z., Chang, W.-Y., Chang, H.-Y. & Liu, C.-H. Rapid heterogeneous liver-cell on-chip patterning via the enhanced field-induced dielectrophoresis trap. *Lab Chip* **6,** 724 (2006).

226. Hongling, L. *et al.* Preliminary Research of Off-Line Bioartificial Liver on Patients with Hbv Related Acute-On-Chronic Liver Failure. *J. Infect. Dis. Ther.* **4,** 6–13 (2016).

227. Patel, P., Okoronkwo, N. & Pyrsopoulos, N. T. Future Approaches and Therapeutic Modalities for Acute Liver Failure. *Clin. Liver Dis.* **22,** 419–427 (2018).

228. Grant, R., Hay, D. C. & Callanan, A. From scaffold to structure: the synthetic production of cell derived extracellular matrix for liver tissue engineering. *Biomed. Phys. Eng. Express* (2018).

229. Bye, F. J. *et al.* Postproduction processing of electrospun fibres for tissue engineering. *J. Vis. Exp.* (2012).

230. Hotaling, N. a., Bharti, K., Kriel, H. & Simon, C. G. DiameterJ: A validated open source nanofiber diameter measurement tool. *Biomaterials* **61,** 327–338 (2015).

231. Shearer, H., Ellis, M. J., Perera, S. P. & Chaudhuri, J. B. Effects of Common Sterilization Methods on the Structure and Properties of Poly(D,L Lactic-Co-Glycolic Acid) Scaffolds. *Tissue Eng.* **12,** 2717–2727 (2006).

232. PARKER, R. C., MORGAN, J. F. & MORTON, H. J. Nutrition of animal cells in tissue culture. III. Effect of ethyl alcohol on cell survival and multiplication. *J. Cell. Comp. Physiol.* **36,** 411–20 (1950).

233. Ghobeira, R. *et al.* Effects of different sterilization methods on the physico-chemical and bioresponsive properties of plasma-treated polycaprolactone films. *Biomed. Mater.* **12,** 015017 (2017).

234. Malik, Y. S., Maherchandani, S. & Goyal, S. M. Comparative efficacy of ethanol and isopropanol against feline calicivirus, a norovirus surrogate. *Am. J. Infect. Control* **34,** 31–35 (2006).

235. Vlodavsky, I. *et al.* Mammalian heparanase: involvement in cancer metastasis, angiogenesis and normal development. *Semin. Cancer Biol.* **12,** 121–129 (2002).

236. Ramchandran, R. *et al.* Antiangiogenic Activity of Restin, NC10 Domain of Human Collagen XV: Comparison to Endostatin. *Biochem. Biophys. Res. Commun.* **255,** 735–739 (1999).

237. Calve, S., Odelberg, S. J. & Simon, H.-G. A transitional extracellular matrix instructs cell behavior during muscle regeneration. *Dev. Biol.* **344,** 259–271 (2010).

238. Barnes, C. A. *et al.* The surface molecular functionality of decellularized extracellular matrices. *Biomaterials* **32,** 137–143 (2011).

239. Keane, T. J. & Badylak, S. F. The host response to allogeneic and xenogeneic biological scaffold materials. *J. Tissue Eng. Regen. Med.* (2014).

240. Keane, T. J., Londono, R., Turner, N. J. & Badylak, S. F. Consequences of ineffective decellularization of biologic scaffolds on the host response. *Biomaterials* **33,** 1771–1781 (2012).

241. Brown, B. N. & Badylak, S. F. Extracellular matrix as an inductive scaffold for functional tissue reconstruction. *Transl. Res.* **163,** 268–285 (2014).

242. Keane, T. J., Swinehart, I. & Badylak, S. F. Methods of Tissue Decellularization Used for Preparation of Biologic Scaffolds and In-vivo Relevance. *Methods* (2015).

243. Hudson, T. W. *et al.* Optimized Acellular Nerve Graft Is Immunologically Tolerated and Supports Regeneration. *Tissue Eng.* **10,** 1641–1651 (2004).

244. Hwang, J. *et al.* Molecular Assessment of Collagen Denaturation in Decellularized Tissues using a Collagen Hybridizing Peptide. *Acta Biomater.* (2017).

245. Meyer, S. R. *et al.* Comparison of aortic valve allograft decellularization techniques in the rat. *J. Biomed. Mater. Res. Part A* **79A,** 254–262 (2006).

246. Faulk, D. M. *et al.* The effect of detergents on the basement membrane complex of a biologic scaffold material. *Acta Biomater.* **10,** 183–193 (2014).

247. Lu, H., Hoshiba, T., Kawazoe, N. & Chen, G. Comparison of decellularization techniques for preparation of extracellular matrix scaffolds derived from three-dimensional cell culture. *J. Biomed. Mater. Res. A* **100,** 2507–16 (2012).

248. Dong, X. *et al.* RGD-modified acellular bovine pericardium as a bioprosthetic scaffold for tissue engineering. *J. Mater. Sci. Mater. Med.* **20,** 2327–2336 (2009).

249. Parmar, P. A. *et al.* Collagen-mimetic peptide-modifiable hydrogels for articular cartilage regeneration. *Biomaterials* **54,** 213–25 (2015).

250. Bellis, S. L. Advantages of RGD peptides for directing cell association with biomaterials. *Biomaterials* **32,** 4205–10 (2011).

251. Inomata, K., Oga, A., Kawauchi, S., Furuya, T. & Sasaki, K. Global genomic changes induced by two-stage carcinogen exposure are precancerous alterations in non-transformed human liver epithelial THLE-3 cells. *Int. J. Oncol.* **27,** 925–31 (2005).

252. Fogh, J. Cultivation, characterization, and identification of human tumor cells with emphasis on kidney, testis, and bladder tumors. *Natl. Cancer Inst. Monogr.* 5–9 (1978).

253. Dalby, B. *et al.* Advanced transfection with Lipofectamine 2000 reagent: primary neurons, siRNA, and high-throughput applications. *Methods* **33,** 95–103 (2004).

254. Ohki, E. ., Tilkins, M. ., Ciccarone, V. . & Price, P. . Improving the transfection efficiency of post-mitotic neurons. *J. Neurosci. Methods* **112,** 95–99 (2001).

255. Cardarelli, F. *et al.* The intracellular trafficking mechanism of Lipofectamine-based transfection reagents and its implication for gene delivery. *Sci. Rep.* **6,** 25879 (2016).

256. Terry, C., Dhawan, A., Mitry, R. R., Lehec, S. C. & Hughes, R. D. Optimization of the Cryopreservation and Thawing Protocol for Human Hepatocytes for Use in Cell

Transplantation. *Liver Transplant.* **16,** 229–237 (2010).

257. Sagias, F. G. *et al.* N-Acetylcysteine Improves the Viability of Human Hepatocytes Isolated From Severely Steatotic Donor Liver Tissue. *Cell Transplant.* **19,** 1487–1492 (2010).

258. Dalet, C., Fehlmann, M. & Debey, P. Use of Percoll density gradient centrifugation for preparing isolated rat hepatocytes having long-term viability. *Anal. Biochem.* **122,** 119–123 (1982).

259. Papadopoulos, N. G. *et al.* An improved fluorescence assay for the determination of lymphocyte-mediated cytotoxicity using flow cytometry. *J. Immunol. Methods* **177,** 101–11 (1994).

260. Promega Corporation. CellTiter-Blue® Cell Viability Assay Protocol. *Promega.Com* 1–15 (2013).

261. Mosmann, T. Rapid colorimetric assay for cellular growth and survival: application to proliferation and cytotoxicity assays. *J. Immunol. Methods* **65,** 55–63 (1983).

262. Dragan, A. I. *et al.* Characterization of PicoGreen Interaction with dsDNA and the Origin of Its Fluorescence Enhancement upon Binding. *Biophys. J.* **99,** 3010–3019 (2010).

263. Doumas, B. T., Watson, W. A. & Biggs, H. G. Albumin standards and the measurement of serum albumin with bromcresol green. *Clin. Chim. Acta* **258,** 21–30 (1997).

264. Kilgore, J. A., Dolman, N. J. & Davidson, M. W. A Review of Reagents for Fluorescence Microscopy of Cellular Compartments and Structures, Part III: Reagents for Actin, Tubulin, Cellular Membranes, and Whole Cell and Cytoplasm. in *Current Protocols in Cytometry* **67,** 12.32.1-12.32.17 (John Wiley & Sons, Inc., 2014).

265. Kapuscinski, J. DAPI: a DNA-specific fluorescent probe. *Biotech. Histochem.* **70,** 220–33 (1995).

266. van Roy, F. & Berx, G. The cell-cell adhesion molecule E-cadherin. *Cell. Mol. Life Sci.* **65,** 3756–3788 (2008).

267. Keirnan, J. Formaldehyde, formalin, paraformaldehyde and glutaraldehyde: What they are and what they do. *Micros. Today* **00,** 8–12 (2000).

268. Bozzola, J. J. & Russell, L. D. *Electron microscopy : principles and techniques for biologists*. (Jones and Bartlett, 1999).

269. Callanan, A., Davis, N. F., Walsh, M. T. & McGloughlin, T. M. Mechanical characterisation of unidirectional and cross-directional multilayered urinary bladder matrix (UBM) scaffolds. *Med. Eng. Phys.* **34,** 1368–74 (2012).

270. Srikar, V. T. & Spearing, S. M. A Critical Review of Microscale Mechanical Testing Methods Used in the Design of Microelectromechanical Systems. *Exp. Mech.* **43,** 238–247 (2003).

271. Akhtar, R. *et al.* Nanoindentation of histological specimens: Mapping the elastic properties of soft tissues. *J. Mater. Res.* **24,** 638–646 (2009).

272. Oliver, W. C. & Pharr, G. M. An improved technique for determining hardness and elastic modulus using load and displacement sensing indentation experiments. *Journal of Materials Research* **7,** 1564–1583 (2011).

273. Lakes, R. Foam Structures with a Negative Poisson's Ratio. *Science (New York, N.Y.)* **235,** 1038–1040 (1987).

274. Greaves, G. N., Greer, A. L., Lakes, R. S. & Rouxel, T. Poisson's ratio and modern materials. *Nat. Mater.* **10,** 823–37 (2011).

275. Szymanski, J. M., Zhang, K. & Feinberg, A. W. Measuring the poisson's ratio of fibronectin using engineered nanofibers. *Sci. Rep.* **7,** (2017).

276. Livak, K. J. & Schmittgen, T. D. Analysis of relative gene expression data using real-time quantitative PCR and the 2-ÄÄCT method. *Methods* **25,** 402–408 (2001).

277. Chomczynski, P. A reagent for the single-step simultaneous isolation of RNA, DNA and proteins from cell and tissue samples. *Biotechniques* **15,** 532–4, 536–7 (1993).

278. Tan, S. C. & Yiap, B. C. DNA, RNA, and protein extraction: The past and the present. *J. Biomed. Biotechnol.* **2009,** (2009).

279. Ye, J. *et al.* Primer-BLAST: a tool to design target-specific primers for polymerase chain reaction. *BMC Bioinformatics* **13,** 134 (2012).

280. Bartlett, M. S. Properties of Sufficiency and Statistical Tests. *Proc. R. Soc. A Math. Phys. Eng. Sci.* **160,** 268–282 (1937).

281. Meier, U. A note on the power of Fisher's least significant difference procedure. *Pharm. Stat.* **5,** 253–263 (2006).

282. McHugh, M. L. Multiple comparison analysis testing in ANOVA. *Biochem. Medica* 203–209 (2011).

283. Badylak, S. F. The extracellular matrix as a scaffold for tissue reconstruction. *Semin. Cell Dev. Biol.* **13,** 377–383 (2002).

284. Egeblad, M., Rasch, M. G. & Weaver, V. M. Dynamic interplay between the collagen scaffold and tumor evolution. *Curr. Opin. Cell Biol.* **22,** 697–706 (2010).

285. Butcher, A. L., Offeddu, G. S. & Oyen, M. L. Nanofibrous hydrogel composites as mechanically robust tissue engineering scaffolds. *Trends Biotechnol.* **32,** 564–570 (2014).

286. Garrigues, N. W., Little, D., Sanchez-Adams, J., Ruch, D. S. & Guilak, F. Electrospun Cartilage-Derived Matrix Scaffolds for Cartilage Tissue Engineering. *J Biomed Mater Res A* **102,** 3998–4008 (2014).

287. He, M., Callanan, A., Lagaras, K., Steele, J. A. M. & Stevens, M. M. Optimization of SDS exposure on preservation of ECM characteristics in whole organ decellularization of rat kidneys. *J. Biomed. Mater. Res. Part B Appl. Biomater.* 1–9 (2016).

288. Peloso, A. *et al.* Current achievements and future perspectives in whole-organ bioengineering. *Stem Cell Res. Ther.* **6,** (2015).

289. Backliwal, G. *et al.* Valproic acid: A viable alternative to sodium butyrate for enhancing protein expression in mammalian cell cultures. *Biotechnol. Bioeng.* **101,** 182–189 (2008).

290. Dokmanovic, M., Clarke, C. & Marks, P. A. Histone Deacetylase Inhibitors: Overview and Perspectives. *Mol. Cancer Res.* **5,** 981–989 (2007).

291. Yang, W. C. *et al.* Addition of Valproic Acid to CHO Cell Fed-Batch Cultures Improves Monoclonal Antibody Titers. *Mol. Biotechnol.* 1–8 (2013).

292. Klatt, D. *et al.* Viscoelastic properties of liver measured by oscillatory rheometry and multifrequency magnetic resonance elastography. *Biorheology* **47,** 133–141 (2010).

293. Cozzolino, A. M. *et al.* Modulating the Substrate Stiffness to Manipulate Differentiation of Resident Liver Stem Cells and to Improve the Differentiation State of Hepatocytes. **2016,** (2016).

294. Mansouri, N. The influence of topography on tissue engineering perspective. *Mater. Sci. Eng. C* **61,** 906–921 (2016).

295. Davis, N. F., Mooney, R., Callanan, A., Flood, H. D. & McGloughlin, T. M. Augmentation cystoplasty and extracellular matrix scaffolds: an ex vivo comparative study with autogenous detubularised ileum. *PLoS One* **6,** e20323 (2011).

296. Discher, D. E., Janmey, P. & Wang, Y.-L. Tissue cells feel and respond to the stiffness of their substrate. *Science* **310,** 1139–43 (2005).

297. Carlsson, R., Engvall, E., Freeman, A. & Ruoslahti, E. Laminin and fibronectin in cell adhesion: enhanced adhesion of cells from regenerating liver to laminin. *Proc. Natl. Acad. Sci.* **78,** 2403–2406 (1981).

298. Matsuzawa, A., Matsusaki, M. & Akashi, M. Construction of three-dimensional liver tissue models by cell accumulation technique and maintaining their metabolic functions for long-term culture without medium change. *J. Biomed. Mater. Res. A* 1–11 (2014).

299. Sell, S. a. *et al.* The use of natural polymers in tissue engineering: A focus on electrospun extracellular matrix analogues. *Polymers (Basel).* **2,** 522–553 (2010).

300. Crapo, P. M., Gilbert, T. W. & Badylak, S. F. An overview of tissue and whole organ decellularization processes.

301. Hay, D. C. *et al.* Efficient differentiation of hepatocytes from human embryonic stem cells exhibiting markers recapitulating liver development in vivo. *Stem Cells* **26,** 894–902 (2008).

302. Broutier, L. *et al.* Culture and establishment of self-renewing human and mouse adult liver and pancreas 3D organoids and their genetic manipulation. *Nat. Protoc.* **11,** 1724–43 (2016).

303. Li, Q. *et al.* Proteomic analysis of naturally-sourced biological scaffolds. *Biomaterials* **75,** 37–46 (2016).

304. Xiang, J. *et al.* Decellularized spleen matrix for reengineering functional hepatic-like tissue based on bone marrow mesenchymal stem cells. *Organogenesis* **12,** 128–142 (2016).

305. Chen, G. Y. & Nuñez, G. Sterile inflammation: sensing and reacting to damage. *Nat. Rev. Immunol.* **10,** 826–37 (2010).

306. Villarin, B. L. *et al.* Polymer Supported Directed Differentiation Reveals a Unique Gene Signature Predicting Stable Hepatocyte Performance. *Adv. Healthc. Mater.* (2015).

307. Godoy, P. *et al.* Gene network activity in cultivated primary hepatocytes is highly similar to diseased mammalian liver tissue. *Arch. Toxicol.* **90,** 1–17 (2016).

308. Xu, W. S., Parmigiani, R. B. & Marks, P. Histone deacetylase inhibitors: molecular mechanisms of action. *Oncogene* **26,** 5541–5552 (2007).

309. Kruh, J. Effects of sodium butyrate , a new pharmacological agent , on cells in culture. *Mol. Cell. Biochem.* **42,** 65–82 (1982).

310. Oniscu, G. C. *et al.* In situ normothermic regional perfusion for controlled donation after circulatory death - The United Kingdom experience. *Am. J. Transplant.* **14,** 2846–2854 (2014).

311. Callanan, A., Davis, N. F., McGloughlin, T. M. & Walsh, M. T. Development of a rotational cell-

seeding system for tubularized extracellular matrix (ECM) scaffolds in vascular surgery. *J. Biomed. Mater. Res. Part B Appl. Biomater.* **102,** 781–788 (2014).

312. Su, W. T., Liu, Y. J. & Huang, T. Y. Nanofibers promote HepG2 aggregate formation and cellular function. *Genet. Mol. Res.* **15,** (2016).

313. Hazama, K., Asayama, S. & Kawakami, H. Up-Regulation of Gene Expression by Transfection to Hepatocyte Spheroids. *Mol. Pharm.* (2012).

314. Lee, M. H. *et al.* Hepatocyte-Targeting Single Galactose-Appended Naphthalimide: A Tool for Intracellular Thiol Imaging in Vivo. *J. Am. Chem. Soc.* **134,** 1316–1322 (2012).

315. Lu, C., Xu, W., Zhang, F., Shao, J. & Zheng, S. Nrf2 Knockdown Disrupts the Protective Effect of Curcumin on Alcohol-Induced Hepatocyte Necroptosis. *Mol. Pharm.* **13,** 4043–4053 (2016).

316. Narsinh, K. H. *et al.* Generation of adult human induced pluripotent stem cells using nonviral minicircle DNA vectors. *Nat. Protoc.* **6,** 78–88 (2010).

317. Cachat, E. *et al.* 2- and 3-Dimensional Synthetic Large-Scale De Novo Patterning By Mammalian Cells Through Phase Separation. *Sci. Rep.* **6,** 20664 (2016).

318. Chen, A. Y., Zhong, C. & Lu, T. K. Engineering Living Functional Materials. *ACS Synth. Biol.* **4,** 8–11 (2015).

319. Zhou, D. *et al.* Highly branched poly(β-amino ester)s for skin gene therapy. *J. Control. Release* (2016).

320. Cutlar, L. *et al.* A Non-Viral Gene Therapy for Treatment of Recessive Dystrophic Epidermolysis Bullosa. *Exp. Dermatol.* 818–820 (2016).

321. Deltcheva, E. *et al.* CRISPR RNA maturation by trans-encoded small RNA and host factor RNase III. *Nature* **471,** 602–609 (2011).

322. Jinek, M. *et al.* A Programmable Dual-RNA–Guided DNA Endonuclease in Adaptive Bacterial Immunity. *Science (80-.).* **337,** 816–821 (2012).

323. Fonfara, I., Richter, H., Bratovič, M., Le Rhun, A. & Charpentier, E. The CRISPR-associated DNA-cleaving enzyme Cpf1 also processes precursor CRISPR RNA CRISPR–Cas systems that provide defence against mobile genetic elements in bacteria and archaea have evolved a variety of mechanisms to target and cleave RNA or DNA. *Nature* **532,** 517–523 (2016).

324. Kay, M. A., He, C.-Y. & Chen, Z.-Y. A robust system for production of minicircle DNA vectors. *Nat. Biotechnol.* **28,** 1287–1289 (2010).

325. Yi, H. *et al.* A New Strategy to Deliver Synthetic Protein Drugs: Self-reproducible Biologics Using Minicircles. *Sci. Rep.* **4,** 5961 (2014).

326. Munye, M. M. *et al.* Minicircle DNA Provides Enhanced and Prolonged Transgene Expression Following Airway Gene Transfer. *Sci. Rep.* **6,** 23125 (2016).

327. Schaefer, K. A. *et al.* Unexpected mutations after CRISPR-Cas9 editing in vivo. *Nat. Methods* **14,** 547–548 (2017).

328. Sibbald, B. Death but one unintended consequence of gene-therapy trial. *CMAJ* **164,** 1612 (2001).

329. Romero, Z., Toscano, M., Unciti, J., Molina, I. & Martin, F. Safer Vectors for Gene Therapy of Primary Immunodeficiencies. *Curr. Gene Ther.* **9,** 291–305 (2009).

330. Pisetsky, D. S. The origin and properties of extracellular DNA: from PAMP to DAMP. *Clin. Immunol.* **144,** 32–40 (2012).

331. Huleihel, L. *et al.* Matrix-bound nanovesicles within ECM bioscaffolds. *Sci. Adv.* **2,** e1600502–e1600502 (2016).

332. Kubow, K. E. *et al.* Mechanical forces regulate the interactions of fibronectin and collagen I in extracellular matrix. *Nat. Commun.* **6,** 8026 (2015).

333. Sottile, J. & Hocking, D. C. Fibronectin Polymerization Regulates the Composition and Stability of Extracellular Matrix Fibrils and Cell-Matrix Adhesions. *Mol. Biol. Cell* **14,** 3546–3559 (2002).

334. Pankov, R. & Yamada, K. M. Fibronectin at a glance. *J. Cell Sci.* **115,** 3861–3863 (2002).

335. Seliskar, M. & Rozman, D. Mammalian cytochromes P450-Importance of tissue specificity. *Biochim. Biophys. Acta - Gen. Subj.* **1770,** 458–466 (2007).

336. Medine, C. N. *et al.* Developing high-fidelity hepatotoxicity models from pluripotent stem cells. *Stem Cells Transl. Med.* **2,** 505–9 (2013).

337. Badylak, S. F., Dziki, J. L., Sicari, B. M., Ambrosio, F. & Boninger, M. L. Mechanisms by which acellular biologic scaffolds promote functional skeletal muscle restoration. *Biomaterials* **103,** 128–136 (2016).

338. Meng, F. W., Slivka, P. F., Dearth, C. L. & Badylak, S. F. Solubilized extracellular matrix from brain and urinary bladder elicits distinct functional and phenotypic responses in macrophages. *Biomaterials* **46,** 131–40 (2015).

339. Davis, N. F., Coakley, D. N., Callanan, A., Flood, H. D. & McGloughlin, T. M. Evaluation of xenogenic extracellular matrices as adjuvant scaffolds for the treatment of stress urinary incontinence. *Int. Urogynecol. J.* **24,** 2105–10 (2013).

340. Burton, T. P., Corcoran, A. & Callanan, A. The effect of electrospun polycaprolactone scaffold morphology on human kidney epithelial cells. *Biomed. Mater* **13,** (2018).

341. Burton, T. P., Corcoran, A. & Callanan, A. The effect of electrospun polycaprolactone scaffold morphology on human kidney epithelial cells. *Biomed. Mater.* **13,** 015006 (2017).

342. Casasola, R., Thomas, N. L., Trybala, A. & Georgiadou, S. Electrospun poly lactic acid (PLA) fibres: Effect of different solvent systems on fibre morphology and diameter. *Polym. (United Kingdom)* **55,** 4728–4737 (2014).

343. Rafael Auras, Lim, L.-T., Selke, S. E. M. & Tsuji, H. *Poly(Lactic Acid): Synthesis, Structures, Properties, Processing, and Applications*. (2010).

344. Iwasaki, A. *et al.* Molecular mechanism responsible for fibronectin-controlled alterations in matrix stiffness in advanced chronic liver fibrogenesis. *J. Biol. Chem.* **291,** 72–88 (2016).

345. Zollinger, A. J. & Smith, M. L. Fibronectin, the extracellular glue. *Matrix Biol.* (2016).

346. George, E. L., Georges-Labouesse, E. N., Patel-King, R. S., Rayburn, H. & Hynes, R. O. Defects in mesoderm, neural tube and vascular development in mouse embryos lacking fibronectin. *Development* **119,** 1079–1091 (1993).

347. Gorell, E., Nguyen, N., Lane, A. & Siprashvili, Z. Gene therapy for skin diseases. *Cold Spring Harb Perspect Med* **4,** a015149 (2014).

348. Mazza, G. *et al.* Rapid production of human liver scaffolds for functional tissue engineering by high shear stress oscillation-decellularization. *Sci. Rep.* **7,** 5534 (2017).

349. Zhang, H., Zhang, Y., Ma, F., Bie, P. & Bai, L. Orthotopic transplantation of decellularized liver scaffold in mice. **8,** 598–606 (2015).

350. Hussein, K. H., Park, K.-M., Kang, K.-S. & Woo, H.-M. Heparin-gelatin mixture improves vascular reconstruction efficiency and hepatic function in bioengineered livers. *Acta Biomater.* **38,** 82–93 (2016).

351. Chia, S. M. *et al.* Hepatocyte encapsulation for enhanced cellular functions. *Tissue Eng.* **6,** 481–95 (2000).

352. Hodgkinson, C. P., Wright, M. C. & Paine, a J. Fibronectin-mediated hepatocyte shape change reprograms cytochrome P450 2C11 gene expression via an integrin-signaled induction of ribonuclease activity. *Mol. Pharmacol.* **58,** 976–81 (2000).

353. Felmlee, D. J., Grün, D. & Baumert, T. F. Zooming in on liver zonation. *Hepatology* **67,** 784–787 (2018).

354. Wang, Y. *et al.* ECM proteins in a microporous scaffold influence hepatocyte morphology, function, and gene expression. *Sci. Rep.* **6,** 37427 (2016).

355. Kennedy, K. M., Bhaw-Luximon, A. & Jhurry, D. Cell-matrix mechanical interaction in electrospun polymeric scaffolds for tissue engineering: Implications for scaffold design and performance. *Acta Biomater.* **50,** 41–55 (2016).

356. Gao, Y. *et al.* Stem Cell Reports Ar ticle Distinct Gene Expression and Epigenetic Signatures in Hepatocyte-like Cells Produced by Different Strategies from the Same Donor. (2017).

357. Sullivan, G. J. *et al.* Generation of functional human hepatic endoderm from human induced pluripotent stem cells. *Hepatology* **51,** 329–35 (2010).

358. Baxter, M. *et al.* Phenotypic and functional analyses show stem cell-derived hepatocyte-like cells better mimic fetal rather than adult hepatocytes. *J. Hepatol.* **62,** 581–589 (2015).

359. Li, M. *et al.* Electrospun protein fibers as matrices for tissue engineering. *Biomaterials* **26,** 5999–6008 (2005).

360. Wang, X., Li, W. & Kumar, V. A method for solvent-free fabrication of porous polymer using solid-state foaming and ultrasound for tissue engineering applications. *Biomaterials* **27,** 1924–9 (2006).

361. Ulery, B. D., Nair, L. S. & Laurencin, C. T. Biomedical Applications of Biodegradable Polymers. *J. Polym. Sci. B. Polym. Phys.* **49,** 832–864 (2011).

362. Malikmammadov, E., Endogan Tanir, T., Kiziltay, A., Hasirci, V. & Hasirci, N. PCL and PCL-based materials in biomedical applications. *J. Biomater. Sci.* **29,** 863–893 (2018).

363. Munir, N. & Callanan, A. Novel phase separated polycaprolactone/collagen scaffolds for cartilage tissue engineering. *Biomed. Mater.* **13,** 051001 (2018).

364. Lübberstedt, M. *et al.* Serum-free culture of primary human hepatocytes in a miniaturized hollow-fibre membrane bioreactor for pharmacological *in vitro* studies. *J. Tissue Eng. Regen. Med.* **9,** 1017–1026 (2015).

365. Hagbard, L. *et al.* Developing defined substrates for stem cell culture and differentiation. *Philos. Trans. R. Soc. Lond. B. Biol. Sci.* **373,** (2018).

366. Villarin, B. L. *et al.* Polyurethane: Stable Cell Phenotype Requires Plasticity: Polymer Supported Directed Differentiation Reveals a Unique Gene Signature Predicting Stable

Hepatocyte Performance (Adv. Healthcare Mater. 12/2015). *Adv. Healthc. Mater.* **4,** 1819 (2015).

367. Greenhough, S., Medine, C. N. & Hay, D. C. Pluripotent stem cell derived hepatocyte like cells and their potential in toxicity screening. *Toxicology* **278,** 250–255 (2010).

368. Gramignoli, R. *et al.* Development and application of purified tissue dissociation enzyme mixtures for human hepatocyte isolation. *Cell Transplant.* **21,** 1245–60 (2012).

369. Guguen-Guillouzo, C. *Isolation and culture of animal and human hepatocytes*. *Methods in Molecular Biology* (2002).

370. Gonçalves, L. A., Vigário, A. M. & Penha-Gonçalves, C. Improved isolation of murine hepatocytes for in vitro malaria liver stage studies. *Malar. J.* **6,** 169 (2007).

371. Vogel, C. & Marcotte, E. M. Insights into the regulation of protein abundance from proteomic and transcriptomic analyses. *Nat. Rev. Genet.* **13,** 227–232 (2012).

372. Khositseth, S. *et al.* Quantitative Protein and mRNA Profiling Shows Selective Post-Transcriptional Control of Protein Expression by Vasopressin in Kidney Cells. *Mol. Cell. Proteomics* **10,** M110.004036 (2011).

373. Haque, K. A. *et al.* Performance of high-throughput DNA quantification methods. *BMC Biotechnol.* **3,** 20 (2003).

374. Ramirez, C. N., Antczak, C. & Djaballah, H. Cell viability assessment: toward content-rich platforms. *Expert Opin. Drug Discov.* **5,** 223–33 (2010).

375. Matos, L. L. de, Trufelli, D. C., de Matos, M. G. L. & da Silva Pinhal, M. A. Immunohistochemistry as an important tool in biomarkers detection and clinical practice. *Biomark. Insights* **5,** 9–20 (2010).

376. He, M. *et al.* Artificial Polymeric Scaffolds as Extracellular Matrix Substitutes for Autologous Conjunctival Goblet Cell Expansion. *Investig. Opthalmology Vis. Sci.* **57,** 6134 (2016).

377. Wang, Y. *et al.* Defined and Scalable Generation of Hepatocyte-like Cells from Human Pluripotent Stem Cells. *J. Vis. Exp.* e55355–e55355 (2017).

378. Rashidi, H., Alhaque, S., Szkolnicka, D., Flint, O. & Hay, D. C. Fluid shear stress modulation of hepatocyte-like cell function. *Arch. Toxicol.* 3–7 (2016).

379. Massey, V. L. *et al.* The hepatic "matrisome" responds dynamically to injury: Characterization of transitional changes to the extracellular matrix in mice. *Hepatology* (2016).

380. Bell, C. C. *et al.* Characterization of primary human hepatocyte spheroids as a model system for drug-induced liver injury, liver function and disease. *Sci. Rep.* **6,** 25187 (2016).

381. Sasaki, K. *et al.* Construction of three-dimensional vascularized functional human liver tissue using a layer-by-layer cell coating technique. *Biomaterials* **133,** 263–274 (2017).

382. Sun, D. *et al.* Effects of gelling bath on the physical properties of alginate gel beads and the biological characteristics of entrapped HepG2 cells. *Biotechnol. Appl. Biochem.* **65,** 263–273 (2018).

383. Heslop, J. A. *et al.* Mechanistic evaluation of primary human hepatocyte culture using global proteomic analysis reveals a selective dedifferentiation profile. *Arch. Toxicol.* (2016).

384. Rogers, A. B. REVIEW ARTICLE: Stress of Strains: Inbred Mice in Liver Research. *Gene Expr.* (2018).

Appendix 1

Supplementary information

Supplementary figure 1; Immunohistochemistry demonstrating penetration of ECM proteins into electrospun scaffold. Data taken from Chapter 3; a drug induced hybrid protein:polycaprolactone scaffolds for liver tissue engineering

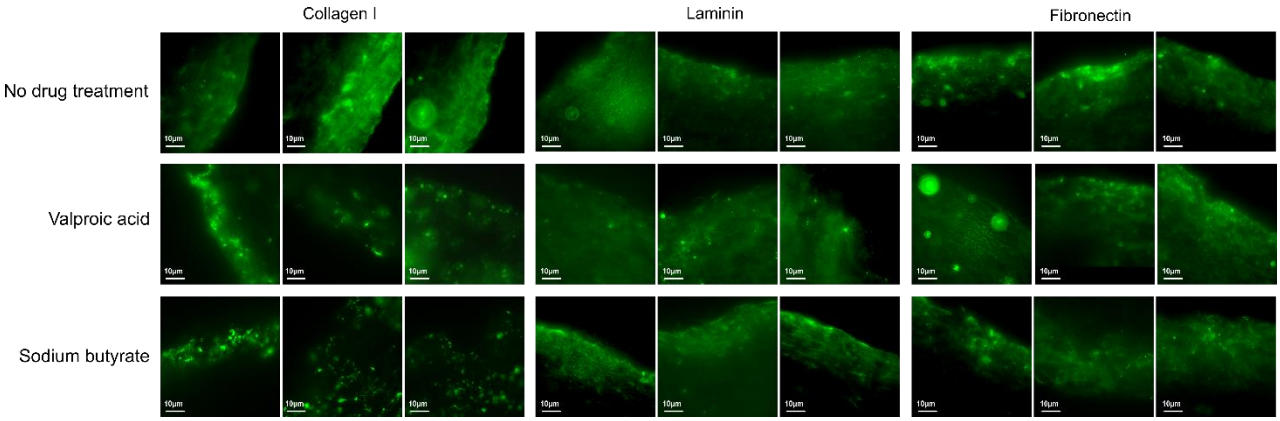

Supplementary figure 2; Raman spectra of decellularized constructs demonstrating changes in scaffolds ECM composition. Data taken from Chapter 5; the production of synthetically derived fibronectin scaffolds for liver tissue engineering

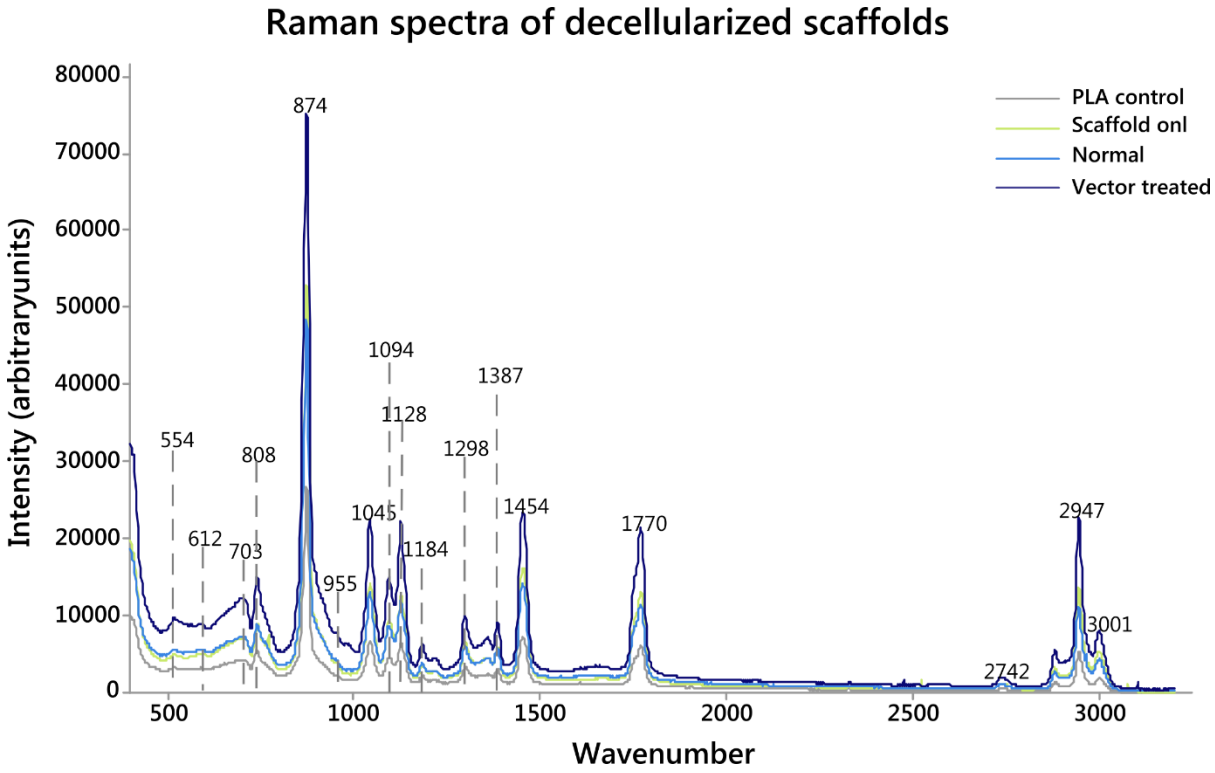

Raman spectroscopy is a method used for label free characterisation of organic materials. It uses laser spectroscopy to measure a vibrational spectrum of covalent bonds, with each frequency being specific to part of a molecule (e.g., CH2 groups in lipids, beta-sheet proteins, RNA). The relative proportions of each of such chemistries gives rise to a “fingerprint” spectrum specific to each material or collection of molecules e.g. to cell phenotype. Using raman spectroscopy allows us to analyse scaffolds woithout

damage being incurred by methods such as immunohistochemistry, and allows us to use minimal sample sizes.

Supplementary figure 3; Full vector sequence. Data taken from Chapter 5; the production of synthetically derived fibronectin scaffolds for liver tissue engineering

AAGCTTGCATGCCTGCAGGTCGACTCTAGGCACATAAAGAAAAACATAACTAACCAAGCTGCAGCCGAGACA
GTGAAAAGAACCGTTAAAACGGTTTGTTTTAAATAAACTGAATTATTTAGAGTCATTTCTTTGGTAGGAAAGTA
CATTGGCACGTAAAGGAGCCCAAAGCAATCTGTGGAAAGCCCAGGCTGGGAGCCCAGCAGTTTGCATCCCCT
CCTGGCGTGTACCTAAGGGTTTCTTAATTGTGTGGTTTCTAAATCTTCCAGAGGGTTTGTCTCATTCACTTCCAC
TTCGGTGCACAATACTTGGACGCGGATTTACTGTCTTAGCATCTATCGGTGGCCCTTCGATTGAGGCTGAACCT
GAGGCCCACTTCTTCAGCTTGTTAAGGAGAGCACAAGCACCAGAAGAGGCTGACCCGGCAGACCTGTGGGCA
TTTTTAACAAGGGCCTCCTGGGTCTGTGGGAGGCAGGCTTACATAAGGTGCAAATTAGAAATATAAATAATAA
GCCCATATCAATTTGTCATCTTTTTTTAAGCTCAAGTTTTGAAAGACCCCACCTGTAGGTTTGGCAAGCTAGCTT
AAGTAACGCCATTTTGCAAGGCATGGAAAATACATAACTGAGAATAGAGAAGTTCAGATCAAGGTTAGGAAC
AGAGAGACAGCAGAATATGGGCCAAACAGGATATCTGTGGTAAGCAGTTCCTGCCCCGCTCAGGGCCAAGAA
CAGTTGGAACAGGAGAATATGGGCCAAACAGGATATCTGTGGTAAGCAGTTCCTGCCCCGGCTCAGGGCCAA
GAACAGATGGTCCCCAGATGCGGTCCCGCCCTCAGCAGTTTCTAGAGAACCATCAGATGTTTCCAGGGTGCCC
CAAGGACCTGAAATGACCCTGTGCCTTATTTGAACTAACCAATCAGTTCGCTTCTCGCTTCTGTTCGCGCGCTTC
TGCTCCCCGAGCTCAATAAAAGAGCCCACAACCCCTCACTCGGCGCGCCAGTCCTCCGATAGACTGCGTCGCC
CGGGTACCCGTGTTCTCAATAAACCCTCTTGCAGTTGCATCCGACTCGTGGTCTCGCTGTTCCTTGGGAGGGTC
TCCTCTGAGTGATTGACTACCCGTCAGCGGGGTCTTTCATTTGGAGGTTCCACCGAGATTTGGAGACCCCTGCC
CAGGGACCACCGACCCCCCCGCCGGGAGGTAAGCTGGCCAGCAACTTATCTGTGTCTGTCCGATTGTCTAGTG
TCTATGACTGATTTTATGCGCCTGCGTCGGTACTAGTTAGCTAACTAGCTCTGTATCTGGCGGACCCGTGGTGG
AACTGACGAGTTCGGAACACCCGGCCGCAACCCTGGGAGACGTCCCAGGGACTTCGGGGGCCGTTTTTGTGG
CCCGACCTGAGTCCTAAAATCCCGATCGTTTAGGACTCTTTGGTGCACCCCCCTTAGAGGAGGGATATGTGGT
TCTGGTAGGAGACGAGAACCTAAAACAGTTCCCGCCTCCGTCTGAATTTTTGCTTTCGGTTTGGGACCGAAGC
CGCGCCGCGCGTCTTGTCTGCTGCAGCATCGTTCTGTGTTGTCTCTGTCTGACTGTGTTTCTGTATTTGTCTGAA
AATATGGGCCCGGGCTAGACTGTTACCACTCCCTTAAGTTTGACCTTAGGTCACTGGAAAGATGTCGAGCGGA
TCGCTCACAACCAGTCGGTAGATGTCAAGAAGAGACGTTGGGTTACCTTCTGCTCTGCAGAATGGCCAACCTT
TAACGTCGGATGGCCGCGAGACGGCACCTTTAACCGAGACCTCATCACCCAGGTTAAGATCAAGGTCTTTTCA
CCTGGCCCGCATGGACACCCAGACCAGGTCCCCTACATCGTGACCTGGGAAGCCTTGGCTTTTGACCCCCCTCC
CTGGGTCAAGCCCTTTGTACACCCTAAGCCTCCGCCTCCTCTTCCTCCATCCGCCCCGTCTCTCCCCCTTGAACCT
CCTCGTTCGACCCCGCCTCGATCCTCCCTTTATCCAGCCCTCACTCCTTCTCTAGGCGCCCCCATATGGCCATAT
GAGATCTTATATGGGGCACCCCCGCCCCTTGTAAACTTCCCTGACCCTGACATGACAAGAGTTACTAACAGCCC
CTCTCTCCAAGCTCACTTACAGGCTCTCTACTTAGTCCAGCACGAAGTCTGGAGACCTCTGGCGGCAGCCTACC
AAGAACAACTGGACCGACCGGTGGTACCTCACCCTTACCGAGTCGGCGACACAGTGTGGGTCCGCCGACACC
AGACTAAGAACCTAGAACCTCGCTGGAAAGGACCTTACACAGTCCTGCTGACCACCCCCACCGCCCTCAAAGT
AGACGGCATCGCAGCTTGGATACACGCCGCCCACGTGAAGGCTGCCGACCCCGGGGGTGGACCATCCTCTAG
ACTGCCATGGCCGAGTACAAGCCCACGGTGCGCCTCGCCACCCGCGACGACGTCCCCCGGGCCGTACGCACC
CTCGCCGCCGCGTTCGCCGACTACCCCGCCACGCGCCACACCGTCGACCCGGACCGCCACATCGAGCGGGTCA
CCGAGCTGCAAGAACTCTTCCTCACGCGCGTCGGGCTCGACATCGGCAAGGTGTGGGTCGCGGACGACGGCG
CCGCGGTGGCGGTCTGGACCACGCCGGAGAGCGTCGAAGCGGGGGCGGTGTTCGCCGAGATCGGCCCGCGC
ATGGCCGAGTTGAGCGGTTCCCGGCTGGCCGCGCAGCAACAGATGGAAGGCCTCCTGGCGCCGCACCGGCCC
AAGGAGCCCGCGTGGTTCCTGGCCACCGTCGGCGTCTCGCCCGACCACCAGGGCAAGGGTCTGGGCAGCGCC
GTCGTGCTCCCCGGAGTGGAGGCGGCCGAGCGCGCCGGGGTGCCCGCCTTCCTGGAGACCTCCGCGCCCCGC
AACCTCCCCTTCTACGAGCGGCTCGGCTTCACCGTCACCGCCGACGTCGAGTGCCCGAAGGACCGCGCGACCT
GGTGCATGACCCGCAAGCCCGGTGCCTGACGCGGCCGCCTCCGGCCATTAGCCATATTATTCATTGGTTATAT
AGCATAAATCAATATTGGCTATTGGCCATTGCATACGTTGTATCCATATCATAATATGTACATTTATATTGGCTC
ATGTCCAACATTACCGCCATGTTGACATTGATTATTGACTAGTTATTAATAGTAATCAATTACGGGGTCATTAG
TTCATAGCCCATATATGGAGTTCCGCGTTACATAACTTACGGTAAATGGCCCGCCTGGCTGACCGCCCAACGA
CCCCCGCCCATTGACGTCAATAATGACGTATGTTCCCATAGTAACGCCAATAGGGACTTTCCATTGACGTCAAT

GGGTGGAGTATTTACGGTAAACTGCCCACTTGGCAGTACATCAAGTGTATCATATGCCAAGTACGCCCCCTAT
TGACGTCAATGACGGTAAATGGCCCGCCTGGCATTATGCCCAGTACATGACCTTATGGGACTTTCCTACTTGGC
AGTACATCTACGTATTAGTCATCGCTATTACCATGGTGATGCGGTTTTGGCAGTACATCAATGGGCGTGGATA
GCGGTTTGACTCACGGGGATTTCCAAGTCTCCACCCCATTGACGTCAATGGGAGTTTGTTTTGGCACCAAAATC
AACGGGACTTTCCAAAATGTCGTAACAACTCCGCCCCATTGACGCAAATGGGCGGTAGGCATGTACGGTGGG
AGGTCTATATAAGCAGAGCTCGTTTAGTGAACCGTCAGATCGCCTGGAGACGCCATCCACGCTGTTTTGACCT
CCATAGAAGACACCGGGACCGATCCAGCCTCCGCGGCCCCAAGCTTATAACTTCGTATAGCATACATTATACG
AAGTTATAGATCCAATATTATTGAAGCATTTATCAGGGTTATTGTCTCATGAGCGGATACATATTTGAATGTAT
TTAGAAAAATAAACAAATAGGGGTTCCGCGCACATTTCCCCGAAAAGTGCCACCTGACGTTCGAGGATCCGG
ATTAGTCCAATTTGTTAAAGACAGGATATCAGTGGTCCAGGCTCTAGTTTTGACTCAACAATATCACCAGCTGA
AGCCTATAGAGTACGAGCCATAGATAAAATAAAAGATTTTATTTAGTCTCCAGAAAAAGGGGGGAATGAAAG
ACCCCACCTGTAGGTTTGGCAAGCTAGCTTAAGTAACGCCATTTTGCAAGGCATGGAAAATACATAACTGAGA
ATAGAGAAGTTCAGATCAAGGTTAGGAACAGAGAGACAGCAGAATATGGGCCAAACAGGATATCTGTGGTA
AGCAGTTCCTGCCCCGCTCAGGGCCAAGAACAGTTGGAACAGGAGAATATGGGCCAAACAGGATATCTGTGG
TAAGCAGTTCCTGCCCCGGCTCAGGGCCAAGAACAGATGGTCCCCAGATGCGGTCCCGCCCTCAGCAGTTTCT
AGAGAACCATCAGATGTTTCCAGGGTGCCCCAAGGACCTGAAATGACCCTGTGCCTTATTTGAACTAACCAAT
CAGTTCGCTTCTCGCTTCTGTTCGCGCGCTTCTGCTCCCCGAGCTCAATAAAAGAGCCCACAACCCCTCACTCG
GCGCGCCAGTCCTCCGATAGACTGCGTCGCCCGGGTACCCGTGTTCTCAATAAACCCTCTTGCAGTTGCATCCG
ACTCGTGGTCTCGCTGTTCCTTGGGAGGGTCTCCTCTGAGTGATTGACTACCCGTCAGCGGGGTCTTTCAGTTT
CTCCCACCTACACAGGTCTCACTAACATTCCTGATGTGCCGCAGGGACTCCGTCAGCCCGGTTTTTGTTTATAA
TAAAATGCAAGAACAGTGTTCCCTTCAAGCCAGACTACATCCTGACTCTCGGCTTTATAAAAGAATGTTGAAG
GGCTCTGTGGACTATCTGCCACACGACTTTTTAAGATTTTTATGCCTCCTGGATGAGGGATTTAGTCAATCTAT
CCTCGTCTATTTTGCTGGCTTCTCCGTATTTTAAATTTCTAGTTTGCACTCCCTTCCTGAGAGCACGGCGATTGC
AGAGTAGTTAATACTCTGAGGGCAGGCTTCTGTGAAAAGGTTGCCTGGGCTCAGTGTGAGATTTTGCCATAAA
AAGGGGTCCTGCCCCTGTGTACAGACAGATCGGAATCTAGAGTGCATACTCAGAGTCCCCGCGGTTCCGGGG
CTCTGATCTCAGGGCATCTTTGCCTAGAGATCCTCTACGCCGGACGCATCGTGGCCCTCGAATTAATTCGTAAT
CATGGTCATAGCTGTTTCCTGTGTGAAATTGTTATCCGCTCACAATTCCACACAACATACGAGCCGGAAGCATA
AAGTGTAAAGCCTGGGGTGCCTAATGAGTGAGCTAACTCACATTAATTGCGTTGCGCTCACTGCCCGCTTTCC
AGTCGGGAAACCTGTCGTGCCAGCTGCATTAATGAATCGGCCAACGCGCGGGGAGAGGCGGTTTGCGTATTG
GGCGCTCTTCCGCTTCCTCGCTCACTGACTCGCTGCGCTCGGTCGTTCGGCTGCGGCGAGCGGTATCAGCTCA
CTCAAAGGCGGTAATACGGTTATCCACAGAATCAGGGGATAACGCAGGAAAGAACATGTGAGCAAAAGGCC
AGCAAAAGGCCAGGAACCGTAAAAAGGCCGCGTTGCTGGCGTTTTTCCATAGGCTCCGCCCCCCTGACGAGC
ATCACAAAAATCGACGCTCAAGTCAGAGGTGGCGAAACCCGACAGGACTATAAAGATACCAGGCGTTTCCCC
CTGGAAGCTCCCTCGTGCGCTCTCCTGTTCCGACCCTGCCGCTTACCGGATACCTGTCCGCCTTTCTCCCTTCGG
GAAGCGTGGCGCTTTCTCATAGCTCACGCTGTAGGTATCTCAGTTCGGTGTAGGTCGTTCGCTCCAAGCTGGG
CTGTGTGCACGAACCCCCCGTTCAGCCCGACCGCTGCGCCTTATCCGGTAACTATCGTCTTGAGTCCAACCCGG
TAAGACACGACTTATCGCCACTGGCAGCAGCCACTGGTAACAGGATTAGCAGAGCGAGGTATGTAGGCGGTG
CTACAGAGTTCTTGAAGTGGTGGCCTAACTACGGCTACACTAGAAGGACAGTATTTGGTATCTGCGCTCTGCT
GAAGCCAGTTACCTTCGGAAAAAGAGTTGGTAGCTCTTGATCCGGCAAACAAACCACCGCTGGTAGCGGTGG
TTTTTTTGTTTGCAAGCAGCAGATTACGCGCAGAAAAAAAGGATCTCAAGAAGATCCTTTGATCTTTTCTACGG
GGTCTGACGCTCAGTGGAACGAAAACTCACGTTAAGGGATTTTGGTCATGAGATTATCAAAAAGGATCTTCAC
CTAGATCCTTTTAAATTAAAAATGAAGTTTTAAATCAATCTAAAGTATATATGAGTAAACTTGGTCTGACAGTT
ACCAATGCTTAATCAGTGAGGCACCTATCTCAGCGATCTGTCTATTTCGTTCATCCATAGTTGCCTGACTCCCCG
TCGTGTAGATAACTACGATACGGGAGGGCTTACCATCTGGCCCCAGTGCTGCAATGATACCGCGAGACCCAC
GCTCACCGGCTCCAGATTTATCAGCAATAAACCAGCCAGCCGGAAGGGCCGAGCGCAGAAGTGGTCCTGCAA
CTTTATCCGCCTCCATCCAGTCTATTAATTGTTGCCGGGAAGCTAGAGTAAGTAGTTCGCCAGTTAATAGTTTG
CGCAACGTTGTTGCCATTGCTACAGGCATCGTGGTGTCACGCTCGTCGTTTGGTATGGCTTCATTCAGCTCCGG
TTCCCAACGATCAAGGCGAGTTACATGATCCCCCATGTTGTGCAAAAAAGCGGTTAGCTCCTTCGGTCCTCCGA
TCGTTGTCAGAAGTAAGTTGGCCGCAGTGTTATCACTCATGGTTATGGCAGCACTGCATAATTCTCTTACTGTC
ATGCCATCCGTAAGATGCTTTTCTGTGACTGGTGAGTACTCAACCAAGTCATTCTGAGAATAGTGTATGCGGC
GACCGAGTTGCTCTTGCCCGGCGTCAATACGGGATAATACCGCGCCACATAGCAGAACTTTAAAAGTGCTCAT

CATTGGAAAACGTTCTTCGGGGCGAAAACTCTCAAGGATCTTACCGCTGTTGAGATCCAGTTCGATGTAACCC
ACTCGTGCACCCAACTGATCTTCAGCATCTTTTACTTTCACCAGCGTTTCTGGGTGAGCAAAAACAGGAAGGCA
AAATGCCGCAAAAAAGGGAATAAGGGCGACACGGAAATGTTGAATACTCATACTCTTCCTTTTTCAATATTATT
GAAGCATTTATCAGGGTTATTGTCTCATGAGCGGATACATATTTGAATGTATTTAGAAAAATAAACAAATAGG
GGTTCCGCGCACATTTCCCCGAAAAGTGCCACCTGACGTCTAAGAAACCATTATTATCATGACATTAACCTATA
AAAATAGGCGTATCACGAGGCCCTTTCGTCTCGCGCGTTTCGGTGATGACGGTGAAAACCTCTGACACATGCA
GCTCCCGGAGACGGTCACAGCTTGTCTGTAAGCGGATGCCGGGAGCAGACAAGCCCGTCAGGGCGCGTCAG
CGGGTGTTGGCGGGTGTCGGGGCTGGCTTAACTATGCGGCATCAGAGCAGATTGTACTGAGAGTGCACCATA
TGCGGTGTGAAATACCGCACAGATGCGTAAGGAGAAAATACCGCATCAGGCGCCATTCGCCATTCAGGCTGC
GCAACTGTTGGGAAGGGCGATCGGTGCGGGCCTCTTCGCTATTACGCCAGCTGGCGAAAGGGGGATGTGCT
GCAAGGCGATTAAGTTGGGTAACGCCAGGGTTTTCCCAGTCACGACGTTGTAAAACGACGGCCAGTGCCGCG
GCCGCATAACTTCGTATAGCATACATTATACGAAGTTATCAGTCGACACCATGTCTGAATCAGGCTTTAAACTG
TTGTGCCAGTGCTTAGGCTTTGGAAGTGGTCATTTCAGATGTGATTCATCTAGATGGTGCCATGACAATGGTG
TGAACTACAAGATTGGAGAGAAGTGGGACCGTCAGGGAGAAAATGGCCAGATGATGAGCTGCACATGTCTT
GGGAACGGAAAAGGAGAATTCAAGTGTGACCCTCATGAGGCAACGTGTTATGATGATGGGAAGACATACCA
CGTAGGAGAACAGTGGCAGAAGGAATATCTCGGTGCCATTTGCTCCTGCACATGCTTTGGAGGCCAGCGGGG
CTGGCGCTGTGACAACTGCCGCAGACCTGGGGGTGAACCCAGTCCCGAAGGCACTACTGGCCAGTCCTACAA
CCAGTATTCTCAGAGATACCATCAGAGAACAAACACTAATGTTAATTGCCCAATTGAGTGCTTCATGCCTTTAG
ATGTACAGGCTGACAGAGAAGATTCCCGAGAGTAAGGAAGCTTTCTAGACCATTCGTTTGGCGCGCGGGCCC

Supplementary figure 4; Example albumin BCG assay calibration curve

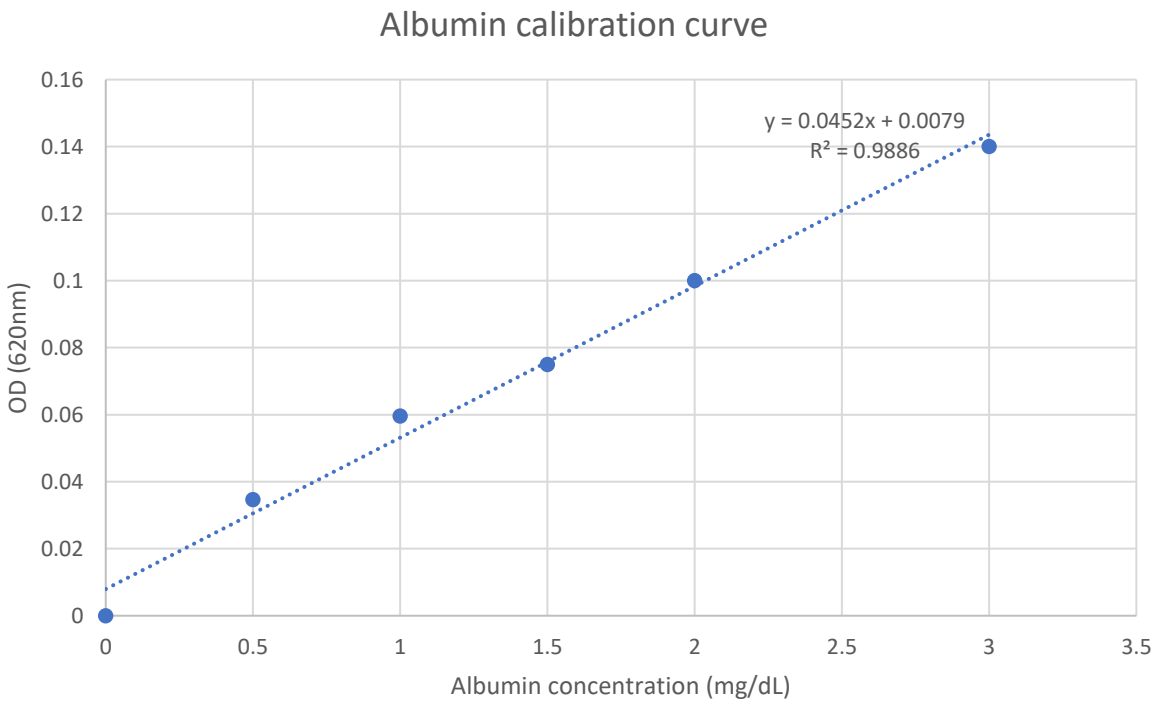

Supplementary figure 5; Example picogreen calibration curve

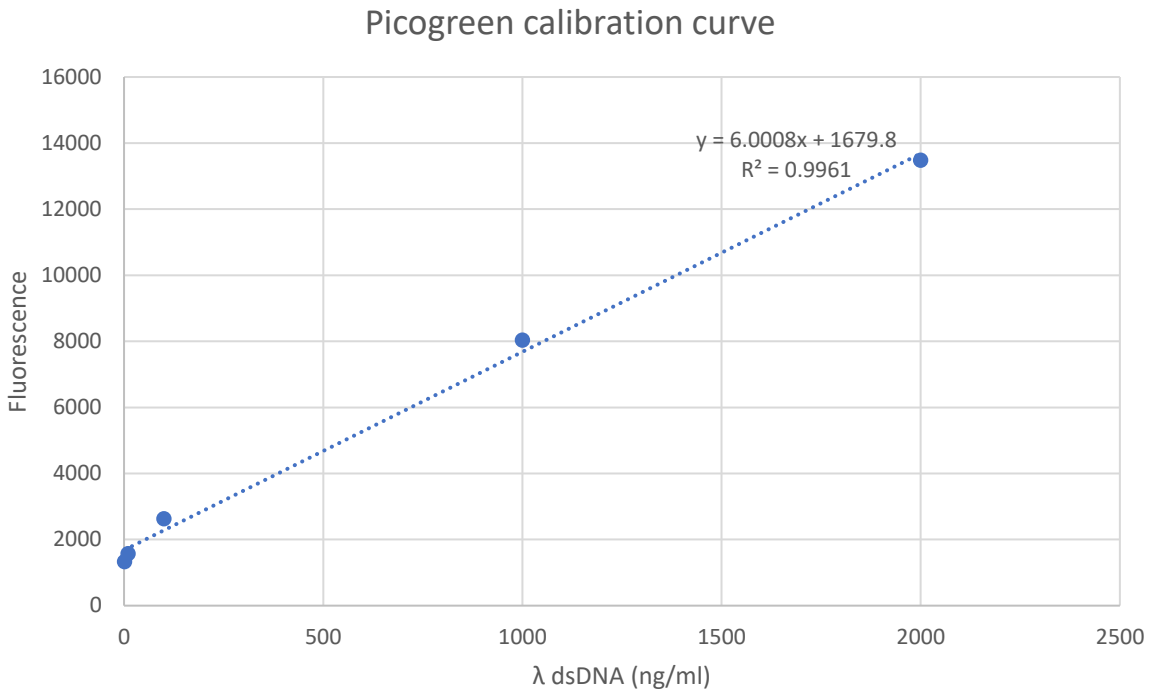

Supplementary figure 6; Example cell titre blue calibration curve

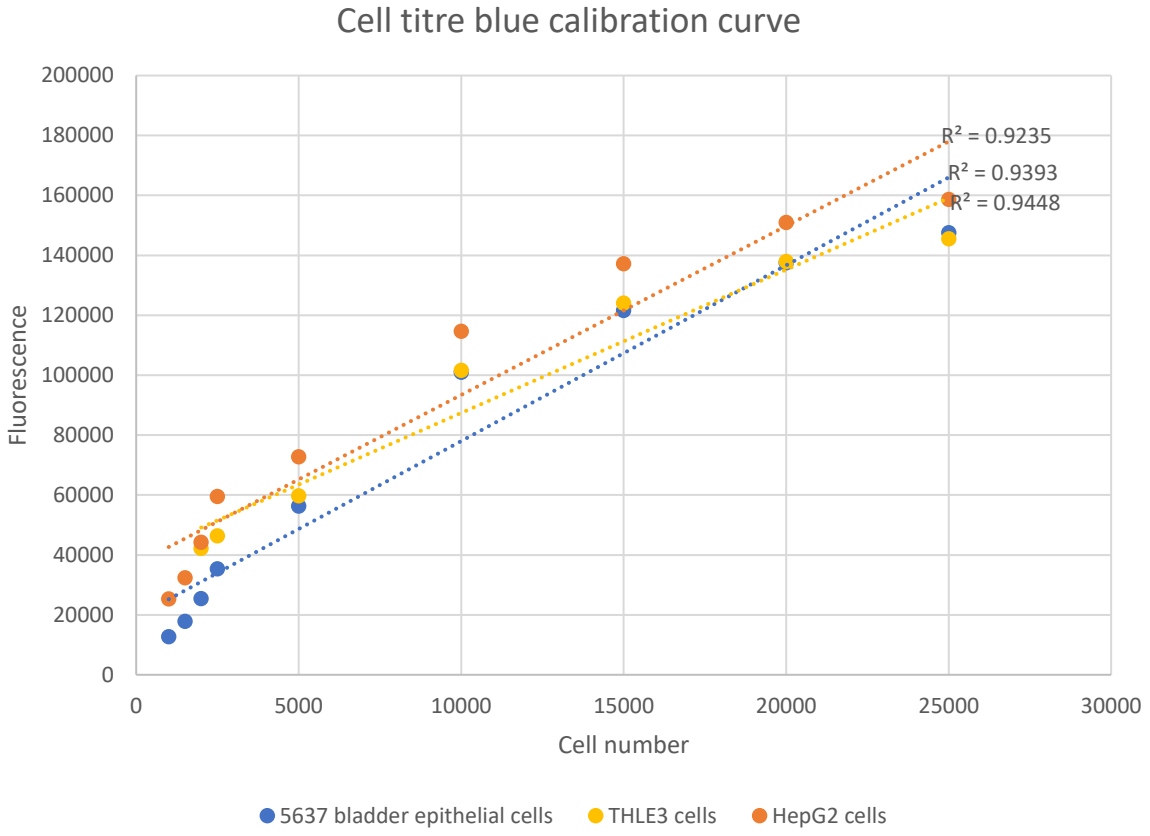

Supplementary figure 7; Example MTT calibration curve

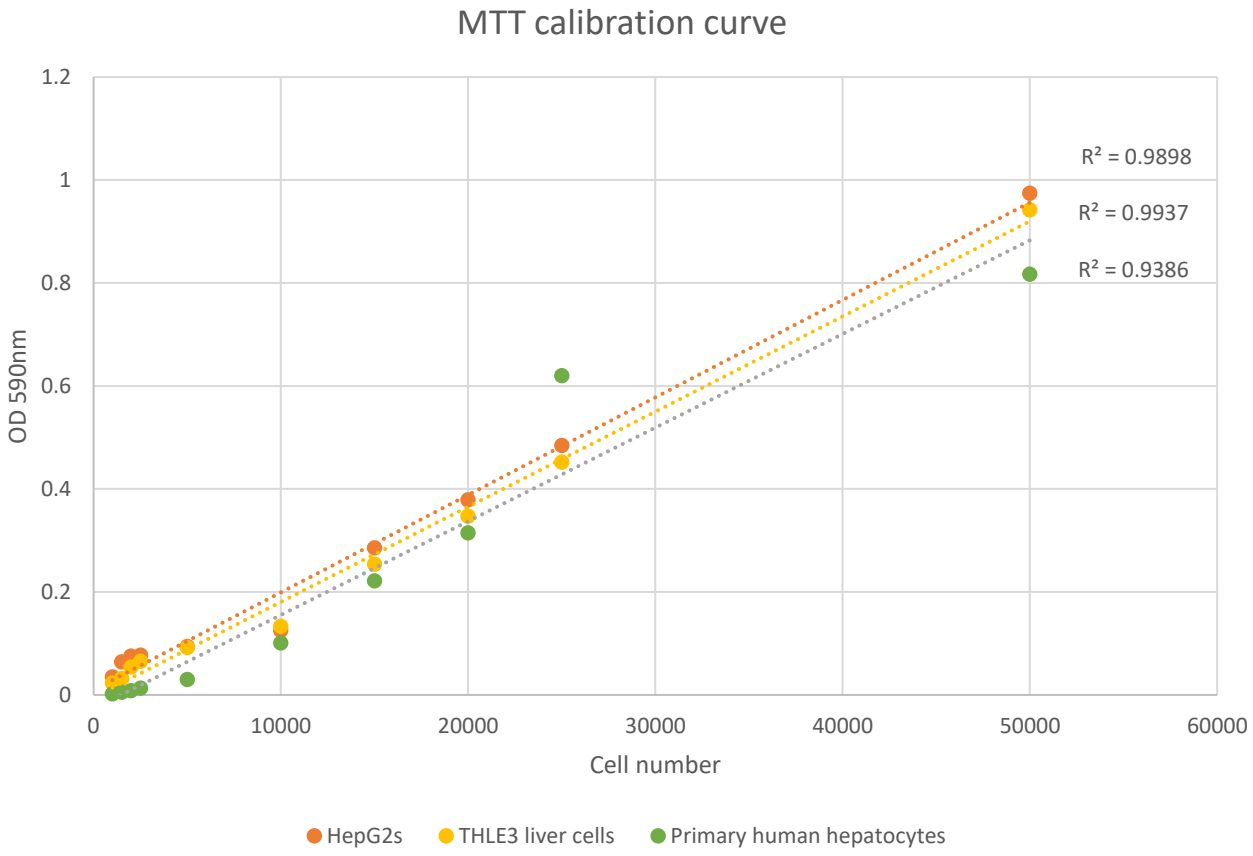

Supplementary figure 8; SEM of HepG2 cultures at 3/5 days on frozen drug derived ECM:PLA scaffolds vs non-frozen (normal) and scaffold only condition

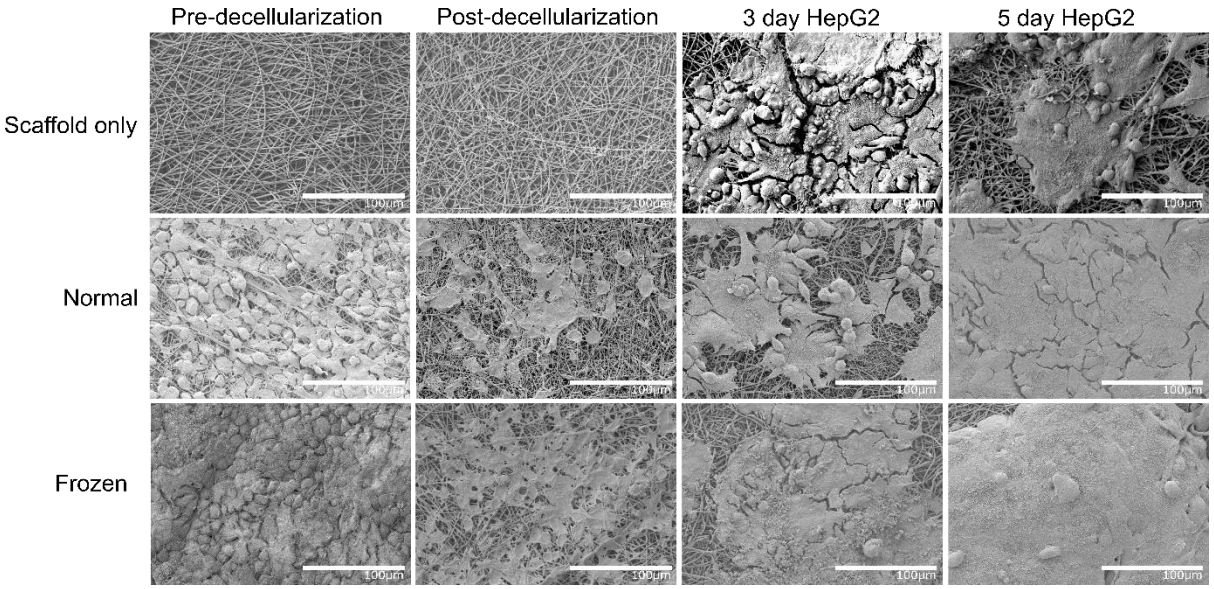

Supplementary figure 9; Cell titre blue of HepG2 cultures at 3/5 days on frozen drug derived ECM:PLA scaffolds vs non-frozen (normal) and scaffold only condition. N = 6, one way ANOVA with Games-Howell post hoc testing. *** = p<0.001.

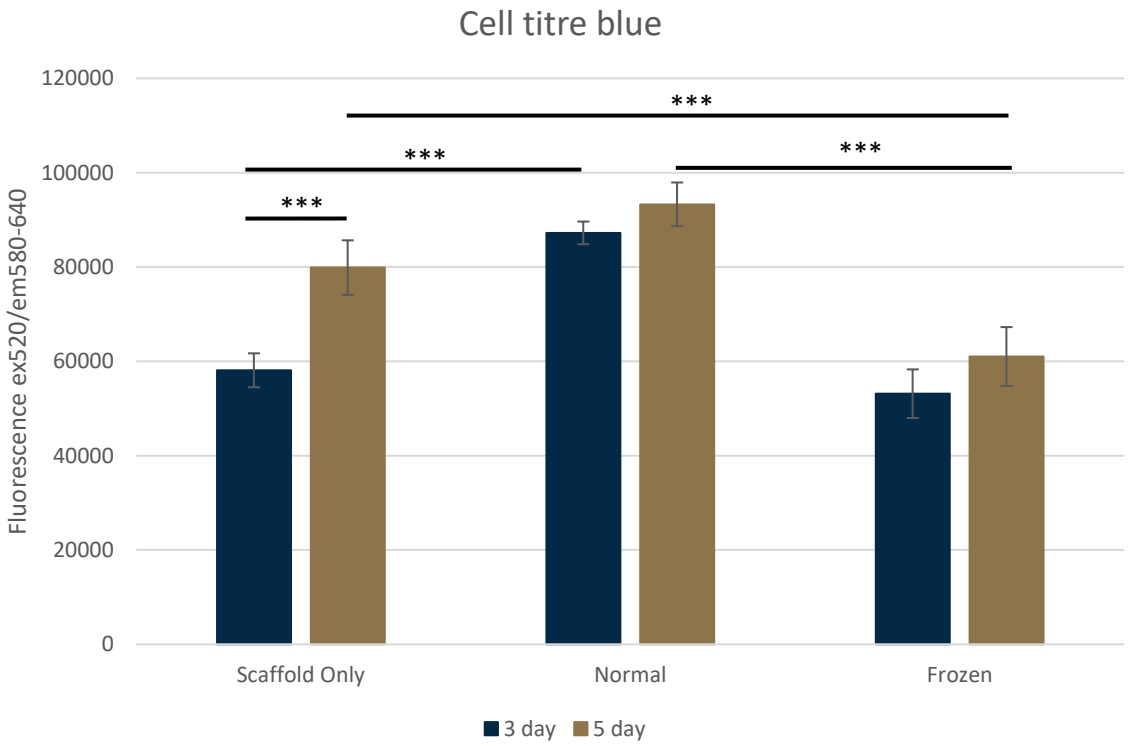

Supplementary figure 10; Gene expression analyses of HepG2 cultures at 3/5 days on frozen drug derived ECM:PLA scaffolds vs non-frozen (normall) and scaffold only condition. N = 6, one way ANOVA with Games-Howell post hoc testing. * = p<0.05. Results normalised to GAPDH and relatice to tissue culture plastic at the same timepoints.

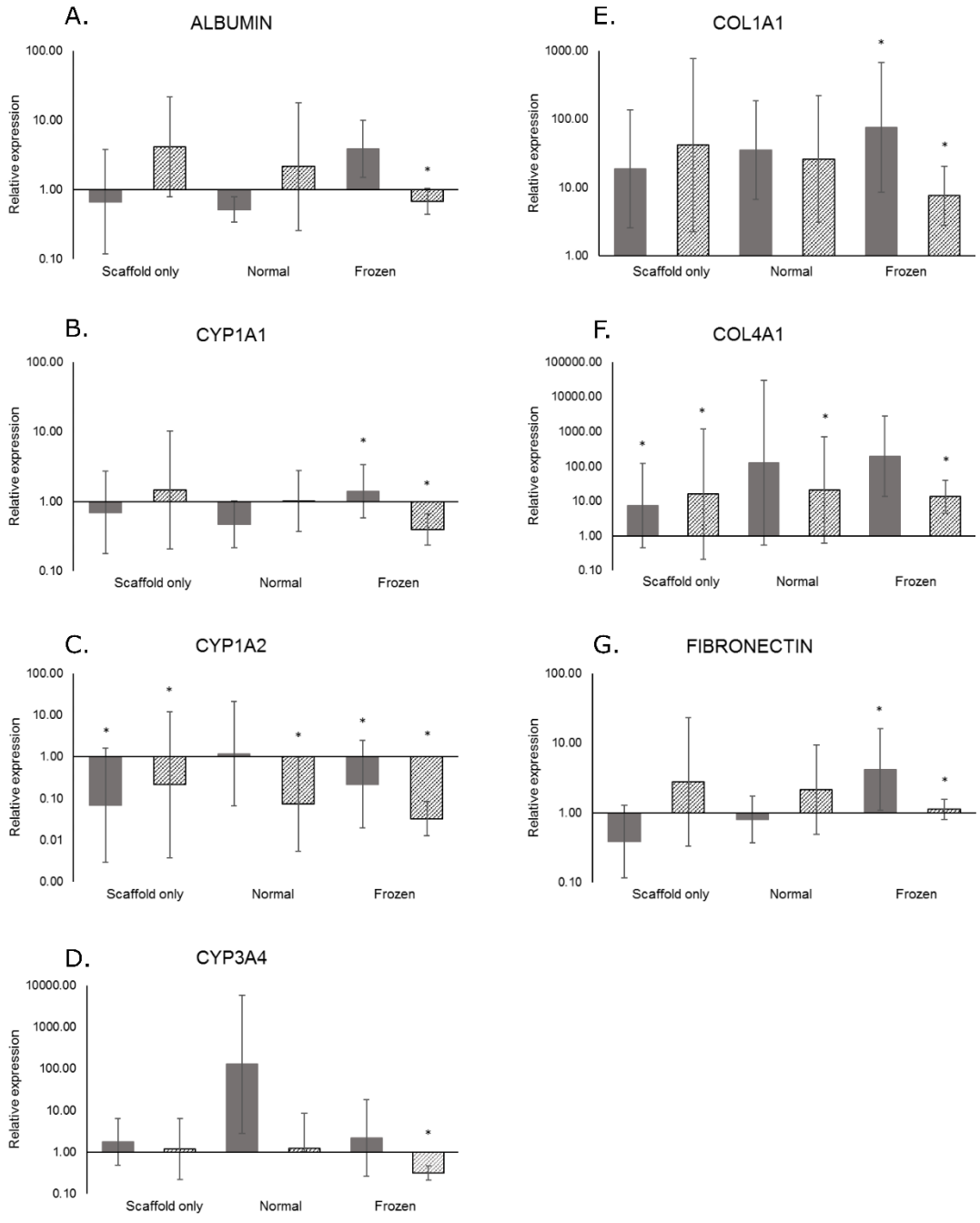

Supplementary figure 11; Cell titre blue analyses of 5637 cell cultures at varying concentrations of histone deacetylase inhibitors. 750uM chosen because of the similarity in cell titre blue results between drugs.

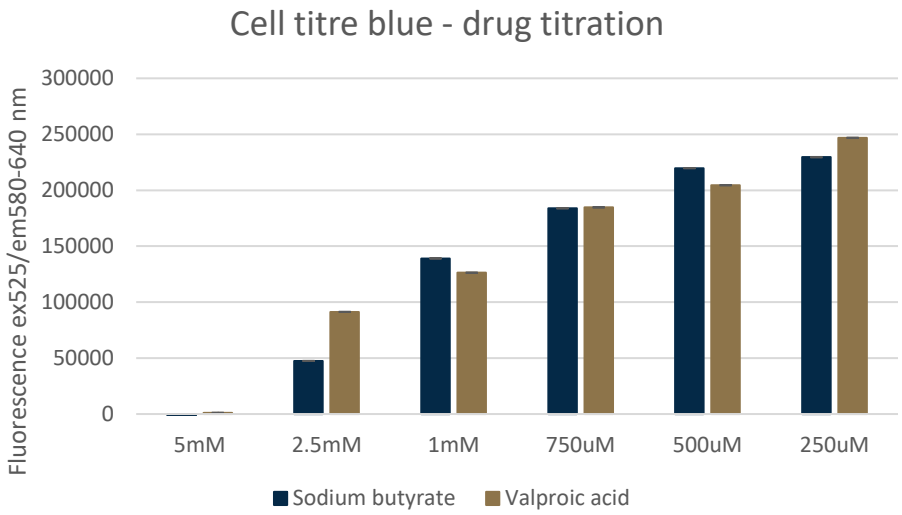

Supplementary figure 12; Cell titre blue analyses of 5637 cell on different percentages of PCL and different coatings. 5637 cells were chosen because of their survival in histone deacetylase inhibitors (Sup Fig 10) and their robustness on various scaffolds.

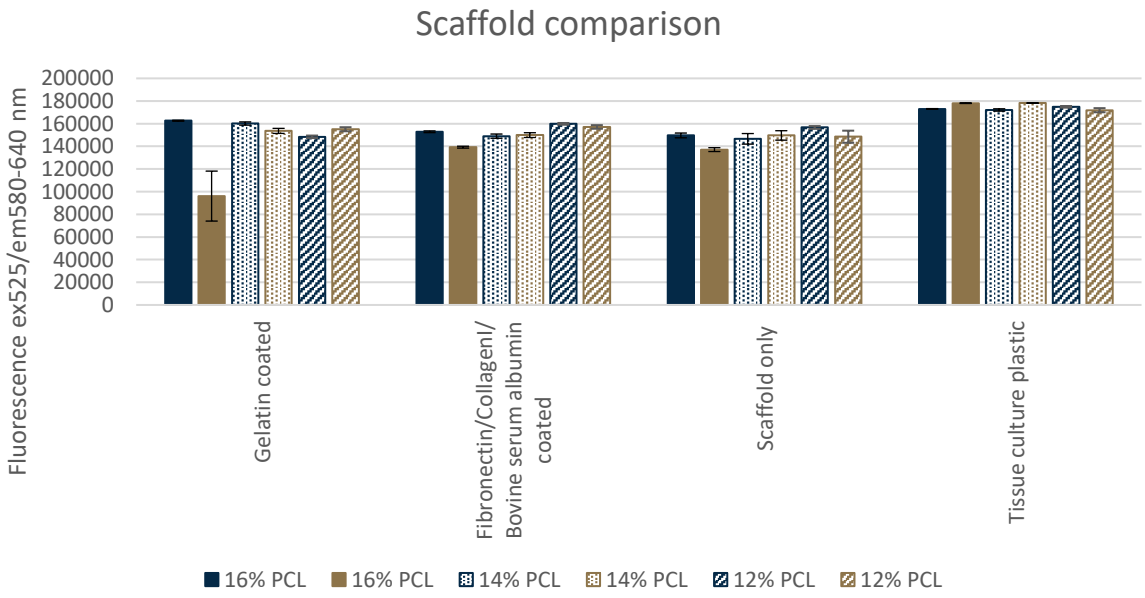

Appendix 2

A Drug-Induced Hybrid Electrospun Poly-Capro Lactone: Cell-Derived Extracellular Matrix Scaffold for Liver Tissue Engineering

TISSUE ENGINEERING: Part A
Volume 00, Number 00, 2017

DOI: 10.1089/ten.tea.2016.0419

termis
Tissue Engineering
& Regenerative Medicine
International Society

ORIGINAL ARTICLE

A Drug-Induced Hybrid

Electrospun Poly-Capro-Lactone: Cell-Derived Extracellular Matrix Scaffold for Liver Tissue Engineering

Rhiannon Grant, MSc,[1] David C. Hay, PhD,[2] and Anthony Callanan, PhD[1]

Liver transplant is the only treatment option for patients with end-stage liver failure, however, there are too few donor livers available for transplant. Whole organ tissue engineering presents a potential solution to the problem of rapidly escalating donor liver shortages worldwide. A major challenge for liver tissue engineers is the creation of a hepatocyte microenvironment; a niche in which liver cells can survive and function optimally. While polymers and decellularized tissues pose an attractive option for scaffold manufacturing, neither alone has thus far proved sufficient. This study exploited cell's native extracellular matrix (ECM) producing capabilities using two different histone deacetylase inhibitors, and combined these with the customizability and reproducibility of electrospun polymer scaffolds to produce a ''best of both worlds'' niche microenvironment for hepatocytes. The resulting hybrid poly-capro-lactone (PCL)-ECM scaffolds were validated using HepG2 hepatocytes. The hybrid PCL-ECM scaffolds maintained hepatocyte growth and function, as evidenced by metabolic activity and DNA quantitation. Mechanical testing revealed little significant difference between scaffolds, indicating that cells were responding to a biochemical and topographical profile rather than mechanical changes. Immunohistochemistry showed that the biochemical profile of the drug-derived and nondrugderived ECMs differed in ratio of Collagen I, Laminin, and Fibronectin. Furthermore, the hybrid PCL-ECM scaffolds influence the gene expression profile of the HepG2s drastically; with expression of Albumin, Cytochrome P450 Family 1 Subfamily A Polypeptide 1, Cytochrome P450 Family 1 Subfamily A Polypeptide 2, Cytochrome P450 Family 3 Subfamily A Polypeptide 4, Fibronectin, Collagen I, and Collagen IV undergoing significant changes. Our results demonstrate that drug-induced hybrid PCL-ECM scaffolds provide a viable, translatable platform for creating a niche microenvironment for hepatocytes, supporting *in vivo* phenotype and function. These scaffolds offer great potential for tissue engineering and regenerative medicine strategies for whole organ tissue engineering.

Keywords: liver tissue engineering, electrospun scaffolds, acellular biological matrices, drug induced, 3D liver cell culture

Introduction

As a result of rapidly increasing incidence and mor- using different polymers and manufacturing techniques to tality, a chronic shortage of liver donors, and a lack of support cell growth and differentiation;[7–10] fluid dynamics, biology, medicine, and engineering and encompasses a wide range of scientific disciplines, including polymer chemistry,

[1] Institute for Bioengineering, School of Engineering, University of Edinburgh, Edinburgh, United Kingdom.
[2] MRC Scottish Centre for Regenerative Medicine, University of Edinburgh, Edinburgh, United Kingdom.

viable new pharmaceuticals there is an urgent need for a solution for patients with liver disease.[1–4] A significant proportion of research focuses on working toward a liver ''organoid''; organs created in a laboratory that can function as a liver *in vivo*.[5,6] Such tissue engineering lies at the interface of designing bioreactors and micro-fluidic devices in which to grow cells;[11–14] and molecular biology, manipulating the molecular environment and response of cells[15–17] in an attempt to recapitulate an environment in which hepatocytes, the functioning cells of the liver, can function long term.

1

While scientists can maintain liver organoids within a laboratory environment, decades worth of scientific research has failed to translate this into an organ that could be used for patient transplant.[5,6] This in part is due to the complexities of recapitulating a vital part of the *in vivo* multicellular environment, the extracellular matrix (ECM).[18]

Multiple methods have been employed in an attempt to provide hepatocytes with an optimal environment; in particular decellularization of whole livers and novel threedimensional (3D) tissue-engineered scaffolds. Decellularization provides a whole organ ECM-based bioscaffold with the potential to maintain the 3D site-specific architecture and highly conserved sinusoidal ECM gradient required for hepatocyte function upon their repopulation of the organ.[18] Several studies have repopulated decellularized organs with hepatocytes and endothelial cells, which subsequently survive and exhibit some level of function.[19–23] However, this approach still requires precious donor organs, sourced from potentially immunogenic human or animal donors, and methods used are not without their drawbacks.

Detergents such as sodium dodecyl sulfate, Triton-X100, and sodium deoxycholate are employed to strip the ECM of cells. These detergents disrupt native tissue ultrastructure, decrease glycosaminoglycan content, and reduce collagen integrity[26,27] and disrupt lipid–lipid, lipid–protein, and protein–protein interactions.[28] Scaffold manufacture employs engineering technologies to create a synthetically derived structure, which mimics the characteristics of the native ECM. There are several different methods of creating a scaffold, and they can be made from a myriad of substances; both natural and synthetic.[29]

Hydrogels have been of particular interest to liver tissue engineers, gels biofuctionalized with collagen I enhance P450 (Cyp450) activity, cell adhesion markers, and innate hepatocyte fibronectin production.[30] Gels biofunctionalized with galactose increased albumin (Alb) production and promoted the proliferation of hepatocytes.[31] Viability and hepatic functions of primary hepatocytes are improved by culturing them in hydrogels made with liver ECM,[32] and when encapsulated in collagen-alginate composite hydrogels.[33] Polyethylene glycol hydrogels have been shown to augment cell–cell interactions of bipotential mouse embryonic liver cells, subsequently improving their survival and function,[34] however, incorporating ECM components into scaffolds at the manufacturing stage has proved challenging, with the harsh solvents require to solubilize major components of ECM alter their microstructure and functionality.[35,36] Ongoing research demonstrates great promise, however to date no scaffold has been created which allows hepatocytes to function as well as they do *in vivo*.[11,37]

Both ECM components and scaffolds have shown great promise in tissue engineering.[9,10,15] With these considerations in mind, we combined decellularization and scaffold engineering to create a novel environment in which hepatocytes thrive (Supplementary Fig. S1; Supplementary Data are available online at www.liebertpub.com/tea). By manipulating ECM production using pharmaceuticals and exploiting polymer characteristics we created a novel hybrid polymer-ECM platform for liver tissue

engineering. To validate the platform we used cells representative of the liver (HepG2s).

Materials and Methods

Electrospinning

A 12% wt/vol solution of poly-capro-lactone (PCL; SigmaAldrich) and hexafluoroisopropanol (Manchester Organics) was dissolved overnight at room temperature with agitation. Solutions were placed into a 10mL syringe and pumped using syringe pump EP-H11 (Harvard Apparatus) into the EC-DIG electrospinning system (IME Technologies) via a 27G bore needle under the following parameters Table 1.

Table 1. Electrospinning Parameters

Volume per hour (mL)	*Total volume (mL)*	*Mandrel:needle distance (cm)*	*Positive charge (kV)*	*Negative charge (kV)*	*Mandrel rotation (rpm)*	*Needle movement (mm/s)*
1.8	8	21	12	-2	250	100

Conditions under which the electrospun poly-capro-lactone scaffold was fabricated.

The mandrel was coated in nonstick aluminium foil for collecting the electrospun fibers. The sheets of electrospun fibers were allowed to dry overnight in a fume hood when the electrospinning session was completed. The average fiber size was 1.14mm as calculated by ImageJ plugin

''Diameter J'' (Fig. 1).[38]

Plasma coating

Ten millimeter discs of scaffold were cut from the dry fiber sheet. The scaffolds were soaked in 70% ethanol for 30min, rinsed three times in phosphate-buffered saline (PBS) for 15min each, and allowed to dry completely at room temperature. We then freeze dried the scaffolds overnight in a FreeZone 4.5 freeze-drier (Labconco) before plasma coating (Harrick Plasma) at 10.2 W for 30s. Scaffolds were removed from the plasma chamber and placed into an antibiotic/antimycotic treatment solution of Eagles Minimal Essential Media supplemented with 10% fetal bovine serum (FBS),2mMl-glutamineand100U/mLpenicillin,100mg/mL streptomycin, and 0.25mg/mL Fungizone (amphotericin B) Anti-Anti solution (Gibco) for 1h.

Initial layer cell seeding and culture

Scaffolds were removed from the antibiotic/antimycotic treatment solution and rinsed three times for 15min each in complete media; Eagles Minimal Essential Media supplemented with 10% FBS, 2mM l-glutamine, 100U/mL penicillin, and 100mg/mL streptomycin (Gibco). They were then placed into a fresh 48-well tissue culture plate.

5637 human urinary bladder epithelials (ATCC) were trypsinized using standard methods from tissue culture flasks and counted using the trypan blue exclusion method. About $1 \cdot 10^4$ cells at passage 23 were suspended in 100mL

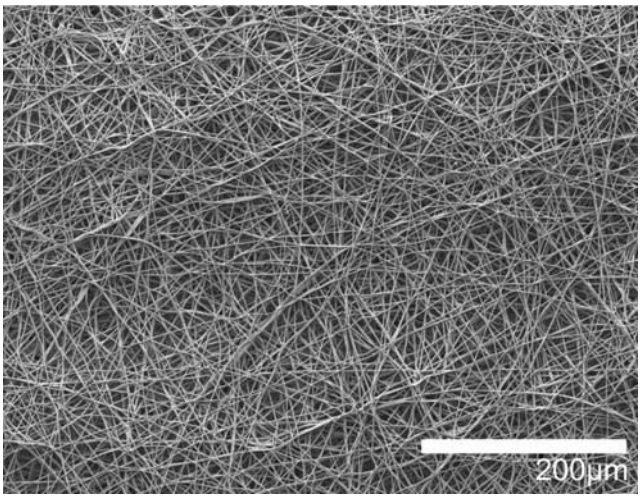

FIG. 1. Characterization of electrospun scaffolds. The scaffolds were assessed for consistency and fiber size via SEM and subsequent image analysis. Fibers consistently displayed a meandiameter of1.14mmasdeterminedbyDiameterJ,[34] n=4. 200·magnification. SEM, scanning electron microscopy.

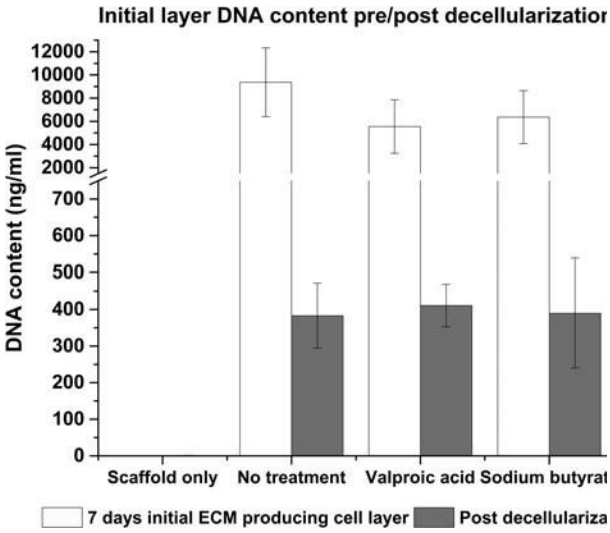

FIG. 2. Confirmation of decellularization. Decellularization was confirmed using the Quant-IT Picogreen dsDNA assay and SEM (not shown). Additionally, CellTiter-Blue cell viability assay was performed on the decellularized scaffolds (data not shown).

of complete media and seeded directly on to the scaffolds. The cells were allowed to incubate in this small volume on the scaffolds for 2h, before an additional 400mL of complete media was added.

Media was changed after 24h to either 750mM valproic acid (VA) or 750mM sodium butyrate (NaB; SigmaAldrich) in complete media and changed every 48h. Controls were scaffold only, that is, not seeded with an initial cell layer and no drug treatment that is, the initial layer cultured in drug-free complete media only. Drug concentrations and initial layer cells were chosen following results of a drug response curve for each histone deacetylase inhibitor (iHDAC) (data not shown). VA and NaB are used as epigenetic control mechanisms of gene transcription. They function by inhibiting HDACs (as iHDACs) to modulate chromatin structure, creating an open, transcriptionally active euchromatin configuration at gene coding and regulatory regions of the chromosome. This renders the chromatin accessible to transcription factors, and facilitates gene transcription.[39]

VA and NaB are both commonly used in industry, particularly antibody production due to their ability to upregulate protein production in such a manner.[40,41] This initial layer of cells was cultured for 7 days at 37C and 5% CO_2 in a humidified incubator.

Decellularization

Decellularization was performed using methods adjusted from Lu *et al.*,[42] under sterile conditions at room temperature (19–22C) and agitation (Fig. 2). Scaffolds were washed in PBS for 15min and then rinsed in 10mM Trisbuffered saline (TBS) for 15min.

The scaffolds were submerged in a 0.1% vol/vol Triton X-100 (Sigma-Aldrich), 1.5M potassium chloride (Acros Organics), and 50mM TBS for 4h. They were rinsed for 15min in 10mM TBS before being submerged in fresh 10mM TBS overnight.

Scaffolds were given a final rinse in 10mM TBS for 15min before being incubated in complete media for 15min and then transferred to new 48-well plates for seeding.

Functional layer cell seeding and culture

HepG2 cells were trypsinized using standard methods from tissue culture flasks and counted using the trypan blue exclusion method. About $3 \cdot 10^5$ cells at passage 17 were suspended in 100mL of complete media and seeded directly on to the scaffolds. The cells were allowed to incubate in this small volume on the scaffolds for 2h, before an additional 400mL of complete media was added.

Media was changed after 24h and changed every 48h after the initial 24h adherence and recovery period. This functional layer (FL) of cells was cultured using standard methods for either 3 or 5 days at 37C and 5% CO_2 in a humidified incubator.

Live/Dead viability/cytotoxicity assay

To determine cellular viability, cell/scaffold constructs were incubated with 10mm calcein and 2mm ethidium ho-modimer-1 (Ethd-1) for 30min as part of the two color live/dead assay (Molecular Probes). Calcein is actively converted to calcein-AM in living cells, which then appear green when excited during fluorescence microscopy. Ethd-1 only accumulates in dead cells, which subsequently appear red. The method allows differentiation between dead and viable cells. The scaffolds were rinsed three times in $CaCl_2$/$MgCl_2$-free PBS to remove excess dye and placed onto a standard microscope slide with a 25mm glass coverslip (VWR). All images were captured using a Zeiss Axio Imager fluorescent microscope (COIL; University of Edinburgh) at 40 ·magnification and postprocessed using ImageJ.

CellTiter-Blue Cell viability assay

The assay was performed according to manufacturer's instruction (Promega). For each condition group, n=3. Importantly, cell/scaffolds constructs were moved into fresh 48-well plates to prevent reading activity from tissue culture plastic bound cells. Measurements were read in a Modulus II microplate reader at an excitation wavelength of 525nm and emission wavelength of 580–640nm and reported as fluorescence.

Picogreen DNA quantification

The Quant-IT Picogreen dsDNA assay kit (Life Technologies) was employed to establish the efficiency of the decellularization method in removing cellular material and to estimate cell number on the cell/scaffold constructs. The assay was performed according to manufacturer instructions. In brief, constructs (n=6) were digested in a solution of $CaCl_2$ and $MgCl_2$-free PBS (Sigma), containing 2.5U/mL papain extract (Sigma), 5mM cysteine-HCl (Sigma), and 5mM ethylenediaminetetraaceticacid (Sigma) and incubated overnight at 60C. Picogreen solution was added to the digests and fluorescent intensity measurements read in a Modulus II microplate reader at an excitation wavelength of 480nm and emission wavelength of 510–570nm. A standard l dsDNA curve of graded known concentrations was used to calibrate fluorescence intensity versus dsDNA concentration.

Sectioning and staining

The samples were rinsed three times in PBS (Gibco) for 15min each, then fixed in 4% v/v formalin buffered in saline for 15min at room temperature. After rinsing with fresh PBS, constructs were embedded in low melting temperature polyester wax (Electron Microscopy Supplies) using methods adapted from Steele *et al.*[9] In brief, samples are dehydrated through 70–100% ethanol, then incubated in 50:50 ethanol:wax overnight at 45C overnight with agitation. The samples were moved into 100% wax for 3h at 45C and then fresh 100% wax for 1h at 45C. Samples were embedded and allowed 72h to fully cure before sectioning.

Immunohistochemical staining was undertaken using antibodies for Collagen I (Stratech), Laminin (Stratech), and Fibronectin (Sigma). All images were captured using a Coherent Anti-Stokes Raman Scattering system (Bioimaging Facility, University of Edinburgh) at 10· and 100· magnification and postprocessed using ImageJ.

Scanning electron microscopy

Scanning electron microscopy (SEM) was used to characterize the scaffold architecture. Samples were rinsed three times in PBS for 15min each, then fixed in 2.5% v/v glutaraldehyde (Fisher Scientific) in 0.1M phosphate buffer (PB) (pH 7.4) at 4C overnight. They were then rinsed three times in 0.1M PB before being postfixed in 1% v/v osmium tetroxide (Electron Microscopy Supplies) buffered with 0.1M PB. Samples were again rinsed three times in 0.1M PB and dehydrated through an ethanol gradient (30–100%). They were dried by placing them in hexamethyldisilazane (Sigma), which was allowed to evaporate off at room temperature overnight. We mounted the samples onto SEM chucks using double-sided carbon tape and coated them with a thin layer of gold and

palladium alloy (Polaron Sputtercoater). All images were captured at 5kV using a Hitach S-4700 SEM (BioSEM; University of Edinburgh).

Mechanical testing

Nanoindentation experiments were undertaken to establish the dynamic properties of scaffolds and decellularized ECM/scaffold constructs using the Keysight/Agilent 5200 nano indenter testing system.

Scaffolds and constructs were subject to indentation by a DCM II actuator flat-ended cylindrical punch (D=100mm) using a max load of 1 gf. All nanoindentation experiments were carried out on fresh, hydrated, unfixed samples that were adhered to the chuck using double-sided tape. A total of 36 indentations were carried out on each sample, 50nm apart. Indent sites were selected using the high precision X–Y stage within the testing system (Agilent). Poissons ratio was assumed to be 0.5 for each sample.[43,44] Allowable drift rate was 0.1nm/s. A NanoSuite (Keysight Technologies) test method ''G-Series DCM CSM Flat Punch Complex Modulus'' was used for all testing.[45,46]

Gene expression analysis

RNA was extracted from constructs using standard TRIzol (Fisher Scientific) methods and purified using Qiagen's RNeasy spin column system. cDNA was synthesized using the Promega's ImProm-II Reverse Transcription System.

Quantitative real-time polymerase chain reaction was performed using the LightCycler 480 Instrument II (Roche Life Science) and Sensifast SYBR High-ROX (Bioline) system. Results were normalized to HepG2s of the same passage number grown on tissue culture plastic and compared to the housekeeping gene glyceraldehyde-3-phosphate dehydrogenase. Analysis was performed using the 2-DDCt method,[47] n=4. Alb, Cytochrome P450 Family 1 Subfamily A Polypeptide 1 (Cyp1A1), Cytochrome P450 Family 1 Subfamily A Polypeptide 2 (Cyp1A2), Cytochrome P450 Family 3 Subfamily A Polypeptide 4 (Cyp3A4), Collagen Type I alpha 1, Collagen Type 4 alpha 1, and Fibronectin Type 1 were investigated, forward and reverse primers (Sigma) are detailed in Supplementary Table S1.

Statistical analysis

One-way analysis of variance and Tukey *post hoc* testing were performed and graphs generated using Origin software (OriginLab). A minimum of n=3 and max of n=6 was used for all analysis. Study groups were as follows; Scaffold only, No drug treatment, treatment with VA, and treatment with NaB. HepG2 cells were grown on each scaffold for 3 and 5 day time points.

Results

Cell attachment and survival on scaffolds

When compared to normal ECM (N-ECM), a lower number of HepG2s adhered to each of the drug-induced scaffold-ECM constructs, and to the scaffold alone (Fig. 3); demonstrating that ''normal'' ECM is efficient for cell seeding purposes. Scaffold only (SO), valproic acid ECM (VA-ECM) and sodium butyrate ECM (NaB-ECM)

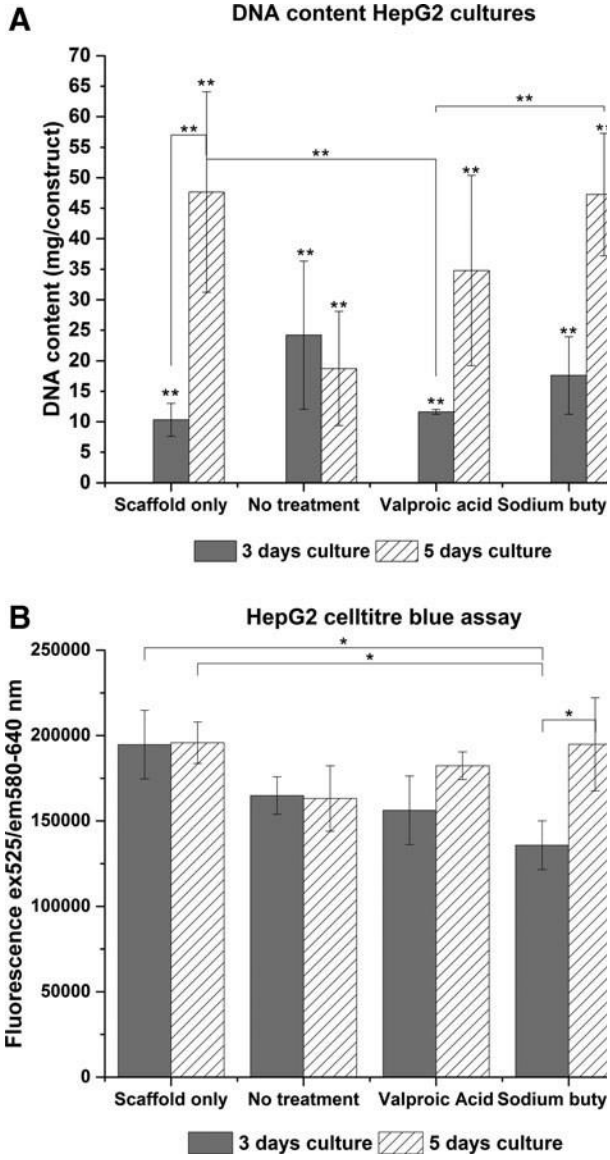

FIG. 3. Seeding efficiency/viability on scaffolds. Cell adherence was assessed by Quant-IT Picogreen dsDNA assay (A) and further confirmed by CellTiter-Blue Cell viability assay (B). One-way ANOVA with Tukey *post hoc* testing. *p<0.05, **p<0.01. Error bars represent SD. SD, standard deviation; ANOVA, analysis of variance.

conditions demonstrate longer term maintenance or the HepG2s, however, (Fig. 3) and results are confirmed by both CellTiter-Blue viability and Picogreen DNA quantitation. Live/dead viability/cytotoxicity images (Fig. 4) further demonstrates the metabolic viability of the functional HepG2 cell layer (FL), although it should be noted that imaging reveals the FL was not yet confluent at 5 days culture, as further confirmed by SEM images (Fig. 5).

Mechanical characterization of scaffolds

Interestingly, mechanical differences between the scaffold construct were negligible (Fig. 6). No significant differences in storage (Fig. 6A) or loss (Fig. 6B) modulus between the four conditions (Supplementary Tables S2 and S3).

Testing was performed at frequencies experienced by the human liver *in vivo*.[48] Storage modulus (G¢) ranged from

3.58–0.12 to 4.64–0.43MPa and loss modulus (G¢¢) from 0.55–0.03 to 1.17–0.07 at the frequencies detailed in Supplementary Tables S2 and S3. This reassures us that differences in cell attachment, viability, and function are due to differences in the biochemical and topographical profile of the hybrid scaffolds, as opposed to potential dynamic differences to which cells are known to be so sensitive.[49–52]

Biochemical characterization of the hybrid polymer-ECM scaffolds

Differences in the biochemical profile of the different ECMs were demonstrated by immunohistochemistry performed on the hybrid scaffold sections (Fig. 7). Hepatic phenotype has long been known to be influenced by ECM proteins; particularly Collagen I, Laminin, and Fibronectin,[15,53,54] all of which are present on the scaffolds to varying degrees.

Laminin is of particular importance in the regenerating liver and for cell adhesion, and it is increased in injured or developing states.[55,56] Laminin is present in each construct, but it appears to be most prevalent in NaB-ECM scaffolds (Fig. 7J). These constructs demonstrate higher ‘‘maintenance’’ of the HepG2s; that is cell number and viability increases between 3 and 5 days (Fig. 3).

Collagen I is one of the major components of normal liver ECM.[53,54] Collagen I is most prevalent on NaB-ECM scaffold constructs (Fig. 7I), followed by VA-ECM (Fig. 7E) and N-ECM (Fig. 7A) scaffold constructs. When compared to the N-ECM scaffold constructs, these demonstrate improved maintenance of the

HepG2 cell layer (Fig. 3), although not in comparison to the SO conditions.

Fibronectin is also ubiquitous in healthy liver ECM[53,57] and is present under each of the conditions, but is most prevalent on NaB-ECM scaffolds (Fig. 7K). SEM of the hybrid scaffolds appears to confirm the fibrillary nature of the Collagen I-enriched NaB (Fig. 5J) and VA-ECMs (Fig. 5G) and the smoother morphology of the Lamininenriched N-ECM (Fig. 5D).

The ECMs present have penetrated the scaffold in each case, and each protein is present on each scaffold, indicating the robustness and reproducibility of the method (Supplementary Fig. S2 n=3).

Gene expression of HepG2s in response to hybrid polymer-ECM scaffolds

Multiple genes associated with liver function were assayed for gene expression (Fig. 8). Alb expression is a marker of liver cell differentiation and function and Cytochrome P450 (Cyp) are involved in metabolism of toxic compounds and products of endogenous metabolism such as

bilirubin in the liver.[6,17]

Alb mRNA expression increases between day 3 and 5 as expected, but at day 5 is upregulated in comparison to HepG2s grown on tissue culture plastic in all conditions; with the highest levels observed in SO and N-ECM conditions. Additionally, Alb mRNA expression is downregulated at day 3 in SO and NaB-ECM conditions (Fig. 8A).

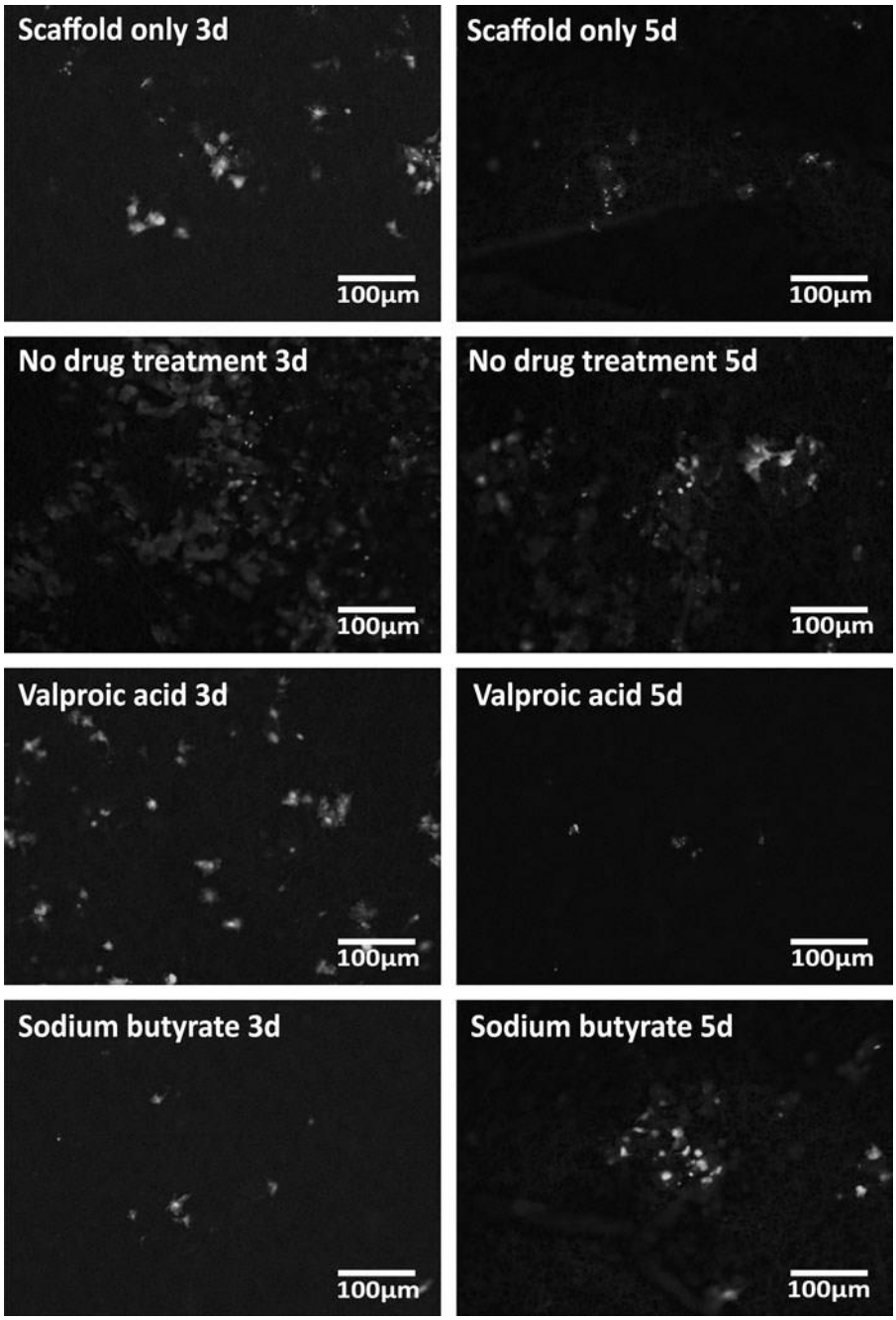

FIG. 4. Live/Dead viability/cytotoxicity assay. Viability of the FL was assessed by live/dead viability/cytotoxicity staining assay. Results demonstrate the FL is metabolically viable at all assessed time points. 40· magnification. FL, functional layer.

Cyp1A1 mRNA expression is consistently upregulated in comparison to tissue culture plastic (Fig. 8B). Cyp1A2 mRNA expression is hugely upregulated in comparison to tissue culture plastic (*1000–38,000-fold), with the highest levels observed at 3 days on VA-ECM scaffold constructs, and levels at day 5 consistently lower than those at day 3 (Fig. 8C). Cyp3A4 mRNA expression follows a similar pattern, barring the NaB-ECM scaffolds; where expression levels at day 5 are higher than those of day 3. Additionally, the highest levels of expression are observed on SO at day 3 of culture (Fig. 8D).

Additionally, we assayed for three ECM genes, key components of the liver microenvironment; Fibronectin (Fig. 8E), Collagen I (Fig. 8F), and Collagen IV (Fig. 8G). While hepatocytes are not the major producers of ECM proteins in the liver,[53] the expression of such genes are of interest with regards to the cells further modulation of its environment considering the plastic nature of the ECM.[58] Fibronectin mRNA levels are higher in each condition than in that of HepG2s grown on tissue culture plastic, and

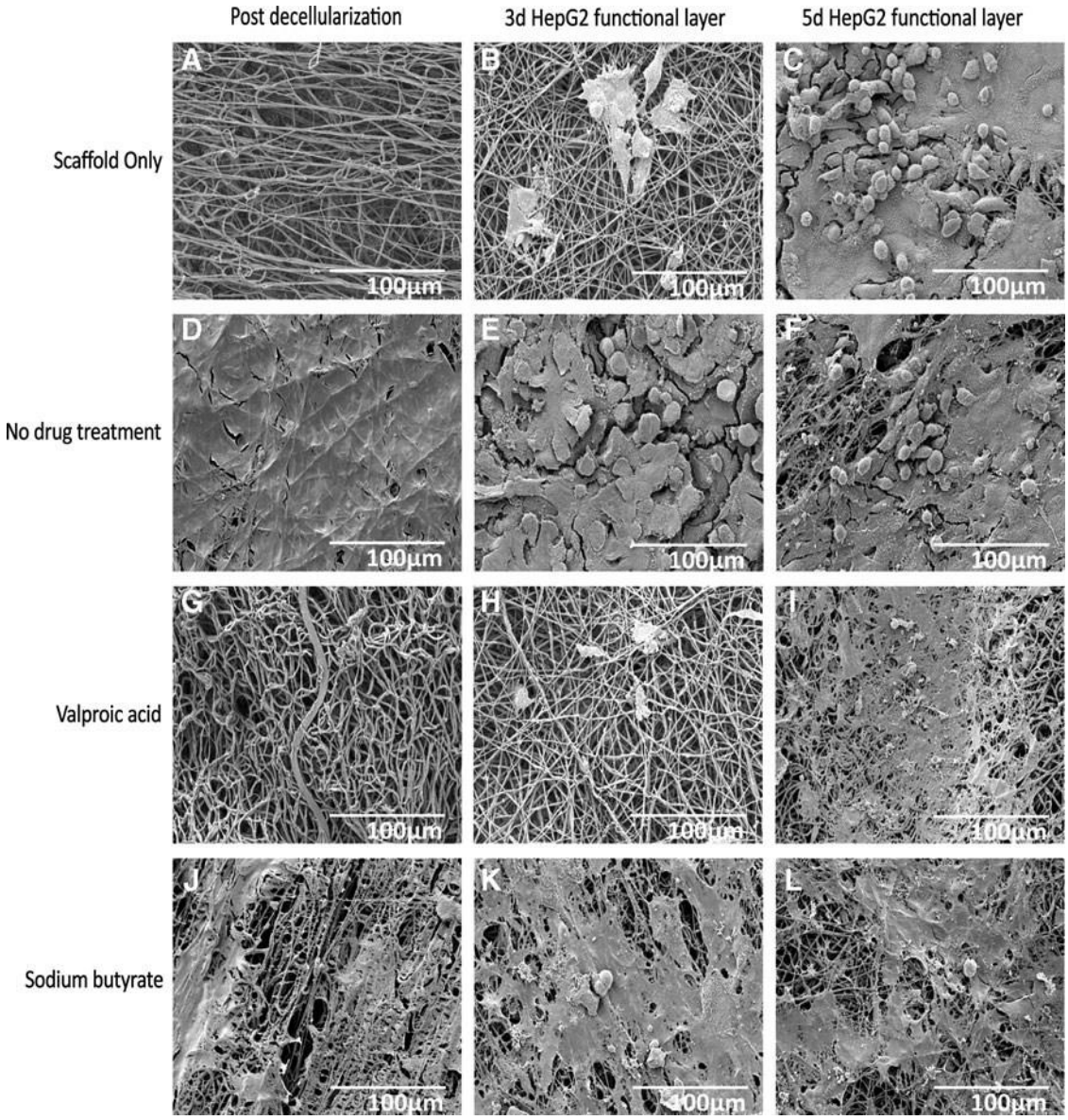

FIG. 5. SEM of scaffold-ECM constructs and functional cell layers. SEM images of the decellularized scaffold-ECM constructs (A, D, G, and J) and functional cell layers at 3 (B, E, H, and K) and 5 (C, F, I, and L) days culture. Topographical differences are clearly evident on decellularized constructs. 500· magnification.

highest levels are observed at day 3 on VA-ECM scaffold constructs, subsequently dropping to less than a third of day 3 levels by day 5. This may be in response to fibronectin levels observed in Figure 7, where the highest fibronectin levels observed (Fig. 7K) correspond with the lowest mRNA expression in the HepG2s. Collagen I mRNA expression is upregulated in every condition. Levels increase at day 5 in SO and NaB-ECM conditions; N-ECM and VA-ECM conditions follow the opposite trend with lowest levels observed in NaB-ECM conditions at day 3. The highest level of gene expression is observed on the scaffold with correspondingly increased Collagen I levels; NaB-ECM (Fig. 7I). Collagen IV mRNA levels are decreased in comparison to tissue culture plastic.

While the authors refrain from speculation without further analysis, the alterations in mRNA levels indicate that the drug-induced ECMs have a profound effect on liver cellular behavior.

Discussion

Fabrication of a hybrid polymer-ECM scaffold is an important avenue for liver tissue engineering, overcoming the shortage of donor organs and

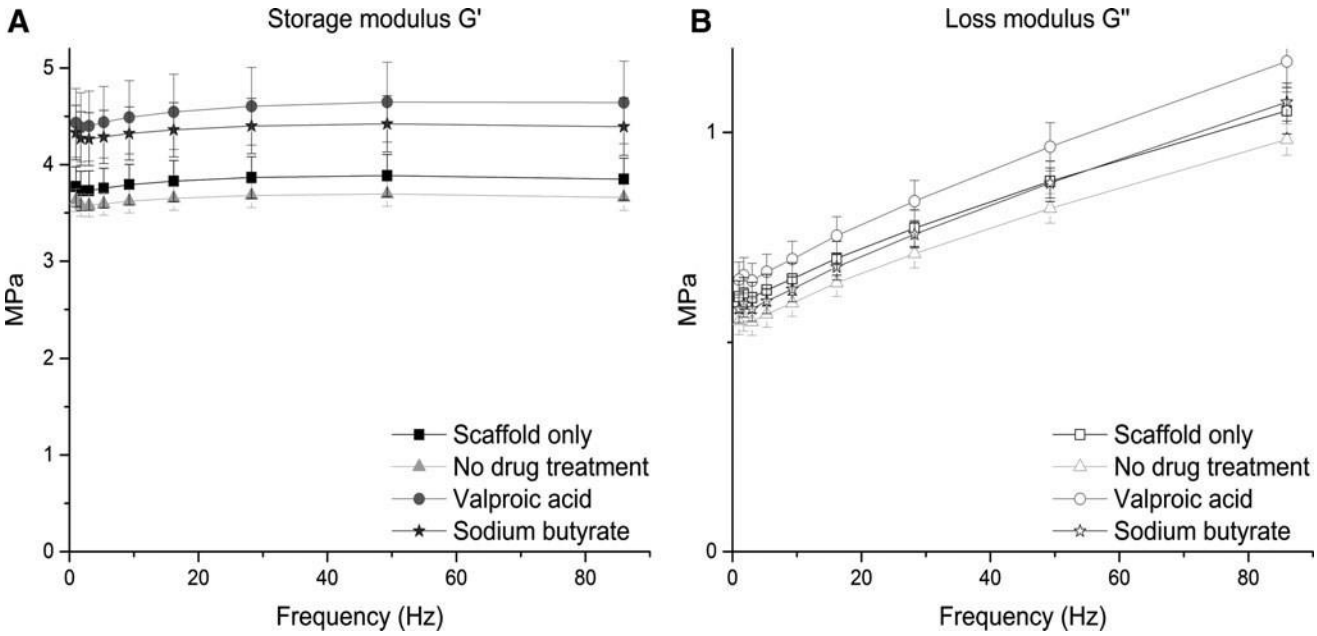

FIG. 6. Mechanical characterization of decellularized scaffolds. Decellularized ECM/scaffold constructs were subject to nanoindentation experiments to assess their dynamic properties. Results demonstrate no significant differences in storage (A) or loss (B) modulus between the four conditions (Supplementary Tables S2 and S3). ECM, extracellular matrix.

issues regarding animal-sourced biomaterials and creating a platform that can produce consistent, clinically translatable scaffolds for liver cell survival and function. An electrospun fiber approach was taken in the study to mimic the morphology of healthy fibrillary collagen,[59,60] which may explain cells favoring environments with more Collagen I. We selected PCL for the fabrication of electrospun scaffolds as it possesses FDA approval for use in medical devices due to its biodegradable nature and elasticity.[9]

The ECM is highly plastic, subject to constant modification and varies massively between tissues,[61] with each tissue possessing its own specific ECM ''recipe'', composed of water, proteins, and polysaccharides, driven by a dialog between various cellular components and the microenvironment within the tissue.[58,62] As the ECM is such a dynamic structure, it stands to reason that its production and maintenance will be influenced by its surrounding environment in 3D culture.[63]

We used two different iHDACs to manipulate the cellular environment and alter the ECM production; NaB is widely used in industry to increase yield recombinant protein yields in mammalian cells. VA (ValA) is an FDA-approved anticonvulsant, which also functions as an iHDAC to increase

recombinant protein yields.[40] By using iHDACs we can influence gene expression via their role in deacetylation, the process by which DNA renders itself less transcriptionally active. Inhibiting this process in cells results in hyperacetylation of histones and subsequently an increase in

transcriptional activity.[39]

Our results indicate not only that the iHDACs significantly alter the production and consistency of the ECM, but also that this technique is robust and reproducible and the ECM it produces, when harnessed in combination with 3D scaffolding technologies, creates a biofuctionalized scaffold, which significantly alters the behavior of liver cells.

The ECM produced by a bladder epithelial may be different to that of a liver cell; however, several decellularized ECM products on the market are in clinical use to regenerate tissues from which they are not derived, including

ALLOPATCH HD, MatriStem, and Tutoplast Pericardium.[64] Indeed, hepatocytes are often cultured on ''ECM'' surfaces that are not derived from liver, commonly using Matrigel, a product derived from murine sarcoma, which is as yet undefined and experiences batch to batch variability.[15,65–68]

The promising field of whole organ decellularization is hampered by the availability of human livers, and researchers are subsequently investigating alternative organ and cells sources, such as spleen, bone marrow mesenchymal stem cells,[69,70] and various animal sources of livers.[37] One of the main advantages of using decellularized native liver ECM is conservation of the *highly conserved sinusoidal ECM gradient required* to allow hepatocytes to repopulate in their specific niches. The complex ECM of the liver remains a topic of investigation in each of its states, diseased, regenerating, and healthy.[53,55,71,72]

To assess the performance of the hybrid scaffolds, we investigated the attachment and function of a commonly used liver cell line, HepG2s, at 3 and 5 days post-replating when cultured *in vitro* on the hybrid scaffolds versus scaffold alone.

HepG2s were derived from the hepatocarcinoma of a 15-yearold Caucasian male. They are often used because they are virus-free, possess liver-specific functions such as ammonia metabolism and albumin synthesis, and secrete some growth factors such as insulin and insulin-like growth factor II.[73] We analyzed cell attachment and viability, and gene expression of both liver function genes and ECM genes at both 3 and 5 day time points. Additionally, we validated the decellularization of the ECM producing cell layer and performed immunohistochemicalanalysesofthe hybridscaffold-ECMconstructsupon which the HepG2s were seeded.

While this work is a robust proof of principle regarding manipulation of ECM production, and has produced a novel hybrid polymer-ECM scaffold with great potential for liver tissue engineering, further work is required to analyze results and increase translatability. While HepG2s are a highly valuable research resource, they are derived from a carcinoma and as such criticism of their *in vitro* relevance abounds within the scientific community. It is important to undertake future work using primary or stem cell-derived hepatocytes and incorporate other stimuli such as fluid flow to combat such criticism. Furthermore, while hepatocytes, the major parenchymal cell of the liver, make up more than 70% of the cellular mass, they do not exist in isolation and the nonparenchymal cells play an essential role in the *in vivo* liver[71,74]; future studies should look to include these cells.

In addition, recognizing the value of proteomic and functional assays (such as enzyme-linked immunosorbent assays) in analyzing the function of the primary/stem cellderived hepatocytes will be important for future validation of the scaffolds, however, at this time these were deemed unnecessary considering the critique of the HepG2 cell line. Additionally, care should be taken to ensure decellularization agents are completely removed from the scaffolds, due to their deleterious effect on both cells and ECM.[24] While such considerations are of importance, this study clearly

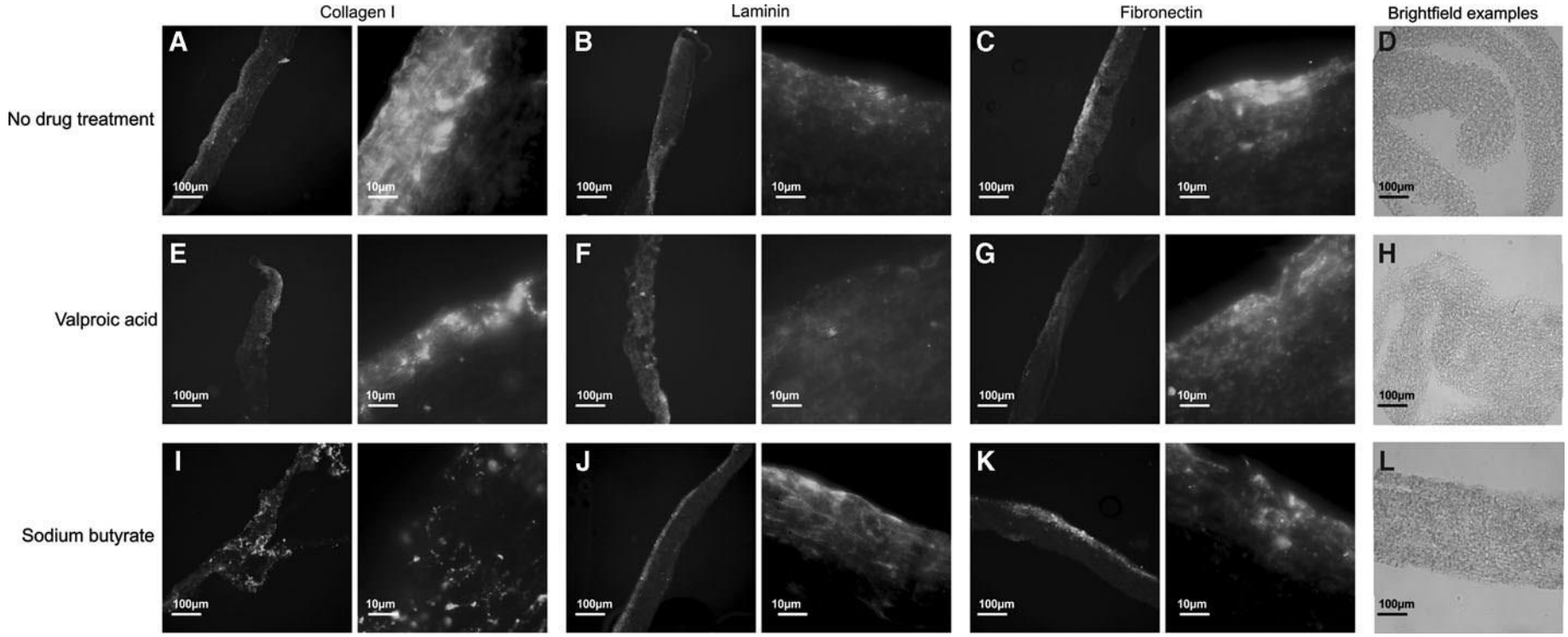

FIG.7. Immunohistochemicalinvestigation.Immunohistochemistrystainingofthedecellularized ECM/scaffoldconstructsrevealedsignificantdiffere ncesinECMcom-ponents.StainswereperformedforCollagenI (A,E, and I),Laminin (B,F, and J),andFibronectin (C,G, and K),postprocessedusingImageJ.10 · and100 · magnification. Brightfieldimages (D,H, and L) providedfor information. ((

(

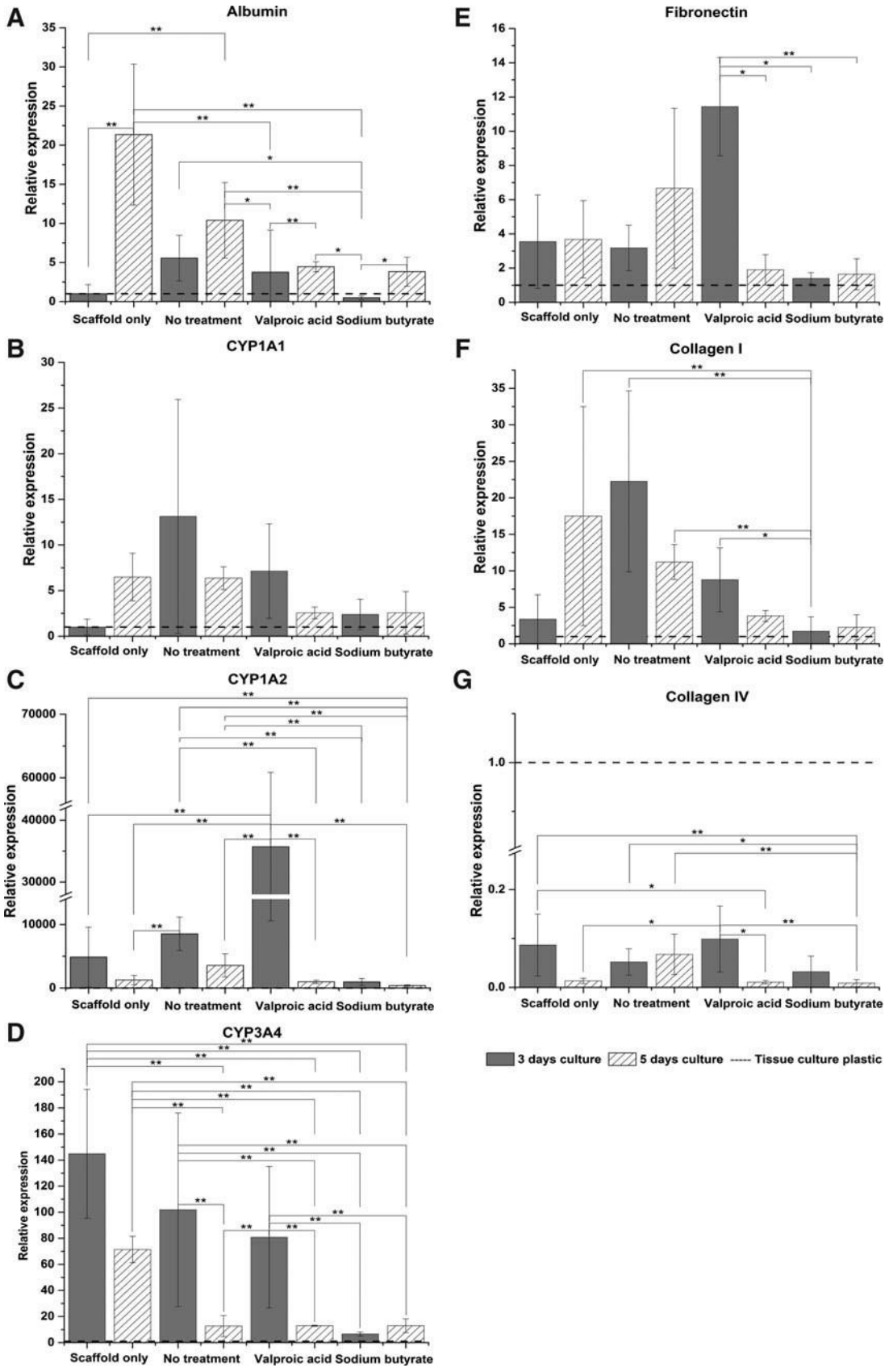

FIG. 8. Quantitative polymerase chain reaction analysis of functional cell layer. Quantitative analysis of gene expression was undertaken on the functional cell layer at 3 and 5 days culture, compared to that of HepG2s of

the same passage and culture periods grown on tissue culture plastic (Fig. 7). mRNA levels of Albumin (A), Cyp1A1 (B), Cyp1A2 (C), CYP3A4 (D), Fibronectin (E) Collagen I (F), and Collagen IV (G) are represented as fold difference relative to tissue culture plastic controls and relative to the housekeeping gene GAPDH. One-way ANOVA with Tukey-*post hoc* testing and $n=4$. *$p<0.05$, **$p<0.01$. Error bars represent SD. GAPDH, glyceraldehyde-3-phosphate dehydrogenase.

demonstrates the potential of these hybrid polymer-ECM scaffolds for tissue engineering and provides a robust initial platform for further research.

Conclusion

This study developed a new method of creating hybrid polymer-ECM scaffolds by manipulating cells using electrospun scaffold technologies, clinically relevant iHDACs and methods easily modified to fulfill good manufacturing practice regulation. To do so, a sacrificial, ECM-producing cell layer was seeded onto a novel electrospun scaffold and then treated with VA or NaB to biofuctionalize the scaffold with ECM components. Scaffolds with untreated cells and no initial cell layer at all were used as controls. The initial cell layer was removed with a detergent-based decellularization method, and the resulting hybrid polymer-ECM scaffolds seeded with a liver cell line for validation. The work was validated using robust methods such as Q-PCR, mechanical quantification, and SEM. Drug-induced hybrid polymer-ECM scaffolds had a significant positive influence on the gene expression profile, attachment, and survival of liver cells.

Our data demonstrates promise as a unique method of inducing and altering the production of ECM and that the hybrid scaffolds exert influence upon cells *in vitro*, as well as future potential as an implantable treatment platform for liver disease patients.

These scaffolds show great potential not only for the future of liver tissue engineering and patient treatment, but are easily adaptable for other organs and tissues. Additionally, they are a useful tool for the development of 3D liver cell platforms, which can be used for *in vivo* cell analysis and novel pharmaceutical research.

Acknowledgments

The authors would like to thank Dr. Vlastimil Srnsen for technical help, Prof. Alistair Elfick for use of lab facilities (IBioE, University of Edinburgh) and Prof. Stuart Forbes for use of equipment (SCRM, University of Edinburgh). We would also like to thank Steve Mitchell (BioSEM), Dr. David Kelly (COIL), and Dr. Tony Corcoran (Bioimaging Facility) for their imaging expertise (University of Edinburgh). This work is funded by an Engineering & Physical Sciences Research Council [EPSRC] doctoral training partnership studentship, UK Regenerative Medicine Platform II [RMPII] grant MR/L022974/1 and MRC computational and chemical biology of the stem cell niche grant (CCBN) MR/L012766/1.

Disclosure Statement

No competing financial interests exist.

References

1. NHS Blood and Transplant. Organ donation and transplantation Activity Report 2014–2015. [Epub ahead of print]; DOI: 10.1016/B978-0-12-373932-2.00158-7, 2016.
2. Williams, R., *et al.* The Lancet commissions addressing liver disease in the UK: a blueprint for attaining excellence in health care and reducing premature mortality from lifestyle issues of excess consumption of alcohol, obesity, and viral hepatitis. Lancet 384, 1953, 2014.
3. British Association for the Study of the Liver and BritishSociety of Gastroenterology. A time to act: improving liver health and outcomes in liver disease. National Plan Liver Services UK, 2009, pp. 1–52. Available at: http://www.bsg .org.uk/sections/liver-articles/the-national-plan-for-liverservices-uk-2009.html (Accessed April 11, 2017).
4. Muriel, P., and Rivera-Espinoza, Y. Beneficial drugs forliver diseases. J Appl Toxicol 28, 93, 2008.
5. Takebe, T., *et al.* Vascularized and complex organ buds from diverse tissues via mesenchymal cell-driven condensation. Cell Stem Cell 16, 556, 2015.

6. Takebe, T., *et al.* Vascularized and functional human liver from an iPSC-derived organ bud transplant. Nature 499, 481, 2013.

7. Celiz, A.D., *et al.* Discovery of a novel polymer for human pluripotent stem cell expansion and multilineage differentiation. Adv Mater [Epub ahead of print]; DOI: 10.1002/ adma.201501351, 2015.

8. Villarin, B.L., *et al.* Polymer supported directed differentiation reveals a unique gene signature predicting stable hepatocyte performance. Adv Healthc Mater [Epub ahead of print]; DOI: 10.1002/adhm.201500391, 2015.

9. Steele, J.A.M., *et al.* Combinatorial scaffold morphologies for zonal articular cartilage engineering. Acta Biomater 10, 2065, 2014.

10. Chung, S., *et al.* Responsive poly (g-glutamic acid) fibres for biomedical applications. J Mater Chem B 1, 1397, 2013.

11. Baptista, P.M., Moran, E.C., Vyas, D., et al. Fluid flowregulation of revascularization and cellular organizationin a bioengineered liver platform. Tissue Eng Part C Methods 22, 199, 2016.

12. Palakkan, A.A., *et al.* Polarisation and functional characterisation of hepatocytes derived from human embryonic and mesenchymal stem cells. Biomed Rep 3, 626, 2015.

13. Sabetkish, S., *et al.* Whole-organ tissue engineering: decellularization and recellularization of three-dimensional matrix liver scaffolds. J Biomed Mater Res A 103, 1498, 2015.

14. Torok, E., *et al.* Primary human hepatocytes on biodegradable poly(l-lactic acid) matrices: a promising model for improving transplantation efficiency with tissue engineering. Liver Transplant 13, 465, 2011.

15. Cameron, K., *et al.* Recombinant laminins drive the differentiation and self-organization of hESC-derived hepatocytes. Stem Cell Rep 5, 1, 2015.

16. Szkolnicka, D., Farnworth, S.L., Lucendo-Villarin, B., andHay, D.C. Deriving functional hepatocytes from pluripotent stem cells. Curr Protoc Stem Cell Biol 30, 1G.5.1, 2014.

17. Hay, D.C., *et al.* Highly efficient differentiation of hESCs to functional hepatic endoderm requires ActivinA and Wnt3a signaling. Proc Natl Acad Sci U S A 105, 12301, 2008.

18. He, M., and Callanan, A. Comparison of methods for wholeorgan decellularisation in tissue engineering of bio-artificial organs. Tissue Eng Part B Rev 19, 194, 2012.

19. De Kock, J., *et al.* Simple and quick method for whole-liver decellularization: a novel in vitro three-dimensional bioengineering tool? Arch Toxicol 85, 607, 2011.

20. Baptista, P.M., *et al.* The use of whole organ decellularization for the generation of a vascularized liver organoid. Hepatology 53, 604, 2011.

21. Barakat, O., *et al.* Use of decellularized porcine liver for engineering humanized liver organ. J Surg Res 173, e11, 2012.

22. Wu, Q., *et al.* Optimizing perfusion-decellularization methods of porcine livers for clinical-scale whole-organ bioengineering. Biomed Res Int 2015, 1, 2015.

23. Zhou, P., *et al.* Decellularization and recellularization of rat livers with hepatocytes and endothelial progenitor cells. Artif Organs 40, E25, 2016.

24. He, M., Callanan, A., Lagaras, K., Steele, J.A.M., andStevens, M.M. Optimization of SDS exposure on preservation of ECM characteristics in whole organ decellularization of rat kidneys. J Biomed Mater Res Part B Appl Biomater [Epub ahead of print]; DOI: 10.1002/ jbm.b.33668, 2016.

25. Peloso, A., *et al.* Current achievements and future perspectives in whole-organ bioengineering. Stem Cell Res Ther 6, 107, 2015.

26. Woods, T., and Gratzer, P.F. Effectiveness of three extraction techniques in the development of a decellularized bone-anterior cruciate ligament-bone graft. Biomaterials 26, 7339, 2005.

27. Funamoto, S., *et al.* The use of high-hydrostatic pressure treatment to decellularize blood vessels. Biomaterials 31, 3590, 2010.

28. Cebotari, S., *et al.* Detergent decellularization of heart valves for tissue engineering: toxicological effects of residual detergents on human endothelial cells. Artif Organs 34, 206, 2010.

29. Naderi, H., Matin, M.M., and Bahrami, A.R. Review paper: critical issues in tissue engineering: biomaterials, cell sources, angiogenesis, and drug delivery systems. J Biomater Appl 26, 383, 2011.

30. Kim, M.H., *et al.* Phenotypic regulation of liver cells in a biofunctionalized three-dimensional hydrogel platform. Integr Biol [Epub ahead of print]; DOI: 10.1039/C5IB00269A, 2016.

31. Vasanthan, K.S., Sethuraman, S., and Parthasarathy, M.Electrochemical evidence for asialoglycoprotein receptormediated hepatocyte adhesion and proliferation in three dimensional tissue engineering scaffolds. Anal Chim Acta 890, 83, 2015.

32. Lee, J.S., *et al.* Liver extracellular matrix providing dual functions of two-dimensional substrate coating and threedimensional injectable hydrogel platform for liver tissue engineering. Biomacromolecules 15, 206, 2014.

33. No, D.Y., Jeong, G.S., and Lee, S.-H. Immune-protectedxenogeneic bioartificial livers with liver-specific microarchitecture and hydrogel-encapsulated cells. Biomaterials 35, 8983, 2014.

34. Underhill, G.H., Chen, A.A., Albrecht, D.R., and Bhatia,S.N. Assessment of hepatocellular function within PEG hydrogels. Biomaterials 28, 256, 2007.

35. Zeugolis, D.I., *et al.* Electro-spinning of pure collagen nano-fibres—just an expensive way to make gelatin? Biomaterials 29, 2293, 2008.

36. Dong, B., Arnoult, O., Smith, M.E., and Wnek, G.E.Electrospinning of collagen nanofiber scaffolds from benign solvents. Macromol Rapid Commun 30, 539,

    2009.

37. Faulk, D.M., Wildemann, J.D., and Badylak, S.F. Decellularization and cell seeding of whole liver biologic scaffolds composed of extracellular matrix. J Clin Exp Hepatol 5, 69, 2015.

38. Hotaling, N.A., Bharti, K., Kriel, H., and Simon, C.G.DiameterJ: a validated open source nanofiber diameter measurement tool. Biomaterials 61, 327, 2015.

39. Dokmanovic, M., Clarke, C., and Marks, P.A. Histonedeacetylase inhibitors: overview and perspectives. Mol Cancer Res 5, 981, 2007.

40. Backliwal, G., *et al.* Valproic acid: a viable alternative to sodium butyrate for enhancing protein expression in mammalian cell cultures. Biotechnol Bioeng 101, 182, 2008.

41. Yang, W.C., *et al.* Addition of valproic acid to CHO cell fed-batch cultures improves monoclonal antibody titers. Mol Biotechnol 56, 421, 2014.

42. Lu, H., Hoshiba, T., Kawazoe, N., and Chen, G. Comparison of decellularization techniques for preparation of extracellular matrix scaffolds derived from three-dimensional cell culture. J Biomed Mater Res A 100, 2507, 2012.

43. Lakes, R. Foam structures with a negative Poisson's ratio.Science 235, 1038, 1987.

44. Greaves, G.N., Greer, A.L., Lakes, R.S., and Rouxel, T.Poisson's ratio and modern materials. Nat Mater 10, 823, 2011.

45. Oliver, W.C., and Pharr, G.M. An improved technique fordetermining hardness and elastic modulus using load and displacement sensing indentation experiments. J Mater Res 7, 1564, 2011.

46. Akhtar, R., *et al.* Nanoindentation of histological specimens: mapping the elastic properties of soft tissues. J Mater Res 24, 638, 2009.

47. Livak, K.J., and Schmittgen, T.D. Analysis of relative geneexpression data using real-time quantitative PCR and the 2A¨ A¨ CT method. Methods 25, 402, 2001.

48. Klatt, D., *et al.* Viscoelastic properties of liver measured by oscillatory rheometry and multifrequency magnetic resonance elastography. Biorheology 47, 133, 2010.

49. Cozzolino, A.M., *et al.* Modulating the substrate stiffness to manipulate differentiation of resident liver stem cells and to improve the differentiation state of hepatocytes. Stem Cells Int 2016, 5481493, 2016.

50. Mansouri, N. The influence of topography on tissue engineering perspective. Mater Sci Eng C 61, 906, 2016.

51. Davis, N.F., Mooney, R., Callanan, A., Flood, H.D., andMcGloughlin, T.M. Augmentation cystoplasty and extracellular matrix scaffolds: an ex vivo comparative study with autogenous detubularised ileum. PLoS One 6, e20323, 2011.

52. Discher, D.E., Janmey, P., and Wang, Y.-L. Tissue cellsfeel and respond to the stiffness of their substrate. Science 310, 1139, 2005.

53. Martinez-Hernandez, A., and Amenta, P.S. The hepatic extracellular matrix I. Components and distribution in normal liver. Virchows Arch A Pathol Anat Histopathol 423, 1, 1993.

54. Dunn, J.C., Yarmush, M.L., Koebe, H.G., and Tompkins,R.G. Hepatocyte function and extracellular matrix geometry: long-term culture in a sandwich configuration. FASEB J 3, 174, 1989.

55. Martinez-Hernandez, A., and Amenta, P.S. The extracellular matrix in hepatic regeneration. FASEB J 9, 1401, 1995.

56. Carlsson, R., Engvall, E., Freeman, A., and Ruoslahti, E.Laminin and fibronectin in cell adhesion: enhanced adhesion of cells from regenerating liver to laminin. Proc Natl Acad Sci U S A 78, 2403, 1981.

57. Matsuzawa, A., Matsusaki, M., and Akashi, M. Construction of three-dimensional liver tissue models by cell accumulation technique and maintaining their metabolic functions for long-term culture without medium change. J Biomed Mater Res A 103, 1554, 2015.

58. Badylak, S.F. The extracellular matrix as a scaffold fortissue reconstruction. Semin. Cell Dev Biol 13, 377, 2002.

59. McCullen, S.D., Autefage, H., Callanan, A., Gentleman, E.,and Stevens, M.M. Anisotropic fibrous scaffolds for articular cartilage regeneration. Tissue Eng Part A 18, 2073, 2012.

60. Sell, S.A., *et al.* The use of natural polymers in tissue engineering: a focus on electrospun extracellular matrix analogues. Polymers (Basel) 2, 522, 2010.

61. Butcher, A.L., Offeddu, G.S., and Oyen, M.L. Nanofibroushydrogel composites as mechanically robust tissue engineering scaffolds. Trends Biotechnol 32, 564, 2014.

62. Egeblad, M., Rasch, M.G., and Weaver, V.M. Dynamicinterplay between the collagen scaffold and tumor evolution. Curr Opin Cell Biol 22, 697, 2010.

63. Faulk, D.M., Johnson, S.A., Zhang, L., and Badylak, S.F.Role of the extracellular matrix in whole organ engineering. J Cell Physiol 229, 984, 2014.

64. Crapo, P.M., Gilbert, T.W., and Badylak, S.F. An overviewof tissue and whole organ decellularization processes. Biomaterials 32, 3233, 2011.

65. Hay, D.C., *et al.* Efficient differentiation of hepatocytes from human embryonic stem cells exhibiting markers recapitulating liver development in vivo. Stem Cells 26, 894, 2008.

66. Takebe, T., *et al.* Generation of a vascularized and functional human liver from an iPSC-derived organ bud transplant. Nat Protoc 9, 396, 2014.

67. Broutier, L., *et al.* Culture and establishment of selfrenewing human and mouse adult liver and pancreas 3D organoids and their genetic manipulation. Nat Protoc 11, 1724, 2016.

68. Li, Q., *et al.* Proteomic analysis of naturally-sourced biological scaffolds. Biomaterials 75, 37, 2016.

69. Xiang, J., *et al.* Decellularized spleen matrix for reengineering functional hepatic-like tissue based on bone marrow mesenchymal stem cells. Organogenesis 12, 128, 2016.

70. Gao, R., *et al.* Hepatocyte culture in autologous decellularized spleen matrix. Organogenesis 11, 16, 2015.

71. Godoy, P., *et al.* Recent advances in 2D and 3D in vitro systems using primary hepatocytes, alternative hepatocyte sources and non-parenchymal liver cells and their use in investigating mechanisms of hepatotoxicity, cell signaling and ADME. Arch Toxicol 87, 1315, 2013.

72. Martinez-Hernandez, A., and Amenta, P.S. The hepatic extracellular matrix II. Ontogenesis, regeneration and cirrhosis. Virchows Arch A Pathol Anat Histopathol 423, 77, 1993.

73. Costantini, S., Di Bernardo, G., Cammarota, M., Castello,G., and Colonna, G. Gene expression signature of human HepG2 cell line. Gene 518, 335, 2013.

74. Chen, G.Y., and Nun˜ez, G. Sterile inflammation: sensing and reacting to damage. Nat Rev Immunol 10, 826, 2010.

Address correspondence to:

Anthony Callanan, PhD

Institute for Bioengineering

School of Engineering

University of Edinburgh

King's Buildings

Mayfield Road

Edinburgh EH9 3JL

United Kingdom

E-mail: anthony.callanan@ed.ac.uk

Received: October 10, 2016

Accepted: February 21, 2017 Online Publication Date: May 3, 2017

Appendix 3;

From scaffold to structure: the synthetic production of cell derived extracellular matrix for liver tissue engineering

Biomedical Physics & Engineering Express

ENDORSED BY IPEM Institute of Physics and Engineering in Medicine

ACCEPTED MANUSCRIPT • OPEN ACCESS

From scaffold to structure: the synthetic production of cell derived extracellular matrix for liver tissue engineering

To cite this article before publication: Rhiannon Grant *et al* 2018 *Biomed. Phys. Eng. Express* in press
https://doi.org/10.1088/2057-1976/aacbe1

Manuscript version: Accepted Manuscript

From scaffold to structure: the synthetic production of cell derived extracellular matrix for liver tissue engineering

Rhiannon Grant MSc, David Hay PhD, Anthony Callanan PhD

Institute for Bioengineering, School of Engineering, University of Edinburgh, King's Buildings, Mayfield Road, Edinburgh, EH9 3JL

Corresponding author; anthony.callanan@ed.ac.uk

Rhiannon Grant MSc

Email	rhiannon.grant@ed.ac.uk
Telephone	+44 (0)1316517077
Fax	+44 (0)131 650 6554

David C Hay PhD

Email	davehay@talktalk.net
Telephone	+44 (0)1316519500
Fax	+44 (0)131 651 9501

Anthony Callanan PhD

Email	anthony.callanan@ed.ac.uk
Telephone	+44 (0)1316507355
Fax	+44 (0)131 650 6554

Abstract

Liver transplant is the only curative treatment option for patients with end -stage liver failure, however there are few donor livers available for transplant. Tissue engineering of a human liver would potentially solve the problem of escalating donor shortages. A major challenge presents itself in the form of the hepatic extracellular matrix (ECM); a finely controlled *in vivo* niche which supports hepatocytes and plays a critical role in the development of liver disease Polymers and decellularized tissues each provide some of the necessary biological cues for the hepatocytes, however, neither alone has proved sufficient. Equally, the ability to fine tune the microenvironment using bioactive molecules presents researchers with the opportunity to create personalised niches for hepatocytes , representing both normal and diseased phenotypes. This study combines cell derived ECM with a fibronectin vector and electrospun scaffolding techniques to produce a platform for creating customisable ECM microenvironments for hepatocytes (Abstract image). The resulting poly -L-lactic acid - extracellular matrix (PLA-ECM) scaffolds were validated using HepG2 hepatocytes.

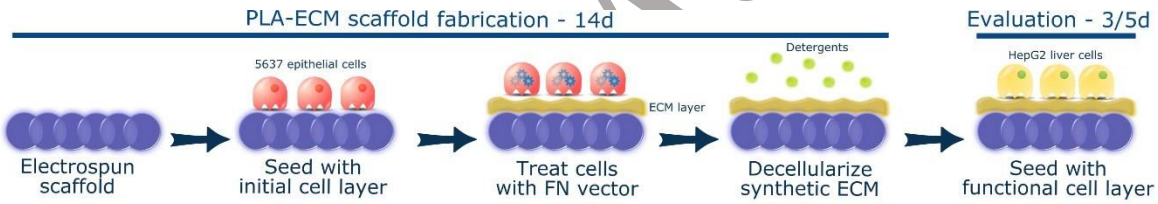

Abstract image . Methodology used to biofuctionalize electrospun scaffolds with synthetically derived ECM.

As expected, statistically significant mechanical differences were observed between the synthetically derived ECM (SD -ECM) scaffolds and normal ECM (N -ECM) scaffolds , confirming that the ECM has been altered by the fibronectin producing vector. The PLA-ECM scaffolds maintained hepatocyte growth and function and influence the gene expression of key hepatic genes. Furthermore, immunohistochemistry showed SD and N-ECMs differed in ratios of Collagen I, Laminin and Fibronectin.

Our results demonstrate that hybrid PLA-ECM scaffolds and the synthetic production of ECM provide a viable, translatable platform for customising microenvironments for hepatocytes.

This technology offers a potential solution to current obstacles in regenerative medic ine, disease modelling and whole organ tissue engineering.

Introduction

In the US alone, as of August 20th 2017, the Organ Procurement and Transplantation Network (OPTN) estimates 14,158 patients are waiting for a donor liver. With a lack of viable new pharmaceuticals, liver transplant remains the sole treatment option for end-stage disease patients [1]. Liver disease is an increasing burden on the health of the Western world, with both incidence and mortality increasing rapidly since 1970 [2]. Demand for donor livers far outstrips supply, and the incidence of liver disease shows no signs of slowing down [3].

Tissue engineers seek to solve this problem by engineering liver 'organoids'; laboratory created organs which can function as a liver in vivo [4–7]. The 3D environment exerts extensive influence on the behaviour and function of hepatocytes [6,8]. With this in mind, tissue engineers employ scaffold manufacturing technologies to create structures which encompass key characteristics of the native 3D ECM [9–14]. Several different methods of creating a scaffold are in use, and they can be made from a myriad of substances; both natural and synthetic [15], and enhanced with bio-decoration methods [8]. There has been particular focus on decellularization, which provides an ECM bioscaffold with the 3D site-specific vasculature required for hepatocyte function upon their repopulation of the organ [16]. Decellularized organs have been repopulated with hepatocytes and endothelial cells which subsequently survive and exhibit some level of function, clearly demonstrating the importance of the ECM in supporting hepatocyte survival and phenotype [17–21]. However, decellularization requires a human or animal source of whole, undamaged organs and while research is showing great promise, the field is fragmented and to date no scaffold has been created which allows hepatocytes to function as well as in vivo [22,23].

Synthetic biology and genetic engineering are vital tools for tissue engineers and have been used to alter gene expression, enhance intracellular imaging and study fundamental processes in hepatocytes [24–26]. Recently, synthetic biology tools have been successfully employed to direct both stem cell lineage and fate in 3D constructs[27,28], in the manipulation of biofilms for cell culture [29] and in the production of therapeutic proteins in *in vivo* systems [30,31]

demonstrating the ability of synthetic biology techniques to manipulate 3D environments and thus their potential benefit to the field of tissue engineering. Groundbreaking CRISPR [32–34] and minicircle vector [35–37] technologies have made the idea of therapeutic gene editing in humans a viable reality, however concerns exist regarding the safety and subsequently, the translatability of such tools with regards to patient treatment. Heavily publicised and tragic events such as the 1999 death of 18 year old Jesse Gelsinger [38] and the 2002 clinical trial in which four children developed leukaemia following gene therapy for their Severe Combined Immune Deficiency disease [39] have led to obvious worries regarding the safety of gene therapies. The inflammatory and immune modulating effects of damage-associated molecular patterns (DAMPs) such as foreign DNA fragments [40] are well documented, however clinical use of decellularized ECM in exogenic and allogenic form has demonstrated great promise, giving no immune response and showing regenerative potential. This paves the way for using synthetic biology to tissue engineer the ideal ECM environment. The ideal ECM would utilise synthetic biology and genetic technologies to their utmost, considerable, potential but remove any risk from the tools used; such as the genetically modified cells themselves.

Table 1; Advantages of a combinatorial approach to tissue engineering of liver environments.

	Polymer scaffolds		**Decellularized tissues**		**Vector technology**		**Combinatorial approach**
✓	Reproducible	✓	Provides biochemical cues of ECM	✓	Customizable protein profile	✓	Mechanically & proteomically customizable
✓	Mechanically customizable	✓	Vasculature exists within tissue	✓	Rapid production of desired proteins	✓	Cell lines used - donors avoided
✘	Does not provide complex biochemical cues of ECM	✘	Limited donors & donor safety	✘	Vector safety concerns	✓	Vectors removed - safety concerns abated

With the potential of synthetic biology for manipulation of protein pr oduction in mind, we set out to address this problem; developing a novel bio -active hybrid scaffold which possesses the potential for customizatioon of the ECM microenvironment. To date, no bioengineers have combined the promising fields of scaffold manufacture, decellularized tissue and synthetic biology. Here we report the first use of a sacrificial, transfected cell line to bio-functionalise an electrospun polymer scaffold for liver tissue engineering. We have successfully decellularized the bio-functionalised scaffold, and validated the platform using cells representative of the liver, HepG2s.

Materials and Methods

Electrospinning

A 10% wt/vol solution of poly-L-lactic acid (Goodman) and hexafluoroisopropanol (Manchester Organics) was dissolved overnight at room temperature with agitation. Solutions were placed into a 10ml syringe and pumped usi ng syringe pump EP -H11 (Harvard Apparatus) into the EC-DIG electrospinning system (IME technologies) via a 27G bore needle under the following parameters;

Table 2; Electrospinning parameters

Volume per hour	Total volume	Mandrel:needle distance	Positive charge	Negative charge	Mandrel rotation	Needle movement
0.5ml	10ml	14 cm	16kV	-3kV	250rpm	100mm/s

The mandrel was coated in non-stick aluminium foil for collecting the electrospun fibres. The sheets of electrospun fibres were allowed to dry overnight in a fume hood when the electrospinning session was completed. The average fibre size was 1.48µm as cal culated by ImageJ plugin 'DiameterJ' [41].

Scaffold Preparation

10mm discs of scaffold were cut from the dry fibre sheet. The scaffolds were soaked in 70% isopropyl alcohol for 10 minutes , rinsed three times in phosphate buffered saline for 15

minutes each and allowed to dry completely at room temperature. Scaffolds were placed into an antibiotic/antimycotic treatment solution of Dulbeccos Minimal Essential Media supplemented with 100U/ml penicillin, 100µg/ml streptomycin, 0.25µg/ml Fungizone® (amphotericin B) Anti-Anti solution (Gibco) for 1 hour.

Initial Layer Cell Seeding and Culture

Scaffolds were removed from the antibiotic/antimycotic treatment solution and rinsed three times for 15 minutes each in complete media; Dulbeccos Minimal Essential Media supplemented with 10% foetal bovine serum, 2mM L-glutamine, 100U/ml penicillin and 100µg/ml streptomycin (Gibco). They were then placed into a fresh 48 well tissue culture plate.

5637 human urinary bladder epithelials (ATCC) were cultured and expanded as per supplier recommendations, using the media described above. Cells for scaffold seeding were trypsinized using 0.25% Trypsin-EDTA (Gibco) from tissue culture flasks and counted using the trypan blue exclusion method. 1×10^5 cells at passage 23 were suspended in 100µl of complete media and seeded directly on to the scaffolds. The cells were allowed to incubate in this small volume on the scaffolds for 2 hours, before an additional 400µl of complete media was added.

Media was changed after 24 hours using standard methods and subsequently changed every 48 hours. Controls were scaffold only, i.e. not seeded with an initial cell layer and a 'normal' initial layer i.e. untransfected cells. Initial layers of cells were cultured for 7 days at 37ºC and 5% CO_2 in a humidified incubator.

Fibronectin Vector

Vectors were obtained from the DNASU plasmid repository. In brief, the human fibronectin gene (FN1) was placed into a retroviral expression vector, PJ1520. The insert sequence was verified by sequence analysis and restriction enzyme digest by DNASU. The vector was obtained in DH5-alpha T1 phage resistance *Escheria coli* glycerol stock. We cultured the E. coli under selective conditions; 100µg/ml ampicillin, 34µg/ml chloramphenicol and 7%wt/vol

sucrose in LB media. Plasmid extractions were performed using Cambridge Bioscience's Zyppy™ plasmid extraction kit following manufacturer's methods.

Transfections

Transfections were performed using Invitrogen Lipofectamine 3000 ®. Following titration experiments, a concentration of 1µg plasmid DNA and 0.75µL lipofectamine reagent per scaffold was chosen. The initial layer of 5637 epi thelials was cultured on the scaffolds under standard conditions for 7 days. Transfection was performed on the 7 th day. Scaffold -cell constructs were then placed into selective media containing 150µg/ml puromycin. The cell - scaffold constructs were cultured under selection for a further 7 days to allow production of the vector derived fibronectin before being decellularized.

Decellularization

Decellularization was performed under sterile conditions at room temperature (19 - 22ºC) and with agitation. Scaffolds were placed into 50ml falcon tubes and placed on a rotator at 20RPM. Scaffolds were washed with phosphate buffered saline (PBS) for 15 minutes and then rinsed in 10mM tris buffered saline (TBS) for 15 minutes.

The scaffolds were submerged in a 0.1% vd/vol Triton X-100 (Sigma-Aldrich) 1.5M potassium chloride (Acros Organics) 50mM TBS for 4 hours. They were rinsed for 15 minutes in 10mM TBS before being submerged in fresh 10mM TBS overnight.

Scaffolds were given a final rinse in 10mM TBS for 15 minutes before being incubated in complete media for 15 minutes and then transferred to new 48 well plates for seeding.

Functional layer Cell Seeding and Culture

HepG2 cells were trypsinized using standard methods from tissue culture flasks and counted using the trypan blue exclusion method. 1 x 10^5 cells at passage 17 were suspended in 100µl of complete media and seeded directly on to the scaffolds. The cells were allowed to incubate

in this small volume on the scaffolds for 2 hours, before an additional 400µl of complete media was added.

Media was changed after 24 hours and changed every 48 hours after the initial 24 hour adherence and recovery period. This functional layer (FL) of cells was cultured using standard methods for either 3 or 5 days at 37ºC and 5% CO_2 in a humidified incubator.

Live/Dead® Viability/Cytotoxicity assay

To determine cellular viability, cell/scaffold constructs were incubated with 10µm calcein and 2µm ethidium ho-modimer-1 (Ethd-1) for 30 minutes as part of the two colour live/dead assay (Molecular Probes). Calcein is actively converted to calcein -AM in living cells, which then appear green when excited during fluorescence microscopy. Ethd-1 only accumulates in dead cells, which subsequently appear red. The method allows differentiation between dead and viable cells. The scaffolds were rinsed three times in $CaCl_2$/$MgCl_2$ free PBS to remove excess dye and placed onto a standard microscope slide with a 25mm glass coverslip (VWR). All images were captured using a Zeiss Axio Imager fluorescent microscope (COIL, University of Edinburgh) at 40x magnification and post processed using ImageJ.

CellTiter-Blue® Cell viability assay

The assay was performed according to manufacturer's instruction (Promega). For each condition group, n = 5. Importantly, cell/scaffolds constructs were moved into fresh 48 well plates to prevent reading activity from tissue culture plastic bound cells. Measurements were read in a Modulus™ II microplate reader at an excitation wavelength of 525 nm and emission wavelength of 580-640 nm and reported as fluorescence.

Albumin quantification

A bromocresol green (BCG) albumin assay (Sigma) was used to quantify serum albumin produced by the HepG2 functional cell layer over 24 hours at 3 and 5 day timepoints. The

assay was performed acc ording to manufacturer's instructions and results read at an absorbance of 620 nm in a Modulus™ II microplate reader.

Picogreen® DNA quantification

The Quant-IT™ Picogreen® dsDNA assay kit (Life Technologies™) was employed to establish the efficiency of the decellularization method in removing cellular material and to estimate cell number on the cell/scaffold constructs. The assay was performed according to manufacturer instructions. In brief, constructs (n = 5) were digested in a solution of $CaCl_2$ and $MgCl_2$ free PBS (Sigma), containing 2.5 U/ml papain extract (Sigma) 5 mM cysteine -HCl (Sigma) and 5 mM EDTA (Sigma) and incubated for 48 hours at 60°C. Picogreen solution was added to the digests and fluorescent intensity measurements read in a Modu lus™ II microplate reader at an excitation wavelength of 480 nm and emission wavelength of 510 -570 nm. A standard λ dsDNA curve of graded known concentrations was used to calibrate fluorescence intensity vs dsDNA concentration.

Sectioning and staining

The samples were rinsed three times in PBS (Gibco) for 15 minutes each, then fixed in 4% v/v formalin buffered in saline for 15 minutes at room temperature. After rinsing with fresh PBS, constructs were embedded in low melting temperature polyester wax (Electr on Microscopy Supplies) using methods adapted from Steele et al. (2014). In brief, samples are dehydrated through 70-100% ethanol, then incubated in 50:50 ethanol:wax overnight at 45ºC overnight with agitation. The samples were moved into 100% wax for 3 hours at 45ºC and then fresh 100% wax for 1 hour at 45ºC. Samples were e mbedded and allowed 72 hours to fully cure before sectioning. Immunohistochemical staining was undertaken using antibodies for Collagen I (Stratech), Laminin (Stratech) and Fibronectin (Sigma). All images were captured using a Zeiss Axio Imager system (Ce ntre Optical Instrumentation Laboratory, University of Edinburgh) at 40x magnification and post processed using ImageJ.

Scanning Electron Microscopy

SEM was used to characterise the scaffold architecture. Samples were rinsed three times in PBS for 15 minu tes each, then fixed in 2.5% v/v glutaraldehyde (Fisher Scientific) in 0.1M phosphate buffer (PB) (pH 7.4) at 4ºC overnight. They were then rinsed three times in 0.1M PB before being post -fixed in 1% v/v osmium tetroxide (Electron Microscopy Supplies) buffered with 0.1M PB. Samples were again rinsed three times in 0.1M PB and dehydrated through an ethanol gradient (30 -100%). They were dried by placing them in hexamethyldisilazane (HDMS, Sigma) which was allowed to evaporate off at room temperature overnight. We mounted the samples onto SEM chucks using double sided carbon tape and coated them with a thin layer of gold and palladium alloy (Polaron Sputtercoater).

All images were captured at 5 kV using a Hitach S -4700 SEM (BioSEM, University of Edinburgh).

Mechanical Testing

Nanoindentation experiments were undertaken to establish the dynamic properties of scaffolds and decellularized ECM/scaffold constructs using the Keysight/Agilent 5200 nano indenter testing system.

Scaffolds and constructs were subject to indentation by a DCM II actuator flat-ended cylindrical punch (D = 100µm) using a max load of 1g -f. All nanoindentation experiments were carried out on fresh, hydrated (suspended in PBS), unfixed samples in a stainless steel well chuck. A total of 36 inde ntations were carried out on each sample, 50nm apart. Indent sites were selected using the high precision X-Y stage within the testing system (Agilent). Poissons ratio was assumed to be 0.5 for each sample [42,43]. Allowable drift rate was 0.1nm/s. A NanoSuite (Keysight Technologies) test method “G-Series DCM CSM Flat Punch Complex Modulus” was used for all testing [44,45].

Gene Expression analysis

RNA was extracted from const ructs using standard Trizol (Fisher Scientific) methods and purified using Qiagen's RNeasy spin column system. cDNA was synthesised using the Promega's ImProm-II™ Reverse Transcription System.

Quantitative real -time polymerase chain reaction (qRT -PCR) was performed using the LightCycler® 480 Instrument II (Roche Life Science) and Sensifast™ SYBR ® High-ROX (Bioline) system. Results were normalized to HepG2s of the same passage number grown on tissue culture plastic and compared to the housekeeping gene Glyce raldehyde-3-Phosphate Dehydrogenase (GAPDH). Analysis was performed using the 2–[delta][delta] Ct method [46,47], n = 5. Albumin (Alb), Cytochrome P450 Family 1 Subfamily A Polypeptide 1 (Cyp1A1), Cytochrome P450 Family 1 Subfamily A Polypeptide 2 (Cyp1A2), Cytochrome P450 Family 3 Subfamily A Polypeptide 4 (Cyp3A4), Collagen Type I alpha 1 (Col1A1), Collagen Type 4 alpha 1 (Col4A1) and Fibronectin Type 1 (FN1) were investigated, forward and reverse primers (Sigma) are detailed in Supplementary Table 1.

Statistical Analysis

One-way ANOVAs with Fishers, Games -Howell and Tukey [48–50] post-hoc testing were performed using Minitab 17 Statistical Software and graphs generated using Origin software (OriginLab, Northampton, MA). Error bars indicate standard deviation. A minimum of n = 3 and max of n = 6 was used for all analysis.

Results

Cell attachment and survival on scaffolds

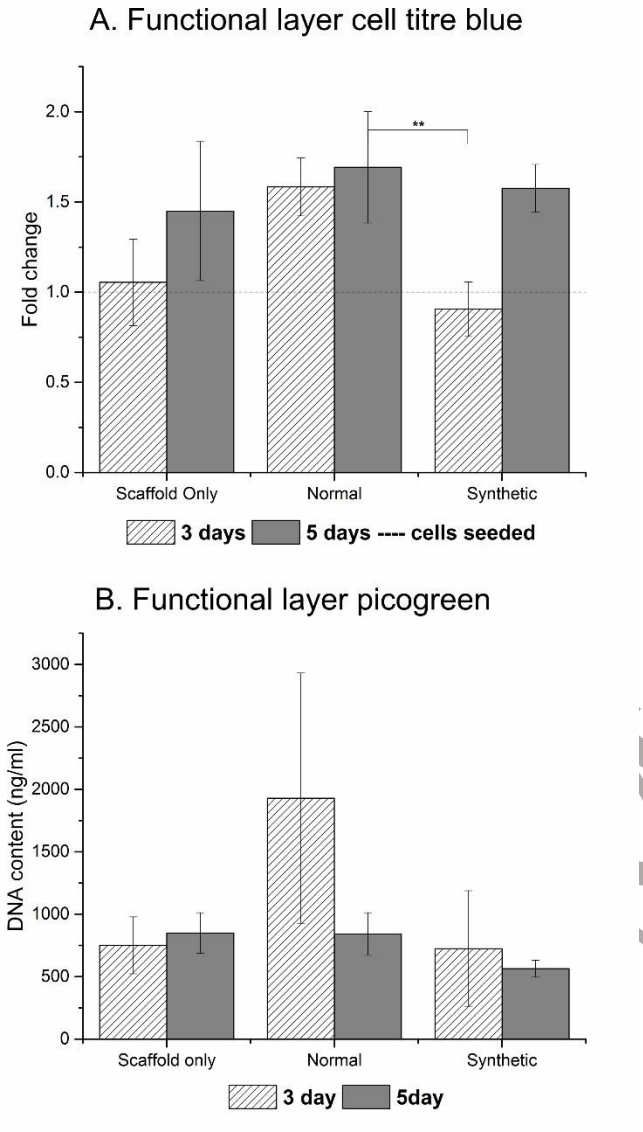

Figure 1. Cell titre blue assay indicating metabolic activity (A) and DNA quantitation of the functional layer (B). One way ANOVA with Games Howell post hoc testing, ** = p value <0.01.

When compared to normal ECM derived from untransfected cells (N-ECM) and the scaffold alone (SO), a lower number of HepG2s adhered to the synthetically derived vector driven (SD -ECM) scaffold-ECM constructs (Fig. 1). According to the CellTiter-Blue® results (Fig. 1 A), the SD ECM layer maintained the growth of the HepG2s between days 3 and 5. However, this result is not concurrent with the Picogreen® DNA quantitation (Fig. 1B). This is most likely due to different data extraction methods and validation methods in the Picogr een and CellTiter - Blue assays. Both assays possess depth dependencies with regards to their efficiency and effectiveness in extracting data from fibrous scaffold constructs. Additionally, the assays were validated using 2D monolayer cell cultures. This would explain high standard deviations in the Picogreen® DNA quantitation dataset and slight different trends observed between the assays. These finding are corroborated by our recent published work of cells on electrospun scaffolds [14]. Live/Dead® Viability/Cytotoxicity images (Fig. 2) demonstrate the metabolic viability of the functional HepG2 cell layer (FL), and that at day 5 the cells appear to be confluent and living, with low levels of cell death in each condition.

Mechanical characterisation of scaffolds

Reassuringly, both storage (G') and loss (G") modulus demonstrate significant differences between the three conditions (Fig. 3). Fibronectin is known to influence both the mechanical profile of the ECM [51,52] and influence the maintenance and structure of o ther vital ECM proteins, such as collagen [53]. Equally, cells are known to respond to the mechanical and topographical influenc e a scaffold exerts [54].

Testing was performed at frequencies experienced by the human liver in vivo [55]. Storage modulus (G') ranged from 22.92±9.14 to 12.29±0.14 MPa and loss modulus (G'') from 2.45±0.93 to 0.15±0.02 MPa at the frequencies detailed in supplementary tables 2 and 3.

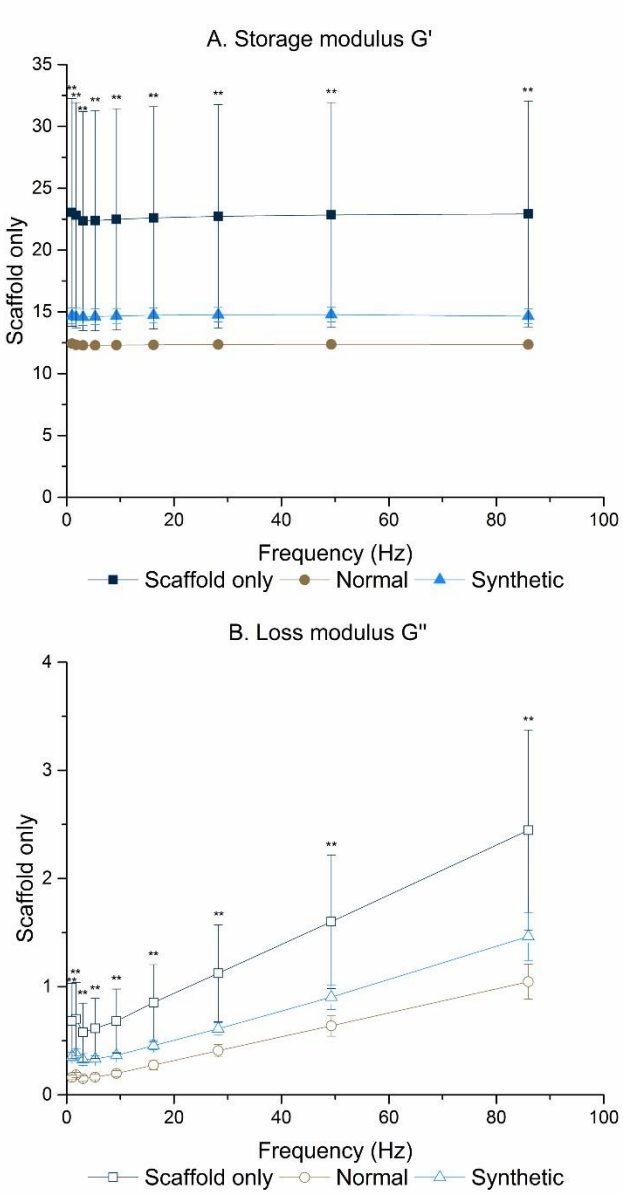

Figure 3. Significant mechanical differences were observed between all scaffold conditions. One way ANOVA with Games H owell post hoc testing, ** = p value <0.01.

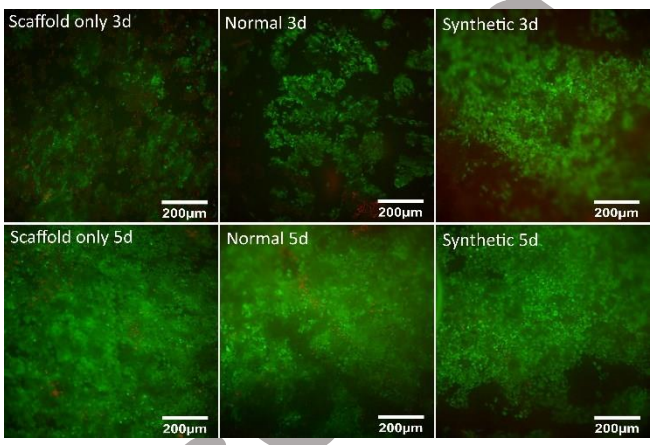

Figure 2. Live Dead imaging demonstrating the living functional layer present at each time point, with minimal cell death.

Biochemical characterisation of the hybrid polymer-ECM scaffolds

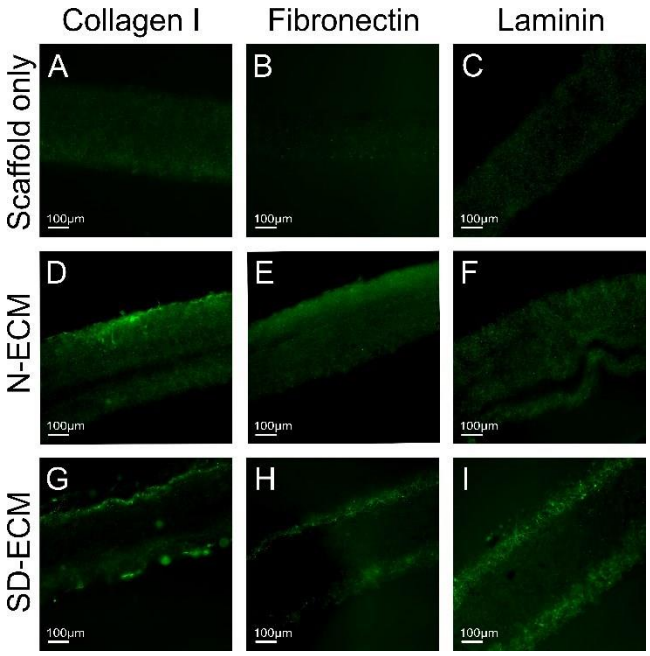

Figure 4. IHC staining showing the retention of major liver ECM proteins Collagen I (D, G), Fibronectin (E, H) and Laminin (F, I) following decellularization. Additionally, SO condition shows no positive staining as expec ted (A, B, C).

Differences in the biochemical profile of the different ECMs were demonstrated by immunohistochemistry performed on decellularized hybrid scaffold sections (Fig. 4). Hepatic cells are very responsive to extracellular matrix proteins; particularly Collagen I, Laminin and Fibronectin [56–58]. Fibronectin is ubiquitous in healthy liver [59,60], and antibody staining reveals altered levels of fibronectin in the synthetically derived ECM, as expected due to the introduction of the fibronectin vector (Fig. 4H). ECM proteins do not exist in isolation, and fibronectin is known to influence the generation and laydown of other ECM proteins including collagen I and laminin [53,61], as evidenced in Fig. 4G and 4I when compared to N-ECM. The N-ECM is collagen I rich (Fig. 4D) with some fibronectin and laminin also present (Fig. 4E & 4F). Of note is that the SD-ECM appears to be concentrated on the outer layers of the electrospun scaffold. This could be due to the transfected cells being in fewer number than those which were not transfected (N-ECM), so they did not penetrate the scaffold to the same extent.

Gene expression of HepG2s in response to hybrid polymer-ECM scaffolds

Genes associated with both liver function and ECM production were ass ayed for gene expression (Fig. 5). Albumin expression, a marker of approp riate liver cell differentiation and function, appears upregulated between day 3 and day 5 in each condition , confirming appropriate development of the cells. At day 5, expression is significantly upregulated in comparison to HepG2s grown on tissue culture plastic (TCP) on the SD-ECM constructs; with

the highest levels of expression observed in SO and SD-ECM conditions. Additionally, albumin mRNA expression is downregulated in comparison to TCP at day 3 in all conditions (Fig. 5A). Cytochrome P450s (Cyp) are a family of enzymes involved in metabolism of xenobiotics and toxic compounds in the liver [62–64]. Cyp1A1 mRNA expression is significantly altered in comparison to TCP (Fig. 5B); upregulated at day 3 and downregulated at day 5. Cyp1A2 mRNA expression is consistently significantly downregulated in all but one condition; day 3 N-ECM (Fig. 5C). Cyp3A4 mRNA expression is upregulated in every condition, with a significant upregulation observed in response to SD-ECM (Fig. 5D).

In addition, we assayed for three ECM genes important for normal liver composition [59,65]; Fibronectin (Fig. 5E), Collagen I (Fig. 5F) and Collagen IV (Fig. 5G). Considering the plastic nature of ECM, these genes are of interest with regards to ongoing modification of the tissue microenvironment despite hepatocytes not being the main producers of ECM proteins in the liver [59,66].

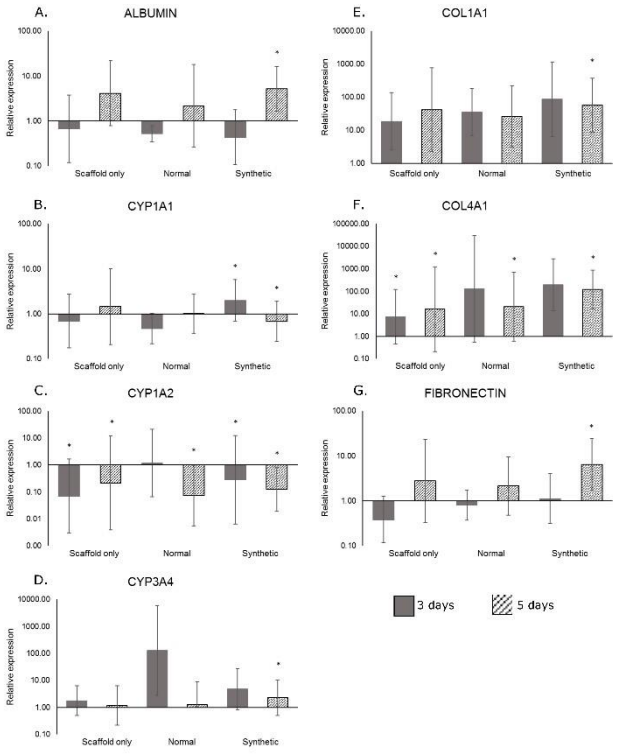

Figure 5. Q-PCR results showing significant changes in expression of major liver genes when compared to TCP, Albumin (A), CYP1A1 (B), CYP1A2 (C), CYP3A4 (D) an ECM genes Col 1A1 (E), Col 4A1 (F) and Fibronectin (G) between the hybrid scaffolds and tissueculture plastic. (A, C, D, E, F, G) = One way ANOVA with Games Howell post hoc testing, * = p value <0.05. (B) = One way ANOVA with Tukey post hoc testing, * = p value <0.05.

Collagen I is consistently upregulated, with significant upregulation observed at day 5 on SD-ECM. Equally, Fibronectin mRNA expression is significantly upregulated on day 5 SD-ECM constructs, though downregulated at day 3 on SO and N-ECM constructs. Collagen IV mRNA expression is consistently upregulated in each condition, with significant changes observed in all but day 3 N-ECM and SD-ECM. While such

alterations in gene expression are promising, we refrain from further assumption regarding cell response without further proteomic and functional analyses.

Albumin production

Albumin levels are indicative of hepatocyte health and response to the microenvironment [57]. Each condition results in differing levels of albumin production, with significant differences in protein levels observed between SO and SD-ECM at both 3 days and 5 days (Fig. 6), indicating that the N-ECM encouraged albumin production more than SD-ECM.

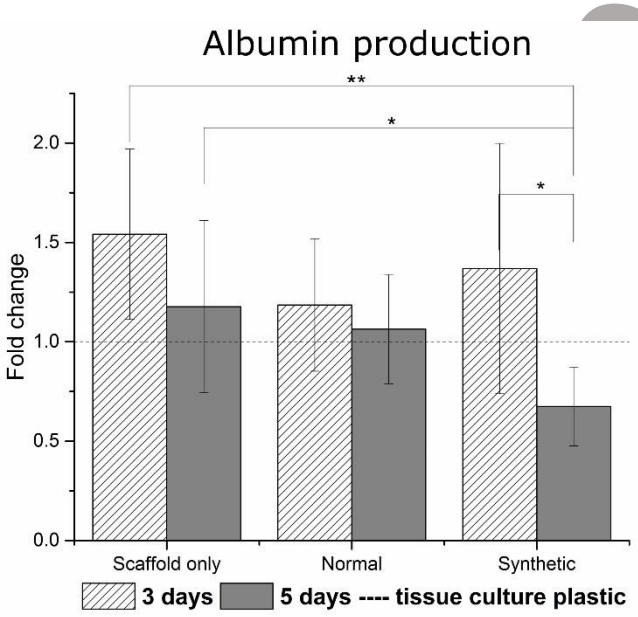

Figure 6. Albumin production between conditions, showing significant changes between SO and SD -ECM conditions at both time points. One way ANOVA with Games Howell post hoc testing, * = p value <0.05. ** = p value <0.01.

Confirmation of decellularization

Decellularization was confirmed using Picogreen® DNA quantitation (Fig. 7G) and histological staining (Fig. 7 A-F). A tenfold reduction in DNA combined with visual confirmation of an absence of DAPI nuclear staining and Phalloidin -514 actin staining on

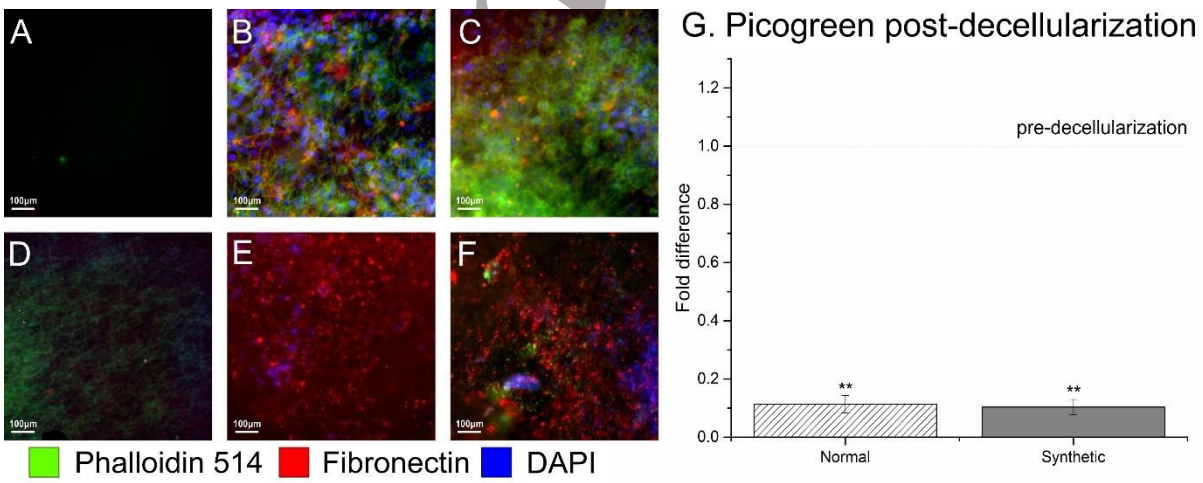

Figure 7. Effectively decellularized constructs, with minimum remnant DNA detected by IHC (E,F) or picogreen (G). Scaffolds pre-decellularization shown in (A), (B) and (C). One way ANOVA with Games Howell post hoc testing, ** = p value <0.05. Scaffold only (A, D), N-ECM (B,E) and SD-ECM (C, F)

decellularized constructs, plus the presence of fibronectin antibody staining on both the N -ECM and SD -ECM decellularized constructs (Fig. 7E&F) provides evidence of efficient decellularization methods, and that synthetically derived fibronectin is present on the hybrid scaffolds.

Discussion

The extracellular matrix provides a microenvironment for cells which is not yet fully understood, nor replicable by existing manufacturing methods [16,67–69]. By manipulating human cells to produce a customizable blend of ECM components, and combining this with replicable electrospun scaffolds and decellularization methods we overcome the shortage of donor derived ECM bioscaffolds and the issues regarding animal -sourced biomaterials [16,70]. Additionally, this platform has the potential to be used to model not only 'healthy' ECM microenvironments, but also those of disease and developing states.

By using fibrous electrospun scaffolds we mimic the morphology of healthy fibrillary collagen [10,11,71,72]. PLA was used to fabricate the scaffolds, chosen for its compatibility with hepatocytes [56] and its use in multiple types of medical device due to its predictable biodegradation rate and mechanical properties [73,74].

Fibronectin was chosen as our protein to synthetically overexpress due to its vital role in the liver [51,75] and its interaction with other ECM components such as collagen and laminin [52,53]. Fibronectin is a large dimeric adhesive glycoprotein which exists in both cellular and plasma forms, with roles in regenerating tissues, embryonic development and regulation of cell behaviours such as adhesion and migration[76]. The role of fibronectin in the liver is still unclear, with inhibition of fibronectin production or deposition improving fibrosis outcomes [77,78]. However its vital role in the hepatic ECM is demonstrated by mutant mice who were specifically null in only the liver for both plasma and cellular fibronectin. The fibronectin -null livers not only de velop highly disorganized/diffuse collagenous ECM networks, but when fibrogenesis was induced the null livers experienced more extensive fibrosis; t hought to be

due to fibronectin s role in regulating TGF -β1 bioavailability [75]. Additionally, homozygous fibronectin null mutants display early embryonic lethality, while heterozygotes (with 50% of the normal plasma fibronectin levels) appear normal; suggesting a dos e dependent role for fibronectin in development [79].

As an initial assessment of these novel hybrid scaffold s we investigated the attachment and function of a commonly used liver cell line, HepG2s, when cultured on the synthetically derived hybrid scaffolds versus a wild type 'normal' hybrid scaffold and the scaffold alone. The HepG2 cell line was derived from t he hepatocarcinoma of a 15 year old Caucasian male. They are often used because they are virus free, possess liver specific functions such as ammonia metabolism and albumin synthesis and secrete some growth factors [80]. We analysed cell attachment and viability, albumin production and gene expression of both liver function genes and ECM genes at 3 and 5 day time points. Additionally, we validated our decellularization method and performed both immunohistochemical and raman spectrum analyses (data not shown) of the hybrid scaffold-ECM constructs upon which the HepG2s were seeded.

Our results indicate not only that synthetically derived ECMs provide a viable method of biofunctionalising electrospun polymer scaffolds, but that the composition of the synthetically derived ECM -polymer hybrid scaffolds influences liver cells. That albumin production is significantly altered between SO and SD-ECM conditions, but not N-ECM conditions supports this assertion. Gene expression of key hepatic genes was altered on day 5 of SD -ECM conditions in every gene tested, whereas SO and N -ECM conditions only influence CYP1A2 and COL4A1 expression; demonstrating that the composition of the ECM is highly influential in tissue engineering. This in turn leads to questions regarding donor -donor variability of current decellularization work and its influence upon hepatic behaviour and a need for more reproducible hepatic microenvironments that this platform provides.

The researchers responsible recognise that, while this study forms a robust initial proof of principle regarding the exploitation of synthetic biology for scaffold manufac ture, and has produced a novel hybrid synthetically derived ECM - polymer scaffold with great potential for

liver tissue engineering, further work is required to analyse results and increase translatability. Vector technologies and synthetic biology present obvious concerns with regards to patient safety [30,81], and care should be taken to ensure all bacterial/ viral constructs are removed from the ECM layer. Detergent based methods used to strip the ECM of cells can be detrimental to the bioscaffold [70,82], disrupting native tissue ultrastructure, decreasing glycosaminoglycan (GAG) content and reducing collagen integrity [83,84] as well as disrupting lipid-lipid, lipid-protein and protein-protein interactions [85]. Care should be taken to optimise this procedure in the future. HepG2s provide a convenient method of initial viability testing of the scaffolds, but they are derived from a carcinoma and as such criticism of their clinical relevance is well placed. Further studies will utilise primary or stem cell derived hepatocytes to combat such criticism. Additionally, recognition of the value of further proteomic and functional assays (such as ELISAs and Alkaline Phosphatase quantitation) in analysing the function of hepatocytes will be vital for expanding this work, however at this time these were deemed unnecessary considering the obvious critiques of the use of the HepG2 cell line. Further, the importance of ensuring decellularization agents are removed from the constructs should not be underestimated, due to their influence upon cells and ECM [21,70]. While such criticisms are important to consider, this work clearly demonstrates the potential of synthetic biology for the design of bespoke ECMs and provides a robust initial platform upon which further, improved studies can be built.

Conclusion

This study demonstrates a novel method of creating a biologically bespoke hybrid ECM-polymer scaffold; utilising clinically translatable electrospun scaffold technologies and synthetic biology methods both easily modified to fulfil Good Manufacturing Practice (GMP) guidelines. In order to achieve this, a sacrificial ECM-producing cell layer was transfected using a protein producing fibronectin vector on an electrospun scaffold, biofuctionalizing the scaffold with a biologically bespoke ECM. Scaffolds with wild type untransfected cells and no initial cell layer at all were used as controls. This sacrificial cell layer was successfully removed

with a detergent based method and the hybrid synthetically derived ECM -polymer scaffolds seeded with HepG2 liver cells for validation . Results were validated using multiple well characterized methods, including mechanical quantitation, Q-PCR and immunohistochemistry. The synthetically derived PLA-ECM scaffolds exert biological influence upon liver cells, manipulating their microenvironm ent and resulting in alterations in gene expression profile, protein synthesis and cell attachment and survival. Such data demonstrates promise as a unique method of creating biologically bespoke ECMs and exerting influence upon cell populations both *in vivo* and *in vitro*.

These novel scaffolds exhibit great promise both as an implantable patient treatment for liver tissue engineering, for adaptation to other tissues and as a useful tool for development of 3D liver cell culture platforms with potential forboth *in vivo* cell analysis and novel pharmaceutical research.

Acknowledgements

The authors would like to thank Prof Alistair Elfick for use of lab facilities (IBioE, University of Edinburgh). We would also like to thank Steve Mitchell (BioSEM) andDr David Kelly (COIL) (University of Edinburgh). This work is funded by an Engineering & Physical Sciences Research Council [EPSRC] doctoral training partnership studentship, UK Regenerative Medicine Platform II [RMPII] grant MR/L022974/1 and MRC computational and chemical biology of the stem cell niche grant (CCBN) MR/L012766/1.

Author disclosure

The authors declare no competing interests.

1. British Association for the Study of the Liver & British Society of Gastroenterology. A Time to Act: Improving Liver Health and Outcomes in Liver Disease. *Natl. Plan Liver Serv. UK* 1–52 (2009).
2. Williams, R. *et al.* Implementation of the Lancet Standing Commission on Liver Disease in the UK. *Lancet* **386,** 2098–2111 (2015).
3. Wang, H. *et al.* Global, regional, and national life expectancy, all-cause mortality, and cause-specific mortality for 249 causes of death, 1980–2015: a systematic analysis for the Global Burden of Disease Study 2015. *Lancet* **388,** 1459–1544 (2016).

4. Huch, M. *et al.* Long-term culture of genome-stable bipotent stem cells from adult human liver. *Cell* **160,** 299–312 (2015).

5. Ye, J., Shirakigawa, N. & Ijima, H. Hybrid organoids consisting of extracellular matrix gel particles and hepatocytes for transplantation. *J. Biosci. Bioeng.* (2015). doi:10.1016/j.jbiosc.2015.01.004

6. Takebe, T. *et al.* Vascularized and complex organ buds from diverse tissues via mesenchymal cell-driven condensation. *Cell Stem Cell* **16,** 556–565 (2015).

7. Banaeiyan, A. A. *et al.* Design and fabrication of a scalable liver-lobule-on-a-chip microphysiological platform. *Biofabrication* **9,** (2017).

8. Grant, R., Hay, D. & Callanan, A. A Drug-Induced Hybrid Electrospun Poly-Capro-Lactone: Cell-Derived Extracellular Matrix Scaffold for Liver Tissue Engineering. *Tissue Eng. Part A* **23,** 650–662 (2017).

9. Nichol, J. W. *et al.* Cell-laden microengineered gelatin methacrylate hydrogels. *Biomaterials* **31,** 5536–44 (2010).

10. McCullen, S. D., Autefage, H., Callanan, A., Gentleman, E. & Stevens, M. M. Anisotropic Fibrous Scaffolds for Articular Cartilage Regeneration. *Tissue Eng. Part A* **18,** 2073–2083 (2012).

11. Accardi, M. A. *et al.* Effects of fiber orientation on the frictional properties and damage of regenerative articular cartilage surfaces. *Tissue Eng. Part A* **19,** 2300–10 (2013).

12. Steele, J. A. M. *et al.* Combinatorial scaffold morphologies for zonal articular cartilage engineering. *Acta Biomater.* **10,** 2065–2075 (2014).

13. Noszczyk, B. H. *et al.* Biocompatibility of electrospun human albumin: a pilot study. *Biofabrication* **7,** 15011 (2015).

14. Grant, R., Hay, D. & Callanan, A. A drug induced hybrid electrospun PCL - cell derived ECM scaffold for liver tissue engineering. *Tissue Eng. Part A* ten.TEA.2016.0419 (2017). doi:10.1089/ten.TEA.2016.0419

15. Naderi, H., Matin, M. M. & Bahrami, A. R. Review paper: critical issues in tissue engineering: biomaterials, cell sources, angiogenesis, and drug delivery systems. *J. Biomater. Appl.* **26,** 383–417 (2011).

16. He, M. & Callanan, A. Comparison of methods for whole organ decellularisation in tissue engineering of bio-artificial organs. *Tissue Eng. Part B Rev.* **19,** (2012).

17. De Kock, J. *et al.* Simple and quick method for whole-liver decellularization: A novel in vitro three-dimensional bioengineering tool? *Arch. Toxicol.* **85,** 607–612 (2011).

18. Baptista, P. M. *et al.* The use of whole organ decellularization for the generation of a vascularized liver organoid. *Hepatology* **53,** 604–617 (2011).

19. Barakat, O. *et al.* Use of decellularized porcine liver for engineering humanized liver organ. *J. Surg. Res.* **173,** e11–e25 (2012).

20. Wu, Q. *et al.* Optimizing Perfusion-Decellularization Methods of Porcine Livers for Clinical-Scale Whole-Organ Bioengineering. *Biomed Res. Int.* **2015,** 1–9 (2015).

21. Zhou, P. *et al.* Decellularization and Recellularization of Rat Livers With Hepatocytes and Endothelial Progenitor Cells. *Artif. Organs* n/a-n/a (2016). doi:10.1111/aor.12645

22. Faulk, D. M., Wildemann, J. D. & Badylak, S. F. Decellularization and Cell Seeding of Whole Liver Biologic Scaffolds Composed of Extracellular Matrix. *J. Clin. Exp.*

Hepatol. **5,** 69–80 (2015).

23. Kogel, J. Van Der, Bussink, J., Coxon, A., Polverino, A. & M, P. Fluid flow regulation of revascularization and cellular organizationin a bioengineered liver platform. *Tissue Eng. Part C Methods* 1–22 (2016).

24. Hazama, K., Asayama, S. & Kawakami, H. Up-Regulation of Gene Expression by Transfection to Hepatocyte Spheroids. *Mol. Pharm.* (2012).

25. Lee, M. H. *et al.* Hepatocyte-Targeting Single Galactose-Appended Naphthalimide: A Tool for Intracellular Thiol Imaging in Vivo. *J. Am. Chem. Soc.* **134,** 1316–1322 (2012).

26. Lu, C., Xu, W., Zhang, F., Shao, J. & Zheng, S. Nrf2 Knockdown Disrupts the Protective Effect of Curcumin on Alcohol-Induced Hepatocyte Necroptosis. *Mol. Pharm.* **13,** 4043–4053 (2016).

27. Narsinh, K. H. *et al.* Generation of adult human induced pluripotent stem cells using nonviral minicircle DNA vectors. *Nat. Protoc.* **6,** 78–88 (2010).

28. Cachat, E. *et al.* 2- and 3-Dimensional Synthetic Large-Scale De Novo Patterning By Mammalian Cells Through Phase Separation. *Sci. Rep.* **6,** 20664 (2016).

29. Chen, A. Y., Zhong, C. & Lu, T. K. Engineering Living Functional Materials. *ACS Synth. Biol.* **4,** 8–11 (2015).

30. Zhou, D. *et al.* Highly branched poly(β-amino ester)s for skin gene therapy. *J. Control. Release* (2016). doi:10.1016/j.jconrel.2016.06.014

31. Cutlar, L. *et al.* A Non-Viral Gene Therapy for Treatment of Recessive Dystrophic Epidermolysis Bullosa. *Exp. Dermatol.* 818–820 (2016).

32. Deltcheva, E. *et al.* CRISPR RNA maturation by trans-encoded small RNA and host factor RNase III. *Nature* **471,** 602–609 (2011).

33. Jinek, M. *et al.* A Programmable Dual-RNA–Guided DNA Endonuclease in Adaptive Bacterial Immunity. *Science (80-.).* **337,** 816–821 (2012).

34. Fonfara, I., Richter, H., Bratovič, M., Le Rhun, A. & Charpentier, E. The CRISPR-associated DNA-cleaving enzyme Cpf1 also processes precursor CRISPR RNA CRISPR–Cas systems that provide defence against mobile genetic elements in bacteria and archaea have evolved a variety of mechanisms to target and cleave RNA or DNA. *Nature* **532,** 517–523 (2016).

35. Kay, M. A., He, C.-Y. & Chen, Z.-Y. A robust system for production of minicircle DNA vectors. *Nat. Biotechnol.* **28,** 1287–1289 (2010).

36. Yi, H. *et al.* A New Strategy to Deliver Synthetic Protein Drugs: Self-reproducible Biologics Using Minicircles. *Sci. Rep.* **4,** 5961 (2014).

37. Munye, M. M. *et al.* Minicircle DNA Provides Enhanced and Prolonged Transgene Expression Following Airway Gene Transfer. *Sci. Rep.* **6,** 23125 (2016).

38. Sibbald, B. Death but one unintended consequence of gene-therapy trial. *CMAJ* **164,** 1612 (2001).

39. Romero, Z., Toscano, M., Unciti, J., Molina, I. & Martin, F. Safer Vectors for Gene Therapy of Primary Immunodeficiencies. *Curr. Gene Ther.* **9,** 291–305 (2009).

40. Pisetsky, D. S. The origin and properties of extracellular DNA: from PAMP to DAMP. *Clin. Immunol.* **144,** 32–40 (2012).

41. Hotaling, N. a., Bharti, K., Kriel, H. & Simon, C. G. DiameterJ: A validated open source nanofiber diameter measurement tool. *Biomaterials* **61,** 327–338 (2015).

42. Lakes, R. Foam Structures with a Negative Poisson's Ratio. *Science (New York, N.Y.)* **235,** 1038–1040 (1987).

43. Greaves, G. N., Greer, A. L., Lakes, R. S. & Rouxel, T. Poisson's ratio and modern materials. *Nat. Mater.* **10,** 823–37 (2011).

44. Oliver, W. C. & Pharr, G. M. An improved technique for determining hardness and elastic modulus using load and displacement sensing indentation experiments. *Journal of Materials Research* **7,** 1564–1583 (2011).

45. Akhtar, R. *et al.* Nanoindentation of histological specimens: Mapping the elastic properties of soft tissues. *J. Mater. Res.* **24,** 638–646 (2009).

46. Livak, K. J. & Schmittgen, T. D. Analysis of relative gene expression data using real-time quantitative PCR and the 2-ÄÄCT method. *Methods* **25,** 402–408 (2001).

47. Callanan, A., Davis, N. F., McGloughlin, T. M. & Walsh, M. T. Development of a rotational cell-seeding system for tubularized extracellular matrix (ECM) scaffolds in vascular surgery. *J. Biomed. Mater. Res. Part B Appl. Biomater.* **102,** 781–788 (2014).

48. Bartlett, M. S. Properties of Sufficiency and Statistical Tests. *Proc. R. Soc. A Math. Phys. Eng. Sci.* **160,** 268–282 (1937).

49. Meier, U. A note on the power of Fisher's least significant difference procedure. *Pharm. Stat.* **5,** 253–263 (2006).

50. McHugh, M. L. Multiple comparison analysis testing in ANOVA. *Biochem. Medica* 203–209 (2011). doi:10.11613/BM.2011.029

51. Klaas, M. *et al.* The alterations in the extracellular matrix composition guide the repair of damaged liver tissue. *Sci. Rep.* **6,** 27398 (2016).

52. Kubow, K. E. *et al.* Mechanical forces regulate the interactions of fibronectin and collagen I in extracellular matrix. *Nat. Commun.* **6,** 8026 (2015).

53. Sottile, J. & Hocking, D. C. Fibronectin Polymerization Regulates the Composition and Stability of Extracellular Matrix Fibrils and Cell-Matrix Adhesions. *Mol. Biol. Cell* **14,** 3546–3559 (2002).

54. Discher, D. E., Janmey, P. & Wang, Y.-L. Tissue cells feel and respond to the stiffness of their substrate. *Science* **310,** 1139–43 (2005).

55. Klatt, D. *et al.* Viscoelastic properties of liver measured by oscillatory rheometry and multifrequency magnetic resonance elastography. *Biorheology* **47,** 133–141 (2010).

56. Torok, E. *et al.* Primary Human Hepatocytes on Biodegradable Poly(l-Lactic acid) Matrices: A Promising Model for Improving Transplantation Efficiency With Tissue Engineering. *Liver Transplant.* **13,** 465–466 (2011).

57. Loneker, A. E., Faulk, D. M., Hussey, G. S., D'Amore, A. & Badylak, S. F. Solubilized liver extracellular matrix maintains primary rat hepatocyte phenotype in-vitro. *J. Biomed. Mater. Res. A* 1–9 (2015).

58. Gao, R. *et al.* Hepatocyte Culture in Autologous Decellularized Spleen Matrix. *Organogenesis* (2015).

59. Martinez-Hernandez, A. & Amenta, P. S. The hepatic extracellular matrix I. Components and distribution in normal liver. *Virchows Arch. A Pathol. Anat.*

Histopathol. **423,** 1–11 (1993).

60. Cameron, K. *et al.* Recombinant Laminins Drive the Differentiation and Self-Organization of hESC-Derived Hepatocytes. *Stem Cell Reports* **5,** 1–13 (2015).

61. Pankov, R. & Yamada, K. M. Fibronectin at a glance. *J. Cell Sci.* **115,** 3861–3863 (2002).

62. Seliskar, M. & Rozman, D. Mammalian cytochromes P450-Importance of tissue specificity. *Biochim. Biophys. Acta - Gen. Subj.* **1770,** 458–466 (2007).

63. Medine, C. N. *et al.* Developing high-fidelity hepatotoxicity models from pluripotent stem cells. *Stem Cells Transl. Med.* **2,** 505–9 (2013).

64. Palakkan, A. A. *et al.* Polarisation and functional characterisation of hepatocytes derived from human embryonic and mesenchymal stem cells. *Biomed. reports* **3,** 626–636 (2015).

65. Saad, B. *et al.* Crude liver membrane fractions and extracellular matrix components as substrata regulate differentially the preservation and inducibility of cytochrome P-450 isoenzymes in cultured rat hepatocytes. *Eur J Biochem* **213,** 805–814 (1993).

66. Badylak, S. F. The extracellular matrix as a scaffold for tissue reconstruction. *Semin. Cell Dev. Biol.* **13,** 377–383 (2002).

67. Badylak, S. F., Dziki, J. L., Sicari, B. M., Ambrosio, F. & Boninger, M. L. Mechanisms by which acellular biologic scaffolds promote functional skeletal muscle restoration. *Biomaterials* **103,** 128–136 (2016).

68. Meng, F. W., Slivka, P. F., Dearth, C. L. & Badylak, S. F. Solubilized extracellular matrix from brain and urinary bladder elicits distinct functional and phenotypic responses in macrophages. *Biomaterials* **46,** 131–40 (2015).

69. Davis, N. F., Coakley, D. N., Callanan, A., Flood, H. D. & McGloughlin, T. M. Evaluation of xenogenic extracellular matrices as adjuvant scaffolds for the treatment of stress urinary incontinence. *Int. Urogynecol. J.* **24,** 2105–10 (2013).

70. He, M., Callanan, A., Lagaras, K., Steele, J. A. M. & Stevens, M. M. Optimization of SDS exposure on preservation of ECM characteristics in whole organ decellularization of rat kidneys. *J. Biomed. Mater. Res. Part B Appl. Biomater.* 1–9 (2016).

71. Burton, T. P., Corcoran, A. & Callanan, A. The effect of electrospun polycaprolactone scaffold morphology on human kidney epithelial cells. *Biomed. Mater* **13,** (2018).

72. Burton, T. P., Corcoran, A. & Callanan, A. The effect of electrospun polycaprolactone scaffold morphology on human kidney epithelial cells. *Biomed. Mater.* **13,** 15006 (2017).

73. Casasola, R., Thomas, N. L., Trybala, A. & Georgiadou, S. Electrospun poly lactic acid (PLA) fibres: Effect of different solvent systems on fibre morphology and diameter. *Polym. (United Kingdom)* **55,** 4728–4737 (2014).

74. Rafael Auras, Lim, L.-T., Selke, S. E. M. & Tsuji, H. *Poly(Lactic Acid): Synthesis, Structures, Properties, Processing, and Applications*. (2010).

75. Iwasaki, A. *et al.* Molecular mechanism responsible for fibronectin-controlled alterations in matrix stiffness in advanced chronic liver fibrogenesis. *J. Biol. Chem.* **291,** 72–88 (2016).

76. Zollinger, A. J. & Smith, M. L. Fibronectin, the extracellular glue. *Matrix Biol.* (2016).

doi:10.1016/j.matbio.2016.07.011

77. Kawelke, N. *et al.* Fibronectin protects from excessive liver fibrosis by modulating the availability of and responsiveness of stellate cells to active TGF-β. *PLoS One* **6,** e28181 (2011).

78. Altrock, E. *et al.* Inhibition of fibronectin deposition improves experimental liver fibrosis. *J. Hepatol.* **62,** 625–633 (2015).

79. George, E. L., Georges-Labouesse, E. N., Patel-King, R. S., Rayburn, H. & Hynes, R. O. Defects in mesoderm, neural tube and vascular development in mouse embryos lacking fibronectin. *Development* **119,** 1079–1091 (1993).

80. Costantini, S., Di Bernardo, G., Cammarota, M., Castello, G. & Colonna, G. Gene expression signature of human HepG2 cell line. *Gene* **518,** 335–45 (2013).

81. Gorell, E., Nguyen, N., Lane, A. & Siprashvili, Z. Gene therapy for skin diseases. *Cold Spring Harb Perspect Med* **4,** a015149 (2014).

82. Peloso, A. *et al.* Current achievements and future perspectives in whole-organ bioengineering. *Stem Cell Res. Ther.* **6,** (2015).

83. Woods, T. & Gratzer, P. F. Effectiveness of three extraction techniques in the development of a decellularized bone-anterior cruciate ligament-bone graft. *Biomaterials* **26,** 7339–7349 (2005).

84. Funamoto, S. *et al.* The use of high-hydrostatic pressure treatment to decellularize blood vessels. *Biomaterials* **31,** 3590–3595 (2010).

85. Cebotari, S. *et al.* Detergent decellularization of heart valves for tissue engineering: Toxicological effects of residual detergent on human endothelial cells. *Artif. Organs* **34,** 206–210 (2010).